Filing at a Glance

Companies: Garrison Property and Casualty Insurance Company, United Services Automobile Association, USAA Casualty Insurance Company, USAA General Indemnity Company

Product Name: Dwelling Fire Program	SERFF Tr Num: USAA-127801012	State: Arkansas
TOI: 01.0 Property	SERFF Status: Closed-Filed	State Tr Num:
Sub-TOI: 01.0002 Personal Property (Fire and Allied Lines)	Co Tr Num: AR1114530	State Status: Suspended Review
Filing Type: Rate		Reviewer(s): Becky Harrington, Nancy Horton
	Authors: Nick Almendarez, Heather Arriola	Disposition Date: 12/06/2011
	Date Submitted: 11/08/2011	Disposition Status: Filed
Effective Date Requested (New): 02/08/2012		Effective Date (New): 02/22/2012
Effective Date Requested (Renewal): 02/08/2012		Effective Date (Renewal): 02/22/2012

State Filing Description:
referred to Commissioner 12/5; notify co to change effective dates.

General Information

Project Name: Rate Revision	Status of Filing in Domicile: Not Filed
Project Number: AR1114530	Domicile Status Comments:
Reference Organization:	Reference Number:
Reference Title:	Advisory Org. Circular:
Filing Status Changed: 12/06/2011	
State Status Changed: 12/05/2011	Deemer Date:
Created By: Heather Arriola	Submitted By: Heather Arriola
Corresponding Filing Tracking Number:	

Filing Description:
United Services Automobile Association (USAA), USAA Casualty Insurance Company (USAA-CIC), USAA General Indemnity Company (USAA-GIC) and Garrison Property and Casualty Insurance Company (Garrison) are revising the Fire and Allied Lines rates for our Dwelling Fire Program on file with your Department. The overall effect for our proposed changes is 13.1% for the Group. Our rate revision will be effective February 8, 2012.

The enclosed exhibits are provided in support of our proposed rate change.

Company and Contact

Filing Contact Information

Nick Almendarez, Compliance Analyst
A-03-W Insurance Regulatory Compliance
9800 Fredericksburg Road
San Antonio, TX 78288-1033

nick.almendarez@usaa.com
800-531-8722 [Phone] 82844 [Ext]
210-498-5081 [FAX]

Filing Company Information

Garrison Property and Casualty Insurance Company 9800 Fredericksburg Road San Antonio, TX 78284-8496 (800) 531-8722 ext. [Phone]	CoCode: 21253 Group Code: 200 Group Name: USAA FEIN Number: 43-1803614	State of Domicile: Texas Company Type: Stock State ID Number:

United Services Automobile Association 9800 Fredericksburg Road San Antonio, TX 78288 (800) 531-8722 ext. [Phone]	CoCode: 25941 Group Code: 200 Group Name: USAA FEIN Number: 74-0959140	State of Domicile: Texas Company Type: Reciprocal State ID Number:

USAA Casualty Insurance Company 9800 Fredericksburg Road San Antonio, TX 78288 (800) 531-8722 ext. [Phone]	CoCode: 25968 Group Code: 200 Group Name: USAA FEIN Number: 59-3019540	State of Domicile: Texas Company Type: Stock State ID Number:

USAA General Indemnity Company 9800 Fredericksburg Road San Antonio, TX 78288 (800) 531-8722 ext. [Phone]	CoCode: 18600 Group Code: 200 Group Name: USAA FEIN Number: 74-1718283	State of Domicile: Texas Company Type: Stock State ID Number:

Filing Fees

SERFF Tracking Number:	*USAA-127801012*	*State:*	*Arkansas*
First Filing Company:	*Garrison Property and Casualty Insurance Company, ...*	*State Tracking Number:*	
Company Tracking Number:	*AR1114530*		
TOI:	*01.0 Property*	*Sub-TOI:*	*01.0002 Personal Property (Fire and Allied Lines)*
Product Name:	*Dwelling Fire Program*		
Project Name/Number:	*Rate Revision/AR1114530*		

Fee Required?	Yes
Fee Amount:	$100.00
Retaliatory?	No
Fee Explanation:	$100 per independent rate filing
Per Company:	No

COMPANY	AMOUNT	DATE PROCESSED	TRANSACTION #
Garrison Property and Casualty Insurance Company	$0.00	11/08/2011	
United Services Automobile Association	$100.00	11/08/2011	53584549
USAA Casualty Insurance Company	$0.00	11/08/2011	
USAA General Indemnity Company	$0.00	11/08/2011	

Correspondence Summary

Dispositions

Status	Created By	Created On	Date Submitted
Filed	Becky Harrington	12/06/2011	12/06/2011

Objection Letters and Response Letters

Objection Letters				Response Letters		
Status	**Created By**	**Created On**	**Date Submitted**	**Responded By**	**Created On**	**Date Submitted**
No response necessary	Becky Harrington	12/05/2011	12/05/2011			
Pending Industry Response	Becky Harrington	11/09/2011	11/09/2011	Heather Arriola	11/21/2011	11/21/2011

Amendments

Schedule	Schedule Item Name	Created By	Created On	Date Submitted
Supporting Document	HPCS-Homeowners Premium Comparison Survey	Heather Arriola	11/30/2011	11/30/2011
Supporting Document	HPCS-Homeowners Premium Comparison Survey	Heather Arriola	11/28/2011	11/28/2011

Filing Notes

Subject	Note Type	Created By	Created On	Date Submitted

SERFF Tracking Number:	*USAA-127801012*	*State:*	*Arkansas*
First Filing Company:	*Garrison Property and Casualty Insurance Company, ...*	*State Tracking Number:*	
Company Tracking Number:	*AR1114530*		
TOI:	*01.0 Property*	*Sub-TOI:*	*01.0002 Personal Property (Fire and Allied Lines)*
Product Name:	*Dwelling Fire Program*		
Project Name/Number:	*Rate Revision/AR1114530*		

Effective Date Revision	Note To Reviewer	Heather Arriola	12/06/2011	12/06/2011
Effective Dates	Note To Filer	Becky Harrington	12/06/2011	12/06/2011
Change of Effective Date Request	Note To Reviewer	Heather Arriola	12/05/2011	12/05/2011

Disposition

Disposition Date: 12/06/2011
Effective Date (New): 02/22/2012
Effective Date (Renewal): 02/22/2012
Status: Filed
Comment:

Company Name:	**Overall % Indicated Change:**	**Overall % Rate Impact:**	**Written Premium Change for this Program:**	**# of Policy Holders Affected for this Program:**	**Written Premium for this Program:**	**Maximum % Change (where required):**	**Minimum % Change (where required):**
Garrison Property and Casualty Insurance Company	28.600%	13.400%	$7,470	58	$55,746	15.600%	8.600%
United Services Automobile Association	28.600%	13.000%	$255,459	2,727	$1,965,067	16.600%	-3.200%
USAA Casualty Insurance Company	28.600%	13.400%	$63,201	481	$471,648	16.400%	8.200%
USAA General Indemnity Company	28.600%	13.400%	$14,945	124	$111,527	16.000%	9.000%

Overall Rate Information for Multiple Company Filings	
Overall Percentage Rate Indicated For This Filing	28.600%
Overall Percentage Rate Impact For This Filing	13.100%
Effect of Rate Filing-Written Premium Change For This Program	$341,075
Effect of Rate Filing - Number of Policyholders Affected	3,390

SERFF Tracking Number:	*USAA-127801012*	*State:*	*Arkansas*
First Filing Company:	*Garrison Property and Casualty Insurance Company, ...*	*State Tracking Number:*	
Company Tracking Number:	*AR1114530*		
TOI:	*01.0 Property*	*Sub-TOI:*	*01.0002 Personal Property (Fire and Allied Lines)*
Product Name:	*Dwelling Fire Program*		
Project Name/Number:	*Rate Revision/AR1114530*		

Schedule	Schedule Item	Schedule Item Status	Public Access
Supporting Document	Form RF-1 NAIC Loss Cost Data Entry Document--All P&C Lines	Filed	Yes
Supporting Document *(revised)*	HPCS-Homeowners Premium Comparison Survey	Filed	Yes
Supporting Document	HPCS-Homeowners Premium Comparison Survey		Yes
Supporting Document	HPCS-Homeowners Premium Comparison Survey		Yes
Supporting Document	HPCS-Homeowners Premium Comparison Survey		Yes
Supporting Document	NAIC Loss Cost Filing Document for OTHER than Workers' Comp	Filed	Yes
Supporting Document *(revised)*	P&C Actuarial Justification	Filed	Yes
Supporting Document	P&C Actuarial Justification		Yes
Supporting Document	AIR US Earthquake Model	Filed	Yes
Rate	Dwelling Fire Manual Rate Pages	Filed	Yes

Objection Letter

Objection Letter Status	No response necessary
Objection Letter Date	12/05/2011
Submitted Date	12/05/2011
Respond By Date	

Dear Nick Almendarez,

This will acknowledge receipt of the recent response.

This filing is being referred to the Commissioner for review due to the requested increase being greater than 6%.

NOTICE regarding, corrections to filings and scrivener's Errors:

Effective for all filings made on or after June 1, 2011, Arkansas no longer allows the re-opening of closed filings for corrections, changes in effective dates, scrivener's errors, amendments or substantive changes. Please see the General Instructions for how these events will be handled after the effective date of the change."

In accordance with Regulation 23, Section 7.A., this filing may not be implemented until 20 days after the requested amendment(s) and/or information is received.

Sincerely,

Becky Harrington

Objection Letter

Objection Letter Status	Pending Industry Response
Objection Letter Date	11/09/2011
Submitted Date	11/09/2011
Respond By Date	

Dear Nick Almendarez,

This will acknowledge receipt of the captioned filing.

Objection 1

- HPCS-Homeowners Premium Comparison Survey (Supporting Document)

Comment: Additional worksheets were detected when the completed HPCS was run through our program. Addition of worksheets, formulas, or any other modifications to the form are not permitted; the form may not be altered in any way. Re-submit the form as separate worksheets for each company. This is a recurring problem with USAA. Future filings will be rejected.

Objection 2

- P&C Actuarial Justification (Supporting Document)

Comment: Provide the AIR model and data used to calculate the overall indications as described for Fire Exhibit VII.

Objection 3

- P&C Actuarial Justification (Supporting Document)

Comment: Please re-calculate indications for Allied Lines using historical AR data. We are not allowing the use of modeling except for earthquake related losses. (This was addressed in the previous filing.)

Objection 4

Comment: Please remove the hurricane load. (This was addressed in previoius filings.)

Objection 5

Comment: Please provide an estimated loss ratio for the 1st six months of 2011.

NOTICE regarding, corrections to filings and scrivener's Errors:

Effective for all filings made on or after June 1, 2011, Arkansas no longer allows the re-opening of closed filings for

corrections, changes in effective dates, scrivener's errors, amendments or substantive changes. Please see the General Instructions for how these events will be handled after the effective date of the change."

In accordance with Regulation 23, Section 7.A., this filing may not be implemented until 20 days after the requested amendment(s) and/or information is received.

Sincerely,

Becky Harrington

Response Letter

Response Letter Status	Submitted to State
Response Letter Date	11/21/2011
Submitted Date	11/21/2011

Dear Becky Harrington,

Comments:

Response 1

Comments: HPCS Surveys have been separated by company and attached to the filing.

Related Objection 1

Applies To:

- HPCS-Homeowners Premium Comparison Survey (Supporting Document)

Comment:

Additional worksheets were detected when the completed HPCS was run through our program. Addition of worksheets, formulas, or any other modifications to the form are not permitted; the form may not be altered in any way. Re-submit the form as separate worksheets for each company. This is a recurring problem with USAA. Future filings will be rejected.

Changed Items:

Supporting Document Schedule Item Changes

Satisfied -Name: HPCS-Homeowners Premium Comparison Survey

Comment:

No Form Schedule items changed.

No Rate/Rule Schedule items changed.

Response 2

Comments: Please refer to The AIR Earthquake Model for the United States, section 5-14. In addition, Exhibit VII-Fire has been revised to include more detailed information regarding the model.

Related Objection 1

Applies To:

- P&C Actuarial Justification (Supporting Document)

Comment:

Provide the AIR model and data used to calculate the overall indications as described for Fire Exhibit VII.

Changed Items:

Supporting Document Schedule Item Changes

Satisfied -Name: P&C Actuarial Justification

Comment:

Satisfied -Name: AIR US Earthquake Model

Comment:

No Form Schedule items changed.

No Rate/Rule Schedule items changed.

Response 3

Comments: The Allied Lines indications have been revised to remove all models, including the hurricane load. Please refer to Exhibit XII-Allied Lines for the calculation of the Catastrophe Loss and LAE ratio used to develop the indications in the revised Exhibit I-Allied Lines. An explanation of this calculation can be found in the revised Explanatory Memo-Allied Lines.

Related Objection 1

Applies To:

- P&C Actuarial Justification (Supporting Document)

Comment:

Please re-calculate indications for Allied Lines using historical AR data. We are not allowing the use of modeling except for earthquake related losses. (This was addressed in the previous filing.)

Changed Items:

Supporting Document Schedule Item Changes

Satisfied -Name: P&C Actuarial Justification

Comment:

No Form Schedule items changed.

No Rate/Rule Schedule items changed.

Response 4

Comments: Please see response and explanatory exhibits revised 11-21-11 to objection 3.

Related Objection 1

Comment:

Please remove the hurricane load. (This was addressed in previoius filings.)

Changed Items:

No Supporting Documents changed.

No Form Schedule items changed.

No Rate/Rule Schedule items changed.

Response 5

Comments: Please refer to Exhibit A in explanatory exhibits revised 11-21-11.

Related Objection 1

Comment:

Please provide an estimated loss ratio for the 1st six months of 2011.

Changed Items:

No Supporting Documents changed.

No Form Schedule items changed.

SERFF Tracking Number:	*USAA-127801012*	*State:*	*Arkansas*
First Filing Company:	*Garrison Property and Casualty Insurance Company, ...*	*State Tracking Number:*	
Company Tracking Number:	*AR1114530*		
TOI:	*01.0 Property*	*Sub-TOI:*	*01.0002 Personal Property (Fire and Allied Lines)*
Product Name:	*Dwelling Fire Program*		
Project Name/Number:	*Rate Revision/AR1114530*		

No Rate/Rule Schedule items changed.

Sincerely,
Heather Arriola, Nick Almendarez

Note To Reviewer

Created By:

Heather Arriola on 12/06/2011 01:27 PM

Last Edited By:

Becky Harrington

Submitted On:

12/06/2011 02:02 PM

Subject:

Effective Date Revision

Comments:

Please update the new and renewal business effective dates to 02/22/2012. Thank you for your help.

Note To Filer

Created By:

Becky Harrington on 12/06/2011 11:25 AM

Last Edited By:

Becky Harrington

Submitted On:

12/06/2011 02:02 PM

Subject:

Effective Dates

Comments:

Please provide revised effective dates. The Commissioner has reviewed the filing and will accept the requested increase amount.

SERFF Tracking Number:	*USAA-127801012*	*State:*	*Arkansas*
First Filing Company:	*Garrison Property and Casualty Insurance Company, ...*	*State Tracking Number:*	
Company Tracking Number:	*AR1114530*		
TOI:	*01.0 Property*	*Sub-TOI:*	*01.0002 Personal Property (Fire and Allied Lines)*
Product Name:	*Dwelling Fire Program*		
Project Name/Number:	*Rate Revision/AR1114530*		

Note To Reviewer

Created By:

Heather Arriola on 12/05/2011 02:19 PM

Last Edited By:

Becky Harrington

Submitted On:

12/06/2011 02:02 PM

Subject:

Change of Effective Date Request

Comments:

We will be unable to implement this filing by the previously requested effective dates of 02/08/2012 (new and renewal business). I would like to ask that the disposition be suspended until further notification to allow a change of effective date once a decision has been reached. Please notify me when a disposition has been reached and I will provide new effective dates at that time. Thank you.

Heather

Amendment Letter

Submitted Date: 11/30/2011

Comments:

Becky,

I apologize for sending multiple copies of the HPCS forms. I have corrected the tab naming on the Excel forms, as I noted that the tabs had been modified. Thank you.

Changed Items:

Supporting Document Schedule Item Changes:

Satisfied -Name: HPCS-Homeowners Premium Comparison Survey

Comment: I apologize for sending multiple copies of the HPCS forms. I have corrected the tab naming on the Excel forms as I noted that the tabs had been modified. Thank you.

USAA HPCS-Revised 11-30-11.XLS

CIC HPCS-Revised 11-30-11.XLS

GIC HPCS-Revised 11-30-11.XLS

Garrison HPCS-Revised 11-30-11.XLS

Amendment Letter

Submitted Date: 11/28/2011

Comments:

HPCS's have been revised to exclude NAIC Group numbers in the NAIC Number field.

Changed Items:

Supporting Document Schedule Item Changes:

Satisfied -Name: HPCS-Homeowners Premium Comparison Survey

Comment: HPCS have been revised to exclude NAIC Group numbers in the NAIC Number field.

USAA HPCS-Revised 11-28-11.XLS

CIC HPCS-Revised 11-28-11.XLS

GIC HPCS-Revised 11-28-11.XLS

Garrison HPCS-Revised 11-28-11.XLS

Rate Information

Rate data applies to filing.

Filing Method:	File and Use
Rate Change Type:	Increase
Overall Percentage of Last Rate Revision:	13.100%
Effective Date of Last Rate Revision:	12/31/2010
Filing Method of Last Filing:	File and Use

Company Rate Information

Company Name:	Overall % Indicated Change:	Overall % Rate Impact:	Written Premium Change for this Program:	# of Policy Holders Affected for this Program:	Written Premium for this Program:	Maximum % Change (where required):	Minimum % Change (where required):
Garrison Property and Casualty Insurance Company	28.600%	13.400%	$7,470	58	$55,746	15.600%	8.600%

Company Rate Information

Company Name:	Overall % Indicated Change:	Overall % Rate Impact:	Written Premium Change for this Program:	# of Policy Holders Affected for this Program:	Written Premium for this Program:	Maximum % Change (where required):	Minimum % Change (where required):

United Services Automobile Association	28.600%	13.000%	$255,459	2,727	$1,965,067	16.600%	-3.200%

Company Rate Information

Company Name:	Overall % Indicated Change:	Overall % Rate Impact:	Written Premium Change for this Program:	# of Policy Holders Affected for this Program:	Written Premium for this Program:	Maximum % Change (where required):	Minimum % Change (where required):
USAA Casualty Insurance Company	28.600%	13.400%	$63,201	481	$471,648	16.400%	8.200%

Company Rate Information

Company Name:	Overall % Indicated Change:	Overall % Rate Impact:	Written Premium Change for this Program:	# of Policy Holders Affected for this Program:	Written Premium for this Program:	Maximum % Change (where required):	Minimum % Change (where required):
USAA General Indemnity Company	28.600%	13.400%	$14,945	124	$111,527	16.000%	9.000%

Overall Rate Information for Multiple Company Filings

Overall % Rate Indicated: 28.600%

SERFF Tracking Number:	*USAA-127801012*	*State:*	*Arkansas*
First Filing Company:	*Garrison Property and Casualty Insurance Company, ...*	*State Tracking Number:*	
Company Tracking Number:	*AR1114530*		
TOI:	*01.0 Property*	*Sub-TOI:*	*01.0002 Personal Property (Fire and Allied Lines)*
Product Name:	*Dwelling Fire Program*		
Project Name/Number:	*Rate Revision/AR1114530*		

Overall Percentage Rate Impact For This Filing:	13.100%
Effect of Rate Filing - Written Premium Change For This Program:	$341,075
Effect of Rate Filing - Number of Policyholders Affected:	3390

Rate/Rule Schedule

Schedule Item Status:	Exhibit Name:	Rule # or Page #:	Rate Action	Previous State Filing Number:	Attachments
Filed 12/06/2011	Dwelling Fire Manual Rate Pages	DP-R-4-8 and DP-R-9-18	Replacement	USAA-126838790	Rates DP-R-4-8 and DP-R-9-18.pdf

301. BASE PREMIUM COMPUTATION

Fire - Coverages A and C - All Forms

1.

UNITY FIRE PREMIUMS		
Company	COV A	COV C
USAA	$98	$20
USAA-CIC	$144	$33
USAA-GIC	$144	$33
Garrison	$144	$33

2.

TERRITORIAL RELATIVITY		
Coverages A and C		
Terr.	COV A	COV C
ALL	1.000	1.000

3.

PROTECTION/CONSTRUCTION RELATIVITY			
	Prot.	FACTOR	
Const.	Class	COV A	COV C
Masonry	1-3	0.479	0.600
	4	0.585	0.600
	5	0.690	0.680
	6	0.849	0.760
	7	1.294	1.040
	8	1.490	1.120
	8B, 9	1.680	1.320
	10	2.310	1.680
Frame	1-3	0.690	0.760
	4	0.756	0.840
	5	0.849	0.840
	6	1.000	1.000
	7	1.471	1.240
	8	1.840	1.440
	8B, 9	2.670	1.920
**	10	3.490	2.400

** Rate mobile homes as frame

@ Use this limit of liability to develop premiums for policy amounts less than $1,000.

4.

NUMBER OF FAMILIES RELATIVITY		
Number of	Factor	
Families	COV A	COV C
1	1.000	1.000
2	1.100	1.000
3	1.600	1.300
4	1.600	1.300
Construction	P.C.	Factor
Masonry	1-3	2.133
	4	2.400
	5	2.176
	6	2.105
	7	1.808
	8	1.786
	8B, 9	1.818
	10	1.714
Frame	1-3	2.211
	4	2.095
	5	2.238
	6	2.000
	7	1.871
	8	1.750
	8B, 9	1.583
	10	1.467

5.

OCCUPANCY RELATIVITY		
	COV A	COV C
Owner	1.000	1.000
Tenant	1.250	1.000

7.

SEASONAL/NONSEASONAL RELATIVITY		
	COV A	COV C
Non-Seasonal	1.000	1.000
Seasonal		
TERR-ALL	1.000	1.000

6.

Amount of Insurance Relativity Curve		
Limit of Liability	COV A	COV C
$ @1,000	0.310	0.35
2,000	0.346	0.48
3,000	0.382	0.61
4,000	0.419	0.74
5,000	0.455	0.87
6,000	0.491	1.00
7,000	0.528	1.13
8,000	0.564	1.26
9,000	0.600	1.39
10,000	0.637	1.52
11,000	0.673	1.65
12,000	0.709	1.78
13,000	0.746	1.91
14,000	0.782	2.04
15,000	0.818	2.17
16,000	0.855	2.30
17,000	0.891	2.43
18,000	0.927	2.56
19,000	0.964	2.69
20,000	1.000	2.82
21,000	1.016	2.95
22,000	1.033	3.08
23,000	1.049	3.21
24,000	1.065	3.34
25,000	1.082	3.47
26,000	1.098	3.60
27,000	1.114	3.73
28,000	1.131	3.86
29,000	1.147	3.99
30,000	1.163	4.12
31,000	1.180	4.25
32,000	1.196	4.38
33,000	1.212	4.51
34,000	1.229	4.64
35,000	1.245	4.77
36,000	1.261	4.90
37,000	1.278	5.03
38,000	1.294	5.16
39,000	1.310	5.29
40,000	1.327	5.42
41,000	1.343	5.55
42,000	1.359	5.68
43,000	1.376	5.81
44,000	1.392	5.94
45,000	1.408	6.07
46,000	1.425	6.20
47,000	1.441	6.33
48,000	1.457	6.46
49,000	1.474	6.59
50,000	1.490	6.72
Each Add'l $1,000	0.016	0.13

301. BASE PREMIUM

Extended Coverage, Broad and
Special Forms - Coverage A and C

1.

USAA Unity Premiums		
	Cov A	Cov C
Extended Coverage	$99	$9
Broad Form	$47	$9
Special Form	$74	-

USAA-CIC Unity Premiums		
	Cov A	Cov C
Extended Coverage	$144	$12
Broad Form	$71	$20
Special Form	$109	-

USAA-GIC Unity Premiums		
	Cov A	Cov C
Extended Coverage	$144	$12
Broad Form	$71	$20
Special Form	$109	-

GARRISON Unity Premiums		
	Cov A	Cov C
Extended Coverage	$144	$12
Broad Form	$71	$20
Special Form	$109	-

2.

Territorial Relativity					
	EXTENDED COVERAGE FACTOR		BROAD FORM FACTOR		SPECIAL FORM FACTOR
Terr	Cov A	Cov C	Cov A	Cov C	Cov A
ALL	1.000	1.000	1.000	1.000	1.000

4.

Seasonal/Non-Seasonal Relativity					
	EXTENDED COVERAGE FACTOR		BROAD FORM FACTOR		SPECIAL FORM FACTOR
	Cov A	Cov C	Cov A	Cov C	Cov A
Non-Seasonal	1.000	1.000	1.000	1.000	1.000
Seasonal TERR-ALL	1.000	1.000	1.568	1.400	1.406

@ Use this limit of liability to develop premiums for policy amounts less than $1,000.

3.

Amount of Insurance Relativity Curve		
Limit of Liability	COV A	COV C
$ @1,000	0.566	0.17
2,000	0.588	0.33
3,000	0.611	0.50
4,000	0.634	0.67
5,000	0.657	0.83
6,000	0.680	1.00
7,000	0.703	1.17
8,000	0.726	1.34
9,000	0.749	1.50
10,000	0.771	1.67
11,000	0.794	1.84
12,000	0.817	2.00
13,000	0.840	2.17
14,000	0.862	2.33
15,000	0.885	2.50
16,000	0.908	2.67
17,000	0.931	2.84
18,000	0.953	3.00
19,000	0.976	3.17
20,000	1.000	3.34
21,000	1.023	3.51
22,000	1.046	3.67
23,000	1.068	3.84
24,000	1.091	4.00
25,000	1.114	4.17
26,000	1.137	4.34
27,000	1.159	4.51
28,000	1.182	4.68
29,000	1.205	4.85
30,000	1.228	5.02
31,000	1.250	5.19
32,000	1.273	5.36
33,000	1.296	5.53
34,000	1.320	5.70
35,000	1.342	5.87
36,000	1.365	6.04
37,000	1.388	6.21
38,000	1.411	6.38
39,000	1.433	6.55
40,000	1.456	6.72
41,000	1.479	6.89
42,000	1.502	7.06
43,000	1.524	7.23
44,000	1.547	7.40
45,000	1.570	7.57
46,000	1.593	7.74
47,000	1.615	7.91
48,000	1.639	8.08
49,000	1.662	8.25
50,000	1.685	8.42
Each Add'l $1,000	0.023	0.17

Supporting Document Schedules

		Item Status:	Status Date:
Satisfied - Item:	Form RF-1 NAIC Loss Cost Data Entry Document--All P&C Lines	Filed	12/06/2011

Comments:

Attachment:

Form RF-1 USAA Group.pdf

		Item Status:	Status Date:
Satisfied - Item:	HPCS-Homeowners Premium Comparison Survey	Filed	12/06/2011

Comments:

I apologize for sending multiple copies of the HPCS forms. I have corrected the tab naming on the Excel forms as I noted that the tabs had been modified. Thank you.

Attachments:

USAA HPCS-Revised 11-30-11.XLS
CIC HPCS-Revised 11-30-11.XLS
GIC HPCS-Revised 11-30-11.XLS
Garrison HPCS-Revised 11-30-11.XLS

		Item Status:	Status Date:
Bypassed - Item:	NAIC Loss Cost Filing Document for OTHER than Workers' Comp	Filed	12/06/2011
Bypass Reason:	N/A		

Comments:

		Item Status:	Status Date:
Satisfied - Item:	P&C Actuarial Justification	Filed	12/06/2011

Comments:

Attachment:

Explanatory Exhibits Revised 11-21-11.pdf

		Item Status:	**Status Date:**
Satisfied - Item:	AIR US Earthquake Model	Filed	12/06/2011

Comments:

Attachments:

AIR_U.S._Earthquake_Model_Non-Confidential 1.pdf
AIR_U.S._Earthquake_Model_Non-Confidential 2.pdf

NAIC LOSS COST DATA ENTRY DOCUMENT

1.	This filing transmittal is part of Company Tracking #	**AR1114530**

2.	If filing is an adoption of an advisory organization loss cost filing, give name of Advisory Organization and Reference/ Item Filing Number	

		Company Name		Company NAIC Number
3.	**A.**	**United Services Automobile Association**	**B.**	**200-25941**

		Product Coding Matrix Line of Business (i.e., Type of Insurance)		Product Coding Matrix Line of Insurance (i.e., Sub-type of Insurance)
4.	**A.**	**01.0 Property**	**B.**	**01.0002 Personal Property (Fire and Allied Lines)**

5.

(A) COVERAGE (See Instructions)	(B) Indicated % Rate Level Change	(C) Requested % Rate Level Change	FOR LOSS COSTS ONLY (D) Expected Loss Ratio	(E) Loss Cost Modification Factor	(F) Selected Loss Cost Multiplier	(G) Expense Constant (If Applicable)	(H) Co. Current Loss Cost Multiplier
Fire	**20.2% (Group)**	**5.0%**					
Allied Lines	**33.8% (Group)**	**20.0%**					
TOTAL OVERALL EFFECT	**28.6% (Group)**	**13.0%**					

6. *5 Year History Rate Change History

Year	Policy Count	% of Change	Effective Date	State Earned Premium (000)	Incurred Losses (000)	State Loss Ratio	Countrywide Loss Ratio
2006	**1900**	**N/A**	**N/A**	**921**	**329**	**36%**	**49%**
2007	**2011**	**N/A**	**N/A**	**1,034**	**1,087**	**105%**	**51%**
2008	**2181**	**0.0%**	**7/1/2008**	**1,130**	**2,337**	**207%**	**62%**
2009	**2370**	**11.1%**	**2/28/2009**	**1,340**	**1,863**	**139%**	**54%**
2010	**2579**	**12.0%**	**12/31/2010**	**1,591**	**1,119**	**70%**	**56%**

7.

Expense Constants	Selected Provisions
A. Total Production Expense	**11.4%**
B. General Expense	**1.7%**
C. Taxes, License & Fees	**2.7%**
D. Underwriting Profit & Contingencies	**15%**
E. Other (explain)	
F. TOTAL	**30.8%**

8. Apply Lost Cost Factors to Future filings? (Y or N) **N**

9. Estimated Maximum Rate Increase for any Insured (%). Territory (if applicable): **16.6%**

10. Estimated Maximum Rate Decrease for any Insured (%) Territory (if applicable): **-3.2%**

*Note that the RF-1 form submitted with our previous filing (effective 12/31/2010) contained data from our "Other Liability" line of business. That portion of the data has been removed for this filing.

NAIC LOSS COST DATA ENTRY DOCUMENT

1.	This filing transmittal is part of Company Tracking #	**AR1114530**

2.	If filing is an adoption of an advisory organization loss cost filing, give name of Advisory Organization and Reference/ Item Filing Number	

		Company Name		Company NAIC Number
3.	**A.**	**USAA Casualty Insurance Company**	**B.**	**200-25968**

		Product Coding Matrix Line of Business (i.e., Type of Insurance)		Product Coding Matrix Line of Insurance (i.e., Sub-type of Insurance)
4.	**A.**	**01.0 Property**	**B.**	**01.0002 Personal Property (Fire and Allied Lines)**

5.

(A) COVERAGE (See Instructions)	(B) Indicated % Rate Level Change	(C) Requested % Rate Level Change	FOR LOSS COSTS ONLY (D) Expected Loss Ratio	(E) Loss Cost Modification Factor	(F) Selected Loss Cost Multiplier	(G) Expense Constant (If Applicable)	(H) Co. Current Loss Cost Multiplier
Fire	**20.2% (Group)**	**5%**					
Allied Lines	**33.8% (Group)**	**20%**					
TOTAL OVERALL EFFECT	**28.6% (Group)**	**13.4%**					

6. *5 Year History Rate Change History

Year	Policy Count	% of Change	Effective Date	State Earned Premium (000)	Incurred Losses (000)	State Loss Ratio	Countrywide Loss Ratio
2006	**335**	**N/A**	**N/A**	**238**	**195**	**82%**	**38%**
2007	**345**	**N/A**	**N/A**	**260**	**70**	**27%**	**43%**
2008	**394**	**0.0%**	**7/1/2008**	**276**	**272**	**99%**	**44%**
2009	**403**	**11.4%**	**2/28/2009**	**325**	**235**	**72%**	**44%**
2010	**460**	**12.1%**	**12/31/2010**	**384**	**184**	**48%**	**49%**

7.

Expense Constants	Selected Provisions
A. Total Production Expense	**11.2%**
B. General Expense	**1.6%**
C. Taxes, License & Fees	**3.0%**
D. Underwriting Profit & Contingencies	**15.0%**
E. Other (explain)	
F. TOTAL	**30.8%**

8. Apply Lost Cost Factors to Future filings? (Y or N) **N**

9. Estimated Maximum Rate Increase for any Insured (%). Territory (if applicable): ____**16.4%**_____

10. Estimated Maximum Rate Decrease for any Insured (%) Territory (if applicable): ___**N/A**_____

*Note that the RF-1 form submitted with our previous filing (effective 12/31/2010) contained data from our "Other Liability" line of business. That portion of the data has been removed for this filing.

NAIC LOSS COST DATA ENTRY DOCUMENT

1.	This filing transmittal is part of Company Tracking #	**AR1114530**

2.	If filing is an adoption of an advisory organization loss cost filing, give name of Advisory Organization and Reference/ Item Filing Number	

		Company Name		Company NAIC Number
3.	**A.**	**USAA General Indemnity Company**	**B.**	**200-18600**

		Product Coding Matrix Line of Business (i.e., Type of Insurance)		Product Coding Matrix Line of Insurance (i.e., Sub-type of Insurance)
4.	**A.**	**01.0 Property**	**B.**	**01.0002 Personal Property (Fire and Allied Lines)**

5.

(A) COVERAGE (See Instructions)	(B) Indicated % Rate Level Change	(C) Requested % Rate Level Change	FOR LOSS COSTS ONLY (D) Expected Loss Ratio	(E) Loss Cost Modification Factor	(F) Selected Loss Cost Multiplier	(G) Expense Constant (If Applicable)	(H) Co. Current Loss Cost Multiplier
Fire	**20.2% (Group)**	**5.0%**					
Allied Lines	**33.8% (Group)**	**20.0%**					
TOTAL OVERALL EFFECT	**28.6% (Group)**	**13.4%**					

6. *5 Year History Rate Change History

Year	Policy Count	% of Change	Effective Date	State Earned Premium (000)	Incurred Losses (000)	State Loss Ratio	Countrywide Loss Ratio
2006	**1**	**N/A**	**N/A**	**0.2**	**0.4**	**223%**	**245%**
2007	**8**	**N/A**	**N/A**	**2.6**	**1.2**	**46%**	**110%**
2008	**19**	**0.0%**	**7/1/2008**	**10.0**	**6.0**	**61%**	**107%**
2009	**40**	**11.2%**	**2/28/2009**	**22.3**	**134.8**	**604%**	**83%**
2010	**89**	**12.1%**	**12/31/2010**	**52.8**	**181.0**	**343%**	**45%**

7.

Expense Constants	Selected Provisions
A. Total Production Expense	**20.5%**
B. General Expense	**2.5%**
C. Taxes, License & Fees	**3.0%**
D. Underwriting Profit & Contingencies	**15.0%**
E. Other (explain)	
F. TOTAL	**41.0%**

8. Apply Lost Cost Factors to Future filings? (Y or N) **N**

9. Estimated Maximum Rate Increase for any Insured (%). Territory (if applicable): ___**16.0%**_____

10. Estimated Maximum Rate Decrease for any Insured (%) Territory (if applicable): _____**N/A**_____

*Note that the RF-1 form submitted with our previous filing (effective 12/31/2010) contained data from our "Other Liability" line of business. That portion of the data has been removed for this filing.

NAIC LOSS COST DATA ENTRY DOCUMENT

1.	This filing transmittal is part of Company Tracking #	**AR1114530**

2.	If filing is an adoption of an advisory organization loss cost filing, give name of Advisory Organization and Reference/ Item Filing Number	

		Company Name		Company NAIC Number
3.	**A.**	**Garrison Property and Casualty Insurance Company**	**B.**	**200-21253**

		Product Coding Matrix Line of Business (i.e., Type of Insurance)		Product Coding Matrix Line of Insurance (i.e., Sub-type of Insurance)
4.	**A.**	**01.0 Property**	**B.**	**01.0002 Personal Property (Fire and Allied Lines)**

5.

(A) COVERAGE (See Instructions)	(B) Indicated % Rate Level Change	(C) Requested % Rate Level Change	FOR LOSS COSTS ONLY (D) Expected Loss Ratio	(E) Loss Cost Modification Factor	(F) Selected Loss Cost Multiplier	(G) Expense Constant (If Applicable)	(H) Co. Current Loss Cost Multiplier
Fire	**20.2% (Group)**	**5.0%**					
Allied Lines	**33.8% (Group)**	**20.0%**					
TOTAL OVERALL EFFECT	**28.6% (Group)**	**13.4%**					

6. *5 Year History Rate Change History

Year	Policy Count	% of Change	Effective Date	State Earned Premium (000)	Incurred Losses (000)	State Loss Ratio	Countrywide Loss Ratio
2006	**16**	**N/A**	**N/A**	**2.8**	**0.2**	**8%**	**13**
2007	**18**	**N/A**	**N/A**	**10.8**	**3.0**	**28%**	**86**
2008	**32**	**0.0%**	**7/1/2008**	**16.8**	**6.2**	**37%**	**67**
2009	**42**	**11.4%**	**2/28/2009**	**31.1**	**12.7**	**41%**	**51**
2010	**55**	**12.1%**	**12/31/2010**	**42.7**	**19.0**	**44%**	**54**

7.

Expense Constants	Selected Provisions
A. Total Production Expense	**13.6%**
B. General Expense	**1.8%**
C. Taxes, License & Fees	**2.8%**
D. Underwriting Profit & Contingencies	**15.0%**
E. Other (explain)	
F. TOTAL	

8. Apply Lost Cost Factors to Future filings? (Y or N) **N**

9. Estimated Maximum Rate Increase for any Insured (%). Territory (if applicable): **15.6%**

10. Estimated Maximum Rate Decrease for any Insured (%) Territory (if applicable): **N/A**

*Note that the RF-1 form submitted with our previous filing (effective 12/31/2010) contained data from our "Other Liability" line of business. That portion of the data has been removed for this filing.

NAIC Number:	25941
Company Name:	United Services Automobile Association
Contact Person:	Nick Almendarez
Telephone No.:	800-531-8722, ext. 8-2844
Email Address:	nick.almendarez@usaa.com
Effective Date:	2/22/2012

Homeowners Premium Comparision Survey Form
FORM HPCS - last modified August, 2005

USE THE APPROPRIATE FORM BELOW - IF NOT APPLICABLE, LEAVE BLANK

Submit to: *Arkansas Insurance Department*
1200 West Third Street
Little Rock, AR 72201-1904
Telephone: *501-371-2800*
Email as an attachment to: insurance.pnc@arkansas.gov
You may also attach to a SERFF filing or submit on a cdr disk

Survey Form for HO3 (Homeowners) - Use $500 Flat Deductible (Covers risk of direct physical loss for dwelling and other structures; named perils for personal property, replacement cost on dwelling, actual cash value on personal property)

Public Protection Class	Dwelling Value	Washington		Baxter		Craighead		St. Francis		Desha		Union		Miller		Sebastian		Pulaski	
		Brick	*Frame*	*Brick*	*Frame*	*Brick*	*Frame*	*Brick*	*Frame*	*Brick*	*Frame*	*Brick*	*Frame*	*Brick*	*Frame*	*Brick*	*Frame*	*Brick*	*Frame*
3	*$80,000*																		
	$120,000																		
	$160,000																		
6	*$80,000*																		
	$120,000																		
	$160,000																		
9	*$80,000*																		
	$120,000																		
	$160,000																		

Survey Form for HO4 (Renters) - Use $500 Flat Deductible (Named perils for personal property, actual cash value for loss, liability and medical payments for others included)

Public Protection Class	Property Value	Washington		Baxter		Craighead		St. Francis		Arkansas		Union		Miller		Sebastian		Pulaski	
		Brick	*Frame*	*Brick*	*Frame*	*Brick*	*Frame*	*Brick*	*Frame*	*Brick*	*Frame*	*Brick*	*Frame*	*Brick*	*Frame*	*Brick*	*Frame*	*Brick*	*Frame*
3	*$5,000*																		
	$15,000																		
	$25,000																		
6	*$5,000*																		
	$15,000																		
	$25,000																		
9	*$5,000*																		
	$15,000																		
	$25,000																		

Survey Form for DP-2 (Dwelling/Fire) - Use $500 Flat Deductible (Named perils for dwelling and personal property; replacement cost for dwelling, actual cash value for personal property, no liability coverage)

Public Protection Class	Dwelling Value	Washington		Baxter		Craighead		St. Francis		Arkansas		Union		Miller		Sebastian		Pulaski	
		Brick	*Frame*	*Brick*	*Frame*	*Brick*	*Frame*	*Brick*	*Frame*	*Brick*	*Frame*	*Brick*	*Frame*	*Brick*	*Frame*	*Brick*	*Frame*	*Brick*	*Frame*
3	*$80,000*	714.92	787.4	714.92	787.4	714.92	787.4	714.92	787.4	714.92	787.4	714.92	787.4	714.92	787.4	714.92	787.4	714.92	787.4
	$120,000	1022.79	1124.25	1022.79	1124.25	1022.79	1124.25	1022.79	1124.25	1022.79	1124.25	1022.79	1124.25	1022.79	1124.25	1022.79	1124.25	1022.79	1124.25
	$160,000	1330.67	1461.11	1330.67	1461.11	1330.67	1461.11	1330.67	1461.11	1330.67	1461.11	1330.67	1461.11	1330.67	1461.11	1330.67	1461.11	1330.67	1461.11
6	*$80,000*	817.17	894.9	817.17	894.9	817.17	894.9	817.17	894.9	817.17	894.9	817.17	894.9	817.17	894.9	817.17	894.9	817.17	894.9
	$120,000	1163.7	1274.83	1163.7	1274.83	1163.7	1274.83	1163.7	1274.83	1163.7	1274.83	1163.7	1274.83	1163.7	1274.83	1163.7	1274.83	1163.7	1274.83
	$160,000	1510.23	1654.76	1510.23	1654.76	1510.23	1654.76	1510.23	1654.76	1510.23	1654.76	1510.23	1654.76	1510.23	1654.76	1510.23	1654.76	1510.23	1654.76
9	*$80,000*	1088.17	1397.18	1088.17	1397.18	1088.17	1397.18	1088.17	1397.18	1088.17	1397.18	1088.17	1397.18	1088.17	1397.18	1088.17	1397.18	1088.17	1397.18
	$120,000	1541.75	1971.51	1541.75	1971.51	1541.75	1971.51	1541.75	1971.51	1541.75	1971.51	1541.75	1971.51	1541.75	1971.51	1541.75	1971.51	1541.75	1971.51
	$160,000	1995.33	2545.85	1995.33	2545.85	1995.33	2545.85	1995.33	2545.85	1995.33	2545.85	1995.33	2545.85	1995.33	2545.85	1995.33	2545.85	1995.33	2545.85

SPECIFY THE PERCENTAGE GIVEN FOR CREDITS OR DISCOUNTS FOR THE FOLLOWING:

HO3 and HO4 only

Fire Extinguisher	0	%	*Deadbolt Lock*	0	%
Burglar Alarm	2 to 15	%	*Window Locks*	0	%
Smoke Alarm	2 to 15	%	*$1,000 Deductible*	14 to 17	%
			Other (specify)		
					%
			Maximum Credit	varies	%

EARTHQUAKE INSURANCE

IMPORTANT, Homeowners insurance does NOT automatically cover losses from earthquakes. Ask your agent about this coverage.

ARE YOU CURRENTLY WRITING EARTHQUAKE COVERAGE IN ARKANSAS? Yes *(yes or no)*

WHAT IS YOUR PERCENTAGE DEDUCTIBLE? 10 %

	Zone	Brick	Frame
WHAT IS YOUR PRICE PER $1,000 OF COVERAGE?	Highest Risk	$ 1.99	$ 0.35
	Lowest Risk	$ 0.77	$ 0.81

NAIC Number:	25968
Company Name:	USAA Casualty Insurance Company
Contact Person:	Nick Almendarez
Telephone No.:	800-531-8722, ext. 8-2844
Email Address:	nick.almendarez@usaa.com
Effective Date:	2/22/2012

Homeowners Premium Comparision Survey Form
FORM HPCS - last modified August, 2005

USE THE APPROPRIATE FORM BELOW - IF NOT APPLICABLE, LEAVE BLANK

Submit to: *Arkansas Insurance Department*
1200 West Third Street
Little Rock, AR 72201-1904
Telephone: *501-371-2800*
Email as an attachment to: insurance.pnc@arkansas.gov
You may also attach to a SERFF filing or submit on a cdr disk

Survey Form for HO3 (Homeowners) - Use $500 Flat Deductible (Covers risk of direct physical loss for dwelling and other structures; named perils for personal property, replacement cost on dwelling, actual cash value on personal property)

Public Protection Class	Dwelling Value	Washington		Baxter		Craighead		St. Francis		Desha		Union		Miller		Sebastian		Pulaski	
		Brick	*Frame*	*Brick*	*Frame*	*Brick*	*Frame*	*Brick*	*Frame*	*Brick*	*Frame*	*Brick*	*Frame*	*Brick*	*Frame*	*Brick*	*Frame*	*Brick*	*Frame*
3	*$80,000*																		
	$120,000																		
	$160,000																		
6	*$80,000*																		
	$120,000																		
	$160,000																		
9	*$80,000*																		
	$120,000																		
	$160,000																		

Survey Form for HO4 (Renters) - Use $500 Flat Deductible (Named perils for personal property, actual cash value for loss, liability and medical payments for others included)

Public Protection Class	Property Value	Washington		Baxter		Craighead		St. Francis		Arkansas		Union		Miller		Sebastian		Pulaski	
		Brick	*Frame*	*Brick*	*Frame*	*Brick*	*Frame*	*Brick*	*Frame*	*Brick*	*Frame*	*Brick*	*Frame*	*Brick*	*Frame*	*Brick*	*Frame*	*Brick*	*Frame*
3	*$5,000*																		
	$15,000																		
	$25,000																		
6	*$5,000*																		
	$15,000																		
	$25,000																		
9	*$5,000*																		
	$15,000																		
	$25,000																		

Survey Form for DP-2 (Dwelling/Fire) - Use $500 Flat Deductible (Named perils for dwelling and personal property; replacement cost for dwelling, actual cash value for personal property, no liability coverage)

Public Protection Class	Dwelling Value	Washington		Baxter		Craighead		St. Francis		Arkansas		Union		Miller		Sebastian		Pulaski	
		Brick	*Frame*	*Brick*	*Frame*	*Brick*	*Frame*	*Brick*	*Frame*	*Brick*	*Frame*	*Brick*	*Frame*	*Brick*	*Frame*	*Brick*	*Frame*	*Brick*	*Frame*
3	*$80,000*	1137.55	1250.00	1137.55	1250.00	1137.55	1250.00	1137.55	1250.00	1137.55	1250.00	1137.55	1250.00	1137.55	1250.00	1137.55	1250.00	1137.55	1250.00
	$120,000	1633.33	1791.27	1633.33	1791.27	1633.33	1791.27	1633.33	1791.27	1633.33	1791.27	1633.33	1791.27	1633.33	1791.27	1633.33	1791.27	1633.33	1791.27
	$160,000	2129.12	2332.56	2129.12	2332.56	2129.12	2332.56	2129.12	2332.56	2129.12	2332.56	2129.12	2332.56	2129.12	2332.56	2129.12	2332.56	2129.12	2332.56
6	*$80,000*	1293.75	1416.89	1293.75	1416.89	1293.75	1416.89	1293.75	1416.89	1293.75	1416.89	1293.75	1416.89	1293.75	1416.89	1293.75	1416.89	1293.75	1416.89
	$120,000	1849.24	2025.82	1849.24	2025.82	1849.24	2025.82	1849.24	2025.82	1849.24	2025.82	1849.24	2025.82	1849.24	2025.82	1849.24	2025.82	1849.24	2025.82
	$160,000	2404.74	2634.77	2404.74	2634.77	2404.74	2634.77	2404.74	2634.77	2404.74	2634.77	2404.74	2634.77	2404.74	2634.77	2404.74	2634.77	2404.74	2634.77
9	*$80,000*	1712.78	2189.17	1712.78	2189.17	1712.78	2189.17	1712.78	2189.17	1712.78	2189.17	1712.78	2189.17	1712.78	2189.17	1712.78	2189.17	1712.78	2189.17
	$120,000	2435.78	3100.53	2435.78	3100.53	2435.78	3100.53	2435.78	3100.53	2435.78	3100.53	2435.78	3100.53	2435.78	3100.53	2435.78	3100.53	2435.78	3100.53
	$160,000	3158.77	4011.90	3158.77	4011.90	3158.77	4011.90	3158.77	4011.90	3158.77	4011.90	3158.77	4011.90	3158.77	4011.90	3158.77	4011.90	3158.77	4011.90

SPECIFY THE PERCENTAGE GIVEN FOR CREDITS OR DISCOUNTS FOR THE FOLLOWING:

HO3 and HO4 only

Fire Extinguisher	0	%	*Deadbolt Lock*	0	%
Burglar Alarm	2 to 15	%	*Window Locks*	0	%
Smoke Alarm	2 to 15	%	*$1,000 Deductible*	14 to 17	%
			Other (specify)		
					%
			Maximum Credit	varies	%

EARTHQUAKE INSURANCE

IMPORTANT, Homeowners insurance does NOT automatically cover losses from earthquakes. Ask your agent about this coverage.

ARE YOU CURRENTLY WRITING EARTHQUAKE COVERAGE IN ARKANSAS? Yes *(yes or no)*

WHAT IS YOUR PERCENTAGE DEDUCTIBLE? 10 %

	Zone	Brick	Frame
WHAT IS YOUR PRICE PER $1,000 OF COVERAGE?	Highest Risk	$ 1.99	$ 0.35
	Lowest Risk	$ 0.77	$ 0.81

NAIC Number:	18600
Company Name:	USAA General Indemnity Company
Contact Person:	Nick Almendarez
Telephone No.:	800-531-8722, ext. 8-2844
Email Address:	nick.almendarez@usaa.com
Effective Date:	2/22/2012

Homeowners Premium Comparision Survey Form
FORM HPCS - last modified August, 2005

USE THE APPROPRIATE FORM BELOW - IF NOT APPLICABLE, LEAVE BLANK

Submit to: *Arkansas Insurance Department*
1200 West Third Street
Little Rock, AR 72201-1904
Telephone: *501-371-2800*
Email as an attachment to: insurance.pnc@arkansas.gov
You may also attach to a SERFF filing or submit on a cdr disk

Survey Form for HO3 (Homeowners) - Use $500 Flat Deductible (Covers risk of direct physical loss for dwelling and other structures; named perils for personal property, replacement cost on dwelling, actual cash value on personal property)

Public Protection Class	Dwelling Value	Washington		Baxter		Craighead		St. Francis		Desha		Union		Miller		Sebastian		Pulaski	
		Brick	*Frame*	*Brick*	*Frame*	*Brick*	*Frame*	*Brick*	*Frame*	*Brick*	*Frame*	*Brick*	*Frame*	*Brick*	*Frame*	*Brick*	*Frame*	*Brick*	*Frame*
3	*$80,000*																		
	$120,000																		
	$160,000																		
6	*$80,000*																		
	$120,000																		
	$160,000																		
9	*$80,000*																		
	$120,000																		
	$160,000																		

Survey Form for HO4 (Renters) - Use $500 Flat Deductible (Named perils for personal property, actual cash value for loss, liability and medical payments for others included)

Public Protection Class	Property Value	Washington		Baxter		Craighead		St. Francis		Arkansas		Union		Miller		Sebastian		Pulaski	
		Brick	*Frame*	*Brick*	*Frame*	*Brick*	*Frame*	*Brick*	*Frame*	*Brick*	*Frame*	*Brick*	*Frame*	*Brick*	*Frame*	*Brick*	*Frame*	*Brick*	*Frame*
3	*$5,000*																		
	$15,000																		
	$25,000																		
6	*$5,000*																		
	$15,000																		
	$25,000																		
9	*$5,000*																		
	$15,000																		
	$25,000																		

Survey Form for DP-2 (Dwelling/Fire) - Use $500 Flat Deductible (Named perils for dwelling and personal property; replacement cost for dwelling, actual cash value for personal property, no liability coverage)

Public Protection Class	Dwelling Value	Washington		Baxter		Craighead		St. Francis		Arkansas		Union		Miller		Sebastian		Pulaski	
		Brick	*Frame*	*Brick*	*Frame*	*Brick*	*Frame*	*Brick*	*Frame*	*Brick*	*Frame*	*Brick*	*Frame*	*Brick*	*Frame*	*Brick*	*Frame*	*Brick*	*Frame*
3	*$80,000*	1137.55	1250.00	1137.55	1250.00	1137.55	1250.00	1137.55	1250.00	1137.55	1250.00	1137.55	1250.00	1137.55	1250.00	1137.55	1250.00	1137.55	1250.00
	$120,000	1633.33	1791.27	1633.33	1791.27	1633.33	1791.27	1633.33	1791.27	1633.33	1791.27	1633.33	1791.27	1633.33	1791.27	1633.33	1791.27	1633.33	1791.27
	$160,000	2129.12	2332.56	2129.12	2332.56	2129.12	2332.56	2129.12	2332.56	2129.12	2332.56	2129.12	2332.56	2129.12	2332.56	2129.12	2332.56	2129.12	2332.56
6	*$80,000*	1293.75	1416.89	1293.75	1416.89	1293.75	1416.89	1293.75	1416.89	1293.75	1416.89	1293.75	1416.89	1293.75	1416.89	1293.75	1416.89	1293.75	1416.89
	$120,000	1849.24	2025.82	1849.24	2025.82	1849.24	2025.82	1849.24	2025.82	1849.24	2025.82	1849.24	2025.82	1849.24	2025.82	1849.24	2025.82	1849.24	2025.82
	$160,000	2404.74	2634.77	2404.74	2634.77	2404.74	2634.77	2404.74	2634.77	2404.74	2634.77	2404.74	2634.77	2404.74	2634.77	2404.74	2634.77	2404.74	2634.77
9	*$80,000*	1712.78	2189.17	1712.78	2189.17	1712.78	2189.17	1712.78	2189.17	1712.78	2189.17	1712.78	2189.17	1712.78	2189.17	1712.78	2189.17	1712.78	2189.17
	$120,000	2435.78	3100.53	2435.78	3100.53	2435.78	3100.53	2435.78	3100.53	2435.78	3100.53	2435.78	3100.53	2435.78	3100.53	2435.78	3100.53	2435.78	3100.53
	$160,000	3158.77	4011.90	3158.77	4011.90	3158.77	4011.90	3158.77	4011.90	3158.77	4011.90	3158.77	4011.90	3158.77	4011.90	3158.77	4011.90	3158.77	4011.90

SPECIFY THE PERCENTAGE GIVEN FOR CREDITS OR DISCOUNTS FOR THE FOLLOWING:

HO3 and HO4 only

Fire Extinguisher	0	%	*Deadbolt Lock*	0	%
Burglar Alarm	2 to 15	%	*Window Locks*	0	%
Smoke Alarm	2 to 15	%	*$1,000 Deductible*	14 to 17	%
			Other (specify)		
					%
			Maximum Credit	varies	%

EARTHQUAKE INSURANCE

IMPORTANT, Homeowners insurance does NOT automatically cover losses from earthquakes. Ask your agent about this coverage.

ARE YOU CURRENTLY WRITING EARTHQUAKE COVERAGE IN ARKANSAS? Yes *(yes or no)*

WHAT IS YOUR PERCENTAGE DEDUCTIBLE? 10 %

	Zone	Brick	Frame
WHAT IS YOUR PRICE PER $1,000 OF COVERAGE?	Highest Risk	$ 1.99	$ 0.35
	Lowest Risk	$ 0.77	$ 0.81

NAIC Number:	21253
Company Name:	Garrison Property and Casualty Insurance Company
Contact Person:	Nick Almendarez
Telephone No.:	800-531-8722, ext. 8-2844
Email Address:	nick.almendarez@usaa.com
Effective Date:	2/22/2012

Homeowners Premium Comparision Survey Form
FORM HPCS - last modified August, 2005

USE THE APPROPRIATE FORM BELOW - IF NOT APPLICABLE, LEAVE BLANK

Submit to: *Arkansas Insurance Department*
1200 West Third Street
Little Rock, AR 72201-1904
Telephone: *501-371-2800*
Email as an attachment to: insurance.pnc@arkansas.gov
You may also attach to a SERFF filing or submit on a cdr disk

Survey Form for HO3 (Homeowners) - Use $500 Flat Deductible (Covers risk of direct physical loss for dwelling and other structures; named perils for personal property, replacement cost on dwelling, actual cash value on personal property)

Public Protection Class	Dwelling Value	Washington		Baxter		Craighead		St. Francis		Desha		Union		Miller		Sebastian		Pulaski	
		Brick	*Frame*	*Brick*	*Frame*	*Brick*	*Frame*	*Brick*	*Frame*	*Brick*	*Frame*	*Brick*	*Frame*	*Brick*	*Frame*	*Brick*	*Frame*	*Brick*	*Frame*
3	*$80,000*																		
	$120,000																		
	$160,000																		
6	*$80,000*																		
	$120,000																		
	$160,000																		
9	*$80,000*																		
	$120,000																		
	$160,000																		

Survey Form for HO4 (Renters) - Use $500 Flat Deductible (Named perils for personal property, actual cash value for loss, liability and medical payments for others included)

Public Protection Class	Property Value	Washington		Baxter		Craighead		St. Francis		Arkansas		Union		Miller		Sebastian		Pulaski	
		Brick	*Frame*	*Brick*	*Frame*	*Brick*	*Frame*	*Brick*	*Frame*	*Brick*	*Frame*	*Brick*	*Frame*	*Brick*	*Frame*	*Brick*	*Frame*	*Brick*	*Frame*
3	*$5,000*																		
	$15,000																		
	$25,000																		
6	*$5,000*																		
	$15,000																		
	$25,000																		
9	*$5,000*																		
	$15,000																		
	$25,000																		

Survey Form for DP-2 (Dwelling/Fire) - Use $500 Flat Deductible (Named perils for dwelling and personal property; replacement cost for dwelling, actual cash value for personal property, no liability coverage)

Public Protection Class	Dwelling Value	Washington		Baxter		Craighead		St. Francis		Arkansas		Union		Miller		Sebastian		Pulaski	
		Brick	*Frame*	*Brick*	*Frame*	*Brick*	*Frame*	*Brick*	*Frame*	*Brick*	*Frame*	*Brick*	*Frame*	*Brick*	*Frame*	*Brick*	*Frame*	*Brick*	*Frame*
3	*$80,000*	1137.55	1250.00	1137.55	1250.00	1137.55	1250.00	1137.55	1250.00	1137.55	1250.00	1137.55	1250.00	1137.55	1250.00	1137.55	1250.00	1137.55	1250.00
	$120,000	1633.33	1791.27	1633.33	1791.27	1633.33	1791.27	1633.33	1791.27	1633.33	1791.27	1633.33	1791.27	1633.33	1791.27	1633.33	1791.27	1633.33	1791.27
	$160,000	2129.12	2332.56	2129.12	2332.56	2129.12	2332.56	2129.12	2332.56	2129.12	2332.56	2129.12	2332.56	2129.12	2332.56	2129.12	2332.56	2129.12	2332.56
6	*$80,000*	1293.75	1416.89	1293.75	1416.89	1293.75	1416.89	1293.75	1416.89	1293.75	1416.89	1293.75	1416.89	1293.75	1416.89	1293.75	1416.89	1293.75	1416.89
	$120,000	1849.24	2025.82	1849.24	2025.82	1849.24	2025.82	1849.24	2025.82	1849.24	2025.82	1849.24	2025.82	1849.24	2025.82	1849.24	2025.82	1849.24	2025.82
	$160,000	2404.74	2634.77	2404.74	2634.77	2404.74	2634.77	2404.74	2634.77	2404.74	2634.77	2404.74	2634.77	2404.74	2634.77	2404.74	2634.77	2404.74	2634.77
9	*$80,000*	1712.78	2189.17	1712.78	2189.17	1712.78	2189.17	1712.78	2189.17	1712.78	2189.17	1712.78	2189.17	1712.78	2189.17	1712.78	2189.17	1712.78	2189.17
	$120,000	2435.78	3100.53	2435.78	3100.53	2435.78	3100.53	2435.78	3100.53	2435.78	3100.53	2435.78	3100.53	2435.78	3100.53	2435.78	3100.53	2435.78	3100.53
	$160,000	3158.77	4011.90	3158.77	4011.90	3158.77	4011.90	3158.77	4011.90	3158.77	4011.90	3158.77	4011.90	3158.77	4011.90	3158.77	4011.90	3158.77	4011.90

SPECIFY THE PERCENTAGE GIVEN FOR CREDITS OR DISCOUNTS FOR THE FOLLOWING:

HO3 and HO4 only

Fire Extinguisher	0	%	*Deadbolt Lock*	0	%
Burglar Alarm	2 to 15	%	*Window Locks*	0	%
Smoke Alarm	2 to 15	%	*$1,000 Deductible*	14 to 17	%
			Other (specify)		
					%
			Maximum Credit	varies	%

EARTHQUAKE INSURANCE

IMPORTANT, Homeowners insurance does NOT automatically cover losses from earthquakes. Ask your agent about this coverage.

ARE YOU CURRENTLY WRITING EARTHQUAKE COVERAGE IN ARKANSAS? Yes *(yes or no)*

WHAT IS YOUR PERCENTAGE DEDUCTIBLE? 10 %

	Zone	Brick	Frame
WHAT IS YOUR PRICE PER $1,000 OF COVERAGE?	Highest Risk	$ 1.99	$ 0.35
	Lowest Risk	$ 0.77	$ 0.81

USAA Group
Arkansas
Fire and Allied Lines Filing Memorandum (Revised)

USAA Group (USAA, USAA-CIC, USAA-GIC, and Garrison) wishes to revise our Fire and Allied Lines program with an overall effect of 13.1%. The effects by form apply as follows:

USAA Fire	5.0%
USAA Allied Lines	20.0%
USAA Misc	0.0%
USAA Combined	13.0%

USAA-CIC Fire	5.0%
USAA-CIC Allied Lines	19.9%
USAA-CIC Misc	0.0%
USAA-CIC Combined	13.4%

USAA-GIC Fire	5.0%
USAA-GIC Allied Lines	19.9%
USAA-GIC Misc	0.0%
USAA-GIC Combined	13.4%

Garrison Fire	5.0%
Garrison Allied Lines	19.9%
Garrison Misc	0.0%
Garrison Combined	13.4%

USAA Group Combined	13.1%

The proposed changes include revising the Fire and Allied Lines Base Rates. The attached exhibits support these revisions.

An effective date of February 8, 2012 for these revisions will apply to all policies. Details of these revisions are attached.

USAA Group
Arkansas
Fire and Allied Lines Filing Memorandum (Revised)

Attachments in support of this filing:

Explanatory Memo-Fire (Revised)

Exhibit I-Fire	Indicated Rate Change
Exhibit II-Fire	Premium Trend
Exhibit III-Fire	Large Loss Adjustment
Exhibit IV-Fire	Loss Development
Exhibit V-Fire	Loss Trend
Exhibit VI-Fire	Loss Adjustment Expense (LAE)
Exhibit VII-Fire (Revised)	Expected Net Fire Following Earthquake Loss and LAE Ratio
Exhibit VIII-Fire	Expenses
Exhibit IX-Fire	Underwriting Profit Provision
Exhibit A	2011 Loss Ratio
	The AIR Earthquake Model for the United States

Explanatory Memo-Allied Lines (Revised)

Exhibit I-Allied Lines (Revised)	Indicated Rate Change
Exhibit II-Allied Lines	Premium Trend
Exhibit III-Allied Lines	Large Loss Adjustment
Exhibit IV-Allied Lines	Loss Development
Exhibit V-Allied Lines	Loss Trend
Exhibit VI-Allied Lines (Revised)	Loss Adjustment Expense (LAE)
Exhibit VII-Allied Lines	*Withdrawn*

USAA Group
Arkansas
Fire and Allied Lines Filing Memorandum (Revised)

Exhibit VIII-Allied Lines	*Withdrawn*
Exhibit IX-Allied Lines	*Withdrawn*
Exhibit X-Allied Lines	Expenses
Exhibit XI-Allied Lines	Underwriting Profit Provision
Exhibit XII-Allied Lines	Expected Catastrophe Loss and LAE Ratio

USAA Group
Arkansas
Explanatory Memorandum (Revised)
Fire

The attached exhibits are in support of the Fire Rate revision in Arkansas with a proposed effective date of 02/08/2012. Exhibits I-Fire through IX-Fire develop the rate level indication.

Exhibit I-Fire - illustrates USAA Group's Arkansas experience for the latest five accident years ending March 31, 2011 as of June 30, 2011. The indicated rate level change is developed in this exhibit. The proposed change is also provided. A large loss procedure was applied to the losses, which is detailed in Exhibit III-Fire.

Exhibit II-Fire - provides the calculation of the premium trend factors to reflect increasing amounts of insurance, as well as all other distributional changes. The selected factors are based on USAA Group Arkansas data. The current amount factors are based on actual trend to current in average earned premium at present rates (EPPR). The trended amount factor was selected based on the change in annual average EPPR. The data was fitted to an exponential curve.

Exhibit III-Fire - shows the 10-year smoothing technique USAA uses to reflect the excess loss potential in Arkansas. The Large Loss Adjustment establishes an excess loss cut-off as a percentage of the average amount of insurance written for each year. The procedure then removes the portion of developed loss in excess of the cut-off, ratios the excess losses to the developed non-excess (normal) losses, and selects a weighted average of this ratio as the excess loss factor.

Exhibit IV-Fire - displays the calculation of USAA Group loss development factors for Arkansas. Loss data used for these calculations excludes catastrophes.

Exhibit V-Fire - shows the loss trend underlying the rate level indication. Various exponential fits including 20-, 16-, 12-, 8-, and 4-points are shown. The selected current cost factor (CCF) and trended cost factor (TCF) are based on the results of these exponential fits. (Due to the volatility and lack of credibility in Arkansas, the selected Arkansas loss trend was credibility weighted with USAA countrywide loss trend data excluding CA, FL & TX.) The Arkansas credibility-weighted current cost factor and trended cost factor are displayed on Page 2.

Exhibit VI-Fire - develops the loss adjustment expense (LAE) factor used in calculating the indication in Exhibit I-Fire. The factor is based upon USAA countrywide data for calendar-accident years 2007, 2008, and 2009.

Exhibit VII-Fire (Revised) - displays the expected fire following earthquake catastrophe loss and LAE ratio calculation based on a fire following earthquake simulation model developed by AIR Worldwide (AIR), Inc., of Boston, Massachusetts. AIR's Catastrophe Loss Analysis Service models fire following earthquake based on geological, engineering, and property damage data. The models estimate damage by five digit ZIP

code based on various earthquake causative characteristics, including ignition, population, and fire suppression ability. The model generates a large sample of simulated events which are then superimposed on USAA's geographical distribution of exposures by county and ZIP code within the state. USAA uses the statewide estimated average annual loss provided by AIR in calculating the overall indication.

Exhibit VIII-Fire - shows the development of the variable permissible loss and LAE ratio for Arkansas on Page 1. Provisions for other expense categories are based on countrywide data from the Insurance Expense Exhibit while taxes, licenses, and fees are based upon actual Arkansas experience for USAA Group. The calculation of the selected annual expense trend is shown on Page 2. The trend is derived by taking a weighted average of the Employment Cost Index and the Consumer Price Index. The expense trend is used to trend fixed expenses, which are used to develop the indication shown in Exhibit I-Fire.

Exhibit IX-Fire - details USAA Group's method for selecting its underwriting profit and contingency provision, which is included in the permissible loss ratio. A separate explanatory memorandum is included with the exhibit.

USAA Group
Arkansas
Indicated Rate Change
Fire Forms
As of 06/30/2011

Calendar/ Accident Year Ending (1)	Earned Premium at Present Rates (2)	Premium Trend Factor [A] (3)	Prospective Earned Premium at Present Rates (4) = (2) * (3)	Smoothed Developed Incurred Losses Excluding Catastrophes [B] (5)	Loss Trend Factor [C] (6)	LAE Factor [D] (7)	Prospective Incurred Losses and LAE Excluding Catastrophes (8) = (5) * (6) * (7)	Prospective Loss and LAE Ratio Excluding Catastrophes (9) = (8) / (4)	Weight (10)
03/31/2007	$583,866	1.211	$707,062	$151,658	0.791	1.120	$134,357	0.190	0.100
03/31/2008	644,873	1.167	752,567	1,023,672	0.823	1.120	943,580	1.254	0.150
03/31/2009	696,052	1.175	817,861	413,990	0.857	1.120	397,364	0.486	0.200
03/31/2010	813,131	1.104	897,697	1,017,170	0.893	1.120	1,017,333	1.133	0.250
03/31/2011	925,208	1.072	991,823	890,541	0.931	1.120	928,585	0.936	0.300

Five Year Weighted Loss and LAE Ratio Excluding Catastrophes =		0.868
Fire Following Earthquake Catastrophe Loss and LAE Ratio [E] =		0.007
Trended Fixed Expense Ratio [F] =		0.117
Variable Permissible Loss and LAE Ratio [G] =		0.825
Indicated Rate Level Change =	(.868+ 0.007 + 0.117) / 0.825 - 1	20.2%
Proposed Rate Level Change =		5.0%

[A] Developed in Exhibit II-Fire
[B] Developed in Exhibit III-Fire
[C] Developed in Exhibit V-Fire , Page 2 of 2
[D] Developed in Exhibit VI-Fire
[E] Developed in Exhibit VII-Fire
[F] Developed in Exhibit VIII-Fire, Page 2 of 2
[G] Developed in Exhibit VIII-Fire, Page 1 of 2

USAA Group
Arkansas
Premium Trend
Fire Forms

Year Ending Quarter (1)	Total Earned Premium at Present Rates (2)	Earned Exposures (3)	Average Earned Premium at Present Rates (4)	Annual Change (5)	Current Amount Factors 295.50 / (4)
2006/2	562,095.27	2,161.00	260.11		1.136
2006/3	569,140.10	2,188.00	260.12		1.136
2006/4	574,664.22	2,213.00	259.68		1.138
2007/1	583,866.26	2,233.00	261.47		1.130
2007/2	596,346.40	2,265.00	263.29	1.2%	1.122
2007/3	613,543.29	2,314.00	265.14	1.9%	1.115
2007/4	630,740.88	2,358.00	267.49	3.0%	1.105
2008/1	644,872.61	2,376.00	271.41	3.8%	1.089
2008/2	658,333.13	2,401.00	274.19	4.1%	1.078
2008/3	670,917.80	2,445.00	274.40	3.5%	1.077
2008/4	690,319.10	2,515.00	274.48	2.6%	1.077
2009/1	696,051.59	2,581.00	269.68	-0.6%	1.096
2009/2	718,912.29	2,654.00	270.88	-1.2%	1.091
2009/3	742,430.83	2,729.00	272.05	-0.9%	1.086
2009/4	774,900.39	2,798.00	276.95	0.9%	1.067
2010/1	813,131.22	2,834.00	286.92	6.4%	1.030
2010/2	834,404.32	2,894.00	288.32	6.4%	1.025
2010/3	862,465.85	2,961.00	291.28	7.1%	1.014
2010/4	885,576.58	3,051.00	290.26	4.8%	1.018
2011/1	925,207.57	3,131.00	295.50	3.0%	1.000

Trended Amount Factor:

Least Squares Results

Exponential Fits	20 pt	16 pt	12 pt	8 pt	4 pt
Annualized Change:	2.6%	2.8%	3.2%	5.3%	2.9%
R-squared Value:	0.891	0.836	0.757	0.912	0.764
Selected Annual Trend Factor:	1.030				

Premium Trend Factor

Accident Year Ending	Current Amount Factors (1)	Trended Amount Selection (2)	Trended Amount Period [A] (3)	Trended Amount Factors (4) = (2) ^ (3)	Premium Trend Factors (5) = (1) * (4)
03/31/2007	1.130	1.030	2.360	1.072	1.211
03/31/2008	1.089	1.030	2.360	1.072	1.167
03/31/2009	1.096	1.030	2.360	1.072	1.175
03/31/2010	1.030	1.030	2.360	1.072	1.104
03/31/2011	1.000	1.030	2.360	1.072	1.072

[A] From the average earned date in the most recent accident year, 09/30/2010, to the average earned date in the effective period, 02/08/2013

USAA Group
Arkansas
Large Loss Adjustment
Fire Forms
As of 06/30/2011

Calendar/ Accident Year Ending (1)	Average Amount of Insurance (2)	Cutoff 25% of (2) (3)	Incurred Losses Excluding Catastrophes (4)	Loss Development Factors (5)[A]	Developed Losses Excluding Catastrophes (6)	Number of Excess Losses (7)	Large Losses (8)	Excess Losses (9) = (8) - (7) * (3)	Normal Losses (10) = (6) - (9)	Excess Ratio (11) = (9) / (10)	Smoothed Developed Incurred Losses Ex Cats (12)[C]
03/31/2002	$102,390	$25,598	$148,568	1.0000	$148,568	3	$132,551	$55,757	$92,811	0.601	$190,912
03/31/2003	104,958	$26,240	43,975	1.0000	$43,975	0	$0	0	43,975	0.000	$90,457
03/31/2004	118,403	$29,601	228,828	1.0000	$228,828	3	$192,297	103,494	125,334	0.826	$257,812
03/31/2005	133,866	$33,467	39,848	1.0000	$39,848	0	$0	0	39,848	0.000	$81,967
03/31/2006	143,875	$35,969	287,165	1.0000	$287,165	3	$270,394	162,487	124,678	1.303	$256,463
03/31/2007	151,060	$37,765	171,876	1.0000	$171,876	1	$135,913	98,148	73,728	1.331	$151,658
03/31/2008	160,900	$40,225	1,015,172	1.0000	$1,015,172	8	$839,319	517,519	497,653	1.040	$1,023,672
03/31/2009	165,380	$41,345	634,221	1.0000	$634,221	4	$598,342	432,962	201,259	2.151	$413,990
03/31/2010	174,666	$43,667	1,066,657	1.0000	$1,066,657	9	$965,168	572,165	494,492	1.157	$1,017,170
03/31/2011	182,031	$45,508	734,702	1.0051	$738,449	7	$624,073	305,517	432,932	0.706	$890,541
								$2,248,049	$2,126,710		

Weighted Average Excess Ratio [B] = 1.057

Weighted Average Excess Factor = 2.057

[A] Developed in Exhibit IV-Fire

[B] Weighted Average Excess Ratio = Sum of Column (9) / Sum of Column (10)

[C] (12) = (10) * Weighted Average Excess Factor

USAA Group
Arkansas
Loss Development
Incurred Losses Excluding Catastrophes
Fire Forms

Accident Year Ending	15 months	27 months	39 months	51 months	63 months
03/31/2002					148,568
03/31/2003				43,975	43,975
03/31/2004			228,828	228,828	228,828
03/31/2005		39,848	39,848	39,848	39,848
03/31/2006	287,165	287,165	287,165	287,165	287,165
03/31/2007	197,936	171,876	171,876	171,876	171,876
03/31/2008	1,021,991	1,037,758	1,015,172	1,015,172	
03/31/2009	634,221	634,221	634,221		
03/31/2010	1,010,651	1,066,657			
03/31/2011	734,702				

Age-to-Age Factors

Accident Year Ending	15 to 27 Months	27 to 39 Months	39 to 51 Months	51 to 63 Months
03/31/2002				
03/31/2003				1.0000
03/31/2004			1.0000	1.0000
03/31/2005		1.0000	1.0000	1.0000
03/31/2006	1.0000	1.0000	1.0000	1.0000
03/31/2007	0.8683	1.0000	1.0000	1.0000
03/31/2008	1.0154	0.9782	1.0000	
03/31/2009	1.0000	1.0000		
03/31/2010	1.0554			
Latest 3-year Average	1.0236	0.9927	1.0000	1.0000
Latest 4-year Average	0.9848	0.9946	1.0000	1.0000
Latest 5-year Average	0.9878	0.9956	1.0000	1.0000
Latest 3-out-of-5-year Average	1.0051	1.0000	1.0000	1.0000
Selected Age-to-Age Factors	1.0051	1.0000	1.0000	1.0000

Cumulative Factors [A]

	15 to Ultimate	27 to Ultimate	39 to Ultimate	51 to 63 Months
Selected Cumulative Factors	1.0051	1.0000	1.0000	1.0000

[A] Cumulative factors are adjusted to ultimate with a factor of 1.0000

USAA Group
Arkansas
USAA Group CW Excl CA, FL, & TX
Fire Forms

	Calendar Year Paid Frequency				Calendar Year Paid Severity				Calendar Year Paid Pure Premium			
Year Ending Quarter	Series 1 [A]	Annual Change	Series 2 [B]	Annual Change	Series 1 [A]	Annual Change	Series 2 [B]	Annual Change	Series 1 [A]	Annual Change	Series 2 [B]	Annual Change
2006/3	0.0027		0.0035		76,714		30,361		210.37		106.86	
2006/4	0.0014		0.0037		123,270		30,583		167.11		111.75	
2007/1	0.0009		0.0038		87,326		28,797		78.21		110.43	
2007/2	0.0040		0.0037		28,013		30,351		111.31		113.60	
2007/3	0.0065	136.4%	0.0038	7.0%	33,874	-55.8%	32,630	7.5%	219.58	4.4%	122.92	15.0%
2007/4	0.0085	525.7%	0.0039	5.9%	37,662	-69.4%	30,740	0.5%	319.44	91.2%	118.99	6.5%
2008/1	0.0114	1168.8%	0.0040	3.1%	35,876	-58.9%	33,091	14.9%	407.69	421.3%	130.87	18.5%
2008/2	0.0125	214.5%	0.0041	9.4%	29,612	5.7%	31,818	4.8%	369.99	232.4%	130.25	14.7%
2008/3	0.0127	95.6%	0.0042	11.4%	33,876	0.0%	29,950	-8.2%	429.51	95.6%	125.72	2.3%
2008/4	0.0119	40.6%	0.0041	5.8%	27,626	-26.6%	30,043	-2.3%	329.53	3.2%	123.06	3.4%
2009/1	0.0101	-11.4%	0.0040	0.4%	26,258	-26.8%	30,092	-9.1%	264.51	-35.1%	119.47	-8.7%
2009/2	0.0060	-51.8%	0.0040	-1.9%	34,402	16.2%	27,891	-12.3%	207.40	-43.9%	112.05	-14.0%
2009/3	0.0066	-48.0%	0.0039	-6.3%	21,452	-36.7%	28,983	-3.2%	141.49	-67.1%	113.93	-9.4%
2009/4	0.0068	-43.1%	0.0037	-8.7%	31,181	12.9%	29,958	-0.3%	211.74	-35.7%	112.00	-9.0%
2010/1	0.0081	-19.4%	0.0040	-0.5%	38,138	45.2%	27,443	-8.8%	309.52	17.0%	108.40	-9.3%
2010/2	0.0100	66.2%	0.0039	-3.5%	34,409	0.0%	26,076	-6.5%	344.80	66.2%	101.12	-9.8%
2010/3	0.0088	33.1%	0.0042	7.1%	38,241	78.3%	24,143	-16.7%	335.79	137.3%	101.69	-10.7%
2010/4	0.0088	30.3%	0.0045	20.1%	31,696	1.7%	21,744	-27.4%	280.50	32.5%	97.60	-12.9%
2011/1	0.0073	-9.5%	0.0045	13.5%	31,819	-16.6%	22,951	-16.4%	233.74	-24.5%	102.87	-5.1%
2011/2	0.0081	-19.5%	0.0047	20.3%	41,380	20.3%	22,818	-12.5%	333.81	-3.2%	106.47	5.3%
Exponential Fits	R-squared Value	Annualized Change	R-squared Value	Annualized Change	R-squared Value	Annualized Change	R-squared Value	Annualized Change	R-squared Value	Annualized Change	R-squared Value	Annualized Change
20-point fit	0.190	30.7%	0.595	3.8%	0.286	-13.5%	0.652	-6.5%	0.117	13.1%	0.256	-2.9%
16-point fit	0.099	-5.3%	0.415	3.5%	0.031	2.1%	0.868	-9.9%	0.032	-3.3%	0.779	-6.7%
12-point fit	0.207	-9.2%	0.351	4.4%	0.256	10.2%	0.835	-11.6%	0.005	0.0%	0.799	-7.7%
8-point fit	0.127	9.6%	0.845	13.0%	0.365	22.4%	0.856	-16.5%	0.300	34.2%	0.444	-5.6%
4-point fit	0.445	-16.2%	0.873	13.0%	0.065	10.1%	0.133	-4.5%	0.019	-7.7%	0.480	7.9%

[A] Series 1 is based on USAA Group Arkansas data

[B] Series 2 is based on USAA Group CW Excl CA, FL, & TX data

USAA Group
Arkansas
USAA Group CW Excl CA, FL, & TX
Fire Forms

	Series 1 Frequency[A]	Series 2 Frequency[B]	Cred-Weighted Frequency[C]	Series 1 Severity[A]	Series 2 Severity[B]	Cred-Weighted Severity[C]	Cred-Weighted Pure Premium
Current Cost Selection	1.000	1.040	1.038	1.030	0.920	0.925	0.96
Trended Cost Selection	1.000	1.070	1.067	1.100	0.900	0.910	0.971

Loss Trend Factor

Accident Year Ending	Current Cost Selection (1)	Current Cost Period[D] (2)	Current Cost Factor (3) = (1) ^ (2)	Trended Cost Selection (4)	Trended Cost Period[E] (5)	Trended Cost Factor (6) = (4) ^ (5)	Loss Trend Factor (7) = (3) * (6)
03/31/2007	0.960	4.250	0.841	0.971	2.110	0.940	0.791
03/31/2008	0.960	3.250	0.876	0.971	2.110	0.940	0.823
03/31/2009	0.960	2.250	0.912	0.971	2.110	0.940	0.857
03/31/2010	0.960	1.250	0.950	0.971	2.110	0.940	0.893
03/31/2011	0.960	0.250	0.990	0.971	2.110	0.940	0.931

[A] Series 1 is based on USAA Group Arkansas data

[B] Series 2 is based on USAA Group CW Excl CA, FL, & TX data

[C] USAA Group Arkansas is 4.9% credible based on 26 claims; used the Square Root method with a full credibility standard of 10,623 claims.

[D] From the average date of loss in the respective accident year to 12/31/2010

[E] From 12/31/2010 to the average date of loss in the effective period, 02/08/2013

USAA Group
Countrywide
Loss Adjustment Expense (LAE) Factor
All Forms Combined
As of 6/30/2010

Non-Catastrophe Loss Adjustment Expense Factor

Calendar/Accident Year Ending	Incurred Losses	Loss Adjustment Expense	LAE Ratio
12/31/2007	90,452,699	10,382,432	0.115
12/31/2008	91,517,758	11,240,055	0.123
12/31/2009	108,159,666	13,712,416	0.127
Average LAE Ratio			0.122
Selected Non-Catastrophe LAE Factor			1.120

USAA Group

Arkansas

Expected Net Fire Following Earthquake Loss and LAE Ratio

Fire Forms

(1a) Expected Annual Gross Fire Following Cat Losses	$5,503
(1b) Expected Recoveries	$4,088
(1c) Ceded Premium	$6,794
(1) Expected Annual Net Fire Following Earthquake Cat Loss	$6,598
(2) Prospective Earned Premium at Present Rates	$991,823
(3) Fire Following Earthquake Catastrophe Loss and LAE Ratio (1) / (2)	0.007
Selected Fire Following Earthquake Catastrophe Loss and LAE Ratio	0.007

[A] Based on Applied Insurance Research, Inc. (AIR) methodology and assumptions; net losses are based on exposure levels as of 05/31/2010 and trended for loss severity

USAA Group
Arkansas
Fixed and Variable Expense Provisions
Fire Forms

	2009	2010	2-Year Straight Average	Selected
(1) Average General Expenses Per Earned Exposure [A]	$4.18	$3.54		
(2) Selected Annual Expense Trend [B]	2.0%	2.0%		
(3) Trend Period [C]	3.61	2.61		
(4) Projected Average General Expenses Per Earned Exposure (1) * [1.02] ^ (3)	$4.49	$3.73	$4.11	$4.11
(5) Average Other Acquisition Expense Per Written Exposure [A]	$28.03	$32.06		
(6) Selected Annual Expense Trend [B]	2.0%	2.0%		
(7) Trend Period [D]	3.11	2.11		
(8) Projected Average Other Acquisition Expense Per Written Exposure (5) * [1.02] ^ (7)	$29.81	$33.43	$31.62	$31.62
(9) Average Licenses and Fees Expense Per Written Exposure [E]	$1.43	$0.72		
(10) Selected Annual Expense Trend [B]	2.0%	2.0%		
(11) Trend Period [D]	3.11	2.11		
(12) Projected Average Licenses and Fees Expense Per Written Exposure (9) * [1.02] ^ (11)	$1.52	$0.75	$1.14	$1.14
(13) Total Fixed Expense (4) + (8) + (12)				$36.87
(14) Average Projected Premium at Present Rates [F]				$316.27
(15) Projected Fixed Expense Provision (13) / (14)				0.117
(16) Commission and Brokerage	0.0%	0.0%	0.0%	0.0%
(17) Taxes [G]	2.4%	2.5%	2.5%	2.5%
(18) Profit and Contingencies Provision [H]				15.0%
(19) Total Variable Expenses (16) + (17) + (18)				17.5%
(20) Variable Permissible Loss and LAE Ratio 1 - (19)				82.5%

[A] USAA Group Countrywide data
[B] Developed in Exhibit VIII-Fire, Page 2 of 2
[C] From the midpoint of the respective year to the average earned date in effective period, 02/08/2013
[D] From the midpoint of the respective year to the average written date in effective period, 08/08/2012
[E] Arkansas USAA Group data
[F] Arkansas USAA Group data for Fire Forms only
[G] Arkansas USAA Group data as a percent of direct written premium
[H] Developed in Exhibit IX-Fire

USAA Group
Countrywide
Calculation of Annual Expense Trend

(1)	Employment Cost Index - Financial activities, excluding incentive paid occupations (annual change over latest 2 years ending 03/31/2011) U.S. Department of Labor	2.1%
(2)	% of Total Acquisition and General Expenses used for Salaries and Employee Relations & Welfare - USAA Group Insurance Expense Exhibit, 2010	54.4%
(3)	Consumer Price Index, All Items - (annual change over latest 2 year ending 03/31/2011)	2.5%
(4)	Annual Expense Trend - { (1) * (2) } + { (3) * [1 - (2)] }	2.3%
Selected Annual Expense Trend		2.0%

USAA GROUP
ARKANSAS FIRE
UNDERWRITING PROFIT PROVISION
EXPLANATORY MEMORANDUM

This exhibit is submitted in support of the underwriting profit and contingency provision included in the permissible loss ratio.

UNDERWRITING PROFIT PROVISION

The target underwriting profit and contingency provision needed to achieve our desired overall profit level is developed on Page 2. The selected target rate of return is 10.0% on GAAP (generally accepted accounting principles) equity.

The target underwriting return on an after-tax basis is derived by subtracting the after-tax investment rate of return on GAAP surplus from the target rate of return. This target underwriting rate of return is then adjusted to a before-tax basis, using the current corporate tax rate of 35.0%, and then divided by the premium-to-surplus ratio to yield the target underwriting profit and contingency provision.

TARGET RATE OF RETURN

Results from the Capital Asset Pricing Model (CAPM), commonly used in evaluating investments, suggest a required rate of return around 8.0%. Historically, the CAPM has consistently supported a 10.0% rate of return. However, the unusually poor market performance in recent years has impacted the results. We still believe 10.0% is a reasonable rate of return and is consistent with our historical selection.

The data points used in the CAPM method are published historical values from Value Line, Inc.'s *Investment Survey* (as of 7/30/10) and from Ibbotson Associates' 2010 Stocks, Bonds, Bills & Inflation (SBBI) Yearbook. The companies composing the "P&C Insurance Industry", as identified by Value Line, Inc., were selected to determine the appropriate rate of return for a P&C company.

INVESTMENT RATE OF RETURN

The investment rate of return is determined by dividing the estimated investment earnings by the Countrywide Fire allocation of USAA Group surplus. The estimated investment earnings are calculated by applying a selected after-tax rate of return to the total funds subject to investment.

The selected after-tax rate of return is a weighted average after-tax return, using the projected proportion of the portfolio held in each component as weight. The composition of the portfolio is projected for 2011 and 2012 and an after-tax return for each year is calculated.

USAA GROUP
ARKANSAS FIRE
UNDERWRITING PROFIT PROVISION

A.	Target Rate of Return (% of GAAP Surplus)		
	1.	Capital Asset Pricing Model	8.0%
	2.	Selected Target Rate of Return	10.0%
B.	Target Underwriting Rate of Return (% of GAAP Surplus)		
	1.	Investment Rate of Return After Tax	1.9%
	2.	Target Underwriting Return After Tax (A2) - (B1)	8.1%
	3.	Target Underwriting Return Before Tax (B2) / (1.00 - 0.35)	12.5%
C.	Target Underwriting Profit Provision (% of Direct Earned Premium)		
	1.	Direct Written Premium / GAAP Surplus Ratio	0.661
	2.	Indicated Underwriting Profit Provision (B3) / (C1)	18.9%
	3.	Selected Underwriting Profit Provision	15.0%

USAA GROUP
ARKANSAS
LOSS RATIOS AS OF 6/30/2011

	Calendar Year Losses Incurred	Calendar Year Premiums Earned	Loss Ratio
Fire	790,148	460,955	171.4%
Allied Lines	1,410,985	744,722	189.5%
Total	2,201,133	1,205,677	182.6%

USAA Group
Arkansas
Explanatory Memorandum (Revised)
Allied Lines

The attached exhibits are in support of the Allied Lines Rate revision in Arkansas with a proposed effective date of 02/08/2012. Exhibits I-Allied Lines through XI-Allied Lines develop the rate level indication.

Exhibit I-Allied Lines (Revised) - illustrates USAA Group Arkansas experience for the latest five accident years ending March 31, 2011 as of June 30, 2011. The indicated rate level change is developed in this exhibit. The proposed change is also provided. A large loss procedure was applied to the losses, which is detailed in Exhibit III-Allied Lines.

Exhibit II-Allied Lines - provides the calculation of the premium trend factors to reflect increasing amounts of insurance, as well as all other distributional changes. The selected factors are based on USAA Group Arkansas data. The current amount factors are based on actual trend to current in average earned premium at present rates (EPPR). The trended amount factor was selected based on the change in annual average EPPR. The data was fitted to an exponential curve.

Exhibit III-Allied Lines - shows the 10-year smoothing technique USAA uses to reflect the excess loss potential in Arkansas. The Large Loss Adjustment establishes an excess loss cut-off as a percentage of the average amount of insurance written for each year. The procedure then removes the portion of developed loss in excess of the cut-off, ratios the excess losses to the developed non-excess (normal) losses, and selects a weighted average of this ratio as the excess loss factor.

Exhibit IV-Allied Lines - displays the calculation of USAA Group loss development factors for Arkansas. Loss data used for these calculations excludes catastrophes.

Exhibit V-Allied Lines - shows the loss trend underlying the rate level indication. Various exponential fits including 20-, 16-, 12-, 8-, and 4-points are shown. The selected current cost factor (CCF) and trended cost factor (TCF) are based on the results of these exponential fits. (Due to the volatility and lack of credibility in Arkansas, the selected Arkansas loss trend was credibility weighted with USAA countrywide loss trend data excluding CA, FL & TX.) The Arkansas credibility-weighted current cost factor and trended cost factor are displayed on Page 2.

Exhibit VI-Allied Lines (Revised) - develops the loss adjustment expense (LAE) factors used in calculating the indication in Exhibit I-Allied Lines (Revised). The factors are based upon USAA countrywide data for calendar-accident years 2007, 2008, and 2009.

Exhibit VII-Allied Lines - *Withdrawn*

Exhibit VIII-Allied Lines - *Withdrawn*

Exhibit IX-Allied Lines - *Withdrawn*

Exhibit X-Allied Lines - shows the development of the variable permissible loss and LAE ratio for Arkansas on Page 1. Provisions for other expense categories are based on countrywide data from the Insurance Expense Exhibit while taxes, licenses, and fees are based upon actual Arkansas experience for USAA Group. The calculation of the selected annual expense trend is shown on Page 2. The trend is derived by taking a weighted average of the Employment Cost Index and the Consumer Price Index. The expense trend is used to trend fixed expenses, which are used to develop the indication shown in Exhibit I-Allied Lines (Revised).

Exhibit XI-Allied Lines - details USAA Group's method for selecting its underwriting profit and contingency provision, which is included in the permissible loss ratio. A separate explanatory memorandum is included with the exhibit.

Exhibit XII-Allied Lines - Page 1 illustrates the calculation of the Arkansas historical catastrophe loss and LAE ratio used to determine the indication in Exhibit I-Allied Lines (Revised). We are utilizing a procedure based on the methodology presented in "Pricing the Catastrophe Exposure in Homeowners Ratemaking" by David H. Hays and W. Scott Farris. The catastrophe losses are considered fully developed. The historical catastrophe loss is divided by the amount of insurance (AOI) in force for each of the last twelve accident years. The mean and standard deviation of these ratios is calculated, along with a t-statistic. A 55% confidence was selected on a state basis to reflect the variability of losses within the twelve-year experience period and to ensure that our countrywide catastrophe provision is sufficient in the long-run. The final catastrophe provision is applied to prospective amount of insurance in force. The selected AOI trend is displayed on Page 2. Exhibit VI-Allied Lines (Revised) derives the selected catastrophe LAE factor.

USAA Group
Arkansas
Indicated Rate Change
Allied Lines Forms
As of 06/30/2011

Accident Year Ending (1)	Earned Premium at Present Rates (2)	Premium Trend Factor [A] (3)	Prospective Earned Premium at Present Rates (4) = (2) * (3)	Smoothed Developed Incurred Losses Excluding Catastrophes [B] (5)	Loss Trend Factor [C] (6)	LAE Factor [D] (7)	Prospective Incurred Losses and LAE Excluding Catastrophes (8) = (5) * (6) * (7)	Prospective Loss and LAE Ratio Excluding Catastrophes (9) = (8) / (4)	Weight (10)
03/31/2007	$942,880	1.226	$1,155,971	$242,472	1.822	1.120	$494,798	0.428	0.100
03/31/2008	1,045,262	1.177	1,230,273	383,980	1.646	1.120	707,875	0.575	0.150
03/31/2009	1,130,424	1.182	1,336,161	274,655	1.487	1.120	457,421	0.342	0.200
03/31/2010	1,357,239	1.081	1,467,175	1,333,619	1.343	1.120	2,005,976	1.367	0.250
03/31/2011	1,512,263	1.072	1,621,146	442,644	1.214	1.120	601,854	0.371	0.300

Five Year Weighted Loss and LAE Ratio Excluding Catastrophes =		0.651
Catastrophe Loss and LAE Ratio [E] =		0.556
Trended Fixed Expense Ratio [F] =		0.094
Variable Permissible Loss and LAE Ratio [G] =		0.826
Indicated Rate Level Change =	(0.651 + 0.556 + 0.094) / 0.826 - 1	57.5%
Proposed Rate Level Change =		20.0%

[A] Developed in Exhibit II-Allied Lines
[B] Developed in Exhibit III-Allied Lines
[C] Developed in Exhibit V-Allied Lines, Page 2 of 2
[D] Developed in Exhibit VI-Allied Lines (Revised)
[E] Developed in Exhibit XII-Allied Lines
[F] Developed in Exhibit VIII-Allied Lines, Page 2 of 2
[G] Developed in Exhibit VIII-Allied Lines, Page 1 of 2

USAA Group
Arkansas
Premium Trend
Allied Lines Forms

Year Ending Quarter (1)	Total Earned Premium at Present Rates (2)	Earned Exposures (3)	Average Earned Premium at Present Rates (4)	Annual Change (5)	Current Amount Factors 483.00 / (4)
2006/2	918,088.87	2,161.00	424.84		1.137
2006/3	924,398.47	2,188.00	422.49		1.143
2006/4	928,712.38	2,213.00	419.66		1.151
2007/1	942,879.55	2,233.00	422.25		1.144
2007/2	965,036.32	2,265.00	426.06	0.3%	1.134
2007/3	994,341.55	2,314.00	429.71	1.7%	1.124
2007/4	1,022,897.13	2,358.00	433.80	3.4%	1.113
2008/1	1,045,261.74	2,376.00	439.92	4.2%	1.098
2008/2	1,067,660.04	2,401.00	444.67	4.4%	1.086
2008/3	1,088,504.75	2,445.00	445.20	3.6%	1.085
2008/4	1,120,924.37	2,515.00	445.70	2.7%	1.084
2009/1	1,130,423.95	2,581.00	437.98	-0.4%	1.103
2009/2	1,173,623.17	2,654.00	442.21	-0.6%	1.092
2009/3	1,220,048.42	2,729.00	447.07	0.4%	1.080
2009/4	1,285,143.69	2,797.00	459.47	3.1%	1.051
2010/1	1,357,238.65	2,833.00	479.08	9.4%	1.008
2010/2	1,395,917.49	2,894.00	482.35	9.1%	1.001
2010/3	1,435,218.19	2,961.00	484.71	8.4%	0.996
2010/4	1,458,909.76	3,051.00	478.17	4.1%	1.010
2011/1	1,512,263.15	3,131.00	483.00	0.8%	1.000

Trended Amount Factor:

Least Squares Results

Exponential Fits	20 pt	16 pt	12 pt	8 pt	4 pt
Annualized Change:	3.2%	3.6%	4.1%	5.5%	-0.4%
R-squared Value:	0.884	0.860	0.789	0.768	0.046
Selected Annual Trend Factor:	1.030				

Premium Trend Factor

Accident Year Ending	Current Amount Factors (1)	Trended Amount Selection (2)	Trended Amount Period [A] (3)	Trended Amount Factors (4) = (2) ^ (3)	Premium Trend Factors (5) = (1) * (4)
03/31/2007	1.144	1.030	2.360	1.072	1.226
03/31/2008	1.098	1.030	2.360	1.072	1.177
03/31/2009	1.103	1.030	2.360	1.072	1.182
03/31/2010	1.008	1.030	2.360	1.072	1.081
03/31/2011	1.000	1.030	2.360	1.072	1.072

[A] From the average earned date in the most recent accident year, 09/30/2010, to the average earned date in the effective period, 02/08/2013

USAA Group
Arkansas
Large Loss Adjustment
Allied Lines Forms
As of 06/30/2011

Calendar/ Accident Year Ending (1)	Average Amount of Insurance (2)	Cutoff 25% of (2) (3)	Incurred Losses Excluding Catastrophes (4)	Loss Development Factors (5)[A]	Developed Losses Excluding Catastrophes (6)	Number of Excess Losses (7)	Large Losses (8)	Excess Losses (9) = (8) - (7) * (3)	Normal Losses (10) = (6) - (9)	Excess Ratio (11) = (9) / (10)	Smoothed Developed Incurred Losses Ex Cats (12)[C]
03/31/2002	$102,390	$25,598	$128,353	1.0000	$128,353	0	$0	$0	$128,353	0.000	$135,541
03/31/2003	104,958	$26,240	226,839	1.0000	$226,839	2	$67,252	14,772	212,067	0.070	$223,943
03/31/2004	118,403	$29,601	187,142	1.0000	$187,142	2	$66,168	6,966	180,176	0.039	$190,266
03/31/2005	133,866	$33,467	147,798	1.0000	$147,798	0	$0	0	147,798	0.000	$156,075
03/31/2006	143,875	$35,969	279,124	1.0000	$279,124	1	$65,405	29,436	249,688	0.118	$263,671
03/31/2007	151,052	$37,763	234,063	1.0000	$234,063	1	$42,212	4,449	229,614	0.019	$242,472
03/31/2008	160,689	$40,172	363,617	1.0000	$363,617	0	$0	0	363,617	0.000	$383,980
03/31/2009	165,333	$41,333	389,857	1.0000	$389,857	1	$171,100	129,767	260,090	0.499	$274,655
03/31/2010	174,667	$43,667	1,271,264	1.0000	$1,271,264	2	$95,065	7,731	1,263,533	0.006	$1,334,291
03/31/2011	182,031	$45,508	414,527	1.0117	$419,377	0	$0	0	419,377	0.000	$442,862
								$193,121	$3,454,313		

Weighted Average Excess Ratio [B] = 0.056

Weighted Average Excess Factor = 1.056

[A] Developed in Exhibit IV-Allied Lines

[B] Weighted Average Excess Ratio = Sum of Column (9) / Sum of Column (10)

[C] (12) = (10) * Weighted Average Excess Factor

USAA Group
Arkansas
Loss Development
Incurred Losses Excluding Catastrophes
Allied Lines Forms

Accident Year Ending	15 months	27 months	39 months	51 months	63 months
03/31/2002					128,353
03/31/2003				227,157	226,839
03/31/2004			187,142	187,142	187,142
03/31/2005		147,798	147,798	147,798	147,798
03/31/2006	276,704	279,124	279,124	279,124	279,124
03/31/2007	238,472	234,063	234,063	234,063	234,063
03/31/2008	362,194	364,117	363,617	363,617	
03/31/2009	381,783	389,857	389,857		
03/31/2010	1,210,733	1,271,264			
03/31/2011	414,527				

Age-to-Age Factors

Accident Year Ending	15 to 27 Months	27 to 39 Months	39 to 51 Months	51 to 63 Months
03/31/2002				
03/31/2003				0.9986
03/31/2004			1.0000	1.0000
03/31/2005		1.0000	1.0000	1.0000
03/31/2006	1.0087	1.0000	1.0000	1.0000
03/31/2007	0.9815	1.0000	1.0000	1.0000
03/31/2008	1.0053	0.9986	1.0000	
03/31/2009	1.0211	1.0000		
03/31/2010	1.0500			
Latest 3-year Average	1.0255	0.9995	1.0000	1.0000
Latest 4-year Average	1.0145	0.9997	1.0000	1.0000
Latest 5-year Average	1.0133	0.9997	1.0000	0.9997
Latest 3-out-of-5-year Average	1.0117	1.0000	1.0000	1.0000
Selected Age-to-Age Factors	1.0117	1.0000	1.0000	1.0000

Cumulative Factors [A]

	15 to Ultimate	27 to Ultimate	39 to Ultimate	51 to 63 Months
Selected Cumulative Factors	1.0117	1.0000	1.0000	1.0000

[A] Cumulative factors are adjusted to ultimate with a factor of 1.0000

USAA Group
Arkansas
USAA Group CW Excl CA, FL, & TX
Allied Lines Forms

	Calendar Year Paid Frequency				Calendar Year Paid Severity				Calendar Year Paid Pure Premium			
Year Ending Quarter	Series 1 [A]	Annual Change	Series 2 [B]	Annual Change	Series 1 [A]	Annual Change	Series 2 [B]	Annual Change	Series 1 [A]	Annual Change	Series 2 [B]	Annual Change
2006/3	0.0379		0.0169		4,296		5,715		162.95		96.50	
2006/4	0.0384		0.0173		3,602		5,745		138.33		99.44	
2007/1	0.0327		0.0184		4,129		6,241		134.99		114.60	
2007/2	0.0305		0.0192		3,866		6,472		117.77		124.57	
2007/3	0.0238	-37.3%	0.0203	20.2%	3,641	-15.2%	6,517	14.0%	86.53	-46.9%	132.24	37.0%
2007/4	0.0212	-44.8%	0.0204	18.1%	4,272	18.6%	6,720	17.0%	90.58	-34.5%	137.38	38.2%
2008/1	0.0244	-25.3%	0.0208	13.1%	4,413	6.9%	6,949	11.4%	107.73	-20.2%	144.36	26.0%
2008/2	0.0312	2.5%	0.0211	9.7%	4,957	28.2%	6,750	4.3%	154.85	31.5%	142.49	14.4%
2008/3	0.0368	54.9%	0.0205	1.3%	4,995	37.2%	6,990	7.2%	183.87	112.5%	143.63	8.6%
2008/4	0.0370	74.4%	0.0203	-0.7%	4,720	10.5%	6,923	3.0%	174.53	92.7%	140.58	2.3%
2009/1	0.0353	44.4%	0.0217	4.7%	4,576	3.7%	6,977	0.4%	161.35	49.8%	151.73	5.1%
2009/2	0.0305	-2.3%	0.0224	6.0%	4,067	-17.9%	7,074	4.8%	124.14	-19.8%	158.30	11.1%
2009/3	0.0370	0.5%	0.0232	12.8%	7,622	52.6%	6,923	-1.0%	282.07	53.4%	160.45	11.7%
2009/4	0.0436	18.0%	0.0234	15.2%	7,724	63.6%	6,918	-0.1%	336.91	93.0%	161.89	15.2%
2010/1	0.0515	46.2%	0.0238	9.4%	7,375	61.1%	6,967	-0.1%	380.05	135.5%	165.68	9.2%
2010/2	0.0591	93.6%	0.0236	5.4%	7,009	72.3%	6,982	-1.3%	414.18	233.6%	164.69	4.0%
2010/3	0.0550	48.7%	0.0241	3.9%	4,664	-38.8%	7,062	2.0%	256.77	-9.0%	169.98	5.9%
2010/4	0.0482	10.5%	0.0247	5.6%	4,386	-43.2%	6,889	-0.4%	211.32	-37.3%	170.19	5.1%
2011/1	0.0383	-25.6%	0.0255	7.4%	4,422	-40.0%	6,877	-1.3%	169.48	-55.4%	175.65	6.0%
2011/2	0.0341	-42.2%	0.0261	10.5%	5,024	-28.3%	6,973	-0.1%	171.51	-58.6%	181.69	10.3%
Exponential Fits	R-squared Value	Annualized Change	R-squared Value	Annualized Change	R-squared Value	Annualized Change	R-squared Value	Annualized Change	R-squared Value	Annualized Change	R-squared Value	Annualized Change
20-point fit	0.321	10.7%	0.957	8.4%	0.224	8.6%	0.576	3.3%	0.318	20.2%	0.925	11.9%
16-point fit	0.493	20.4%	0.931	7.2%	0.096	7.0%	0.297	0.9%	0.286	28.8%	0.958	8.2%
12-point fit	0.138	9.1%	0.949	8.8%	0.001	-0.6%	0.046	-0.2%	0.029	8.4%	0.937	8.5%
8-point fit	0.038	-6.8%	0.901	6.9%	0.771	-30.6%	0.000	0.0%	0.509	-35.3%	0.922	6.8%
4-point fit	0.979	-48.6%	0.992	11.5%	0.240	9.7%	0.176	-1.6%	0.873	-43.6%	0.896	9.7%

[A] Series 1 is based on USAA Group Arkansas data

[B] Series 2 is based on USAA Group CW Excl CA, FL, & TX data

USAA Group
Arkansas
USAA Group CW Excl CA, FL, & TX
Allied Lines Forms

	Series 1 Frequency[A]	Series 2 Frequency[B]	Cred-Weighted Frequency[C]	Series 1 Severity[A]	Series 2 Severity[B]	Cred-Weighted Severity[C]	Cred-Weighted Pure Premium
Current Cost Selection	1.130	1.080	1.085	1.020	1.020	1.020	1.107
Trended Cost Selection	1.000	1.090	1.081	1.020	1.000	1.002	1.083

Loss Trend Factor

Accident Year Ending	Current Cost Selection (1)	Current Cost Period[D] (2)	Current Cost Factor (3) = (1) ^ (2)	Trended Cost Selection (4)	Trended Cost Period[E] (5)	Trended Cost Factor (6) = (4) ^ (5)	Loss Trend Factor (7) = (3) * (6)
03/31/2007	1.107	4.250	1.540	1.083	2.110	1.183	1.822
03/31/2008	1.107	3.250	1.391	1.083	2.110	1.183	1.646
03/31/2009	1.107	2.250	1.257	1.083	2.110	1.183	1.487
03/31/2010	1.107	1.250	1.135	1.083	2.110	1.183	1.343
03/31/2011	1.107	0.250	1.026	1.083	2.110	1.183	1.214

[A] Series 1 is based on USAA Group Arkansas data

[B] Series 2 is based on USAA Group CW Excl CA, FL, & TX data

[C] USAA Group Arkansas is 10.2% credible based on 110 claims; used the Square Root method with a full credibility standard of 10,623 claims.

[D] From the average date of loss in the respective accident year to 12/31/2010

[E] From 12/31/2010 to the average date of loss in the effective period, 02/08/2013

USAA Group
Countrywide
Loss Adjustment Expense (LAE) Factor
All Forms Combined
As of 6/30/2010

Non-Catastrophe Loss Adjustment Expense Factor

Accident Year Ending	Incurred Losses	Loss Adjustment Expense	LAE Ratio
12/31/2007	89,126,770	10,268,737	0.115
12/31/2008	91,517,758	11,240,055	0.123
12/31/2009	108,159,666	13,712,416	0.127
Average LAE Ratio			0.122
Selected Non-Catastrophe LAE Factor			1.120

Catastrophe Loss Adjustment Expense Factor

Accident Year Ending	Incurred Losses	Loss Adjustment Expense	LAE Ratio
12/31/2007	10,272,987	566,720	0.051
12/31/2008	42,469,355	3,227,489	0.076
12/31/2009	29,456,960	751,999	0.026
Average LAE Ratio			0.051
Selected Catastrophe LAE Factor			1.051

USAA Group
Arkansas
Expected Net Hurricane Catastrophe
Loss and LAE Ratio
Allied Lines Forms

WITHDRAWN

(1) Expected Annual Net Hurricane Catastrophe Loss and LAE [A]	$12,273
(2) Prospective Earned Premium at Present Rates	$1,621,146
(3) Hurricane Catastrophe Loss and LAE Ratio (1) / (2)	0.008
Selected Hurricane Catastrophe Loss and LAE Ratio	0.008

[A] Based on Applied Insurance Research, Inc. (AIR) methodology and assumptions; net losses are based on exposure levels as of 05/31/2010 and trended for loss severity.

USAA Group

Arkansas

Expected Net Severe Thunderstorm Loss and LAE Ratio

Allied Lines Forms

(1) Expected Annual Net Severe Thunderstorm Cat Loss	$513,137
(2) Prospective Earned Premium at Present Rates	$1,621,146
(3) Severe Thunderstorm Catastrophe Loss and LAE Ratio (1) / (2)	0.317
Selected Severe Thunderstorm Catastrophe Loss and LAE Ratio	0.317

[A] Based on Applied Insurance Research, Inc. (AIR) methodology and assumptions; net losses are based on exposure levels as of 05/31/2010 and trended for loss severity

WITHDRAWN

USAA Group
Arkansas
Expected Net Winter Storm Loss and LAE Ratio
Allied Lines Forms

WITHDRAWN

(1)	Expected Annual Net Winter Storm Cat Loss	$56,599
(2)	Prospective Earned Premium at Present Rates	$1,621,146
(3)	Winter Storm Catastrophe Loss and LAE Ratio (1) / (2)	0.035
Selected Winter Storm Catastrophe Loss and LAE Ratio		0.035

[A] Based on Applied Insurance Research, Inc. (AIR) methodology and assumptions; net losses are based on exposure levels as of 05/31/2010 and trended for loss severity

USAA Group
Arkansas
Fixed and Variable Expense Provisions
Allied Lines Forms

	2009	2010	2-Year Straight Average	Selected
(1) Average General Expenses Per Earned Exposure [A]	$5.36	$4.70		
(2) Selected Annual Expense Trend [B]	2.0%	2.0%		
(3) Trend Period [C]	3.61	2.61		
(4) Projected Average General Expenses Per Earned Exposure (1) * [1.02] ^ (3)	$5.76	$4.95	$5.36	$5.36
(5) Average Other Acquisition Expense Per Written Exposure [A]	$36.09	$42.16		
(6) Selected Annual Expense Trend [B]	2.0%	2.0%		
(7) Trend Period [D]	3.11	2.11		
(8) Projected Average Other Acquisition Expense Per Written Exposure (5) * [1.02] ^ (7)	$38.38	$43.96	$41.17	$41.17
(9) Average Licenses and Fees Expense Per Written Exposure [E]	$2.38	$1.15		
(10) Selected Annual Expense Trend [B]	2.0%	2.0%		
(11) Trend Period [D]	3.11	2.11		
(12) Projected Average Licenses and Fees Expense Per Written Exposure (9) * [1.02] ^ (11)	$2.53	$1.20	$1.87	$1.87
(13) Total Fixed Expense (4) + (8) + (12)				$48.40
(14) Average Projected Premium at Present Rates [F]				$516.95
(15) Projected Fixed Expense Provision (13) / (14)				0.094
(16) Commission and Brokerage	0.0%	0.0%	0.0%	0.0%
(17) Taxes [G]	2.4%	2.4%	2.4%	2.4%
(18) Profit and Contingencies Provision [H]				15.0%
(19) Total Variable Expenses (16) + (17) + (18)				17.4%
(20) Variable Permissible Loss and LAE Ratio 1 - (19)				82.6%

[A] USAA Group Countrywide data
[B] Developed in Exhibit X-Allied Lines, Page 2 of 2
[C] From the midpoint of the respective year to the average earned date in effective period, 02/08/2013
[D] From the midpoint of the respective year to the average written date in effective period, 08/08/2012
[E] Arkansas USAA Group data
[F] Arkansas USAA Group data for Allied Lines Forms only
[G] Arkansas USAA Group data as a percent of direct written premium
[H] Developed in Exhibit XI-Allied Lines

USAA Group
Countrywide
Calculation of Annual Expense Trend

(1)	Employment Cost Index - Financial activities, excluding incentive paid occupations (annual change over latest 2 years ending 03/31/2011) U.S. Department of Labor	2.1%
(2)	% of Total Acquisition and General Expenses used for Salaries and Employee Relations & Welfare - USAA Group Insurance Expense Exhibit, 2010	54.4%
(3)	Consumer Price Index, All Items - (annual change over latest 2 year ending 03/31/2011)	2.5%
(4)	Annual Expense Trend - { (1) * (2) } + { (3) * [1 - (2)] }	2.3%
Selected Annual Expense Trend		2.0%

USAA GROUP
ARKANSAS EXTENDED COVERAGE
UNDERWRITING PROFIT PROVISION
EXPLANATORY MEMORANDUM

This exhibit is submitted in support of the underwriting profit and contingency provision included in the permissible loss ratio.

UNDERWRITING PROFIT PROVISION

The target underwriting profit and contingency provision needed to achieve our desired overall profit level is developed on Page 2. The selected target rate of return is 10.0% on GAAP (generally accepted accounting principles) equity.

The target underwriting return on an after-tax basis is derived by subtracting the after-tax investment rate of return on GAAP surplus from the target rate of return. This target underwriting rate of return is then adjusted to a before-tax basis, using the current corporate tax rate of 35.0%, and then divided by the premium-to-surplus ratio to yield the target underwriting profit and contingency provision.

TARGET RATE OF RETURN

Results from the Capital Asset Pricing Model (CAPM), commonly used in evaluating investments, suggest a required rate of return around 8.0%. Historically, the CAPM has consistently supported a 10.0% rate of return. However, the unusually poor market performance in recent years has impacted the results. We still believe 10.0% is a reasonable rate of return and is consistent with our historical selection.

The data points used in the CAPM method are published historical values from Value Line, Inc.'s *Investment Survey* (as of 7/30/10) and from Ibbotson Associates' 2010 Stocks, Bonds, Bills & Inflation (SBBI) Yearbook. The companies composing the "P&C Insurance Industry", as identified by Value Line, Inc., were selected to determine the appropriate rate of return for a P&C company.

INVESTMENT RATE OF RETURN

The investment rate of return is determined by dividing the estimated investment earnings by the Texas Extended Coverage allocation of USAA Group surplus. The estimated investment earnings are calculated by applying a selected after-tax rate of return to the total funds subject to investment.

The selected after-tax rate of return is a weighted average after-tax return, using the projected proportion of the portfolio held in each component as weight. The composition of the portfolio is projected for 2011 and 2012 and an after-tax return for each year is calculated.

USAA GROUP
ARKANSAS EXTENDED COVERAGE
UNDERWRITING PROFIT PROVISION

A.	Target Rate of Return (% of GAAP Surplus)		
	1.	Capital Asset Pricing Model	8.0%
	2.	Selected Target Rate of Return	10.0%
B.	Target Underwriting Rate of Return (% of GAAP Surplus)		
	1.	Investment Rate of Return After Tax	1.8%
	2.	Target Underwriting Return After Tax (A2) - (B1)	8.2%
	3.	Target Underwriting Return Before Tax (B2) / (1.00 - 0.35)	12.6%
C.	Target Underwriting Profit Provision (% of Direct Earned Premium)		
	1.	Direct Written Premium / GAAP Surplus Ratio	0.661
	2.	Indicated Underwriting Profit Provision (B3) / (C1)	19.1%
	3.	Selected Underwriting Profit Provision	15.0%

USAA Group
Arkansas
Catastrophe Ratio
Allied Lines Forms
As of 03/31/2011

Accident Year Ending	Total Amount of Insurance in Force/1000	Catastrophe Losses	Cat/AOI Ratio
12/31/1999	159,911	79,195	0.4952
12/31/2000	181,073	9,241	0.0510
12/31/2001	180,987	27,613	0.1526
12/31/2002	182,923	4,851	0.0265
12/31/2003	205,907	3,786	0.0184
12/31/2004	262,734	24,039	0.0915
12/31/2005	303,100	117,550	0.3878
12/31/2006	337,994	88,311	0.2613
12/31/2007	380,148	72,841	0.1916
12/31/2008	427,489	221,871	0.5190
12/31/2009	496,787	1,348,787	2.7150
12/31/2010	579,952	379,795	0.6549

(1) Mean	0.4637
(2) Standard Deviation	0.7401
(3) t-statistic for 55% confidence and 11 degrees of freedom	0.1290
(4) Final Catastrophe Provision (1) + (2) * (3)	0.5592
(5) Selected AOI trend [A]	0.0496
(6) Prospective Amount of Insurance in Force/1000	549,706
(7) Prospective Catastrophe Losses (4) * (6)	857,106
(8) Selected Catastrophe LAE Factor [B]	1.0510
(9) Prospective Catastrophe Loss and LAE (7) * (8)	900,819
(10) Prospective Earned Premium at Present Rates [C]	1,621,146
Catastrophe Loss and LAE Ratio (9) / (10)	0.556

[A] Developed in Exhibit XII-Allied Lines, Page 2 of 2
[B] Developed in Exhibit VI-Allied Lines (Revised)
[C] Developed in Exhibit I-Allied Lines (Revised)

USAA Group
Arkansas
Average Amount of Insurance Trend
Allied Lines Forms

In Force Data as of	Average AOI	Annual Change	12 point fit	6 point fit
12/31/1998	86,969			
12/31/1999	90,447	4.00%	90,103	
12/31/2000	97,614	7.92%	96,342	
12/31/2001	101,507	3.99%	103,012	
12/31/2002	103,816	2.27%	110,144	
12/31/2003	113,136	8.98%	117,770	
12/31/2004	131,302	16.06%	125,924	
12/31/2005	141,437	7.72%	134,643	142,341
12/31/2006	149,159	5.46%	143,965	149,398
12/31/2007	159,592	6.99%	153,933	156,806
12/31/2008	162,791	2.00%	164,591	164,581
12/31/2009	174,006	6.89%	175,986	172,741
12/31/2010	180,221	3.57%	188,171	181,306
Exponential Trend			6.9%	5.0%
R-squared			0.982	0.989
Selected AOI Trend				5.0%

The AIR Earthquake Model for the United States

AIR WORLDWIDE

Revision History

Original writing: September 2009

Last updated: August 2010

Copyright

2009 AIR Worldwide. All rights reserved.

Information in this document is subject to change without notice. No part of this document may be reproduced or transmitted in any form, for any purpose, without the express written permission of AIR Worldwide (AIR).

Trademarks

AIR Worldwide, CATRADER and CATStation are registered trademarks of AIR Worldwide Corporation.

Contact Information

If you have any questions regarding this document, contact:

AIR Worldwide
131 Dartmouth Street
Boston, MA 02116-5134
USA
Tel: (617) 267-6645
Fax: (617) 267-8284

Table of Contents

1 Facts at a Glance 12

1.1 Model Facts 12

1.2 United States — Country Facts 13

1.3 Data Sources 15

1.4 Historical Catalog 16

1.5 Stochastic Catalog 16

1.6 Optimization of the Stochastic Catalog 18

1.7 Model Resolution 19

1.8 Modeled Lines of Business 19

1.9 Modeled Construction and Occupancy Classes 20

1.10 Modeled Industry Losses 20

1.11 The United States Insurance Market 21

1.12 Navigating the Document 22

2 Earthquakes in the Continental United States 23

2.1 Earthquakes: An Overview 23

2.2 United States Earthquake Risk 29

2.3 Significant Historical Earthquakes in the United States 37

3 Event Generation 44

3.1 Modeled Earthquake Variables 44

3.2 Domain of the AIR Earthquake Model for the United States 46

3.3 Regional Seismicity in the Continental United States 47

3.4 Fault Sources 47

3.5 Time Dependence and the Model's Stochastic Catalogs 58

3.6 Validating Stochastic Event Generation 63

4 Local Intensity Calculation 72

4.1 Ground-Shaking Intensity 72

4.2 Attenuation Relationships 72

4.3 Site Amplification Due to Surface Geology *78*

4.4 Liquefaction *83*

4.5 Ground Motion Intensity and Spatial Correlation *85*

4.6 Validating Local Intensity Calculations *88*

5 Damage Estimation **94**

5.1 Building Classification *95*

5.2 Impact of Regional Construction on Building Vulnerability *97*

5.3 Impact of Year Built on Building Vulnerability *98*

5.4 Building Damage Functions *99*

5.5 The Capacity Spectrum Method and the Use of Nonlinear Static Analysis *100*

5.6 Nonlinear Dynamic Analysis *104*

5.7 Development of Damage Functions for Different Construction Classes *108*

5.8 Damage Functions that Include Ground Motion Uncertainty *117*

5.9 Contents Damage *122*

5.10 Additional Living Expenses *122*

5.11 Business Interruption *123*

5.12 Automobile Damage *124*

5.13 Liquefaction Damage *125*

5.14 Fire Following Damage *125*

5.15 Workers' Compensation Losses due to Earthquakes *130*

5.16 Sprinkler Leakage Damage *137*

5.17 Validating the Model's Damage Estimation Module *140*

6 Estimating Damage to Industrial Facilities **153**

6.1 Assessment of Business Interruption Losses for Industrial Facilities *168*

6.2 Validating Damage Functions for Industrial Facilities *170*

7 Insured Loss Calculation **174**

7.1 Aggregating Losses Probabilistically *174*

7.2 Validating Modeled Losses *175*

8 Selected References 178

9 About AIR Worldwide 189

List of Figures

Figure 1. Population Density in the Continental United States 13
Figure 2. Map of the Continental United States showing the ZIP Codes 14
Figure 3. ZIP Codes in San Francisco (a), Los Angeles (b, upper left), and San Diego (b, bottom) 14
Figure 4. Map of Counties in the Continental United States 15
Figure 5. Distribution of Annual Simulated Event Frequency, 10K Time-Dependent Catalog 17
Figure 6. Distribution of Annual Simulated Event Frequency, 10K Time-Independent Catalog 17
Figure 7. Earthquake Risk (Loss Costs) in the Continental United States 20
Figure 8. Components of the AIR Earthquake Model for the United States 22
Figure 9. The Earth's Layers at a Subduction Zone 24
Figure 10. Completeness of Auxiliary and Historical Record Data, Based on Earthquake Source Dimension 28
Figure 11. Sample Gutenberg-Richter Distribution 28
Figure 12. Historical Seismicity and Faults in the Continental United States ($M_W \geq 5.0$) 30
Figure 13. Some of the Major Faults in California 31
Figure 14. The Pacific, Juan de Fuca, and North American Plates in the Cascadia Subduction Zone 33
Figure 15. Historical Seismicity in the New Madrid and Wabash Valley Seismic Zones ($M_W \geq 3.0$) 35
Figure 16. 1906 Rupture of the San Andreas Fault compared to the 1989 Loma Prieta Rupture 41
Figure 17. United States Earthquake Model Domain 46
Figure 18. Subduction Zones and Crustal Faults in the Western United States 48
Figure 19: The San Andreas Peninsula Segment 49
Figure 20. The Cascadia Subduction Zone Fault Model 50
Figure 21. Spatial Variability in the New Madrid Seismic Zone using Five Parallel Fault Traces (USGS) 52
Figure 22. A Logic Tree Used to Capture Uncertainty for the New Madrid Seismic Zone 53
Figure 23. Charleston Fault Source Zones 54
Figure 24. Spatial Distribution of Historical Earthquakes for the Western United States 55
Figure 25. Spatial Distribution of Historical Earthquakes for the Central and Eastern United States 56
Figure 26. Special Seismic Zones in the Central and Eastern United States 57
Figure 27. Special Seismic Zones in the Western United States 58
Figure 28. Faults, Subduction Zones, and Regional Zones Used for the Time-Dependent Catalog 61
Figure 29. 30-Year Rupture Probabilities for Time-Dependent compared to Time-Independent Catalogs 62
Figure 30. Comparison between the Historical and Simulated Magnitude-Frequency Distributions for the United States 64
Figure 31. Comparison between the Historical and Time-Independent Simulated Magnitude-Frequency Distribution for California 64
Figure 32. Magnitude-Frequency Distributions for the Time-Independent Simulated Catalog vs. the USGS Report for the Cascadia Subduction Zone 65
Figure 33. Percentage of Earthquakes on each Branch of the New Madrid Seismic Zone. 66

Figure 34. Portion of the New Madrid Logic Tree showing Unclustered Event Rates 67
Figure 35. Magnitude-Frequency Distribution of Simulated Events for a Single Earthquake Scenario 68
Figure 36. Portion of the New Madrid Logic Tree showing Clustered Event Rates 68
Figure 37. Magnitude-Frequency Distribution of Simulated Events for Correlated Scenarios 69
Figure 38. Magnitude-Frequency Distribution of Simulated Events for Both Single Earthquake and Correlated Scenarios 69
Figure 39. Magnitude Distribution of Simulated Events for the Charleston Seismic Zone 70
Figure 40. Smoothed-Gridded Background Seismicity from the USGS (left) and AIR (right) 71
Figure 41. Ground Motion Attenuation for Earthquakes on Crustal Faults in the Western United States for 0.3 s S_a (g) 75
Figure 42. Ground Motion Attenuation for Earthquakes on Crustal Faults in the Western United States for 1.0 s S_a (g) 75
Figure 43. Ground Motion Attenuation for Subduction Zones in the Pacific Northwest 76
Figure 44. Ground Motion Attenuation for Deep Earthquakes in the Pacific Northwest 77
Figure 45. Ground Motion Attenuation for the Central and Eastern United States 78
Figure 46. Nationwide 500-meter Base Soil Map (left) and Higher Resolution (100-meter) State Soil Map (right) for Western Washington State 80
Figure 47. Several Recent Studies Reveal Positive Correlation between Topographic Slope and Shallow Shear-Wave Velocity 81
Figure 48. Shear-Wave Velocity Map Based on Geological Data only (left) and Augmented Based on Topographic Slope (Right) 82
Figure 49. Alluvial Basins in California, Washington and Nevada 83
Figure 50. Groundwater Depths for Liquefaction-Modeled Areas in the Western (left) and Eastern (right) United States 84
Figure 51. USGS TriNet Map for the Northridge Earthquake (top left), Expected Ground Motion (top right), and the Ratio (bottom) Showing Spatial Correlation of Residuals 86
Figure 52. Multiple Ground Motion Maps with Spatial Correlation and the Corresponding Distribution of Modeled Losses for the 1994 Northridge Earthquake 87
Figure 53. Loss Exceedance Curves with (Green) and without (Blue) Spatial Correlation 88
Figure 54. Comparison between Observed and NGA Predicted Mean Ground Motion with Uncertainty for the 1989 Loma Prieta Earthquake 89
Figure 55. Comparison between Observed and NGA Predicted Mean Ground Motion with Uncertainty for the 1994 Northridge Earthquake 89
Figure 56. U.S. Locations Used for Ground Motion Validation 90
Figure 57. USGS vs. AIR 475-Year Return Period PGA Values 90
Figure 58. USGS vs. AIR 475-Year Return Period 0.3 s S_a Values 91
Figure 59. USGS vs. AIR 475-Year Return Period 1.0 s S_a Values 91
Figure 60. Simulated Liquefaction Severity and Observed Liquefaction Sites, 1989 Loma Prieta Earthquake 92

Figure 61. Simulated Liquefaction Severity and Observed Liquefaction Sites, 1906 San Francisco Earthquake 92
Figure 62. Simulated Liquefaction Severity and Observed Liquefaction Sites, 1994 Northridge Earthquake 93
Figure 63. Simulated Liquefaction Severity and Observed Liquefaction Sites, 2001 Nisqually Earthquake 93
Figure 64. Damage Ratios of Wood Frame Structures of Different Ages after the 1994 Northridge Earthquake 99
Figure 65: Conceptual Flow of Analyses Adopted for Building Damage Functions (adapted from FEMA 440) 100
Figure 66: Schematic Depiction of Static Pushover Analysis used in the Capacity Spectrum Method (excerpted from FEMA 440) 101
Figure 67. Maximum Acceleration and Displacement of a Series of Oscillators 102
Figure 68. The Peak Response of a Structure Determined by its Capacity Curve 103
Figure 69. Maximum Displacement and Building Damage Depends on Ground Motion and Building Characteristics 103
Figure 70. Flow Chart Depicting the Use of NDA to Determine Building Response (Excerpted from FEMA 440) 105
Figure 71. Maximum Peak Inter-Story Drift Ratios (MIDR) and Maximum Peak Floor Accelerations (MPFA) 106
Figure 72. Relationship between Spectral Accelerations at the Fundamental Period of a Building and the Induced MIDR and IDR. 107
Figure 73. Six Failure Modes Captured by NDA for a Four-Story Concrete Moment-Resisting Frame Building (courtesy of Dr. Curt B. Haselton, California State University) 107
Figure 74. Claims Data from the 1994 Northridge Earthquake (Private Insurers) 109
Figure 75. Damage Data from the 1994 Northridge Earthquake for Wood Frame Houses Built after 1976 110
Figure 76. Average Damage Ratios for a Set of Spectral Accelerations 110
Figure 77. Damage Ratios vs. 0.3 s Spectral Acceleration for Wood Frame Houses Built around 1980 111
Figure 78. Damage to Approximately 100 Concrete Tilt-Up Structures after the 1994 Northridge Earthquake 112
Figure 79. Post-Occupancy Tags Corresponding to the Damaged Tilt-Up Structures after the 1994 Northridge Earthquake 113
Figure 80. Damage Distribution for URM Buildings, 1989 Loma Prieta Earthquake 113
Figure 81. Damage Distribution for URM Buildings, 1994 Northridge Earthquake 114
Figure 82. Damage Ratios for URM Buildings for Earthquakes in California and Italy 115
Figure 83. Damage Functions for Various Construction Types in California 115
Figure 84. Damage Functions for Low-Rise RC Frame Buildings 116
Figure 85. Sample Damage Function and Distribution with Non-zero Probabilities of 0% and 100% Loss 117
Figure 86. Mean and Integrated Damage Functions for Wood Frame Structures in California 118

Figure 87. Simulated ShakeMap (colors) vs. Observed (numbers) PGA, 1994 Northridge Earthquake 119
Figure 88. Modeled vs. Observed Sa at 0.3 second (g), 1994 Northridge Earthquake 120
Figure 89. Modeled vs. Observed Sa at 1.0 second (g), 1994 Northridge Earthquake 120
Figure 90. Modeled vs. Observed PGA, 1989 Loma Prieta Earthquake 121
Figure 91. Modeled vs. Observed Sa at 0.3 second (g), 1989 Loma Prieta Earthquake 121
Figure 92. Modeled vs. Observed Sa at 1.0 second (g), 1989 Loma Prieta Earthquake 122
Figure 93. Hypothetical Event Tree of BI Estimation for an Office and a Hotel 123
Figure 94. Primary Model Components in Fire Damage Estimation 126
Figure 95. Source Locations for Fire Engine Data – Continental U.S. and Zoom-in of Los Angeles Area 127
Figure 96. Fire Ignition Data for Selected Historical Earthquakes 128
Figure 97. Sample Ignition Rate Distribution at PGA of 0.4 g 128
Figure 98: Injury Severity Level by Building Damage State for a Reinforced Masonry Building 134
Figure 99: Calculation of Workers' Compensation Loss for an Individual Building 135
Figure 100: General Form of the AIR Sprinkler Leakage Damage Function 137
Figure 101: Relative Ranking of Contents Damage Functions by Occupancy Class 138
Figure 102. Model of an Existing Reinforced Concrete Frame Building that was Instrumented during the 1994 Northridge Earthquake 140
Figure 103. Comparison of Simulated and Recorded Floor Displacement during the 1994 Northridge Earthquake 141
Figure 104. Comparison between USGS MMI Map for the 1994 Northridge Earthquake (left) and AIR Modeled Damage Ratios (right) 142
Figure 105. Comparison between USGS MMI Map for the 1989 Loma Prieta Earthquake and AIR Modeled Damage Ratios 142
Figure 106. Northridge Claims Data and AIR Damage Function for Residential Contents 143
Figure 107. Northridge Claims Data and AIR Damage Function for Residential Additional Living Expenses 143
Figure 108. Modeled vs. Observed Probability Distributions, Mean Damage Ratio 0.026136 144
Figure 109. Modeled vs. Observed Probability Distributions, Mean Damage Ratio 0.17251 144
Figure 110. Observed Ignitions for the 1994 Northridge Earthquake 145
Figure 111. Simulated Ignitions for the 1994 Northridge Earthquake, Assuming 2008 Exposures 145
Figure 112. Exposure Density, Simulated PGA Contours, and Mean Damage Ratios for Combustible Exposures, Repeat of the 1994 Northridge Earthquake 146
Figure 113. Exposure Density, Simulated PGA Contours, and Mean Damage Ratios for Noncombustible Exposures, Repeat of the 1994 Northridge Earthquake 147
Figure 114. Exposure Density, Simulated PGA Contours, and Damage Ratios for Combustible Exposures, Repeat of the 1906 San Francisco Earthquake 148
Figure 115. Exposure Density, Simulated PGA Contours, and Damage Ratios for Noncombustible Exposures, Repeat of the 1906 San Francisco Earthquake 148

Figure 116. Exposure Density, Simulated PGA Contours, and Damage Ratios for Combustible Exposures, Repeat of the 1989 Loma Prieta Earthquake 149
Figure 117. Exposure Density, Simulated PGA Contours, and Damage Ratios for Noncombustible Exposures, Repeat of the 1989 Loma Prieta Earthquake 149
Figure 118. Observed Fire-Following Losses Compared to Mean and Median Modeled Losses for Northridge and Loma Prieta Earthquakes 150
Figure 119: Modeled vs. Observed Fatalities from 29 Historical Earthquakes in the U.S. 152
Figure 120. Some Industrial Facility Components 153
Figure 121. Damage Functions for Industrial Facility Components in California 156
Figure 122. Building Damage Functions in California 158
Figure 123. Building Damage Functions for Various Industrial Facilities in California 158
Figure 124. Damage Functions for Tanks Based on Technical Literature and Reviews, Average Damage from Each Source 159
Figure 125. Damage Functions for On-Grade Tanks Based on Observed Damage Data 159
Figure 126. Pushover Analysis Results for an Open-Frame Structure showing PGA Values at Several Limit States 161
Figure 127. Damage Functions for an Open-Frame Steel Plant Structure 162
Figure 128. Damage Functions for an Open-Frame Steel Dock Structure 162
Figure 129. Damage Functions for an "Anchored" Oil Refinery in California 164
Figure 130. Damage Functions for Unanchored Oil Refinery in California 164
Figure 131. Distribution of Industrial Facility Types for each Seismic Area of the United States 166
Figure 132. Damage Functions for Industrial Facilities in California 166
Figure 133. Damage Functions for Industrial Facilities in Oregon and Washington 167
Figure 134. Damage Functions for Industrial Facilities for All States Outside of California, Oregon, and Washington 167
Figure 135. Time Element Functions for Industrial Facility Components 169
Figure 136. Time Element Functions for Industrial Facilities in California 169
Figure 137. Damage Functions and Observed Damage Data for Chemical Processing Plants in a High Seismicity Area 172
Figure 138. Damage Functions and Observed Damage Data for a Thermo-Power Plant in a High Seismicity Area 173
Figure 139. Damage Functions and Observed Damage Data for Potable Water Systems in a High Seismicity Area 173
Figure 140. Comparison between Actual and Modeled Losses for Key Historical Events (variation in published reported losses is represented by an error bar) 176
Figure 141. Comparison between Actual and Modeled Losses for Less Severe Historical Events (variation in published reported losses is represented by an error bar) 177
Figure 142. Relative Distribution of Modeled vs. Reported Insurable Losses, 1994 Northridge Earthquake 177

List of Tables

Table 1. Distribution of All Simulated Events by Magnitude – 10K Time-Dependent Catalog 17
Table 2. Distribution of All Simulated Events by Magnitude – 10K Time-Independent Catalog 18
Table 3. Modeled Insured Losses for Historical Earthquakes (in billions USD) for Various Lines of Business – Shake and Fire-Following Damage 20
Table 4. Ratios of Short to Long-Term Seismicity Rates 61
Table 5. 30-Year Time-Dependent Rupture Probabilities Compared to Time-Independent 63
Table 6. Characteristic Magnitudes in USGS Model for the Charleston Zone 70
Table 7. Soil Maps Implemented in the AIR Earthquake Model for the U.S. 79
Table 8. Soil Classifications and Average Shear-Wave Velocities 80
Table 9. Independent Variables for Different Construction Classes 94
Table 10: Collapse Probabilities Used in the AIR Earthquake Model for the United States 132
Table 11: Distribution of Nonfatal Injuries for Five California Earthquakes 133
Table 12. Injury Severity Levels Used for Workers' Compensation (FEMA 2009) 133
Table 13: Model Estimates of the Number of Casualties for Two Scenarios of the 1994 Northridge Earthquake 136
Table 14: Comparison of Observed and Modeled Casualties for Selected Historical Earthquakes in California 151
Table 15. Industrial Facility Components used in the AIR Earthquake Model for the United States 155
Table 16. Construction Distribution for Heavy Fabrication and Assembly Plants in each Seismic Zone, for Low-Rise Buildings 157
Table 17. Historical Earthquakes Used for Tank Damage Data 160
Table 18. Historical Earthquakes used for Facility and Component Damage Function Validation 170
Table 19. Some Facilities and Components Validated with Damage Data from Historical Earthquakes 171

1 Facts at a Glance

1.1 Model Facts

Model Name: AIR Earthquake Model for the United States

Release Date: July 2010 (first released in Version 12.0 of the AIR software systems)

Software Systems: CATRADER, CLASIC/2, CATStation

AIR Model Version: 8.2

Modeled Country: Continental United States

Modeled Perils: The perils included in this model are ground shaking, liquefaction, fire following and sprinkler leakage. The effects of tsunami and levee failure are not modeled. Landslides are also not explicitly modeled; however, because modeled losses have been calibrated to and validated against actual reported losses, the impact of landslides on modeled losses is captured implicitly.

Model Abstract: The AIR Earthquake Model for the United States captures the effects of ground shaking, liquefaction, fires following earthquakes, and sprinkler leakage on properties in the continental United States. This is a fully stochastic, event-based model designed for portfolio risk management. The model captures the complex seismicity of the continental United States by generating events along known crustal faults and the Cascadia subduction zone. Through the use of smoothed background seismicity, the model also captures the potential for earthquakes to occur where there has been little or no recorded historical seismic activity. The stochastic event generation process includes determination of the magnitude, location, rupture length and the width, depth, and fault orientation and mechanism. Attenuation relationships, surface geology classification, and site-amplification factors are considered for the local ground-shaking intensity calculations. The engineering component has been extensively validated against published research and observed damage data from historical earthquakes. The damage functions have undergone external peer review. Overall model performance has been validated against historical loss data from various events. The model's fire-following module, which includes fire ignition, spread, and suppression, takes into account the amounts of combustible and noncombustible exposures, the number and location of fire engines, wind speeds, and population counts. The AIR Earthquake Model for the United States has been developed to

meet the wide spectrum of earthquake risk management needs of the insurance industry and accounts for policy conditions that are specific to the United States.

Model Domain: The model domain covers the continental United States, including the 48 conterminous states and Washington, DC. Seismic events generated in the model cover a region well beyond the boundaries of the United States, including Canada, Mexico and offshore subduction zones.

1.2 United States — Country Facts

Population: 310.2 million (est. as of 2010)

GDP (purchasing power parity): USD 14.26 trillion (est. as of 2009)

Per Capita GDP: USD 46,400 (est. as of 2009)

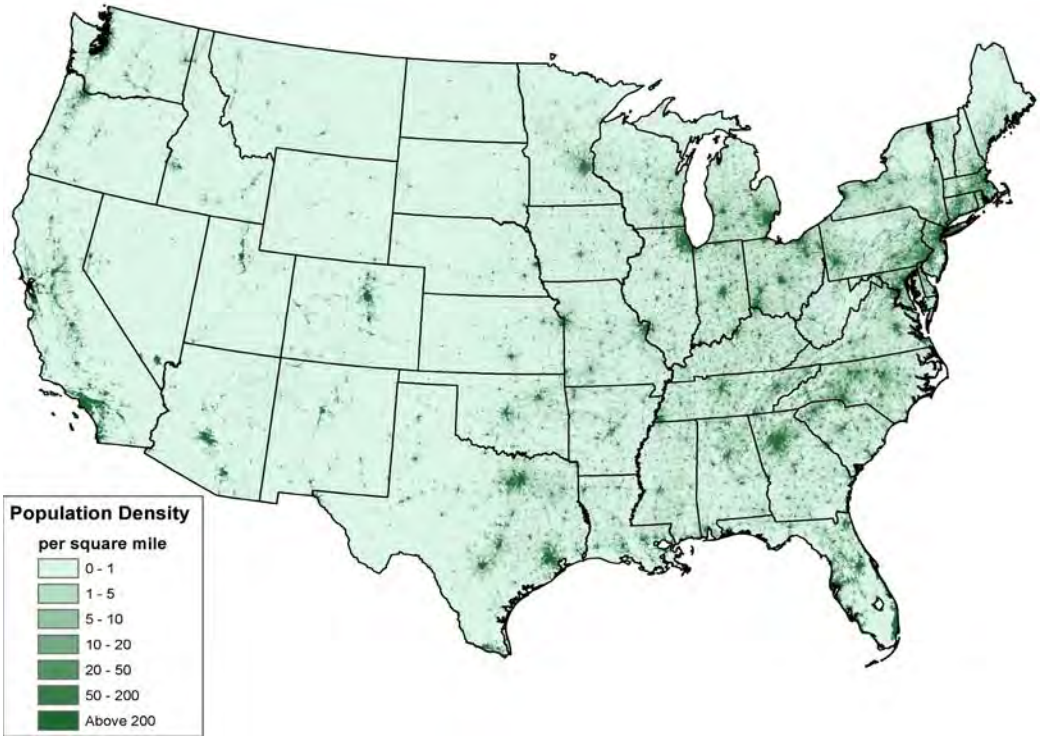

Figure 1. Population Density in the Continental United States

Figure 2 illustrates the density of ZIP Codes in continental United States, of which there are roughly 43,000.

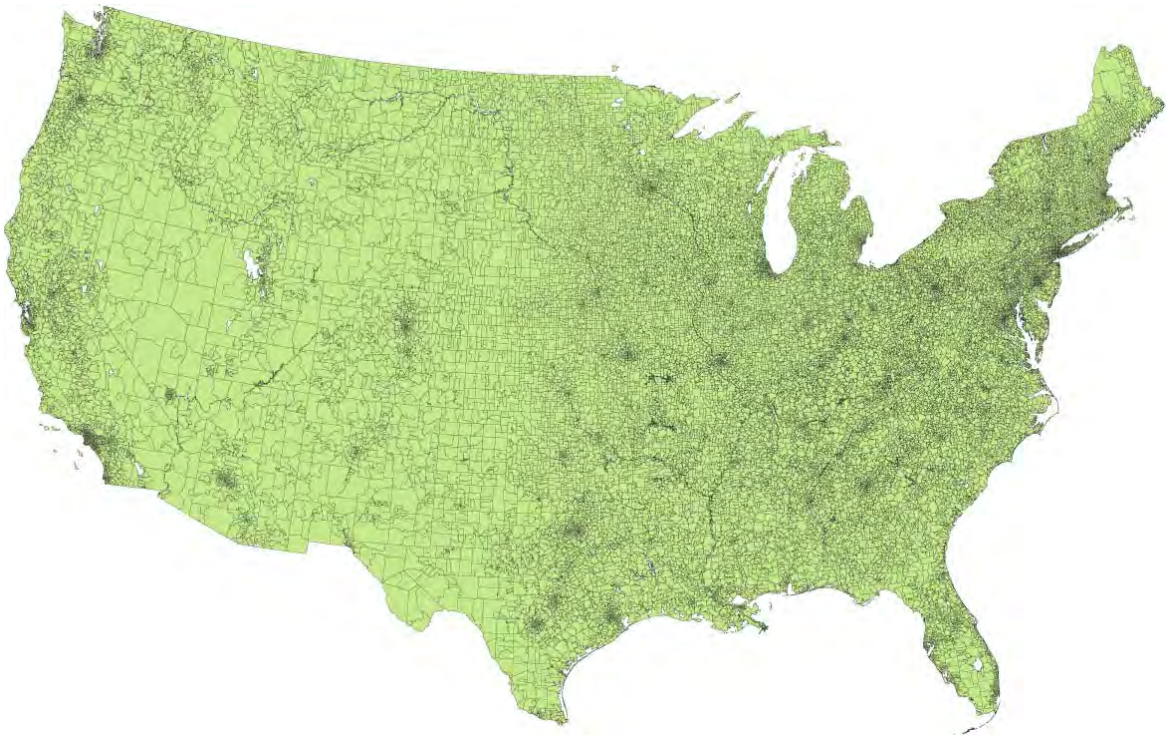

Figure 2. Map of the Continental United States showing the ZIP Codes

Figure 3 shows a zoom-in of ZIP Codes in the San Francisco area on the left and the Los Angeles and San Diego areas on the right.

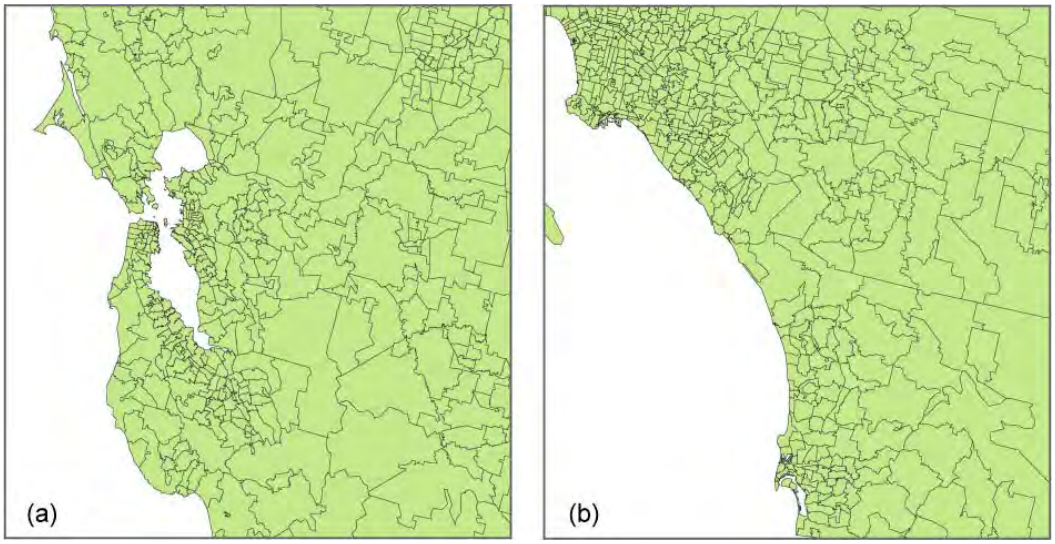

Figure 3. ZIP Codes in San Francisco (a), Los Angeles (b, upper left), and San Diego (b, bottom)

There are 3,109 counties or county equivalents in the continental United States, categorized as follows:

2,980 Counties
64 Parishes in Louisiana
42 Independent Cities (1 in MD 1 in MO, 1 in NV, and the remainder in VA)
1 District (District of Columbia)

Figure 4 shows the counties in the continental United States.

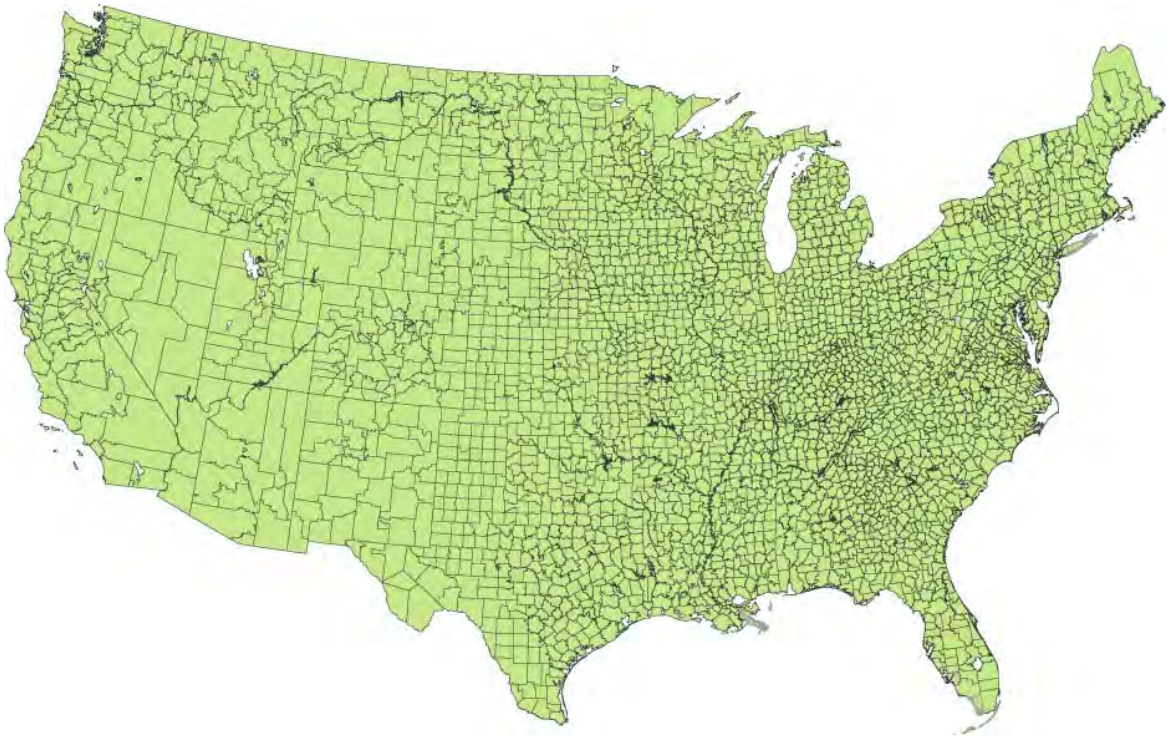

Figure 4. Map of Counties in the Continental United States

1.3 Data Sources

Key data sources used in the development of the AIR Earthquake Model for the United States are as follows:

Event Generation: Data for the model's hazard component came from the 2008 United States Geological Survey (USGS) national earthquake hazard model, which is described in USGS Open-File Report 2008-1128, *Documentation for the 2008 Update of the United States National Seismic Hazard Maps*. This information includes the process for determining event scenarios for the New Madrid Zone, and the zone boundaries in the Charleston area. Data for the time-dependent model incorporates information from the Working Group on California Earthquake Probabilities, using the empirical and fault-specific models from the Uniform California Earthquake Rupture Forecast (UCERF2).

Local Intensity: The AIR model implements attenuation equations, used by the USGS model, developed by Boore and Atkinson (2008), Campbell and Bozorgnia (2008), Chiou and Youngs (2008), and Abrahamson and Silva (2008). Additional equations were used to determine ground motion intensity for areas outside of California. Data on soil conditions and groundwater depth were obtained from the USGS and several state geological surveys. For a complete list of soil data sources, see Table 7. See Section 4 for details on all of the sources for local intensity data and attenuation equations that were used in the model.

Fire Following Module: Fire engine data was collected from individual local fire departments (see Figure 95 for source locations) and wind speed data was obtained from the National Weather Service.

Workers' Compensation Line: Information on injury costs was obtained from the National Council on Compensation Insurance (NCCI); worker counts were obtained from Claritas.

1.4 Historical Catalog

The AIR Earthquake Model for the United States utilizes United States Geological Survey (USGS) seismic information on faults and background seismicity. Much of this information is based on the USGS historical catalog that is described in the publication, *Documentation for the 2008 Update of the United States National Seismic Hazard Maps* (USGS Open-File Report 2008-1128). For the western United States, historical earthquakes of moment magnitude (M_w) 4.0 or greater are considered; for the central United States, the minimum magnitude is mbLg 3.0[1]. Because the damage caused by earthquakes below magnitude M_W 5.0 is very limited in the United States, those events were excluded from the historical catalog which is released with the model.

1.5 Stochastic Catalog

The model incorporates two 10,000-year catalogs of simulated earthquakes: a time-dependent catalog with 68,877 events and a time-independent catalog with 68,570 events.[2] The time-dependent catalog is the standard (recommended and therefore default) catalog. Unless otherwise specified, the exhibits in this document refer to the time-dependent catalog. For more detail on time dependence, see Section 3.5.

[1] mbLg was converted into Mw using relationships from Johnston (Johnston, A.C., 1996a, "Seismic Moment Assessment of Earthquakes in Stable Continental Regions—I. Instrumental Seismicity," *Geophysical Journal International*, 126:381–414)

[2] Note that catalogs of 50,000 and 100,000 years are also available. The 100,000-year time-dependent catalog consists of 685,830 events.

The number of simulated years that contain a particular number of simulated earthquake events is illustrated in the following figures. Figure 5 shows the distribution of annual event frequency for the 10,000-year time-dependent model. Figure 6 shows the distribution of annual event frequency for the 10,000-year time-*in*dependent model.

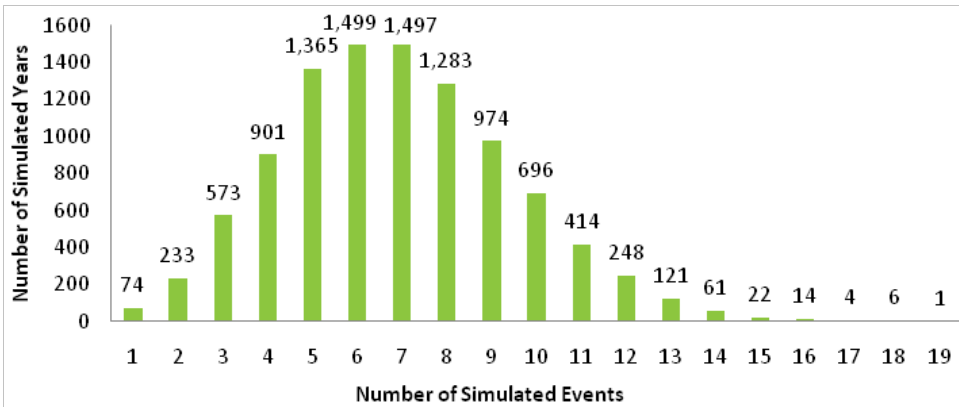

Figure 5. Distribution of Annual Simulated Event Frequency, 10K Time-Dependent Catalog

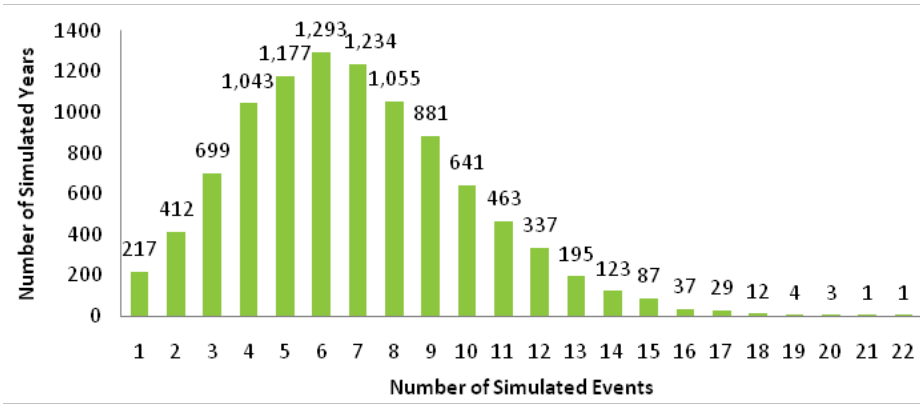

Figure 6. Distribution of Annual Simulated Event Frequency, 10K Time-Independent Catalog

Each event in the stochastic catalogs is associated with an epicenter, magnitude, rupture length and width, azimuth, dip, dip azimuth, depth, and rupture mechanism.

The magnitude distribution of simulated events is shown in the following tables. Table 1 and Table 2 show the magnitude distribution for the 10K time-dependent and time-independent models, respectively. The tables indicate that events of magnitude 5.0 to 5.5 constitute well over 50% of the simulated catalogs.

Table 1. Distribution of All Simulated Events by Magnitude – 10K Time-

Dependent Catalog

Magnitude	≥ 8.0	7.5 to 8.0	7.0 to 7.5	6.5 to 7.0	6.0 to 6.5	5.5 to 6.0	5.0 to 5.5
Event Count	55	208	1,022	3,897	6,793	16,276	40,606
Percentage	0.07%	0.3%	1.5%	5.6%	9.9%	23.6%	58.9%

Table 2. Distribution of All Simulated Events by Magnitude – 10K Time-Independent Catalog

Magnitude	≥ 8.0	7.5 to 8.0	7.0 to 7.5	6.5 to 7.0	6.0 to 6.5	5.5 to 6.0	5.0 to 5.5
Event Count	51	221	1,031	3,912	6,840	16,385	40,110
Percentage	0.07%	0.3%	1.5%	5.7%	9.9%	23.9%	58.5%

1.6 Optimization of the Stochastic Catalog

Several regions of the United States display low levels of historical seismicity. In order to build a stochastic sample of simulated earthquake activity that adequately captures the seismicity in these regions, it was necessary to expand the sample to 1,000,000 years. This one-million-year catalog accurately represents the background seismicity in the areas of lowest seismicity, in accordance with the USGS.

However, loss calculations using a one-million-year catalog require extensive computational resources. In order to deliver catalogs to our clients that are both accurate and computationally efficient, an optimization process has been implemented to obtain a representative extraction from the 1M catalog of 100,000 years (10 times smaller) that minimizes sampling variability (the error that appears in the statistical characteristics of a sample when its size is reduced).

This process consists of a multi-criteria optimization procedure in which three aspects of the catalog are evaluated: the magnitude-rate distributions for each region in the US, the ground motion at specific locations and at specific return periods, and the loss distributions. Maintaining these three main traits of the one million year sample in a smaller 100,000-year sample is a complex endeavor that AIR solves using advanced evolutionary computation techniques. The result is a 100K catalog that performs similarly to the one-million-year catalog, not only with respect to the magnitude-rate distributions but also with respect to ground shaking and loss distribution.

Acknowledging that even catalogs of 100K-year length may still pose unacceptable computational demands when multiple runs are needed, AIR delivers a standard catalog of 10,000 years (and 50,000 years). This smaller catalog is again optimized from the 100K sample in order to obtain a catalog that is representative of the greater set (the sample of 10K must be included in the 100K catalog for software functionality purposes, therefore the extraction is not carried out directly from the one-million-year catalog). In this case, the optimization is performed based on loss distributions at the state level. This is accomplished in an iterative loop, where different potential extractions are evaluated based on the accuracy of the industry exceedance probability (EP) curves rendered by the 10K catalog in comparison to the industry EP curves constructed from the 100K sample. Special interest zones such as New Madrid are also included in the optimization to guarantee that the final 10K extraction yields results comparable to the 100K results even in areas of very low seismicity such as this one.

With these innovative techniques, AIR has succeeded in integrating the high accuracy of very large samples with the computational efficiency of smaller catalogs.

1.7 Model Resolution

The resolution of the surface-geology data used in shake-damage calculations varies from 50 meters for Manhattan island in New York City to 1,020 meters for eastern South Carolina. For most of the continental U.S., the model employs maps of about 500 meters resolution in the central and eastern part of the country, with exceptions in the New Madrid area, Charleston, and the northeast. The resolution used for most of California is 180 meters, with a 90-meter resolution for San Francisco, Los Angeles, and Santa Ana. Data at 190-meter resolution is used for Oregon, and a 90-meter resolution is used for Washington state.

In CLASIC/2, users may input a risk at the level of county, ZIP Code, street address or latitude and longitude. CATRADER industry loss files are developed using ZIP Code resolution industry exposures. CATRADER users may input resolutions at the county or state level; losses are reported at the county level.

1.8 Modeled Lines of Business

The lines of business included in the AIR Earthquake Model for the United States are residential, mobile home, commercial, industrial, automobile and workers' compensation.

1.9 Modeled Construction and Occupancy Classes

Number of Supported Construction Classes: 75

Number of Supported Occupancy Classes: 111

1.10 Modeled Industry Losses

Figure 7 illustrates the relative loss costs for earthquakes in the Continental U.S.

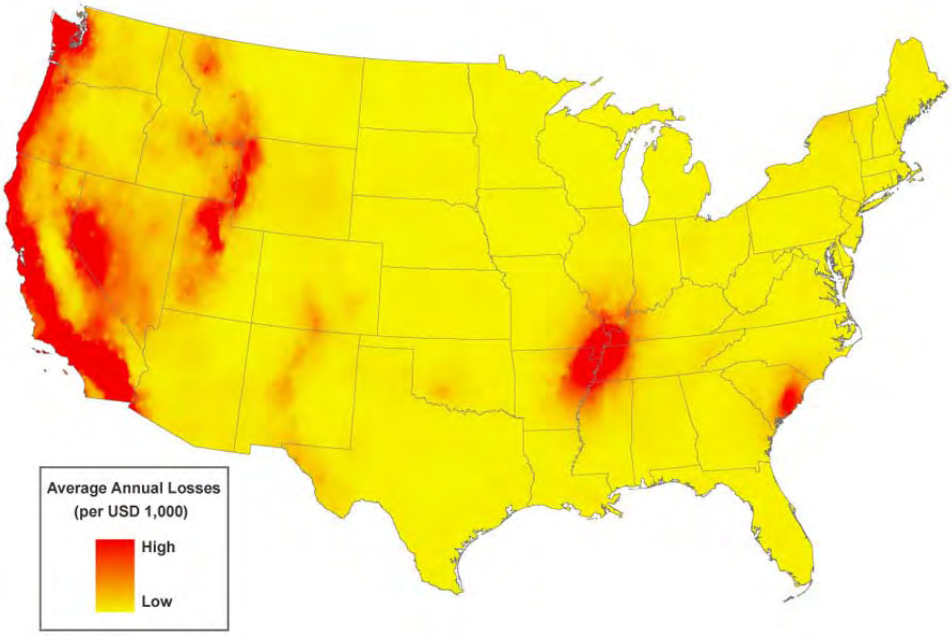

Figure 7. Earthquake Risk (Loss Costs) in the Continental United States

Listed below in Table 3 are modeled **insured** loss estimates for significant historical earthquakes affecting the continental United States based on 2009 (year-end) industry exposures. Please note that the losses *include* the effects of demand surge.

Table 3. Modeled Insured Losses for Historical Earthquakes (in billions USD) for Various Lines of Business – Shake and Fire-Following Damage

Historical Earthquake	Total Losses (USD Billions)
1812 New Madrid, MO	109.288
1906 San Francisco, CA	91.612
1886 Charleston, SC	41.110
1838 San Andreas fault, CA	28.467
1994 Northridge, CA	23.555

1868 Hayward fault, CA	23.006
1857 Fort Tejon, CA	8.664
1989 Loma Prieta, CA	6.342
1933 Long Beach, CA	5.460
1911 Calaveras, CA	4.184

1.11 The United States Insurance Market

The United States property-casualty insurance market is the largest in the world, with premiums totaling approximately USD 419.3 billion in 2009, a decrease of about USD 26.1 billion from 2008. The after-tax return on equity (return on surplus) increased from 1.7% in 2008 to 6.2% in 2009. The policyholder surplus increased to USD 519.3 billion in 2009, from USD 477.2 billion in 2008.

Underwriting results for the property-casualty industry as a whole were relatively solid, due to the absence of major hurricane activity in the United States in 2009, favorable prior-year loss-reserve development, and a sizable reduction in underwriting losses in the mortgage and financial guaranty segments. Losses from catastrophic events totaled approximately USD 14.6 billion, down from USD 28.2 billion in 2008 when Hurricane Ike caused significant underwriting losses.

The earthquake risk in the continental United States is primarily associated with the west coast, with the highest concentration in California, where most of the population (over 36 million) resides along the coast in seismically active areas. North of California is the Cascadia subduction zone, which has the potential of producing massive earthquakes. However, even though the west coast is more seismically active than the rest of the country, 39 states are associated with earthquake risk. Some of the largest earthquakes in U.S. history occurred east of the Rocky Mountains, in New Madrid, Missouri, and Charleston, South Carolina.

Earthquake damage is not covered under standard residential or commercial insurance policies, but is instead available as an endorsement to an existing policy. However, insurers that don't offer coverage for earthquake damage may still be affected by related losses such as those due to fires following an earthquake. These losses can increase due to claims for business interruption and additional living expenses. Cars and other vehicles are covered for earthquake damage under the comprehensive part of an auto insurance policy.

The most costly earthquake in U.S. history is the one that struck Northridge, California, on January 17, 1994. It caused an estimated USD 20 billion in property damage, including USD 12 billion in insured losses. Two years after the

Northridge earthquake, the California Earthquake Authority (CEA) was created to ensure the availability of earthquake coverage for homeowners, which became increasingly hard to obtain due to insurers' fears of insolvency from another massive earthquake. The CEA is now one of the world's leading residential earthquake insurers, with 775,000 policies in force, and 17 participating insurers. However, only about 12% of homeowners in California buy earthquake coverage. This is a decrease from 30% in 1996, due to several factors including the high cost of earthquake coverage and the fact that earthquake insurance is not mandated by mortgage lenders.

The risk of insured losses due to earthquakes has increased in recent years due to increasing urban development in seismically active areas such as California, and the increasing vulnerability of older buildings, which may not have been built or upgraded to current building codes. According to insurance records, direct premiums written for earthquake coverage in California, excluding the CEA, totaled about USD 1.06 billion in 2007, or about 68% of the total earthquake premiums in the United States, which come to about USD 1.56 billion.

1.12 Navigating the Document

Figure 8 illustrates the components of the AIR Earthquake Model for the United States. Section 2 of this document provides a brief overview of earthquakes and earthquake risk in the continental United States. Section 3 details the generation of simulated events that populate the stochastic catalog, and Section 4 describes how ground shaking is modeled locally. Section 5 discusses the model's damage functions for residential, mobile home, commercial, and automobile properties, while Section 6 describes damage functions for industrial facilities. Section 7 discusses insured loss calculation. Section 8 offers selected references and Section 9 provides an overview of AIR Worldwide .

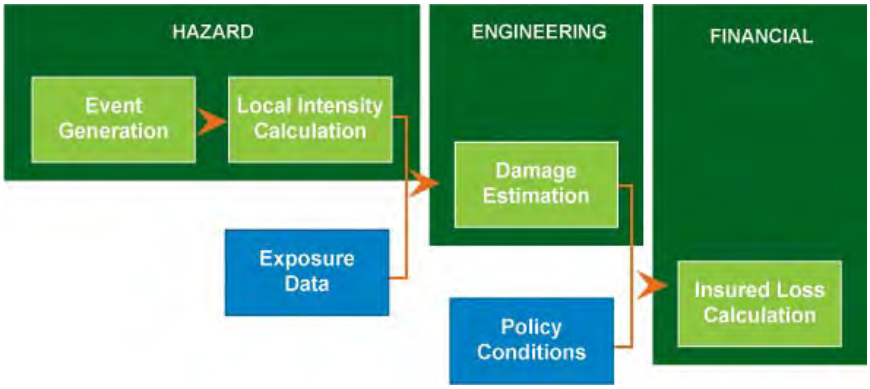

Figure 8. Components of the AIR Earthquake Model for the United States

2 Earthquakes in the Continental United States

This section provides an overview of earthquakes and introduces some important concepts in earthquake modeling.

2.1 Earthquakes: An Overview

An earthquake results from a sudden displacement of rock along a fault. It accompanies a rapid release of energy in the form of seismic waves, which propagate outward from a focus.

The process begins when rocks that experience stress along faults begin to deform as the strain within them builds. When the stress exceeds the strength of the rock and overcomes the friction that resists the relative movement of opposite sides of the fault, the fault ruptures and releases energy. Some of the energy released dissipates as friction along the fault; the rest is transferred as seismic waves that radiate from the initial point of rupture and cause ground motion at the earth's surface.

Faults are rarely found in isolation; instead, they tend to form zones of related fault traces. Long faults may be segmented, with each segment having an individual rupture history and mechanism. Ruptures during a weak to moderate earthquake are believed to be contained within one segment of a fault, but more powerful earthquakes may manifest themselves along multiple segments. Fault zones vary in depth, width, and orientation.

A fault plane can be vertical or sloping in relation to the earth's surface. In sloping faults, the rock volume above the fault plane is known as the hanging wall, and the rock volume below the fault plane is the footwall. One type of earthquake faulting mechanism is dip-slip, which can be subclassified as either normal or reverse faulting. Normal faulting occurs when the hanging wall slips down relative to the footwall, resulting in an extension of crustal matter. Reverse faulting occurs when the hanging wall lifts relative to the footwall, which causes a shortening of the crustal material. Strike-slip faults have a nearly vertical surface; their movement is horizontal, parallel to the strike of the fault surface. Oblique-slip faulting is a combination of strike-slip and normal or reverse faulting.

While faults may form a visible trace on the earth's surface, some remain buried within the earth. These blind faults represent a significant seismic hazard, as they

are often difficult to detect prior to rupture. Hazard assessment of blind faults is challenging and often plagued with uncertainty.

Generally, active faults are those which have demonstrated activity during the last 10,000 years, or during the Holocene period. Potentially-active faults are those that have demonstrated activity during the last 1.65 million years, or during the Quaternary period.

Plate Tectonics

The theory of plate tectonics was developed to explain the evidence for large-scale motion of the earth's continents. The crust and upper mantle form the rigid, strong lithosphere, which is divided into large plates that move relative to one another. The largest plates are the Pacific, North American, South American, Eurasian, African, and Australian plates.

These lithospheric plates move over the asthenosphere, a hot, viscous layer of weak rock that is continuously moving and transferring heat from the interior to the surface of the earth. The boundaries between plates are where most earthquake and volcanic activity occurs.

There are several types of boundaries between neighboring plates. Convergent boundaries occur where two plates move towards one another; if one of these plates sinks, or subducts, beneath the edge of the other plate, a subduction zone is formed (Figure 9). Seismic activity may be particularly rampant in subduction zones.

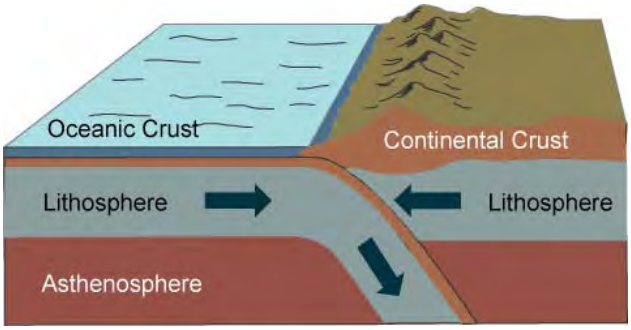

Figure 9. The Earth's Layers at a Subduction Zone

Continental-collision boundaries occur where two low-density plate edges move towards one another; this process may result in crustal rock being thrust upward, which is how linear mountain systems are formed. Divergent boundaries occur where plates move away from one another, which allows for the formation of new crustal material.

Transform boundaries occur where one plate moves past another. Due to massive amounts of friction, however, the plates do not simply glide past each other. Rather, stress builds up in the rocks along the fault until the strain is too great. At that point, the potential energy is released in the form of an earthquake.

While the majority of earthquakes do occur at plate boundaries, intraplate earthquakes can occur along fault zones in the interior of a plate. Large intraplate earthquakes usually have long recurrence intervals, which makes it difficult to estimate the associated risk.

Seismic Waves

Seismic waves transmit tectonic energy through the earth at speeds of up to several miles per second. Seismic waves produce ground motion on the earth's surface that may damage buildings, trees, cars, roads, and other structures. Soil properties, local geological features, and other factors play a role in attenuating or amplifying seismic waves at a given location.

There are several types of seismic waves. Body waves travel through the earth, while surface waves travel along its surface. The two types of body waves that are generated by an earthquake are primary and secondary waves, also known as P waves and S waves, respectively. P waves are fast and capable of traveling through both solids and liquids. These waves exhibit an alternating compression-dilatation motion in the direction of wave propagation. S waves are slower and travel only through solid material. These waves produce a sideways-shearing motion perpendicular to the direction of wave propagation.

Surface waves, which are responsible for the majority of earthquake damage, include Love waves and Rayleigh waves. Love waves move horizontally, perpendicular to the direction of wave propagation. Rayleigh waves are slow waves that move in an elliptical, or rolling, motion. Note that wave amplitude, which is the height of an individual wave cycle, or the maximum displacement, decreases with increasing depth in the earth for these surface waves. The amplitude of a wave is one measure of its destructive potential.

In addition to amplitude, there are several ways to mathematically describe wave activity. The wave frequency is the number of wave cycles per second that pass a reference point. A wave's period is the elapsed time, in seconds, between peaks, or the time it takes one complete cycle of the wave to pass a reference point. The wavelength is the distance between repeating units of a propagating wave of a given frequency at some point in time.

Measuring Earthquake Magnitude and Intensity

The severity of an earthquake can be measured by the damage it inflicts on the earth's surface or by the energy released at its focus, which is where the rupture originates. Earthquake magnitude characterizes the total energy released by an earthquake, while earthquake intensity refers to the resulting level of ground shaking at a particular location and the observed effects of an earthquake on people, buildings, and other features. While the magnitude of an earthquake is a characteristic of the earthquake as a whole, intensity varies from place to place within a disturbed region.

An earthquake's intensity at different locations can be described semi-quantitatively using the Modified Mercalli Intensity (MMI) scale[3], which was developed in its original form in 1902 and is based on observations of shaking severity and its effects at different locations. The MMI at a particular location is based on human judgment and the observed post-event damage. Today, ground motion intensity can be directly measured using strong motion seismographs. The characteristics of ground motion intensity can be quantified by physical parameters such as peak ground acceleration (PGA) and spectral acceleration (Sa). Shaking intensity at a particular location depends not only on earthquake magnitude, but on the local surface geology and the proximity of the location to the earthquake source.

Magnitude is a measure of an earthquake's size. There are several types of earthquake magnitude, including moment magnitude (M_w), Richter magnitude (M_L), body-wave magnitude (M_b), and surface-wave magnitude (M_s). Magnitude scales are generally logarithmic in nature; that is, an increase of one point on a magnitude scale represents approximately a ten-fold increase in wave amplitude and a 30-fold increase in the amount of energy released during the earthquake. AIR models utilize the moment-magnitude scale, which is based on seismic moment. The moment magnitude is defined as:

$M_w = \mu AD$

where

μ = the shear modulus of elasticity

A = the rupture area

D = the average slip over the rupture area

The moment magnitude is considered superior to other magnitude scales because it is based on earthquake source parameters, rather than on a particular type of seismic wave, like the surface-wave magnitude or body-wave magnitude scales, or a particular type of instrument, such as the Richter magnitude scale. The type

[3] Please see http://earthquake.usgs.gov/learning/topics/mercalli.php for a more detailed description of this intensity scale.

and amplitude of the seismic waves that reach an instrument and are recorded depends on earthquake magnitude, the radiation pattern of seismic waves due to different rupture mechanisms, and the complex structures along the propagation path of the seismic waves that are between the source and seismic stations. Different earthquakes can generate different types of seismic waves. Small earthquakes generate seismic waves with short periods while larger earthquakes can generate seismic waves with long to very long periods.

Most seismic waves will saturate beyond a certain magnitude; that is, wave amplitude will not increase beyond that magnitude. Therefore magnitude scales based on the amplitude of a particular type of seismic wave will also experience saturation. Moment magnitude does not have such limitations.

Paleoseismic and Geodetic Data

The modeling of earthquakes requires historical data. For large earthquakes, the catalog is complete further back in time because such events are more likely to have been observed and documented than smaller events. However, improvements in instrument sensitivity and coverage have led to increased recordings of smaller events. The completeness of the historical catalog is therefore a function of time and magnitude.

Paleoseismology and geodetic data are often used to augment instrumentally recorded earthquake catalogs to estimate current seismic hazard. Paleoseismology is the study of the location, timing, and size of prehistoric earthquakes. Prehistoric earthquakes are evidenced by offsets in geologic formations found in exhumed fault zones, signs of rapid uplift or subsidence near coastal areas, laterally offset stream valleys, and liquefaction artifacts, such as sand boils.

The geodetic measurement of fault slip rate is another source of information that is used to supplement historical data. The Global Positioning System (GPS) is now the most widely used technology to measure fault slip rates of crustal deformations in a region. The observed crustal deformation represents elastic strain accumulation in the crust. By calculating the rate at which elastic strain accumulates along a fault or seismic zone, estimates can be made as to how often large earthquakes may occur.

Geodetic data assists in estimating the frequency of large-magnitude earthquakes; for smaller events, the historical earthquake data tends to be more complete. For earthquakes above a given magnitude, which is region-dependent, geodetic and paleoseismic data become more reliable compared to historical earthquake data, as Figure 10 illustrates.

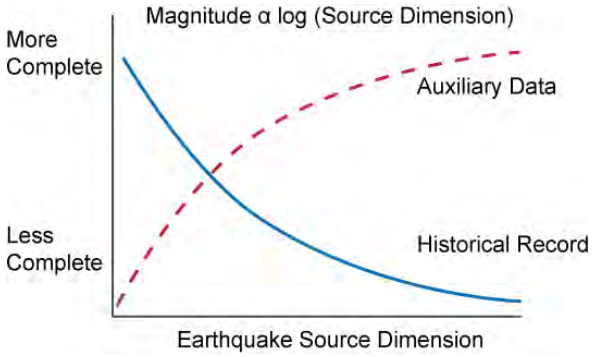

Figure 10. Completeness of Auxiliary and Historical Record Data, Based on Earthquake Source Dimension

The Gutenberg-Richter Relationship

The Gutenberg-Richter (GR) relationship (Figure 11) expresses the association between magnitude and the earthquake occurrence rate on a fault or in a given area, at or above each magnitude. The relationship can be used to provide a more complete picture of seismicity in regions where historical data is lacking, as it holds over a wide variety of magnitudes and locations.

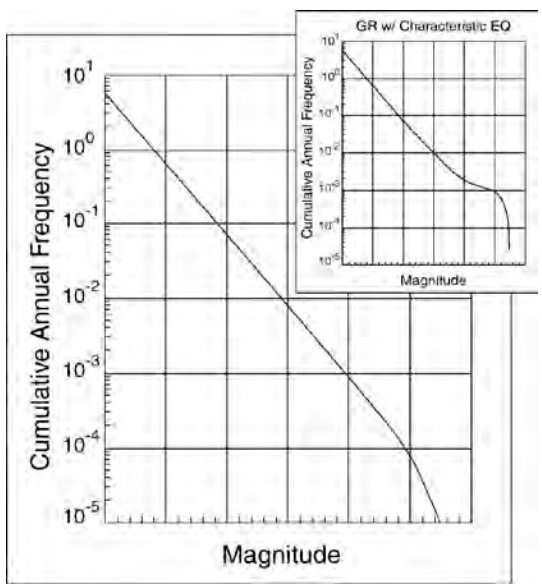

Figure 11. Sample Gutenberg-Richter Distribution

The GR relationship is parameterized by the a-value, which is the logarithm of the earthquake occurrence rate above some reference magnitude, and the b-value, which is the rate at which the logarithm of the cumulative-annual frequency decreases as the magnitude increases. Scientists usually truncate this relationship at a limiting magnitude above which the probability of an earthquake's occurrence becomes zero, as illustrated in Figure 11.

Note that the a-value is plotted as the y-intercept, and the b-value is represented by the slope of the line. The presence of large-magnitude characteristic earthquakes modifies the shape of the magnitude-frequency distribution.

Historical seismicity data, paleoseismic data, and geodetic slip-rate data are used to estimate the upper-bound magnitude of the GR distribution.

Characteristic Earthquakes

The characteristic earthquake concept states that active faults tend to generate earthquakes of about the same magnitude at regular time intervals. This concept is used to simulate seismic activity along active faults. In order to model seismicity using the characteristic earthquake method, the earthquake magnitude and return period must be defined. Magnitude can be estimated from historical data, paleoseismological data, and the length of the fault. The return period is estimated from paleoseismological data, fault slip rates, or seismic-moment rates as estimated from fault slip rates.

2.2 United States Earthquake Risk

Throughout the continental United States, earthquakes are generated along the plate interfaces, within plate slabs, and along crustal faults in the middle of the plates. All parts of the country experience low-intensity tremors year-round, and even destructive earthquakes are not limited to the west coast. Each century has seen one or more large-magnitude earthquakes strike inland regions as well as the west coast, and 39 states are associated with earthquake risk.

The hazard due to earthquakes in the continental United States is largely associated with California, where they pose a continual threat. The high seismic activity in this area is due to the on-land boundary between the Pacific and North American plates, which is located along California's coast. Farther north along the west coast, in the Cascadia region, the Juan de Fuca plate subducts under the North American plate and this activity has generated large damaging earthquakes in the Pacific Northwest, although not as frequently as in California.

Across the Rocky Mountains, in the central and eastern United States, the hazard drops significantly, however notable earthquakes have occurred in this part of the country. Earthquakes in this region are not as frequent as on the west coast, but the geological conditions in the central and eastern regions cause earthquakes of a given magnitude to affect a much larger area than earthquakes of the same magnitude that strike the west coast.

Figure 12 illustrates the historical seismicity of the continental United States.

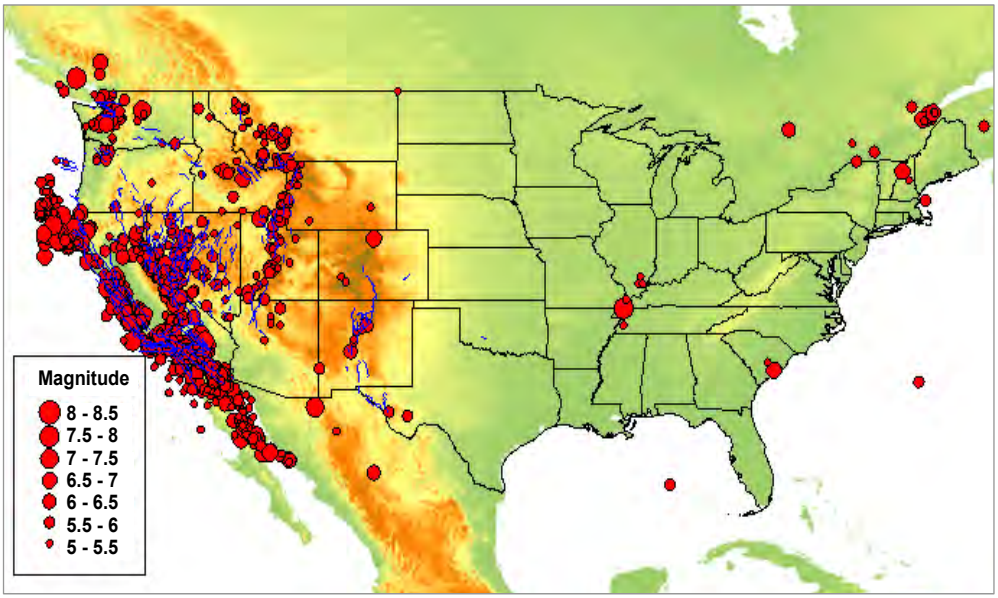

Figure 12. Historical Seismicity and Faults in the Continental United States ($M_W \geq 5.0$)

The seismically active areas in the continental United States are generally distributed among several states, with the highest exposure concentrated along the west coast. California, in particular, has a high exposure due the large and complex fault system, of which the major contributor is the San Andreas fault, as well as other major faults that are part of the San Andreas system. This part of California is also highly populated, with the major cities located along the coastline.

Oregon and Washington also have their highest populations located near the coast. The cities in this area have experienced fewer earthquakes than those in California, but the area is exposed to very large and damaging events due to the massive earthquakes that can be generated from the subducting Juan de Fuca plate. The activity from the plate motion is not limited to the west coast, however. A significant amount of deformation caused by the west coast plate activity affects much of the western interior and has been known to reach areas all the way to the eastern front of the Rocky Mountains.

The central and eastern regions of the country have far fewer earthquakes than the west, but it does have areas with earthquake risk due to intraplate deformation. In the central United States, there is abundant evidence of earthquakes in the Mississippi, Ohio, and Wabash River valleys. Three of the largest historical earthquakes known to strike the continental United States occurred in the winter of 1811–1812 along the New Madrid seismic zone.

In the northeastern and southeastern parts of the nation the earthquake risk is relatively low; however there are notable exceptions including the magnitude 7.3 earthquake that shook Charleston, South Carolina, in 1886, and the magnitude 6.0 earthquake that struck Cape Ann, Massachusetts, in 1755.

California

Earthquakes in the continental United States are mostly associated with the state of California, with good reason. Every year, California experiences approximately 500 earthquakes that are large enough to be felt. Earthquakes pose a continual major threat for the state's 36 million residents, most of whom live along the west coast in some of the most seismically active areas of the region.

California is the site of the on-land boundary between the Pacific and North American plates, which contains a complex system of faults. The right lateral strike-slip motion between the two plates occurs in California at a rate of about 33-37 mm/year, with the Pacific plate (west of the boundary) moving northwest, and the North American (east of the boundary) plate moving southeast. About 70 percent of the slippage is carried along the San Andreas fault, which runs about 1,300 kilometers (808 miles) in length. The fault system also includes a number of major faults running parallel to the San Andreas, such as the Calaveras, Hayward– Rodgers Creek, San Jacinto, and Elsinore faults.

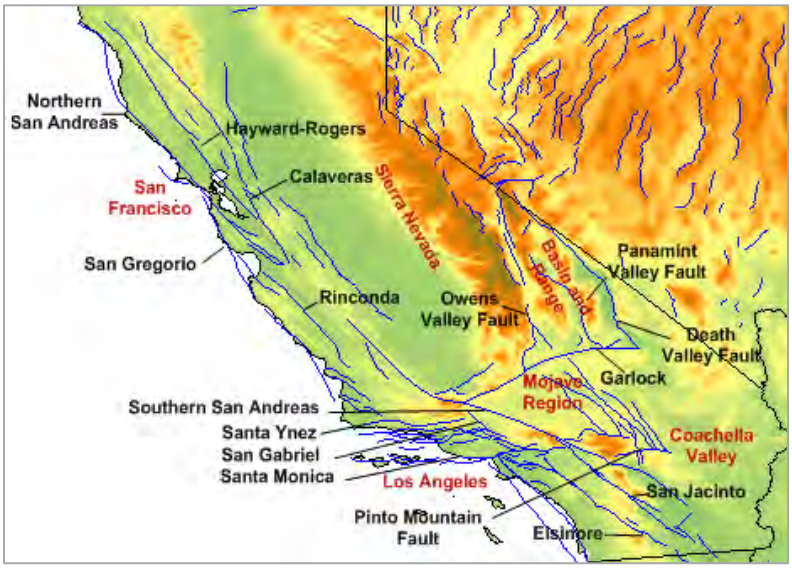

Figure 13. Some of the Major Faults in California

A lower slip rate of about 8-10 mm/year is found near the north part of the Coachella Valley, in southern California, where some of the right-lateral shear from the Pacific-North American plate boundary leaves the San Andreas fault.

This shear continues along right-lateral faults across the Mojave Desert and along the east side of the Sierra Nevada. In California's Basin and Range province, right-lateral faults, including the Death Valley fault system, also accommodate approximately 8 mm/year of right-lateral shear, which is consistent with geodetic deformation rates in the area.

Eastern California – Nevada

A large part of western Nevada is affected by the eastern California shear zone, which runs northwest from the Gulf of California. The movement in this zone is about 10 to 12 mm/year, or about 25 percent of the total movement of the North American plate. Between this shear zone and the San Andreas area are the Sierra Nevada mountains, which move along with the plate that lies under them.

The central Nevada seismic zone, which adjoins seismic zones in southern California, was defined during a series of earthquakes that occurred between 1915 and 1954. The sequence started in October of 1915 when an earthquake of magnitude 7.1 struck Pleasant Valley. In 1932, Cedar Mountain was struck by a magnitude 7.3 shock, which was followed in 1934 by another shock of magnitude 6.5 at Excelsior Mountain. The final earthquakes in the sequence occurred in 1954, when the Carson Sink and Dixie Valley were struck by four earthquakes with magnitudes ranging between 6.6 and 7.1.

Southern Nevada contains a broad seismic area in the west-east direction that reaches from eastern California into Utah. Seismic activity has been observed or recorded in the Pahranagat shear zone and the Caliente region as well as the Goldfield region in the southwestern part of the state. In 1988, two earthquakes of magnitude 3.7 occurred in the Boulder City-Lake Mead area, possibly due to the Mead slope fault. Earthquakes have also struck Las Vegas; in November, 1989, and February, 2001, two relatively small earthquakes with magnitudes around 3.5 were widely felt in the Las Vegas area.

Cascadia Subduction Zone

In January of 1700, an extremely powerful earthquake of magnitude 9.0 struck the Cascadia region, which extends 1,200 kilometers (746 miles) along the west coast from Cape Mendocino, California, through Oregon and Washington, up to Vancouver Island, British Columbia. This earthquake, which is believed to be the largest to have ever occurred in the continental United States, triggered a tsunami that traveled from the American coast to Japan, where it damaged several coastal villages.

The immense earthquake in 1700 was caused by tectonic stresses due to the subduction of the Juan de Fuca plate beneath the North American plate at a rate of about 40 mm/year. The earthquakes in this zone can be extremely powerful, with magnitudes of 8.0 and higher. They can also be deep, and the Cascadia subduction zone has seen earthquakes as deep as 35 kilometers (22 miles). Deep earthquakes have ground motion characteristics that differ from shallower earthquakes, and generally don't produce surface waves as readily as shallow ones.

Figure 14. The Pacific, Juan de Fuca, and North American Plates in the Cascadia Subduction Zone

Some of the earthquakes experienced in this area, in addition to the 1700 event, include three earthquakes of magnitude 7.0 and higher, which struck California's northern coast during the nineteenth century. In November, 1873, a magnitude 7.3 earthquake occurred along the coast near the California-Oregon border. In May, 1878, this same area was the site of an earthquake with a magnitude exceeding 7.0, located about 75 kilometers (47 miles) offshore near the Mendocino fault. Several earthquakes in the Puget Sound area, including ones in the city of Seattle, have cause heavy damage including major events in 1949, 1965, and most recently in 2001.

The Intermountain United States

The Intermountain United States comprises Idaho, Nevada, Arizona, Utah, Montana, New Mexico, Colorado, and Wyoming. It includes the Basin and Range province (in eastern California and Nevada), the Colorado Plateau, the Rocky Mountains, and the Great Plains. The area is the site of the Intermountain Seismic

Belt (ISB), which runs from northwestern Montana through Wyoming, Idaho and Utah, and further into southern Nevada and northern Arizona. Other major seismic zones in the Intermountain region include the Sierra Nevada-Great Basin zone; the central Nevada seismic zone; and the Rio Grande rift.

The ISB includes several fault zones including the Madison and Hebgen faults in Wyoming near Yellowstone National Park and, at the center of the ISB, the Wasatch fault zone in Utah. The Wasatch fault is at the base of the Wasatch mountains, which run along the eastern edge of Ogden, Salt Lake, and Provo, which are the major cities in Utah and home to about 75 percent of the state's population.

Since 1900, the ISB has been the site of 50 earthquakes with magnitudes between 5.5 and 7.5. The two largest earthquakes on record are a magnitude 7.5 earthquake, which struck Hebgen Lake, Montana, in 1959, and a magnitude 7.3 event at Borah Peak, Idaho, in 1983. Most of the earthquakes in this area are shallow, occurring at depths less than 20 kilometers (12 miles).

The Rio Grande rift extends from southern New Mexico northward to central Colorado. It includes the cities of Santa Fe and Albuquerque, where most of New Mexico's population is located. The area near the town of Socorro experienced quite a bit of earthquake activity during the nineteenth century, when a series of 22 shocks struck the area between 1849 and 1850. Socorro also experienced the largest earthquake observed in this region, a magnitude 6.0 shock that struck the area in November, 1906.

Central United States

The central United States is in the stable craton, which stretches from areas east of Denver, Colorado, across the Midwest. Earthquakes do occur in the area however, and when they do, the seismic waves propagate more efficiently due to the geology of the area. In the stable interior, the lithosphere is cooler and thicker than in the western United States, allowing ground motion to travel over a larger distance than on the west coast.

Some areas in the central United States show evidence of significant seismic activity in the past. These include southern Oklahoma, where paleoliquefaction features indicate that two large earthquakes of magnitude 7.0 occurred during the past 3,000 years along the Meers fault. Evidence along the Cheraw fault in southeastern Colorado indicates that earthquakes of a similar magnitude have occurred in that region over the past 10,000 years. More recently, over the past 150 years, eastern Kansas and Nebraska have experienced two earthquakes of magnitude 5.0.

Several times during the past century, moderate earthquakes have been widely felt in the Wabash Valley seismic zone along the southern border of Illinois and Indiana. Throughout the region, between 150 and 200 earthquakes are recorded annually although most are too small to be felt. Liquefaction features in the area indicate seismic activity, including earthquakes with magnitudes of 6.5 to 7.5 with recurrence periods of a few thousand years.

The New Madrid Seismic Zone

The New Madrid seismic zone, and the smaller Wabash Valley seismic zone nearby (Figure 15), are areas of great interest due to the catastrophic earthquake cluster of 18111812, which ruptured the Reelfoot fault. The zone is located in the central Mississippi Valley and encompasses an area that includes northeastern Arkansas, southeastern Missouri, western Tennessee, western Kentucky, and southern Illinois. It is named after the town of New Madrid, Missouri, which was the closest settlement to the epicenter of the 1811–1812 earthquakes. This area is not part of the stable craton but is instead included in the extended margin, which extends along the south and up the Atlantic coast.

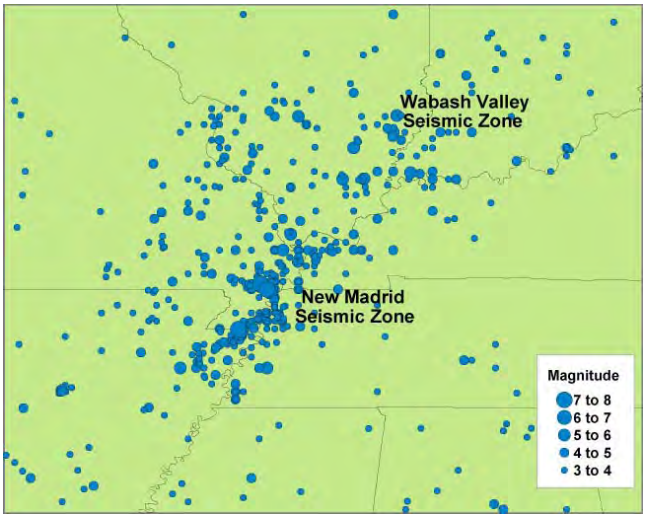

Figure 15. Historical Seismicity in the New Madrid and Wabash Valley Seismic Zones ($M_W \geq 3.0$)

The earthquakes of 1811–1812 occurred over a three-month period, and included three extremely powerful shocks with magnitudes well over 7.0. These earthquakes affected the landscape profoundly; it changed the topography over a very large area of about 600,000 square kilometers (232,000 square miles). The land was raised and sunk in areas. Fissures, sinks, sand blows, and large landslides occurred over a huge area of 78,000–129,000 square kilometers (30,000 – 49,800 square miles). There was, however, no surface rupturing.

Even after 1812 the area experienced hundreds of aftershocks, which continued for several years. Other large earthquakes have also struck the area since that time, including an event of magnitude 6.0, which occurred in January of 1843 and another of magnitude 6.2, which occurred in October of 1895.

The Southeastern United States

Evidence of significant earthquakes in the southeastern United States is provided by paleoliquefaction features in the Atlantic coastal plain. These are associated with nearly vertical faults that formed in the bedrock 220 million years ago, during the Triassic period, when the Atlantic Ocean opened.

Within this region, one of the areas of particular interest is the coastal plain of South Carolina. This is the site of the Middleton Place-Summerville seismic zone, which contains two faults: the deep Woodstock fault, which run northeast, and the shallower Ashley River fault, which runs northwest. Recently there has been little seismic activity in this area; however it is the site of a magnitude 7.3 earthquake, which struck Charleston in 1886.

Seismic activity is also found in northeastern Alabama, northwestern Georgia and eastern Tennessee, where the seismic zone runs parallel to the fold-and-thrust belt of the Appalachian Mountains. The earthquakes in this area generally do not have magnitudes exceeding 4.7, and have not been known to cause damage. There is also no evidence of prehistoric shocks although there is some indication of stress accumulating in the region. If any of the bedrock faults in this region show activity, it could be due to a weak lower crust or increased fluid pressure within the upper crust.

The mid-Atlantic and central Appalachian regions, including Maryland, have experienced some low-level tremors, but it is an area of very low earthquake risk. Maryland contains numerous faults, but none are known to be active.

The Northeastern United States

Similar to the New Madrid and Charleston areas, the northeastern United States has been the site of large intraplate earthquakes. They are rare when compared to the west coast; most earthquakes in the region have small magnitudes and are not widely felt. However, seismic activity is persistent, which indicates that some crustal deformation is occurring.

The most recent significant earthquake in the area occurred on September 25, 1998, when a magnitude 5.2 event struck Pymatuning Reservoir, Pennsylvania. In 1904, an earthquake with an intensity of VII (MMI scale) was recorded in

Eastport, Maine. One of the most severe earthquakes known to occur in the northeast was the Cape Ann earthquake of 1755, which struck the Boston, Massachusetts area with a magnitude of 6.0 causing considerable damage.

The northeast is affected by the Charlevoix seismic zone in eastern Canada, also known as the Charlevoix-Kamouraska seismic zone, located along the St. Lawrence River, about 100 kilometers (62 miles) north of Quebec City. Since 1663 this area has experienced five earthquakes of magnitude 6.0 or greater. Remote sensing indicates strike-slip to reverse faulting on buried crustal faults, and crustal weakness combined with fluid pressure are believed to contribute to the earthquake activity.

2.3 Significant Historical Earthquakes in the United States

Six of the more significant earthquakes in U.S. history are described in this section. They are notable in terms of the long-term effects on the surrounding environment and the damage that was incurred. Major events, such as the 1994 Northridge, California earthquake can also have a permanent effect on building codes and insurance coverage.

New Madrid Region (1811–1812)

Between December 16, 1811, and March 15, 1812, a series of devastating earthquakes struck the interior of the continental United States. The series defined the New Madrid seismic zone, named after New Madrid, Missouri, which was the town closest to the epicenter of the earthquake sequence. During this time period, the area was shaken by over a hundred moderate to large earthquakes with magnitudes between 4.5 and 7.6.

Included in the earthquake sequence was a cluster of very large events: an earthquake with a magnitude of 7.2 on December 16, 1811 (followed by another shock of 7.0), another with a magnitude of 7.1 on January 23, 1812, and the largest with a magnitude of 7.7 on February 7, 1812. Although the first shock was reportedly extremely violent, the two aftershocks that struck six hours later were much more destructive.

Most of the destruction was done to the landscape, which still shows evidence of uprooted forests, massive landslides, sand blows, and fissures covering a very large area of about 600,000 square kilometers (232,000 square miles). Shaking was felt throughout much of the United States and even as far away as Quebec, over an area five times larger than the area affected by the 1906 San Francisco earthquake.

The earthquake generated huge waves along the Mississippi river, throwing boats onto the banks, which in turn collapsed back into the river. Elsewhere along the river, whole islands disappeared. According to records, the only life that was claimed was in New Madrid, due to falling buildings. However, damage to log cabins and chimneys occurred as far away as Ohio, Kentucky, Missouri, and Tennessee.

If this earthquake were repeated today, the estimated losses would be over USD 143 billion in total property losses and over USD 109 billion in insured losses.

Charleston, South Carolina (1886)

On September 1, 1886, Charleston, South Carolina, was struck by the most damaging earthquake to occur in the southeastern United States. The earthquake had a magnitude of 7.3, making it one of the largest shocks on record for eastern North America. It damaged or destroyed most of the buildings in the city of Charleston and killed 60 people. Structural damage was reported as far away as central Alabama, Ohio, eastern Kentucky, Virginia, and West Virginia. Shaking was reported as far away as 1,000 kilometers (620 miles).

Craters and fissures from this earthquake were observed over an area of 1,300 square kilometers (500 square miles). Severe damage was done to 80 kilometers (50 miles) of railroad tracks and the tracks six kilometers (4 miles) northwest of Charleston formed S-shaped curves in places where they were formerly straight.

Sand overflows were widespread in the area, and formed craterlets as wide as 6.4 meters (21 feet). Some of these craterlets spewed water spouts as high as 4.5 to 6 meters (15-19 feet). Fissures one meter wide appeared along canals and stream banks. Wide cracks appeared along the banks of the Ashley River and as the banks collapsed, large trees were uprooted and carried into the river along with the sand.

In the town of Summerville, about 25 kilometers (15 miles) northwest of Charleston, many houses were damaged and displaced. Chimneys constructed independently of the houses had the portion above the rooflines break and fall to the ground. Many chimneys were crushed at the base and consequently sunk through the floors. This type of chimney damage, and the fact that multi-level structures remained standing, indicate that the predominant ground shaking was probably vertical.

Ground shaking from this earthquake was reported as far away as Boston, Massachusetts; Milwaukee, Wisconsin; Chicago, Illinois; Cuba; and Bermuda.

If this earthquake were to repeat today, the estimated losses would be over USD 82 billion in total property losses and over USD 41 billion in insured losses.

San Francisco, California (1906)

The magnitude 7.8 earthquake that struck San Francisco on April 18, 1906, remains one of the most devastating earthquakes in the history of California. It caused an estimated 3,000 deaths and USD 524 million in property loss (1906 dollar values), due to both shake damage and resulting fires. In San Francisco, direct damage from the earthquake was estimated at USD 20 million (1906); outside the city, it was estimated at USD 4 million (1906). Shaking was felt throughout California and in parts of Nevada and Oregon. In San Francisco, shaking was felt for about one minute from the main shock, which was followed by several aftershocks.

The earthquake created the longest fault rupture ever observed in the continental United States. The rupture extended 477 kilometers (296 miles) along the northern San Andreas fault, from northwest of San Juan Bautista to Point Arena, and from there the rupture continues further into the ocean. Horizontal displacement was observed in many areas with the largest at 6.4 meters (21 feet) found near Point Reyes Station in Marin County. The displacement caused by this earthquake, and the strain of the rupture, led to the elastic-rebound theory of earthquakes.

The earthquake devastated San Francisco, destroying or severely damaging structures throughout the city. The pavements buckled; houses of ordinary brick and frame construction were destroyed; sewers and water mains were broken; and streetcar tracks were torn and bent out of shape. The ground was torn and forced into ridges and trees were knocked over. Pipelines were broken, and roads were impassable, shutting off water supply to the city, which in turn made it impossible to fight the fires that ignited due to overturned stoves and broken gas lines. At least 50-60 fires burned the city for four days; the percentage of the total damage attributed to fire is estimated to be between 80% and 90%.

The ground shaking from this earthquake was at destructive intensities as far away as 600 kilometers (373 miles) from the fault. Based on geological effects, the maximum MMI appears to be XI although based on building and infrastructural damage, the maximum MMI was IX.

If this earthquake occurred today, the estimated losses would be over USD 208 billion in total property losses and over USD 91 billion in insured losses.

Loma Prieta, California (1989)

On October 17, 1989, a magnitude 6.9 earthquake struck Nisene Marks State Park in the Santa Cruz Mountains, rupturing a section of the San Andreas fault about 100 kilometers (62 miles) south of San Francisco. This earthquake was the largest to occur along the San Andreas fault since the 1906 earthquake in San Francisco, however the rupture was much smaller. This earthquake however caused 63 deaths, nearly 4,000 injuries, and an estimated USD 6 billion (1989 dollar values) in property damage.

Severe damage occurred throughout the greater San Francisco-Oakland area. In Monterey Bay, liquefaction broke underground pipes and caused significant and widespread damage to many structures including buildings, bridges, highways, and port facilities. Levees and airport runways were also heavily damaged. Liquefaction also occurred in San Francisco's Marina District where the soil conditions (loose sandy fills above deep soil deposits) amplified the ground shaking. In San Francisco and Oakland, reinforced concrete viaducts collapsed, resulting in heavy damage to U.S Highway 101 and Interstate 280 in San Francisco, and to Interstate 880 in Oakland. Traffic was also disrupted for many weeks due to landslides near the earthquake's epicenter in the Santa Cruz Mountains.

Several fires broke out, particularly in the Marina District of San Francisco, and also in Santa Cruz. Several homes were burned down completely and many buildings, including some fire stations, suffered severe fire damage.

However engineered buildings, even those near the epicenter, withstood the ground shaking quite well. Hospitals sustained only minor damage and operations were not interrupted. Only five schools were severely affected, sustaining an estimated USD 81 million in damages. The worst damage was to unreinforced concrete structures with wood frame roofs, and floors supported by unreinforced brick walls. The Pacific Garden Mall in Santa Cruz, which consisted of unreinforced masonry buildings, sustained a great deal of damage.

The first day after the main shock, 51 aftershocks of magnitude 3.0 and higher took place and 16 occurred the following day. Over the next three weeks after the main earthquake, 87 aftershocks with magnitudes 3.0 and higher took place in the region. Considering the earthquake's magnitude, this is fewer aftershocks than would be expected in the region.

The earthquake is sometimes referred to as the "World Series" earthquake, since it occurred at 5:04 p.m. during a World Series game taking place in San Francisco, and consequently became the first earthquake to be broadcast live on television. It

is believed that rush hour traffic was much lighter than usual that day due to people leaving work early or staying in town for the game (both teams were from the area), and that the death toll might have been much higher otherwise.

If this earthquake were to repeat today, the estimated losses would be over USD 19 billion in total property losses, and over USD 6.3 billion in insured losses.

Figure 16 compares the Loma Prieta rupture along the San Andreas fault to the rupture caused by the 1906 San Francisco earthquake.

Figure 16. 1906 Rupture of the San Andreas Fault compared to the 1989 Loma Prieta Rupture

Northridge, California (1994)

On January 17, 1994, once of the most significant earthquakes to occur in California shook the Northridge area. This earthquake had a magnitude of 6.7 and the devastation was profound. It claimed the lives of 60 people, injured over 7,000, and left 20,000 homeless. Throughout the greater Los Angeles area, across several counties, more than 40,000 buildings and structures, including Anaheim stadium, were heavily damaged.

The earthquake affected several freeways when the columns supporting the overpasses collapsed, causing those portions of the freeway to fall onto the freeway beneath. Collapsed overpasses occurred on the Santa Monica, Simi Valley, and the Golden State freeways, among others.

Most of the buildings that were damaged were multi-story wood frame buildings, especially those with a "soft" ground floor, (e.g., those with parking areas or other large open spaces on the ground floor). Unreinforced masonry buildings and houses on steep slopes were also heavily damaged. Eleven hospitals had to be shut down due to heavy damage, which caused other hospitals to be overburdened with incoming patients injured from the earthquake. It should be noted that school buildings, for which earthquake reinforcement is mandatory, survived fairly well.

This earthquake triggered several fires, mostly in the San Fernando Valley but also in Malibu and Venice. As houses shifted, gas pipes broke and water heaters toppled over, causing fires to break out. In the San Fernando Valley, fires broke out amid floods due to rupturing of both gas pipes and water mains.

The earthquake was felt throughout southern California and as far away as Las Vegas, Nevada. Shaking was also reported in Richfield, Utah, and Ensenada, Mexico. The largest recorded acceleration of 1.8 g occurred at Tarzana, about seven kilometers (four miles) south of the epicenter, and several other sites recorded maximum accelerations exceeding 1.0 g. In the mountains, roads were blocked due to rockslides and ground cracks appeared in the Potrero Canyon and at Granada Hills. The maximum uplift of about 15 centimeters (6 inches) was observed in the Santa Susana Mountains.

The Northridge earthquake remains the costliest in recent U.S. history, with estimates for property damage at over USD 15 billion (1994). Due to the overwhelming cost of this earthquake, many insurers stopped offering earthquake insurance, or only offered it at a restricted level. In response, the California Earthquake Authority was created by the California Legislature to make minimal earthquake insurance available on a broad scale.

If this earthquake were repeated today, the estimated losses would be over USD 77 billion in total property losses and over USD 23 billion in insured losses.

Nisqually, Washington (2001)

On February 28, 2001, a magnitude 6.8 earthquake shook the Puget Sound area for 40 seconds. The epicenter was located about 56 kilometers (35 miles) south of Seattle, in the same area as a magnitude 7.1 earthquake that occurred in April of 1949. It is attributed to tensional (normal) faulting in Juan de Fuca Plate, caused by the plate bending as it subducts under the North American plate.

The earthquake caused about 400 injuries along with major damage to several structures in Seattle, Tacoma, and Olympia. The maximum ground-shaking

intensity occurred in Olympia and in the Pioneer Square area of Seattle, while the maximum recorded acceleration of 0.3 g was recorded at Seward Park in Seattle. Ground shaking was reported in central Oregon and in Vancouver, British Columbia. Shaking also occurred as far east as northwestern Montana and in Salt Lake City, Utah.

Landslides, liquefaction, and sand boils were witnessed south of Seattle, in the suburb of Renton, and also in Tacoma and Olympia. Most of the structural damage was to buildings that were near the epicenter, although there was significant damage to unreinforced concrete or masonry buildings in Pioneer Square and areas south of Seattle. At Seattle-Tacoma International Airport, the air traffic control tower was damaged along with several runways. (A new air traffic control tower was built with earthquake-resistant construction.)

Several highways and bridges were significantly damaged. In Olympia, the Fourth Avenue Bridge was nearly destroyed and had to be torn down completely and rebuilt. Just northwest of Olympia, U.S. Highway 101 buckled in several places and a mudslide blocked State Route 3 northeast of Shelton. The Alaskan Way Viaduct, which runs along the Seattle waterfront, also sustained a good deal of damage.

Damage to roads, bridges, transit facilities, buildings and airport runways totaled about USD 7 million (2001). If this earthquake were to recur today, the estimated losses would be over USD 2 billion in total property losses and over USD 667 million in insured losses.

3 Event Generation

The AIR Earthquake Model for the United States captures the effects of ground shaking, liquefaction, and fire damage on insured properties. The hazard component of the model is based on the 2008 United States Geological Survey (USGS) national earthquake hazard model, which is described in USGS Open-File Report 2008-1128, *Documentation for the 2008 Update of the United States National Seismic Hazard Maps*. The details of this update are the result of a collaborative effort by the scientific community at several USGS workshops held around the country, which included active participation by AIR's scientists and engineers.

As part of their report, the USGS released a large number of documents and data that support the revision of their seismic hazard maps. New information from this research was provided on the magnitude-frequency distribution of earthquakes along faults and subduction zones across the continental United States. They also provided reports on an enhanced seismicity study and on the shallow and deep background seismicity at grid points uniformly distributed across the country. To account for both parametric and model uncertainties, the USGS makes extensive use of logic trees.

The current AIR model is based on an extensive review of the latest USGS model, including reviews of the magnitude-frequency distributions for faults and subduction zones in the western United States, the special seismic zones in the central and eastern United States, and the background seismicity. To construct the stochastic catalog, AIR seismologists formulated a procedure that captures the details of the USGS model, on both regional and local scales, and translates that information into catalog-based earthquake scenarios.

The procedure includes detailed reviews of the USGS logic trees on seismicity and ground motion. These logic trees allow the AIR model to capture the epistemic uncertainties on rupture scenarios, fault geometry and locations, magnitudes, faulting mechanisms, and the rupture orientation of the background seismicity that are compatible with the information given by the USGS report.

3.1 Modeled Earthquake Variables

Each event in the model's stochastic catalog(s) is associated with an epicenter, magnitude, rupture length and width, azimuth, dip, dip azimuth, depth, and rupture mechanism.

Epicenter

The epicenter of an earthquake is the location on the earth's surface directly above the point of initial rupture. Understanding the spatial distribution of earthquake epicenters is greatly facilitated when the faults are visible on the surface. In the case of blind faults, their location must be inferred from the seismic activity of the area or by subsurface-sounding techniques; many faults remain undiscovered, however.

The background seismicity component of the AIR Earthquake Model for the United States allows simulated earthquakes to occur anywhere within a seismic source zone to accommodate the uncertainty surrounding the locations of past events. While the distribution of epicenters used in the model generally reflects the historical distribution, smoothing techniques appropriate to each region allow simulated earthquakes to occur where none have been observed in the past.

The modeling of seismicity on subduction zones and faults is based on the epicentral locations of historical and instrumentally-recorded earthquakes, paleoseismic data and GPS data.

Magnitude

Magnitude, a measure of the energy released during an earthquake, is a useful way to compare seismic events. As described in Section 2, a variety of magnitude scales have been used to describe earthquakes. The AIR Earthquake Model for the United States utilizes the moment magnitude scale, M_w. Moment magnitude is a more quantitative and therefore objective measure than the Richter scale, and is applicable over a wider range of ground motions and geographical locations.

Focal Depth

The focal depth is the depth at which a rupture originates. Because seismic waves are attenuated as they travel through the earth, deeper earthquakes of a given magnitude typically cause less damage than those that erupt closer to the surface. Event magnitude and the thickness of the upper layer of the earth's crust shape the distribution parameters that govern focal depth. Crustal thickness can vary considerably across the United States.

Rupture Length

Rupture length is the span of the fault that ruptures during an earthquake. In the AIR Earthquake Model for the United States, rupture length is modeled as a function of the magnitude of the event, with the relationship between rupture length and magnitude determined through empirical regression analysis.

Rupture Azimuth and Dip Angle

Rupture-azimuth and dip angle are parameters that define the orientation of a fault. The rupture azimuth is the angle between true north and the line connecting the rupture plane and the surface of the earth, measured clockwise from north. By convention, the dip azimuth is 90 degrees clockwise of the rupture azimuth. Because energy is distributed along the rupture, a fault's spatial orientation is important for damage estimation.

For earthquakes in each seismic source zone, a preferred azimuth is defined with some range of variation. For characteristic earthquakes, the rupture azimuths are aligned with the fault orientations.

Fault Rupture Mechanism

In the AIR Earthquake Model for the United States, the rupture mechanisms for faults vary widely across the country. See Section 3.4 for a discussion of the fault sources used in different regions.

3.2 Domain of the AIR Earthquake Model for the United States

The region that is covered by the AIR Earthquake Model for the United States comprises the 48 conterminous states and the District of Columbia. Seismic events generated in the model cover a region well beyond the boundaries of the United States to include parts of Canada, Mexico and off-shore subduction zones. The region covers an area that extends from 64° to 127° west longitude and from 24° to 51° north latitude. The model domain is shown in Figure 17.

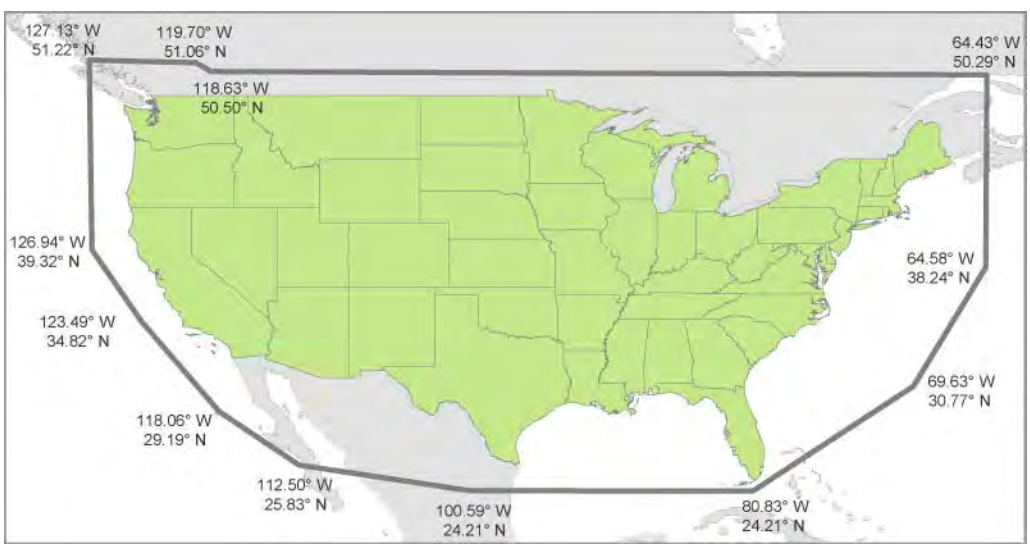

Figure 17. United States Earthquake Model Domain

3.3 Regional Seismicity in the Continental United States

The AIR model makes use of known faults, subduction zones, and special seismic zones, as well as geodetically derived source zones that are identified in the USGS report. In addition, the AIR model uses the USGS smoothed-gridded seismicity information to account for the regional seismicity that is not captured by faults. Details of each of these seismic sources is discussed in the sections that follow.

3.4 Fault Sources

In the AIR Earthquake Model for the United States, the seismicity of the country's faults and the Cascadia subduction zone is based on the information provided in the USGS report. For their 2008 model update, the USGS conducted a comprehensive review of all available information on faults within the continental United States.

This review resulted in the formulation of a very elaborate logic tree that captures various types of parametric and model uncertainties, including uncertainties in the magnitudes of the characteristic earthquakes on faults, and uncertainties for cascading fault scenarios. The recurrence rates for characteristic earthquakes on faults are based on the integration of the paleoseismic, geodetic, and seismic data, depending on the availability of data for each fault.

AIR has developed comparable fault sources by extracting an exhaustive sampling of the USGS fault rates, based on the magnitude-frequency distributions. Using the USGS seismicity information for faults, fault segments, and cascading scenarios, provided in the form of logic trees, AIR constructed a magnitude-frequency distribution for each fault. This magnitude-frequency distribution captures the details of the USGS logic-tree uncertainty for the seismicity for each fault. The magnitude-frequency distributions are used to generate AIR's stochastic catalogs.

Figure 18 shows the subduction zones and crustal faults for the west coast and intermountain seismic belt.

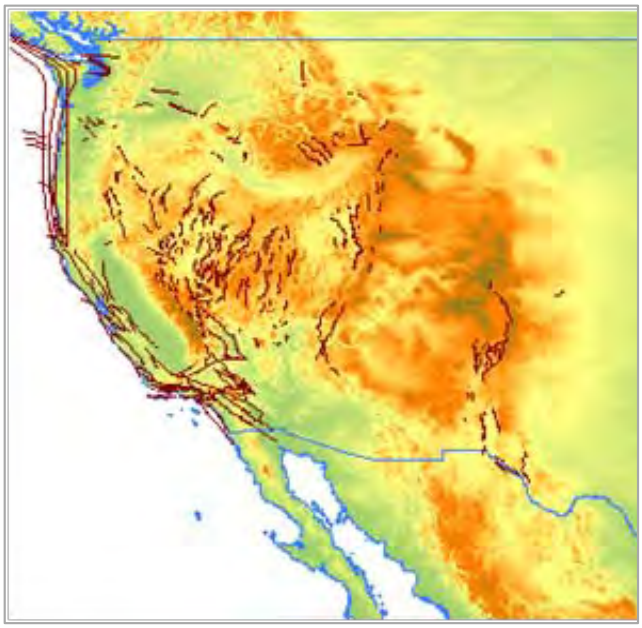

Figure 18. Subduction Zones and Crustal Faults in the Western United States

California

For the state of California, two types of fault sources are identified by the USGS: type-A and type-B faults. Type-A faults are extensively studied and have enough information on the location, timing, and (in some cases) slip rates for previous earthquakes to be used for stress-renewal recurrence time-dependent analysis. In the Uniform California Earthquake Rupture Forecast (UCERF2)[4], there are six type-A faults: San Andreas, San Jacinto, Elsinore, Garlock, Hayward-Rodgers Creek, and Calaveras. The models used for these faults include characteristic earthquakes on specific segments, multi-segment ruptures, and earthquakes that rupture only part of a specific segment.

The San Andreas fault is the most extensively studied fault in the world, and major faults that are part of the greater San Andreas fault system are also considered type-A, such as the Hayward-Rodgers Creek, San Jacinto, Garlock, and Elsinore faults.

The AIR model includes 136 single and cascading scenarios for type-A faults. Type-B faults have slip-rate estimates, but the data on the distribution and timing of previous events are inadequate to model these faults with stress-renewal probabilities. There are 416 type-B faults included in the AIR model.

[4] UCERF2 was released by the 2007 Working Group on California Earthquake Probabilities. See Section 3.5 for more information.

Additionally, the USGS defines a number of areal special seismic zones to capture the seismicity of certain regions that cannot be adequately modeled by faults or background seismicity. The seismicity of these zones are discussed in the Special Zones section below.

Figure 19 below illustrates some of the details of the Peninsula Segment of the San Andreas fault.

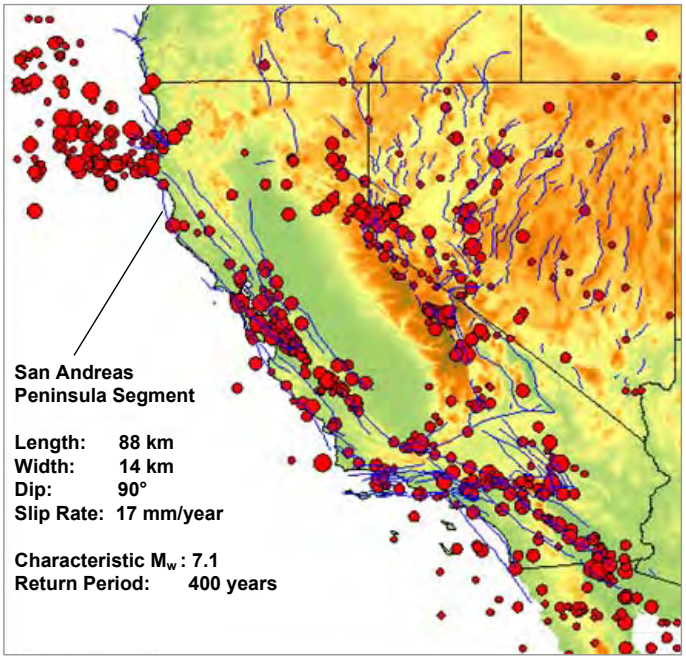

Figure 19: The San Andreas Peninsula Segment

The Cascadia Fault Sources

In the Pacific Northwest (Washington, Oregon, and Idaho) both crustal faults and subduction zones drive the hazard, giving this region a unique seismic setting when compared to the rest of the country. The crustal faults include the South Whidbey Island fault, the Lake Creek-Boundary Creek fault, the Stonewall anticline, and the Boundary Creek fault.

The Cascadia subduction zone extends about 1,200 kilometers from Vancouver Island in British Columbia to Cape Mendocino in California. At these areas, the Explorer, Juan De Fuca, and Gorda plates subduct under the North American plate at about 40 mm/year. Coastal subsidence and tsunami deposits indicate that the recurrence rate of extremely large earthquakes (M8.8–M9.2) in this region is about 500 years.

The rupture models for the Cascadia subduction zone were developed based on thermal models and analogs of shallow-dipping subduction zones used by the

USGS. The ruptures extend through different depth ranges that are typical of the elastic and transitional zones of the earth's crust, and extend down to a depth of 30 kilometers. The AIR model adopts the complex geometry for the Cascadia zone by implementing four different scenarios developed by the USGS that have varied width and dipping angles from north to south.

Figure 20 shows the Cascadia rupture zone faults. In this figure, the "top" (pink line) is the base of the elastic zone, the "middle" (red line) is the midpoint of the transition zone, the "bottom" (brown line) is the base of the transition zone, and the "base" (cyan line) is the base for the model that assumes the ruptures extend to a depth of about 30 km.

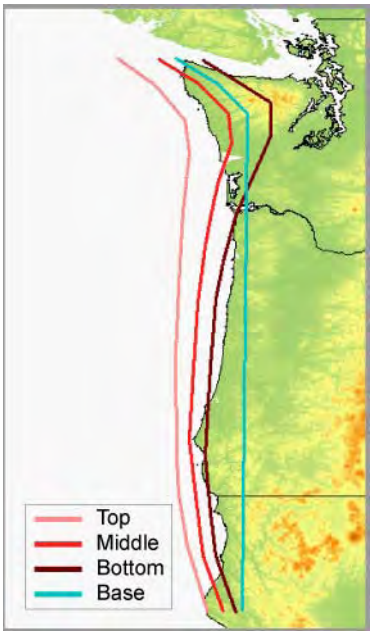

Figure 20. The Cascadia Subduction Zone Fault Model

The USGS model considers two scenarios for the interface earthquakes in the Cascadia subduction zone: one scenario assumes that the entire subduction zone ruptures in a megathrust M9.0 (± 0.2) earthquake; the other scenario assumes that different sections of the subduction zone rupture in smaller M8.0 – 8.8 earthquakes. In both scenarios, the recurrence time for the rupture of the subduction zone, at any point along the zone, is assumed to be 500 years. During the last few years, the M9.0 scenario has been gaining more credibility, and in the latest USGS maps the probability of an M8.8–M9.2 scenario has increased from 0.5, used in 2002, to 0.67.

Intermountain West

The fault sources for the Intermountain West include nearly 300 faults, although this large and diverse area contains thousands of older faults and has a very long history of seismic activity. The AIR modeled faults in the Intermountain West include all Quaternary faults that have documented slip rates (or sufficient data to calculate the slip rates) or rates of large earthquakes that caused permanent geological deformation. All faults with known Holocene surface faulting are included.

The model also takes multi-segment ruptures for some faults into consideration, such as those along Utah's Wasatch fault. For this fault, the model includes a characteristic earthquake of magnitude 7.4.

The New Madrid Seismic Zone

In the latest U.S. Hazard Maps the USGS conducted a major review of the New Madrid seismic zone (NMSZ) and accordingly introduced important changes to the formulation of the seismicity for this special zone, based on the earthquakes of 1811–1812. These changes included updating the spatial distribution of the NMSZ faulting scenario, dividing the NMSZ into three segments (southern, central, and northern), and then modifying the recurrence intervals and magnitude distributions for each segment.

The precise location of the three New Madrid events is uncertain due to the uncertainty in the regional seismotectonic setting, and in the interpretation of data taken at the time of the 1811–1812 earthquakes. Therefore, to account for the spatial variability of future earthquakes in the area, the AIR model uses the process adopted by the USGS, which provides for five hypothetical fault traces. Figure 21 illustrates these fault traces and shows the probability of an earthquake being located along each trace, should one occur. The center trace shows a much higher probability (70%) of being the location of an event than the other four traces on either side.

After carefully reviewing the paleoliquefaction data, the USGS introduced two major changes for the recurrence model. First, for the entire zone, they introduced a 1,000-year rupture scenario with a 10% weighting factor. This reflects observations on the correlation between the changes in the meander patterns of the Mississippi River and large-magnitude earthquakes. The second change pertains to the northern segment, where the USGS assumed a longer recurrence rate of 750 years.

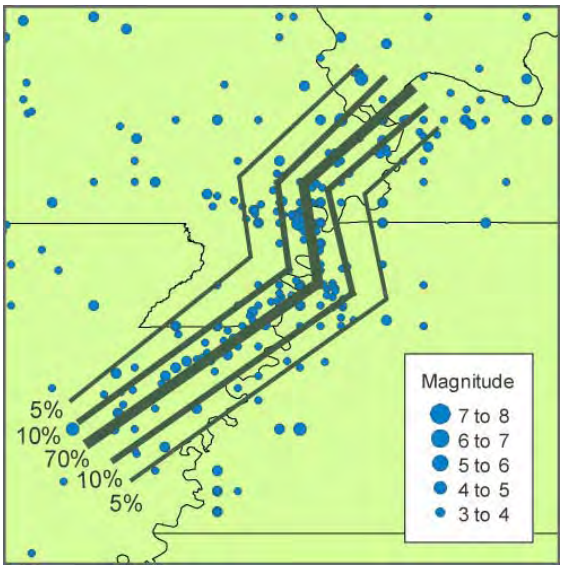

Figure 21. Spatial Variability in the New Madrid Seismic Zone using Five Parallel Fault Traces (USGS)

The USGS now considers temporal clustering for earthquakes on different segments of the NMSZ. This is based on the 1811–1812 events and on geological data, which shows evidence that prehistoric earthquakes on the Reelfoot fault typically occur in sequences of three large earthquakes similar to that observed in 1811–1812.

Accordingly, the USGS considers three scenarios for earthquakes occurring in the NMSZ. In one scenario, which has a 50% weighting factor, no clustering is considered. Under this scenario, the entire NMSZ would rupture in a single earthquake that extends along the entire fault zone.

In the second scenario, earthquake clustering is assumed; in this case, the NMSZ ruptures either in three separate, but temporally correlated, earthquakes on its southern, central, and northern segments, or in two separate, but temporally correlated, ruptures on the central and southern segments. For each segment, the USGS considers four different magnitude scenarios although for the northern segment they use a magnitude range that is lower by 0.2 units.

Figure 22 shows the logic tree used for the New Madrid seismic zone. The northern, central and southern segments are marked as N, C, and S, respectively.

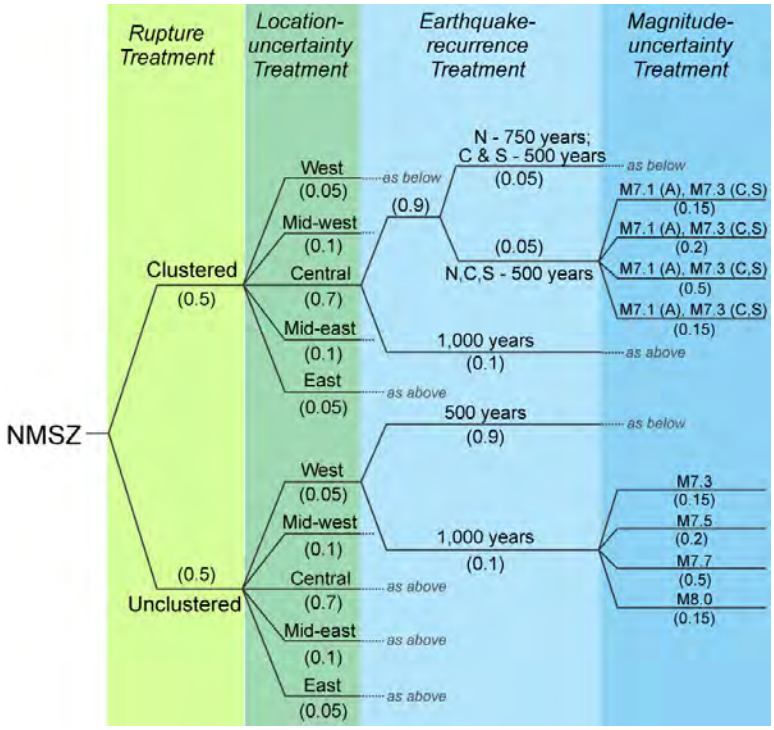

Figure 22. A Logic Tree Used to Capture Uncertainty for the New Madrid Seismic Zone

For the NMSZ, the AIR earthquake model closely follows the USGS model. However, given the number of branches of the logic tree, the number of permutations of magnitude-rate scenarios becomes so large (these include the variations on five rupture scenarios in the east-west direction, the three rupture segments for each scenario, four magnitude values for each segment, the distribution of the recurrence intervals, and the consideration for earthquake clustering on the different segments) that it cannot be fully captured by earthquake scenarios in a typical 100,000-year catalog.

Therefore, to capture this complexity in the AIR catalog, AIR seismologists first constructed an earthquake catalog containing *one million* simulated years, which included all earthquake permutations. Using this large catalog, a regional loss analysis was conducted. An optimization procedure was developed to produce 100,000-year, 50,000-year and 10,000-year catalogs by sampling the extended catalog in such a way that the smaller catalogs maintain the magnitude-frequency distributions over the fault scenarios (in the east-west direction, and over the southern, central, and northern segments) and the regional loss exceedance-probability curves.

The Charleston Zone

The USGS definition of the Charleston seismic zone is based on the occurrence of the M7.3 1886 earthquake and a large volume of paleoliquefaction data. However, there is uncertainty in the location of the causative fault for the 1886 earthquake and other paleoearthquakes. There are geophysical and geological indications that a northeasterly-directed fault zone along the Woodstock lineament might be the causative source.

To account for the uncertainty in the location of future events, USGS defines a small narrow zone that follows the Woodstock lineament and a broader zone that includes an area of known liquefaction features resulting from past earthquakes (Figure 23). This zone extends offshore to include the Helena Banks fault zone, which contains Miocene strata that appear to have been warped from reverse-faulting action. For each zone, the magnitude of the characteristic earthquake is defined by four magnitude values: M6.8, M7.1, M7.3, and M7.5, which are weighted with factors of 0.2, 0.2, 0.45, and 0.15, respectively.

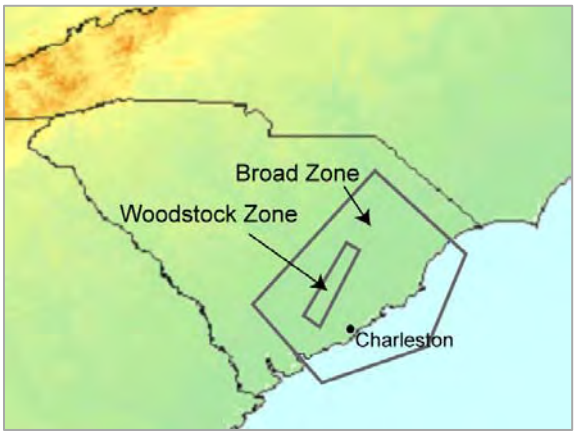

Figure 23. Charleston Fault Source Zones

Smoothed-Gridded Seismicity

The USGS model for the background seismicity in the United States is based on the integration of a number of historical and instrumentally recorded earthquake catalogs. See Section 8 for a full list of references. Gridded seismicity is designed to preserve the pattern of historical seismicity but also to ensure a nonzero probability of future earthquake occurrence.

Figure 24 and Figure 25 show the distribution of past earthquakes in the western, and the central and eastern United States, respectively. After a detailed investigation of the completeness of different catalogs, the USGS formulated a detailed set of completeness times for different magnitude ranges for different

areas in the western, central, and eastern United States. This information is used in conjunction with spatial correlation functions to translate the historical earthquake catalog data to magnitude-frequency distributions within longitude-latitude grid cells.

For California, the USGS assumes completeness for magnitudes of 4.0 and higher since 1933, 5.0 and higher since 1900, and 6.0 and higher since 1850. For the rest of the western United States, the catalog has completeness for magnitudes of 4.0 and higher since 1963, 5.0 and higher since 1930, and 6.0 and higher since 1850.

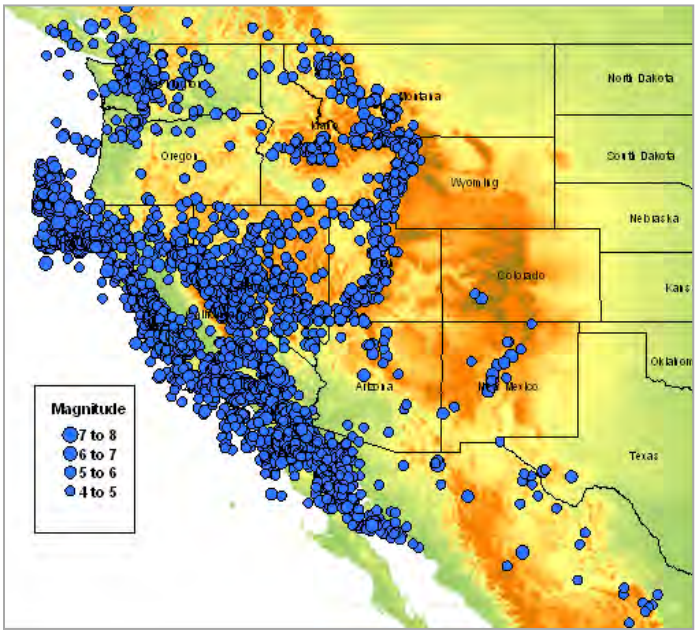

Figure 24. Spatial Distribution of Historical Earthquakes for the Western United States

For areas east of longitude 105°W (just east of the Rocky Mountains in Colorado, near Denver), the catalog is assumed to be complete at magnitudes of 3.0 and higher since 1924, 4.0 and higher since 1860, and 5.0 and higher since 1700.

The formulation of the background seismicity is based on the concept of a positive correlation between the spatial distribution of past and future earthquakes. The scale of this correlation is defined by a distance correlation function that is formulated by processing the spatial distribution of earthquakes in the historical catalog. Using this Gaussian correlation function and the completeness times for different magnitude earthquakes, the USGS calculated the likelihood of different magnitude earthquakes within grid cells.

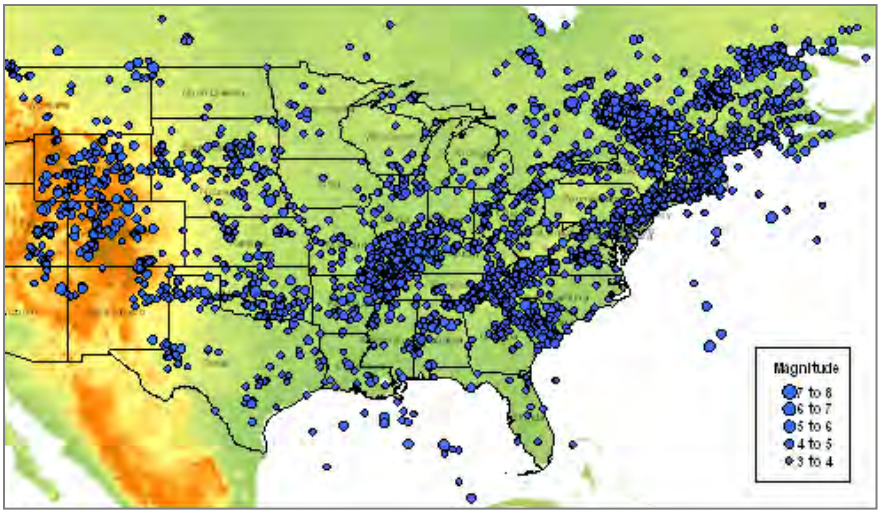

Figure 25. Spatial Distribution of Historical Earthquakes for the Central and Eastern United States

The country is divided into grid cells whose dimensions are 0.1° longitude by 0.1° latitude. The magnitude-frequency distribution of earthquakes for each cell is represented by a Gutenberg-Richter distribution which is the result of integrating different branches of a logic tree that accounts for uncertainty in the catalog earthquake magnitudes, catalog completeness, conversion of different magnitude scales, and maximum magnitudes.

The GR distribution for each cell is represented by an a-value, a b-value and an upper-bound magnitude. The a-value for each cell is determined by quantifying the historical-earthquake occurrence rate within each cell and its adjacent cells. In the central and eastern parts of the country (except for special zones, which are described below), a b-value of 0.95 is used. Upper-bound magnitudes vary: in the stable craton (an area extending from east of the Rocky Mountains into the Midwest (excluding the New Madrid zone), upper-bound magnitudes of 6.6 to 7.1 are used; for earthquakes in the extended margin (an area encompassing the South, mid-Atlantic and Northeast, and includes the New Madrid zone) the upper-bound magnitudes range from 7.1 to 7.7.

For the western United States, the USGS estimated seismicity rates by applying a single smoothed-gridded seismicity model and a b-value of 0.8. For most of the western part of the country the gridded rates are smoothed using a correlation distance of 50 km, for both shallow and deep seismicity. For some zones, an anisotropic smoothing scheme (where the parameters of the Gaussian distribution are direction dependent) is applied in order to provide some smoothing but also keep the modeled seismicity closer to the historical seismicity.

To capture this complexity, AIR seismologists formulated a procedure to integrate the different branches of the USGS logic tree for background seismicity into a single smoothed-seismicity model on grid cells that best reflect the USGS model.

Special Zones

The USGS model considers a number of special zones which are treated differently to account for variations in catalog completeness, maximum magnitude, and b-value. As shown in Figure 26, four special zones are defined in the central and eastern United States, and one is defined in eastern Canada. The average seismicity rates for the eastern Tennessee and New Madrid seismic zones are based on events with magnitudes of 3.0 or larger since 1976. The Wabash Valley zone incorporates a maximum magnitude of 7.5. The Charlevoix zone in eastern Canada incorporates a b-value of 0.76.

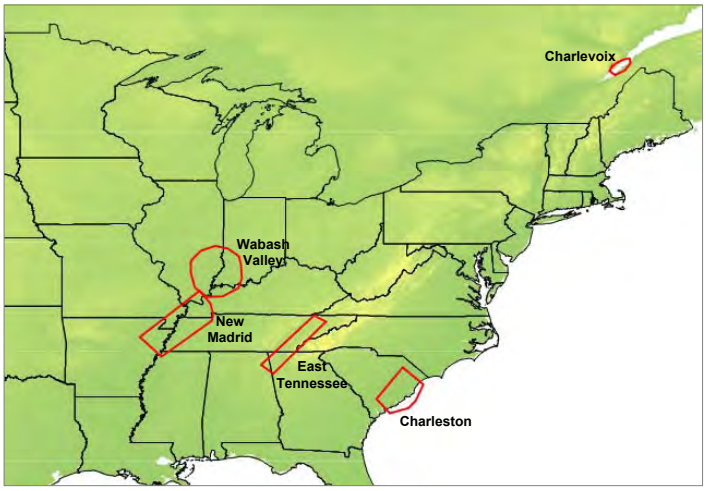

Figure 26. Special Seismic Zones in the Central and Eastern United States

The special zones in the western United States, shown in Figure 27, are mostly concentrated in California. These zones include those that are studied by the Working Group on California Earthquake Probabilities (WGCEP) whose findings are published in the USGS report, *Documentation for the 2008 Update of the United States National Seismic Hazard Maps*. In the figure, some of the zones are identified as shear zones. These are zones whose faults are poorly defined and for which geodetic or seismic data indicate a higher level of shear strain. Note that in the figure, the central Nevada zone is outlined in green to make it easier to see since it overlaps with the western Nevada and Mohawk-Honey Lake shear zones.

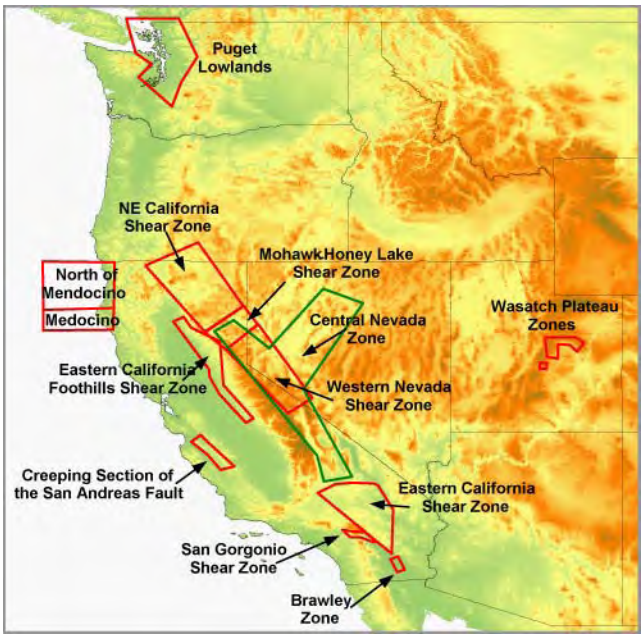

Figure 27. Special Seismic Zones in the Western United States

For the deep seismicity in the Puget Sound region, the USGS assumes completeness since 1963 for M4.0 and greater, and since 1940 for M5.0 and greater, and a b-value of 0.40. For the deep seismicity of northern California, completeness is assumed since 1963 for M4.0 and greater, since 1930 for M5.0 and greater, and since 1850 for M6.0 and greater. A b-value of 0.8 is used for the deep seismicity in this region. Anisotropic smoothing schemes are applied to the Brawley seismic zone, the creeping section of the San Andreas fault in central California, and the Mendocino fracture zone.

3.5 Time Dependence and the Model's Stochastic Catalogs

Since 2001, AIR has offered both time-dependent and time-independent catalogs as part of its U.S. earthquake model. In the current model, the time-dependent catalog is the recommended and therefore default, catalog. However, as in previous years, AIR continues to provide both a time-dependent and a time-independent view. The standard 10,000-year[5] time-dependent catalog contains 68,877 events; the time-independent catalog contains 68,570 events.

By including alternative catalogs, each of which has been developed using rigorous, scientifically defensible methods, the AIR model provides a

[5] Note that catalogs of 50,000 and 100,000 years are also available.

comprehensive view of seismic risk, enabling companies to test the sensitivity of different scientific assumptions.

A time-independent catalog is based on a model that has no memory of earthquake occurrence. In other words, the annual probability of an earthquake occurring along any given fault is independent of when the last similar historical earthquake occurred along that fault. In a model such as this, the number of events occurring on a fault, or within a seismic zone, in different time intervals of the same length, follows a Poisson distribution corresponding to the mean recurrence rate.

For example, suppose a certain fault ruptures with a characteristic earthquake of magnitude 7.0 with an average annual rate of 0.01, which translates to an average of one earthquake every 100 years. A time-independent model consisting of 10,000 simulated years would have 100 such events regardless of when the last historical event occurred.

In the time-dependent models of earthquake occurrence, the probability that an earthquake will occur in the coming year increases with the length of time elapsed since the previous event. Thus in contrast to the time-independent model, the number of such events contained in a time-dependent model consisting of 10,000 simulated years would be very different if the last historical event occurred 10 years ago or 110 years ago. If the last historical event occurred 10 years ago, the probability of another event occurring within the next year would be extremely small, and there would be fewer than 100 such events in the model. If the last historical event occurred 110 years ago, the probability of another event occurring within the next year would be relatively high, and there would be more than 100 such events in the model.

The USGS update of the national seismic hazard maps does not include time-dependence. This is because the primary purpose of the maps is to support the development of building codes, which appropriately reflect a time-independent view of risk. However, it was released at the same time another report was produced by the 2007 Working Group on California Earthquake Probabilities. This report was the second version of the Uniform California Earthquake Rupture Forecast, known as UCERF2. UCERF2 describes the development of a time-dependent rupture model for faults in the state of California, and for large-magnitude earthquakes on the Cascadia subduction zone. It was the first time that a fully consistent and comprehensive time-dependent model became available, and after a thorough review and analysis by AIR seismologists, UCERF2's time-dependent view of risk was implemented as the default catalog in the AIR model.

Time-dependent fault-rupture models better represent the occurrences of characteristic earthquakes on faults, given that adequate information on the statistics of the recurrence intervals and the causative mechanisms for faulting is available. However, compared to a time-independent Poissonian model, the time-dependent model requires more information on fault-rupture history in order to construct a stochastic model for earthquake recurrence intervals on the fault. This requires knowledge of the date of the most recent previous characteristic earthquake, the shape of the probability density distribution for the recurrence intervals (e.g., lognormal or Brownian passage time), and the mean recurrence and aperiodicity values for the recurrence distribution, which measure the scale of randomness for recurrence intervals (that is, aperiodicity measures the extent to which earthquakes do *not* occur at regular intervals, like clockwork).

Due to the lack of detailed knowledge of the causative faults and faulting mechanisms in the central and eastern United States, the seismicity of this part of the country is modeled with time-independent rates. *Therefore, the AIR time-dependent catalog is in fact an integration of the time-dependent seismicity model for characteristic earthquakes on California faults and the Cascadia subduction zone, and the time-independent seismicity model for all other earthquake sources.*

To construct a time-dependent catalog, first the 30-year time-dependent probabilities for characteristic earthquakes on faults in California and the Cascadia subduction zone are calculated. These are converted to the equivalent annual occurrence rates, which are used to generate the time-dependent stochastic catalog for these source zones. These events are then merged with those from the time-independent source zones elsewhere in the United States.

UCERF2 models time dependence in two ways: fault-specific time-dependent rupture probabilities for Type-A faults using a Brownian Passage Time Renewal Model, and a zone-based model that applies "correction factors" based on empirical data to transform long-term seismicity rates into short-term rates.

The UCERF2 Empirical Model

The left-hand panel of Figure 28 shows the faults and subduction zones used for the fault-based model; the regions used for the empirical model are shown on the right.

The empirical model divides California into a number of regions and evaluates the short- and long-term seismicity of those regions. The study took place in 2006, so long-term seismicity is defined as the rate determined between 1850 and 2006. Short-term rates are, in general, estimated by averaging together (with equal weights) average seismicity rates calculated from the 1906-2006, 1942-2006, and

1984- 2006 catalogs. The years 1942 and 1984 represent points of improvement in the seismic network and catalog; and the year 1906 was used to capture the potential influence of the1906 earthquake.

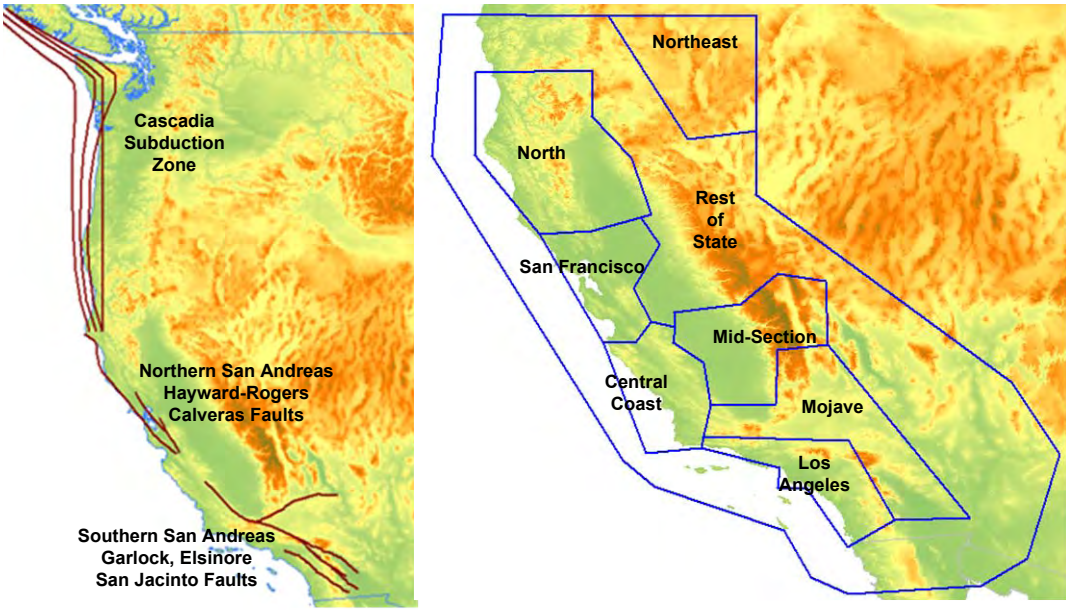

Figure 28. Faults, Subduction Zones, and Regional Zones Used for the Time-Dependent Catalog

Table 4 shows the ratio of short- to long-term seismicity according to UCERF2's empirical region-based model. Note that in every case, the short term time-dependent rate of seismicity is lower than the long term, time-independent rate.

Table 4. Ratios of Short to Long-Term Seismicity Rates

Region	Ratio of Short to Long Term Seismicity
North	0.81 ± 0.63
San Francisco	0.57 ± 0.25
Central Coast	0.69 ± 0.50
Los Angeles	0.55 ± 0.29
Mojave	-
Mid Section	0.61 ± 0.45
Northeast	-
Rest of State	0.86 ± 0.45

The UCERF2 Fault-Specific Model

Estimating time-dependent rupture probabilities for *individual faults* requires good information on such things as the historical recurrence rates of regional earthquakes, and information on the specific fault, such as mean recurrence

interval and the elapsed time since the last occurrence. The interactions between nearby faults and the resulting redistribution of stresses regionally add to the complexity.

For type-A faults, the UCERF2 model used the renewal Brownian passage time model to estimate, for each fault, the 30-year occurrence probability for characteristic earthquakes. This was done using the dates of historical events on those faults. The occurrence probabilities for each fault were then used to estimate the time-dependent occurrence probabilities for all cascading scenarios on these faults.

In integrating the two models, UCERF2 assigns a 70% weight to the fault-based model (Brownian passage time) and a 30% weight to the zone-based model. The AIR Earthquake Model for the United States has implemented time-dependent probabilities in accordance with this recommendation. Accordingly, for type-B faults, the probability values were obtained by taking the weighted average of time-dependent probabilities obtained in the empirical regional model and the time-independent probability values obtained with the Poissonian model.

The Effects of Time-Dependence on Rupture Probabilities

Figure 29 shows the effects of time-dependence on rupture probabilities by comparing the time-dependent rupture scenarios to the time-independent ones. The figure on the left shows the distribution of all faults with 30-year time-dependent probabilities that are *lower* than their 30-year time-independent probabilities. The figure on the right shows the distribution of faults with 30-year time-dependent probabilities that are *higher* than their 30-year time-independent

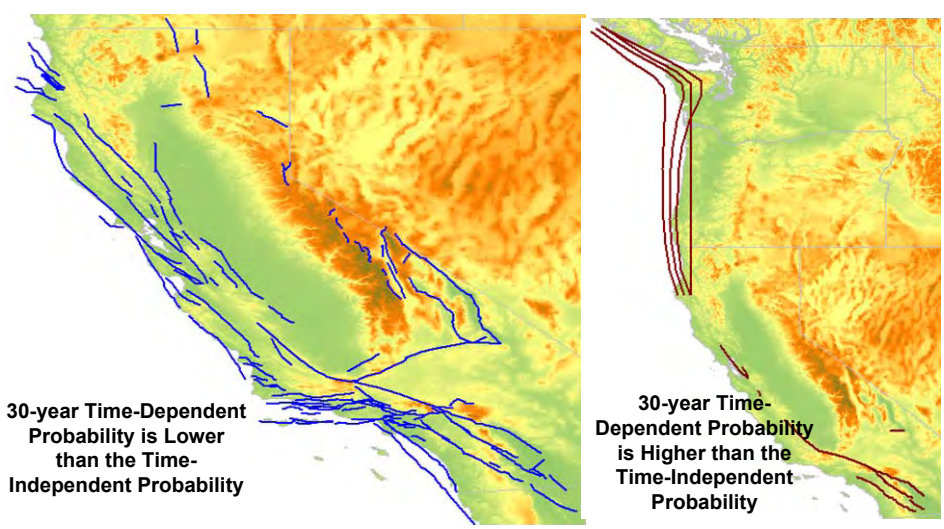

Figure 29. 30-Year Rupture Probabilities for Time-Dependent compared to Time-Independent Catalogs

The 30-year time-dependent probabilities for selected California faults, as published by UCERF2 in 2008, are shown below. They are compared with the Working Group's previous published estimates and the current time-*independent* probabilities. Note that the relatively large increases in the rupture probabilities of the San Jacinto and Elsinore faults are largely the result of the reevaluation of some paleoseismic data on certain segments of the faults and changes to cascading scenarios for those faults.

Table 5. 30-Year Time-Dependent Rupture Probabilities Compared to Time-Independent

Fault	30-Year Time-dependent Probability			30-Year Time-independent Probability
	1995	2003	2008	
S. San Andreas	53%		59%	50%
Hayward-Rogers		27%	31%	23%
San Jacinto	61%		31%	30%
N. San Andreas		23%	21%	22%
Elsinore	24%		11%	13%
Calaveras		11%	7%	7%
Garlock			6%	5%

For the Cascadia subduction zone, AIR followed the USGS method, which uses two sets of earthquakes with 500-year recurrence intervals. The magnitude 9.0 earthquakes are modeled as time-dependent. The last great earthquake occurred here in January 1700, and the time-dependent probability of a M9.0 earthquake in the next 30 years is estimated at 8.0%, compared to a time-independent rupture probability of 5.8%.

3.6 Validating Stochastic Event Generation

The methods used to validate the stochastic catalogs depend on the region of the country. Magnitude-frequency distributions can be provided for both time-independent and time-dependent catalogs for the entire country or for specific regions. For California, the historical record is sufficiently populated that comparisons between simulated and historical magnitude-frequency distributions are appropriate. For the Central and Eastern U.S. and for large magnitude events along the Cascadia subduction zone, where the historical record is sparse, comparisons between the AIR model and the USGS report are used for validation.

Validating the Frequency and Magnitude of Events in the United States

Figure 30 illustrates the magnitude-frequency distributions of simulated and historical earthquakes for the entire continental United States, showing

consistency between the two. The time-dependent and time-independent catalogs are consistent with the historical catalog for events with magnitudes between 5 and 8. The difference between the time-dependent and time-independent catalogs becomes apparent at higher magnitudes.

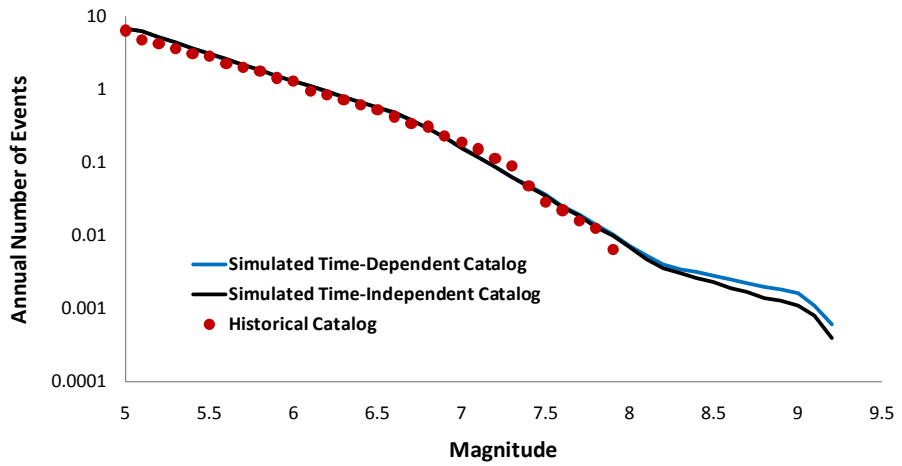

Figure 30. Comparison between the Historical and Simulated Magnitude-Frequency Distributions for the United States

Validating the Frequency and Magnitude of Events in California

Figure 31 displays the magnitude-frequency distributions of time-independent simulated and historical earthquakes in California, showing consistency between the two. Again, the time-dependent catalog's higher rate for large magnitude events is reflected in the figure.

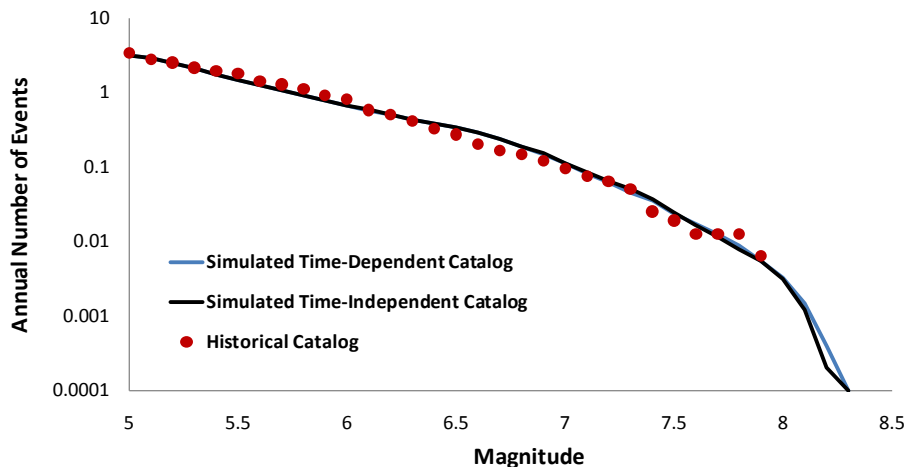

Figure 31. Comparison between the Historical and Time-Independent Simulated Magnitude-Frequency Distribution for California

Validating the Frequency and Magnitude of Events in the Cascadia Subduction Zone

Figure 32 shows a comparison between the cumulative magnitude-frequency distribution for the characteristic interface earthquakes in the Cascadia subduction zone as modeled by the USGS and by AIR. Immediately apparent is the higher rate for the time-dependent catalog compared to the time-independent catalog. For validation purposes, a comparison between the USGS distribution (which is time-independent) and the AIR time-independent distribution is more appropriate.

According to USGS, the recurrence interval for rupturing any location along the Cascadia subduction zone is 500 years. If the interface were modeled by a single M9.0 earthquake, then the plot would have shown a maximum cumulative rate of 0.002 or 1/500 per year. However, the subduction-zone seismicity is modeled by a logic tree and earthquakes with magnitudes ranging from 8.0 to 9.2. Earthquakes smaller than M8.8 do not rupture the entire subduction zone; therefore more of them are required to create a 500-year rupture recurrence at every location along the subduction zone. This fact and the criteria used to balance the seismic moment for the subduction zone are responsible for the difference between the USGS and AIR time-independent magnitude-frequency distributions at the higher magnitudes.

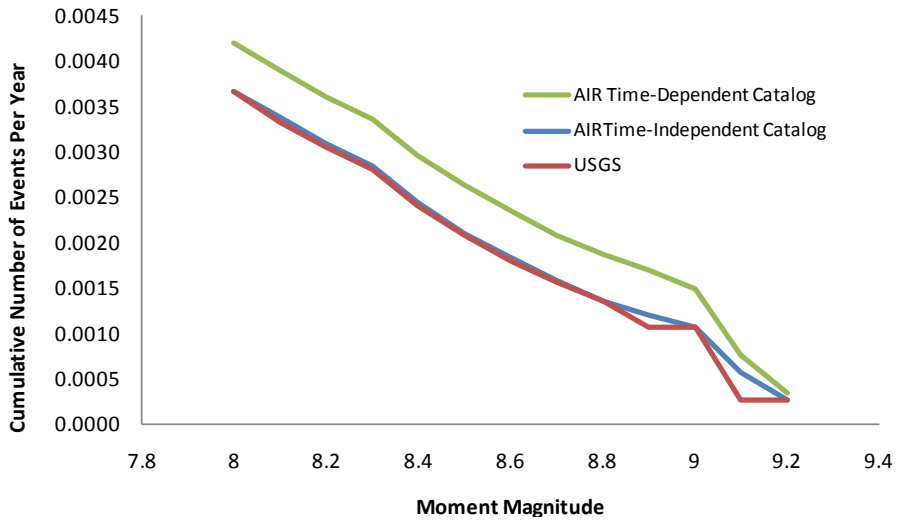

Figure 32. Magnitude-Frequency Distributions for the Time-Independent Simulated Catalog vs. the USGS Report for the Cascadia Subduction Zone

Validating the Frequency and Magnitude of Events in the New Madrid Seismic Zone

The historical catalog contains only one very large historical event for each of the two seismic zones of interest in the central and eastern United States—New Madrid (albeit in the new USGS maps the single New Madrid "event" is now treated as three separate earthquakes) and Charleston. Thus validation in terms of comparing the simulated catalog with the sparse historical catalog is not meaningful. Instead, a more appropriate exercise is to validate AIR earthquake rates against those proposed in new USGS seismic hazard maps.

As shown in Figure 21 in Section 3.4, the USGS proposes five different possible fault traces, each of which has a weighting factor that indicates, in catalog terms, the percentage of earthquakes occurring on that rupture. The rupture trace in the center has the highest weighting factor of 0.7, or 70%. The two traces on either side of the middle trace have weighting factors of 0.1 each, or 10%. The two outer traces have weighting factors of 0.05, or 5%.

Figure 33 shows the percent distribution of simulated earthquakes over the five rupture areas based on the counts from the AIR stochastic catalog. The figure shows complete agreement between the AIR model and the USGS recommended weights for different rupture traces.

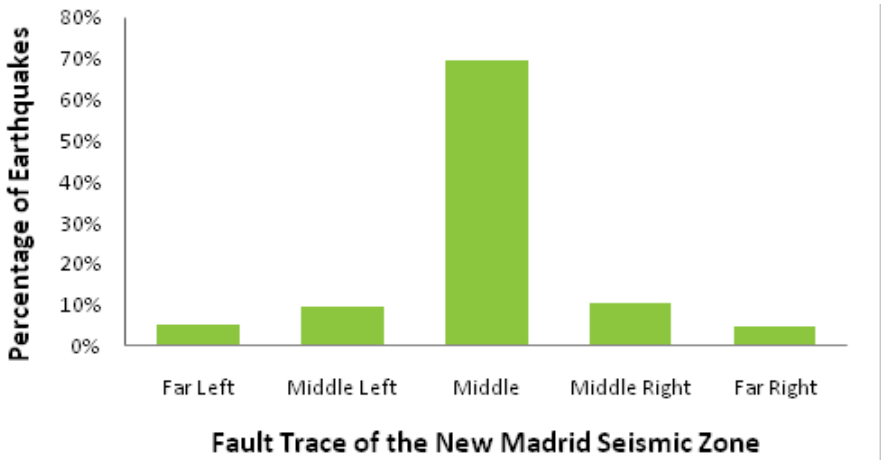

Figure 33. Percentage of Earthquakes on each Branch of the New Madrid Seismic Zone.

The USGS employs a very complex magnitude recurrence model for earthquakes in the NMSZ that consists of a set of correlated and uncorrelated events on the three segments, with different magnitude and recurrence-interval distributions for the northern versus the central and southern segments. The USGS model is reflected in the logic tree shown in Figure 22 in Section 3.4.

The portion of that tree used for determining the event rate for unclustered events is shown in Figure 34. The logic tree shows a probability of 0.9 for a recurrence period of 500 years and a probability of 0.1 for a recurrence of 1,000 years. Using these factors for each recurrence rate, we can calculate a rate of 0.00095 for these unclustered events based on the USGS logic tree.

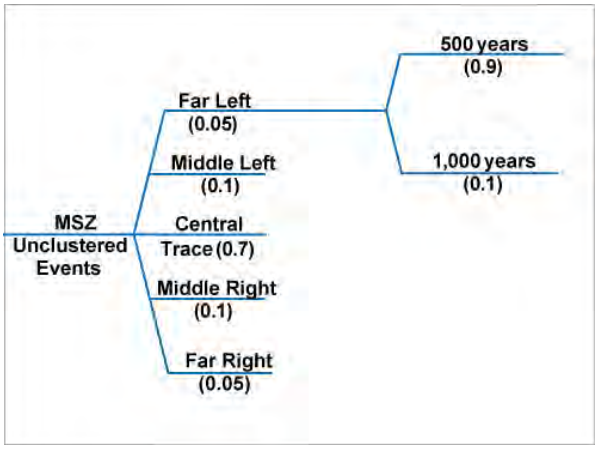

Figure 34. Portion of the New Madrid Logic Tree showing Unclustered Event Rates

Figure 35 shows the magnitude-frequency distribution of AIR simulated events for the unclustered earthquake scenario. In the figure, the cumulative rates indicate the event rates for all events of a given magnitude and higher. For example, the cumulative rate for the M7.1 bar shows the rate for all earthquakes of M 7.1 and higher.

The cumulative rates in this figure reflect the weighted integration of the 500-year and 1,000-year recurrence scenarios for the New Madrid seismic zone as shown in the USGS logic tree, with the 50% weighting factor applied to the single-earthquake scenario. The total rate shown is 0.00092, which is very close to the USGS rate obtained from the logic tree.

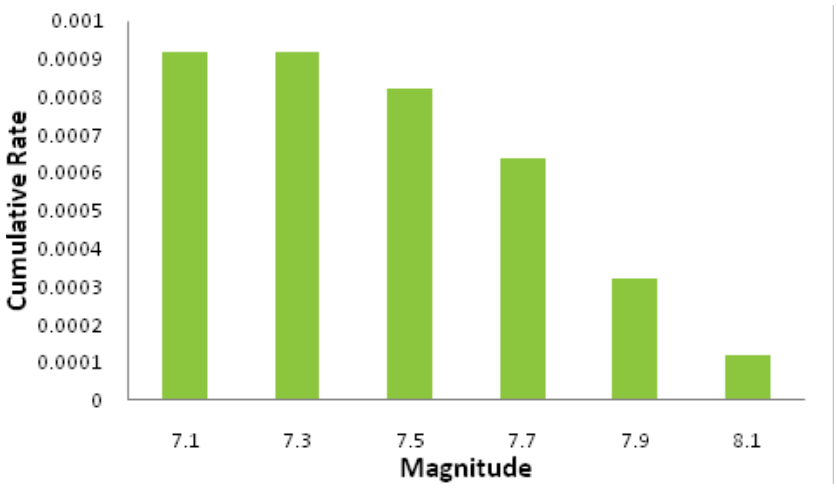

Figure 35. Magnitude-Frequency Distribution of Simulated Events for a Single Earthquake Scenario

For clustered events, the USGS logic tree shows a 500-year recurrence for the southern and central segments, and a 750-year recurrence for a rupture of the northern segment. A portion of the tree used for clustered events in shown in Figure 36.

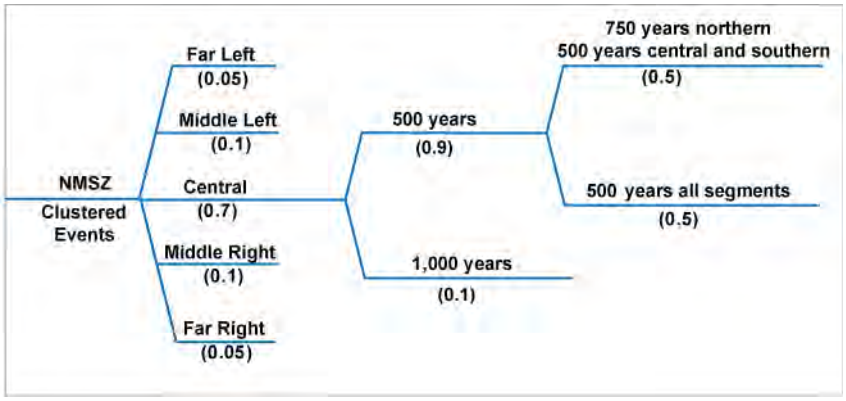

Figure 36. Portion of the New Madrid Logic Tree showing Clustered Event Rates

Figure 37 shows the magnitude-frequency distribution for the New Madrid correlated-triplet scenario event set. The cumulative rates on this figure indicate the weighted integration of the recurrence scenarios shown in the logic tree for clustered events, with the 50% weighting factor applied to clustered events. The total rate shown is 0.00098, which again is very close to the calculated rate of 0.00099 from the USGS logic tree.

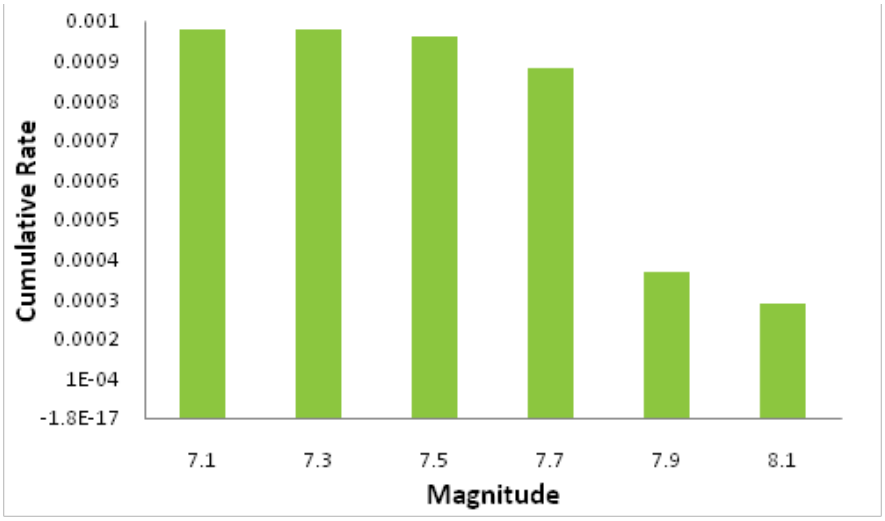

Figure 37. Magnitude-Frequency Distribution of Simulated Events for Correlated Scenarios

The overall magnitude distribution (Figure 38) reflects the magnitude distribution for the south and central segments, and the lower magnitude range for the northern segment.

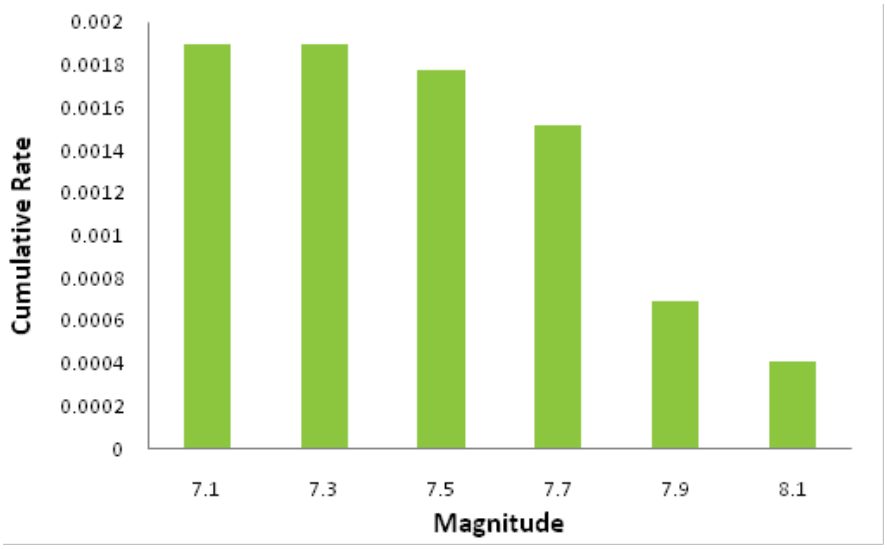

Figure 38. Magnitude-Frequency Distribution of Simulated Events for Both Single Earthquake and Correlated Scenarios

Validating the Magnitude and Frequency of Events in the Charleston Zone

For the Charleston seismic zone, the USGS created a characteristic model for each areal zone. Their magnitudes are shown in with weighting factors. A recurrence time of 550 years was used. The weighting factors were obtained by the USGS

using their areal source zones to account for uncertainty in the location of future earthquakes.

Table 6. Characteristic Magnitudes in USGS Model for the Charleston Zone

Magnitude	Weight
6.8	0.2
7.1	0.2
7.3	0.45

Figure 39 shows the magnitude distribution of AIR simulated events by showing the frequency of events for each magnitude range. The weighting factors used by USGS compare well to the AIR model, showing a highest probability for earthquakes with magnitudes of approximately 7.3.

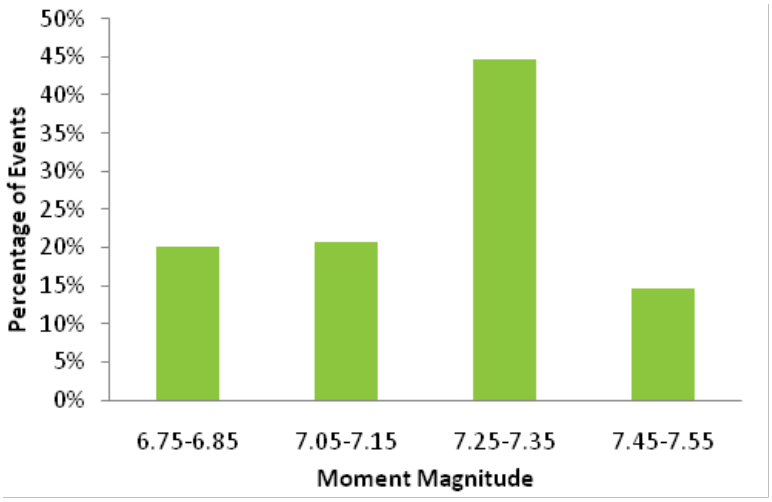

Figure 39. Magnitude Distribution of Simulated Events for the Charleston Seismic Zone

Validating Smoothed Gridded Seismicity

Figure 40 shows a comparison between the spatial distributions of the USGS and AIR's smoothed-seismicity rates using 0.1 degree wide grid cells. The AIR smoothed-seismicity rates are used to produce a one million-year stochastic catalog that is then used to create optimized 10,000-year , 50,000-year and 100,000-year stochastic catalogs in such a way that they satisfy regional magnitude-frequency and loss-distribution requirements—thus the excellent agreement between the USGS and AIR maps shown in Figure 40.

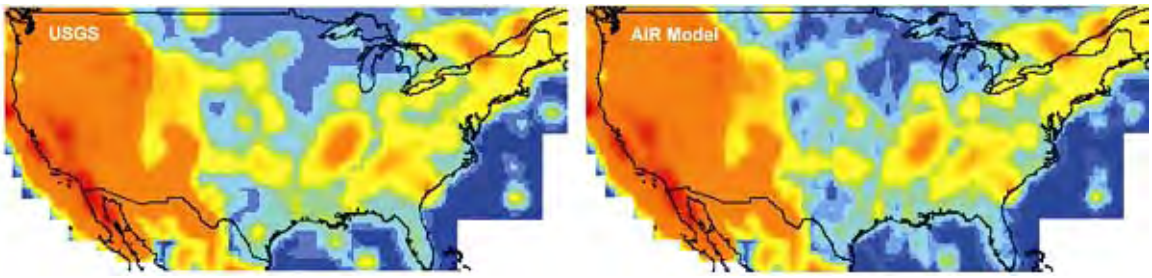

Figure 40. Smoothed-Gridded Background Seismicity from the USGS (left) and AIR (right)

4 Local Intensity Calculation

The measures of intensity used in the AIR Earthquake Model for the United States comprise a variety of ground motion parameters, including spectral acceleration (Sa) at different periods, and Peak Ground Acceleration. Additional detail on how each is implemented in the model can be found in Section 5. This section provides information on the derivation of ground motion parameters by region.

4.1 Ground-Shaking Intensity

In order to analyze damage and loss for each simulated earthquake, the ground motion intensity at each affected surface location must be calculated. This ground motion can range from barely perceptible trembling to violent shaking, depending not only on the magnitude of the event, but also on the distance from the rupture to the affected site, the geological characteristics of the region, and local site conditions.

Ground-shaking intensity is commonly measured in term of peak ground acceleration (PGA) and spectral acceleration (S_a). The peak ground acceleration is the maximum value of the ground acceleration and is typically referred to as motion in the horizontal direction. Spectral acceleration is the maximum response of a simple building, with a single natural frequency of vibration, to earthquake ground motions. S_a approximates what a building experiences as modeled by a particle mass on a massless vertical rod having the same natural period of vibration as the building.

As discussed in more detail in Section 5, different buildings respond differently to the ground motion that occurs during a particular earthquake. A building will be most sensitive to ground motion components that are close to its natural frequency of vibration. Thus, while PGA is the maximum acceleration experienced at a free ground surface, spectral acceleration is more relevant for estimating building damage.

4.2 Attenuation Relationships

Empirical attenuation relationships are practical tools used to estimate ground-shaking intensity in terms of the magnitude, location, and rupture mechanism of an earthquake. These equations describe the rate at which certain ground motion parameters decrease with distance as the waves propagate outward from the rupture site. This decrease is caused by the absorption and scattering of energy as the waves travel through the earth.

The general form of the attenuation functions used in the AIR Earthquake Model for the United States is as follows:

$$S_a = f(M, D, d, F, B, C, T)$$

where

S_a = spectral acceleration or PGA

M = earthquake magnitude

D = distance from rupture plane

d = focal depth

B = basin effect

C = site condition

F = faulting mechanism

T = Natural period of vibration (inverse of frequency)

The AIR model implements attenuation relations for three seismic regions of the continental United States as described below and in accordance with the 2008 USGS seismic hazard maps. For loss analysis, the AIR model uses the weighted average ground motion from different sets of attenuation equations, as recommended by the USGS, with weighting factors defined by the USGS logic trees. This captures the epistemic uncertainty in the calculated ground motion as recommended by the USGS. Peak ground acceleration and different spectral acceleration values are used to formulate the earthquake building response.

For all three regions, the attenuation relations modify the reference shear wave velocity to 760 m/s, which is in accordance with the 2008 USGS update.

Western United States

One of the most important components of the 2008 USGS National Seismic Hazard Maps is the incorporation of new attenuation equations for crustal faults in the Western U.S.

Because of scarce data, the prediction of ground motion at sites very close to faults from large earthquakes was previously heavily guided by "expert opinion, " which concluded that the ground motion under such conditions must be very high. Since the mid 1990s, however, the number of strong motion stations deployed around the globe has multiplied and they have recorded some of the large magnitude earthquakes that have occurred since. To exploit this infusion of new data—more than three times the amount than had previously been available—a multidisciplinary research effort was initiated in 2003. The effort, which ended in

2007, was called the "Next Generation of Ground Motion Attenuation Models" (NGA) project. It focused on predicting ground motion from shallow crustal earthquakes in the WUS in particular and similar active tectonic regions more generally.

Five groups of scientists were tasked with developing the NGA attenuation equations, or ground motion prediction equations. By the time the USGS maps were published, three of the five developers had published their research. Those three—Boore and Atkinson (2008), Campbell and Bozorgnia (2008), and Chiou and Youngs (2008)—were incorporated in the new USGS maps. Shortly thereafter, a fourth NGA equation was published, that of Abrahamson and Silva (2008). AIR has implemented all four equations, weighted equally as recommended by the USGS, in the AIR Earthquake Model for the United States.[6]

The result of the NGA project is a set of attenuation equations that are more reliable and scientifically defensible than any previously produced. Because they use a higher quantity and quality of ground motion data, the NGA equations provide a more realistic (i.e., data-driven) estimate of the ground motion in terms of the faulting mechanisms, focal depth, site location relative to the hanging wall, basin depth, and site conditions.[7]

The NGA equations provide a more realistic estimate of ground motion for large-magnitude earthquakes at close distances thanks, in part, to the 1999 Chi-chi (Ji-ji) M7.6 earthquake, which provided a wealth of data for the near field. The use of ground motion data from international events is appropriate since near-field earthquake ground motion is not very sensitive to regional geological differences and is instead mostly controlled by the source rupture details. Seismological studies on these international earthquakes indicate that they have source mechanisms and rupture details that are very similar to those of crustal earthquakes in the western United States.

Figure 41 shows the ground-shaking attenuation for simulated earthquakes on crustal faults in the western United States with magnitudes of 6.0, 7.0, and 8.0. One of the important features of the new NGA equations is the ground-motion saturation of large-magnitude earthquakes. At large magnitudes, the calculated ground motion at distances below 10 km is relatively insensitive to magnitude compared to previous attenuation equations for crustal earthquakes. That is, earthquakes above a certain magnitude, say M7, appear to produce ground

[6] The fifth GNA equation, developed by I.M. Idriss, has been more controversial and is deemed less credible by some. It was not implemented in the USGS hazard maps.

[7] It is interesting and important to note, however, that despite the use of the same dataset and the strong collaboration among the groups, the equations still show considerable differences in ground motion prediction. The database of recordings is still not sufficiently populated to remove uncertainty altogether.

motions at sites very close to the causative fault that are very similar regardless of the magnitude of the event.

This can be seen in Figure 41, in the spectral values for M7.0 and M8.0 at distances below 10 km. The main reason for this observed saturation is that, for crustal faults beyond certain magnitudes, the fault rupture width does not increase with increasing magnitude. Instead, the magnitude increases because the rupture length increases. For a long rupture area, the contribution of seismic energy from a distant part of the fault (relative to the observation point), is small because waves have to travel a long distance and will be attenuated.

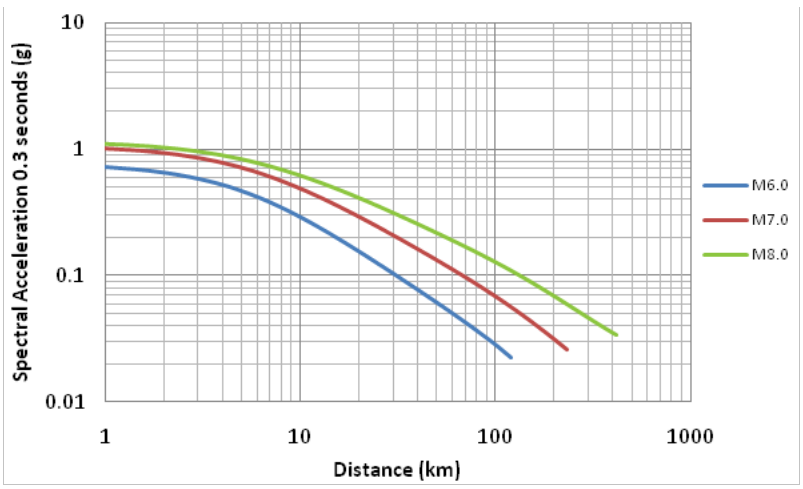

Figure 41. Ground Motion Attenuation for Earthquakes on Crustal Faults in the Western United States for 0.3 s S_a (g)

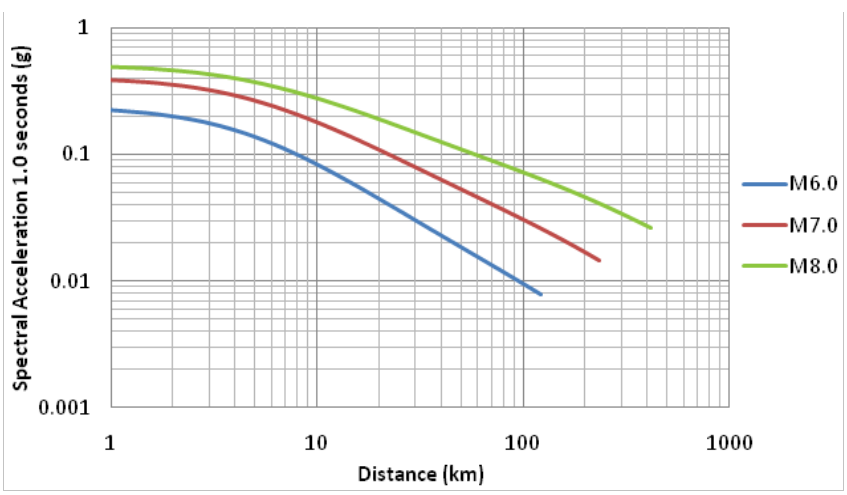

Figure 42. Ground Motion Attenuation for Earthquakes on Crustal Faults in the Western United States for 1.0 s S_a (g)

By the time the 2008 USGS seismic hazard maps were published, three of the new attenuation equations were also published and were incorporated in the new USGS maps. Shortly thereafter, an additional NGA equation was published by Abrahamson and Silva (2008). In the AIR Earthquake Model for the United States, AIR has implemented all four of these equations, weighted equally as recommended by the USGS. The result is a set of attenuation equations that are more reliable and scientifically defensible than any previously produced.

Cascadia Subduction Zone

The NGA equations were developed specifically for crustal faults in active tectonic environments such as California. (They are suitable for similar tectonic regions both inside and outside of the U.S.) However, new attenuation equations were also adopted by the USGS in their 2008 seismic hazard maps for the Pacific Northwest where seismicity is dominated by the Cascadia Subduction Zone.

For subduction zone and deep in-slab events in the Pacific Northwest, an equation published by Zhao et al. (2006) replaced that of Sadigh et al. (1997). The new equation is derived from strong-motion recordings from interface earthquakes in Japan and was weighted equally with Youngs et al. (1997), and Atkinson and Boore (2003), which were also used in the previous maps.

Figure 43 shows the subduction attenuation for the Pacific Northwest (Washington, Oregon, and Idaho) for simulated earthquakes with a magnitude of 9.0. For earthquakes of smaller magnitudes, see Figure 44, which shows the ground motion attenuation for deep earthquakes in the Pacific Northwest.

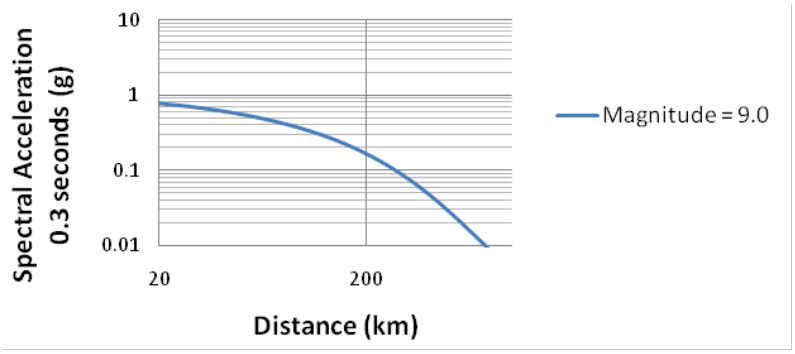

Figure 43. Ground Motion Attenuation for Subduction Zones in the Pacific Northwest

Figure 44 shows attenuation for the Cascadia zone, for deep earthquakes of magnitudes 6.5 and 7.5.

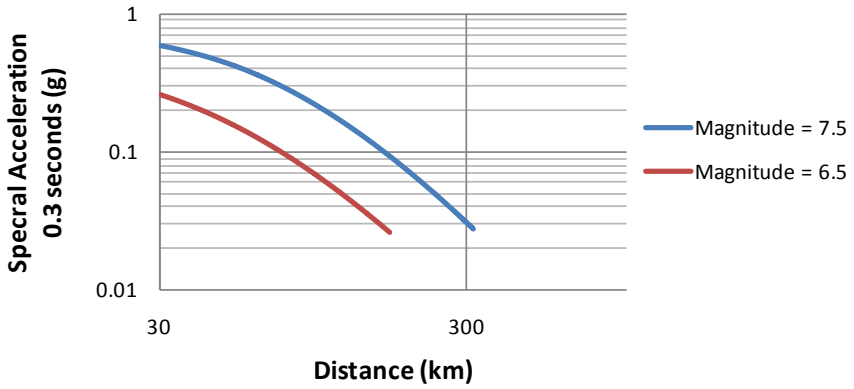

Figure 44. Ground Motion Attenuation for Deep Earthquakes in the Pacific Northwest

Central and Eastern United States

For the central and eastern United States, three attenuation relations from the 2002 USGS hazard maps were retained in the 2008 maps, namely Frankel et al. (1996), Somerville et al. (2001), and Campbell (2003), but four were added: Toro et al. (1997), Atkinson and Boore (2006), Tavakoli and Pezeshk (2005), and Silva et al. (2002). Each is weighted according to the ground motion/tectonic characteristics it was designed to address, which may include magnitude saturation, constant or variable stress drop, or the phenomenon known as the Moho Bounce (whereby seismic waves that initially head downward from the hypocenter bounce off the dense rock of the Earth's mantle and head back to the surface, resonating with direct waves and exacerbating the damage potential).

The number of attenuation equation used by the USGS in this region reflects the high uncertainty in the formulation of the ground motion here and the need to consider many credible models to account for the related epistemic uncertainty.

The attenuation equations for the central and eastern U.S. all are based on stochastic numerical simulations that integrate observations with the latest scientific knowledge of the earthquake rupture process. In general, earthquakes in the central and eastern U.S. tend to have a higher stress drop when compared with earthquakes in the western US. For any given magnitude, this leads to a stronger radiation of ground motion, especially at high frequencies. Also, in this part of the country, the older formation of crustal rocks causes the ground motion to decay more slowly with distance than in the western U.S. The ground motion variability encompassed by different attenuation equations in the CEUS reflects the differences in the experts' opinions on how to formulate and capture these complex phenomena.

The AIR ground motion model for the central and eastern U.S. follows the USGS recommendations and weighting factors for the eight attenuation equations. Figure 45 shows the ground motion attenuation in the central and eastern United States, for simulated earthquakes of magnitude 6.0, 7.0, and 8.0.

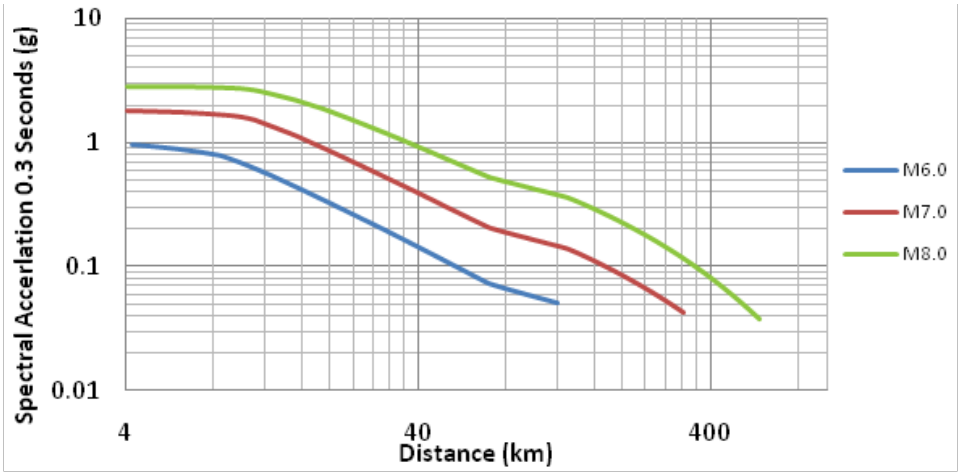

Figure 45. Ground Motion Attenuation for the Central and Eastern United States

4.3 Site Amplification Due to Surface Geology

Local site conditions can dramatically alter the intensity and to some degree the frequency content of the ground motion at a site. Shaking intensity in a given area reflects the local surface geology, as ground-motion intensities vary in part due to these geological properties. The AIR Earthquake Model for the United States uses surficial geological maps and high-resolution topographical data to develop soil classification maps at various scales.

There are three layers of soil maps, each with a different resolution and areal coverage. The first layer is the base soil map that covers the entire continental United States. This map was developed from the unified 1:500,000 digital geological maps in the 48 conterminous states and topographic data, and has a model resolution of about 0.5 km. The second layer covers 17 states, including three on the west coast, nine within the New Madrid seismic zone, and five in the northeast. These state soil maps were developed based on larger scale (1:100,000 to 1:250,000) surficial or quaternary state geological maps. The model resolution for these maps varies from 100 meters to about 500 meters.

The third layer covers local areas with concentrated exposure and significant seismic risk. The model resolution in these maps is 50 to 100 meters. Most of these maps, such as those covering New York City, northeastern New Jersey, southern

Illinois, San Francisco, and Los Angeles, were developed by researchers and geologists in state geological surveys.

Table 7 shows the spatial coverage, data type, resolution and sources of the maps implemented in the AIR model.

Table 7. Soil Maps Implemented in the AIR Earthquake Model for the U.S.

Region	Source Data	Model Resolution (meters)	Reference
New York City	Soil Maps	50	Jacob, K., N. et al 2000
Northeastern New Jersey (8 counties)	Surficial Geological Maps, Borehole Data, Shear Wave Velocity Data	100	New Jersey Geological Survey, 1999 – 2008
Southern Illinois (39 counties)	Soil Maps	100	Bauer, R. A. et al. 2007
Salt Lake City, Utah	Geological Maps	100	Bryant, B. 1990
San Francisco, California	Soil Maps	100	Wentworth, C. M. 1997
Los Angeles, California	Soil Maps	100	Yerkes, R. F. et al. 1997; Morton, D. M. 1999
Portland, Oregon	Soil Maps	100	Beeson, M. H. et al. 1991
Seattle, Washington	Soil Maps	100	Washington State Department of Natural Resources 1993
Charleston, South Carolina	Soil Maps	100	Geological Survey of South Carolina 2003
California	Geologic Maps	200	California Geological Survey 1950-1990
New Jersey	Surficial Geological Maps	100	New Jersey Geological Survey 2006
New York	Surficial Geological Maps	300	New York State Museum Technology Center 1999
Connecticut	Quaternary Geological	300	Connecticut Geological and Natural History Survey 2000; Map 1998
Vermont	Surficial geological Maps	100	Vermont Geological Survey 2008
Massachusetts	Digital Surface Geology Maps	250	Massachusetts Geographic Information System 1999
Illinois	Stack-Unit Mapping of Geological Materials to a Depth of 15 Meters	400	Illinois State Geological Survey 1995, Revision 2004
Washington	Geological Maps	100	Washington Division of Geology and Earth Resources 2005
Oregon	Geological Maps	100	Oregon Department of Geology and Mineral Industries 2004-2009
New Madrid zone (8 states)	Soil maps, Geology, Topography	500	Central United States Earthquake Consortium (CUSEC) 2007
Continental United States (includes Washington D.C.)	Geologic maps, Topography	500	1:500,000 Geologic Maps in 47 states, USGS1997-2007

These maps have not only employed detailed surficial geological data, but also a large amount of shear-wave velocity data in surficial geological materials, estimated based on geotechnical and geophysical methods.

Figure 46 illustrates the difference in the level of detail between the 500-meter base map and a higher resolution map for western Washington.

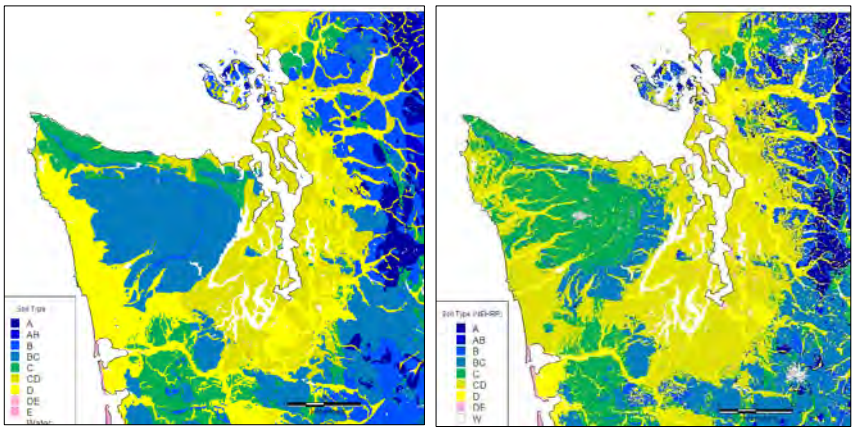

Figure 46. Nationwide 500-meter Base Soil Map (left) and Higher Resolution (100-meter) State Soil Map (right) for Western Washington State

The NEHRP soil types shown in Figure 46 are defined in Table 8, which also lists the average shear-wave velocities for each soil class. Note that intermediate soil types are expressed as a combination of two classes. The average shear-wave velocity for a given soil type is determined from the shear-wave velocities observed in each region that is identified with the soil type.

Table 8. Soil Classifications and Average Shear-Wave Velocities

Soil Class	Description	Average Shear Wave Velocity (m/s)
A	Very hard rock (crystalline rock with few fractures)	1620
AB	Hard rock	1150
B	Firm to hard rock	1050
BC	Firm rock	760
C	Soft to firm rock (gravelly soil and soft rock)	540
CD	Soft rock (gravelly and stiff soil)	370
D	Stiff clay and sandy soil	330
DE	Soft soil to firm soil (silty clay and sand)	280
E	Soft soil (includes bay mud)	160
Special soft soil for New Madrid Zone		220

These soil classifications accommodate variations in ground motion amplification, since the amplification factors are calculated directly from the mean shear-wave velocities. Thus, the soil classifications give a more accurate prediction of ground-motion amplification wherever detailed soil data and shear-wave velocity measurements are available.

Ground motion at each location depends on the magnitude and fault mechanism of the earthquake, the local surface geology, and the propagation path of the seismic waves. Maps detailing the average shear-wave velocity in the upper 30 meters of soil (the 30 meters immediately below the surface of the earth) are used to estimate site amplification. These are known as Vs30 maps.

For some areas of the United States, the model includes more than one geological map. If the low-resolution Vs30 map provides detailed information regarding low-velocity seismic waves, then the data from this map and the higher resolution map(s) are used with equal weight. However, if the low-resolution Vs30 map does not demonstrate adequately detailed information on, then only the high-resolution maps are used.

Topographic Slope Effects

AIR has implemented a methodology recently developed by the USGS for characterizing site conditions; the methodology is used to augment geologic data with topographic data. Recent studies show a positive correlation between the topographic slope and shear wave velocity of surficial material (soils) as shown in Figure 47. This results from the fact that areas characterized by a gentle topographic slope are more likely to accumulate soft soil sediments than areas with steeper slopes.

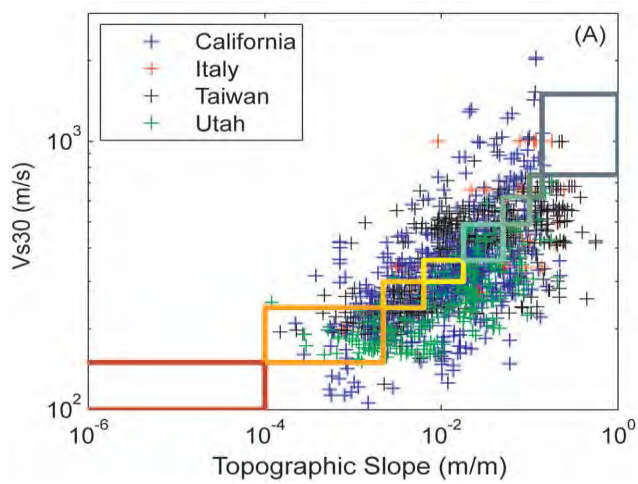

Figure 47. Several Recent Studies Reveal Positive Correlation between Topographic Slope and Shallow Shear-Wave Velocity

AIR has leveraged this relationship to produce far more detailed shear-wave velocity maps used in the formulation of regional site conditions. An example is shown in Figure 48, which illustrates shear-wave velocity maps in the San Francisco area; one based on geological data alone (left-hand panel) and one that takes topographic slope into consideration (right-hand panel).

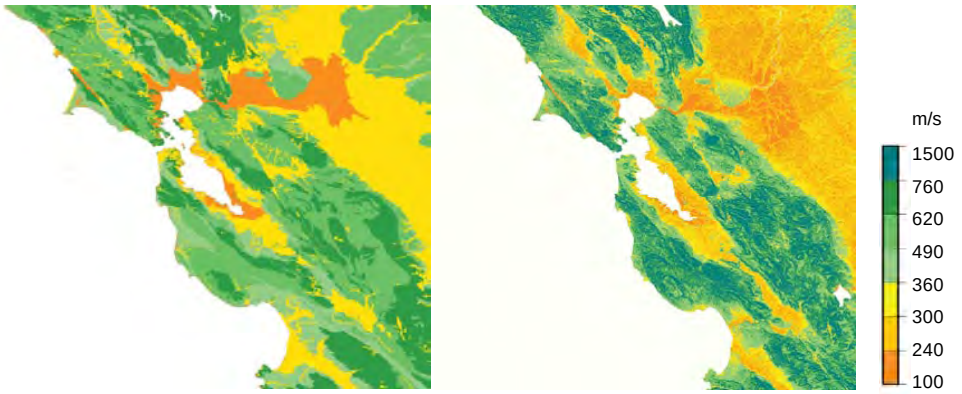

Figure 48. Shear-Wave Velocity Map Based on Geological Data only (left) and Augmented Based on Topographic Slope (Right)

Alluvial Basin Effects

The ground motion on deep alluvial basins can be further amplified above and beyond what would be expected using the near-surface soil stiffness parameter only. If the basin depth is provided for an area, the NGA equations can account for its effect on ground motion.

While the USGS adopted a neutral approach by using a uniform basin depth that had the effect of cancelling out any significant amplifying or deamplifying effect, AIR went further, collecting and implementing depth information at high (0.2 km) resolution for major basins in California, Washington, and Nevada (Figure 49). The AIR model therefore takes full advantage of the capabilities of the NGA equations.

While the impact of basin effects is relatively small, there are implications for tall buildings located on deep basins. All else being equal, the deeper the basin, the greater will be the amplification of long-period ground motion, which resonates with the natural periods of tall, flexible buildings, making them more vulnerable.

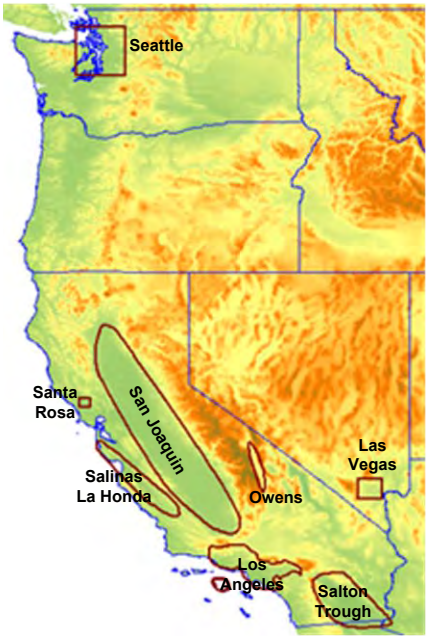

Figure 49. Alluvial Basins in California, Washington and Nevada

4.4 Liquefaction

When an earthquake strikes an area that is saturated with groundwater, the shaking can cause the soil to lose its stiffness due to increased water pressure, and behave like a heavy liquid. When this happens, the soil loses its capability to support structures. Buildings can suddenly tilt or even topple over as the ground beneath them becomes liquefied. Pipelines and ducts can surface, and as the liquefied soil shifts, it can break buried utility lines.

Liquefaction is more likely in areas with granular soils that have poor drainage and are saturated with water. An example would be silty sands, which are found along riverbeds, beaches, dunes, and other areas where sands have accumulated. If the saturated soil lies underneath a dry crust, the ground motion can crack the top dry soil allowing the liquefied sand to erupt through the cracks, creating sand boils. Sand boils can spread through utility openings into building, and damage the building or its electrical system.

During the Loma Prieta earthquake in 1989, a significant amount of the destruction in the Marina District of San Francisco was due to liquefaction. When the Nisqually earthquake struck the Seattle area in 2001, liquefaction caused sand boils and collapsed pits on Harbor Island.

The AIR Earthquake Model for the United States includes a liquefaction component that relies on the availability of accurate data concerning groundwater depth. The AIR model assesses the risk of liquefaction for the seven regions that

have sufficient groundwater-depth data along with a history of liquefaction occurrences during earthquakes. (This data was obtained from the USGS.) These areas include the greater San Francisco and Los Angeles areas; Portland, Oregon; Seattle, Washington; Salt Lake City, Utah; and the New Madrid and Charleston seismic zones. It is important to note that liquefaction is a secondary hazard. Although liquefaction damage alone may be severe on a particular structure, its contribution to the total damage caused by an earthquake is relatively small.

AIR has mapped the groundwater depths for those areas that are included in the liquefaction model. Figure 50 show the areas covered by the AIR model's groundwater depth data in the western (left-hand panel) and eastern (right-hand panel) sections of the country.

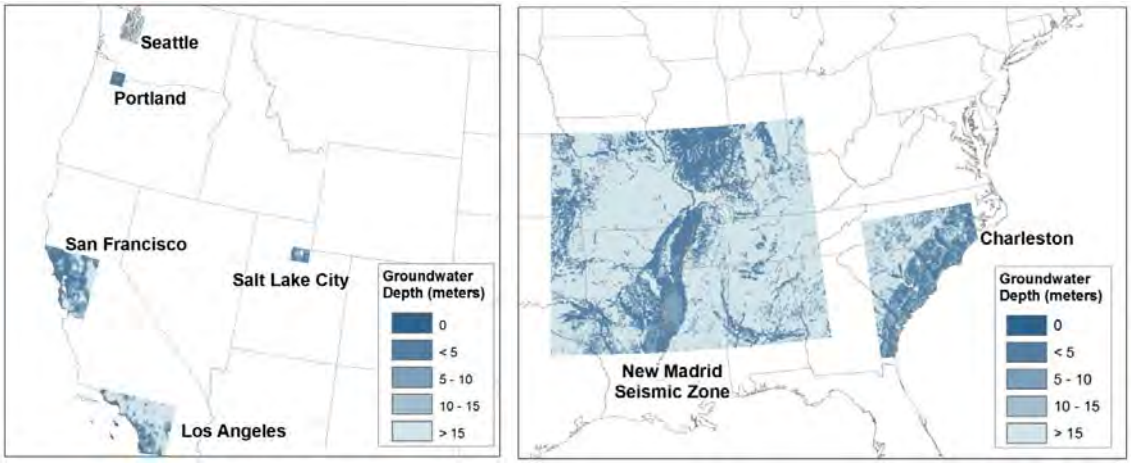

Figure 50. Groundwater Depths for Liquefaction-Modeled Areas in the Western (left) and Eastern (right) United States

The liquefaction estimation method, which compares liquefaction resistance to liquefaction demand, follows collective research summarized by Idriss and Boulanger (2008) and Youd et al. (2001). Liquefaction resistance is dominated by soil strength characterized by shear-wave velocity and groundwater depth, while liquefaction demand is a function of ground motion intensity. The building damage caused by liquefaction is calculated based on liquefaction-induced ground settlement recommended by Ishihara and Yoshimine (1992).

Note that in the AIR Earthquake Model for the United States shake damage and damage caused by liquefaction are combined and are not separable in the software.

4.5 Ground Motion Intensity and Spatial Correlation

The assessment of ground motion intensity has traditionally been based on an approach that used event magnitude, the source-to-site distance, and the local soil conditions. These calculations also accounted for variability in the ground motion, based on observed deviations during historical earthquakes. The variable ground motion intensities were included in the equations by means of a lognormally-distributed error term, also known as a "residual."

Recent studies of these ground motion residuals show that, rather than being randomly distributed through an area during an earthquake, there is a distinct correlation between residuals at one site and residuals at nearby sites. Observations have shown that if the ground motion is higher than expected at a particular site, it is more likely that a nearby site will also experience higher-than-expected ground motion.

Because the USGS national seismic hazard maps are designed to capture the hazard at any given single site, the focus of the USGS and developers of the NGA equations has not been on correlated ground motion. However, such correlation has important implications for *portfolios* of properties held by insurance providers. For example, these pockets of high or low ground motion may be very large and encompass an entire metropolitan area. When a higher-than-expected ground motion pocket occurs in a densely populated area, the losses will be much larger than expected everywhere in that area. The converse is true when a lower-than-expected ground motion pocket occurs in a densely populated area.

The AIR model explicitly takes into account the effects of site-to-site correlation of ground motion intensity measurements when estimating the loss due to seismic activity for spatially extended portfolios.[8, 9] The modeling of ground motion correlation by AIR is therefore a departure from the USGS maps.

Figure 51 provides a visual illustration of ground motion correlation. Figure 51a shows a recreation of the 1994 Northridge earthquake's ground motion footprint using the latest NGA equations without modification. Figure 51b is considerably more complex because it takes output from the NGA equations and modifies it using information on soils and basin effects. Figure 51b represents median ground motion as calculated by the AIR model. Figure 51c, however, is the best estimate of "actual", or observed, ground motion taken from the USGS ShakeMap. (For more

[8] For further technical details, see P. Bazzurro et al., "Effects of Spatial Correlation of Ground Motion Parameters for Multi-Site Seismic Risk Assessment: Collaborative Research with Stanford University and AIR" available on the USGS website at http://earthquake.usgs.gov/research/external/reports/07HQGR0032.pdf.

[9] For further details on the methodology used by AIR to simulated ground motion with spatial correlation, see Park, J., Bazzurro, P. and J.W. Baker "Modeling Spatial Correlation of Ground Motion Intensity Measures for Regional Seismic Hazard and Portfolio Loss Estimation," *Proceedings of ICASP10* (Tokyo, Japan, July 31-August 4, 2007)

about ShakeMap see "Using ShakeMap for Damage Function Calibration" in Section 5.8.)

While the overall comparison between Figure 51b and Figure 51c is reasonably good, the actual ground motion footprint reveals pockets of very high concentrations of ground motion. In this case, the pockets are located in heavily populated areas, which led to losses that were much higher than would otherwise be expected from an earthquake of Northridge's magnitude (M6.7) and epicentral location.

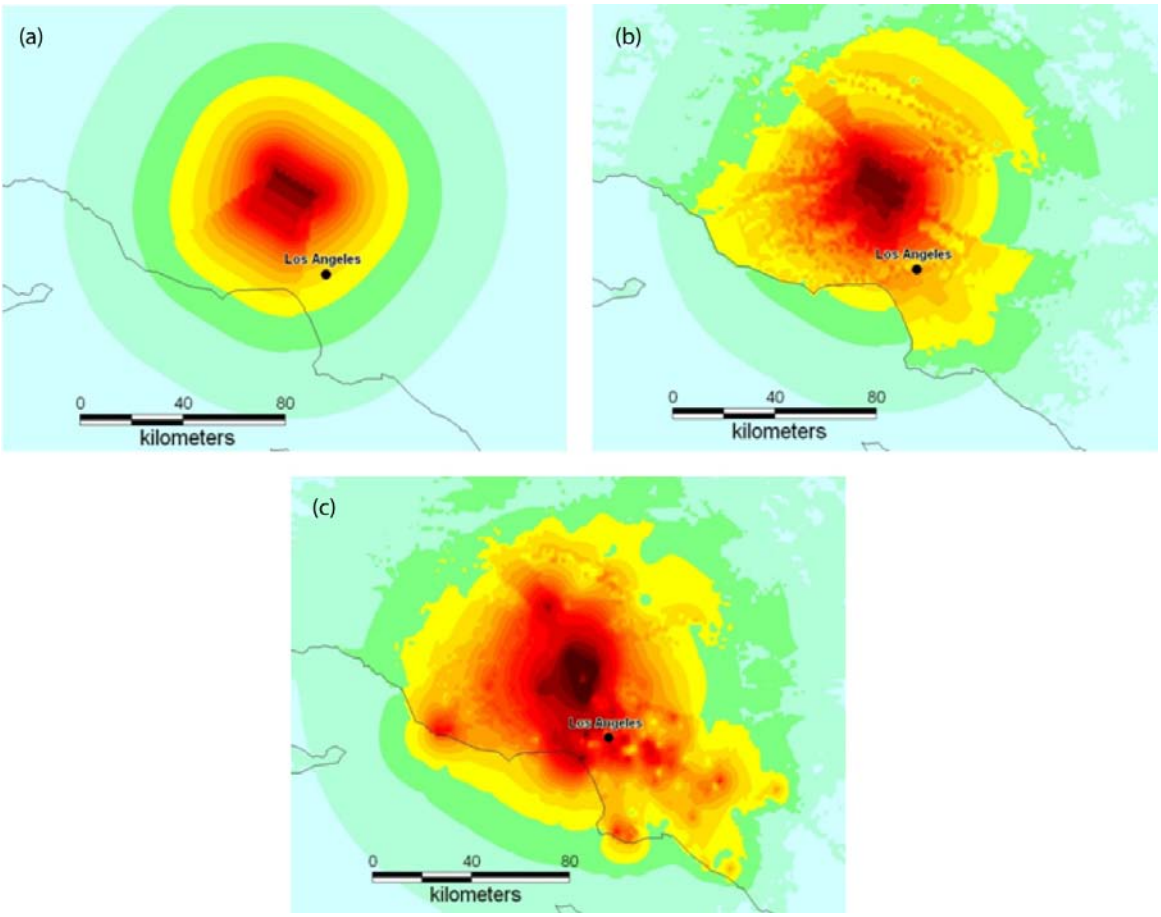

Figure 51. USGS TriNet Map for the Northridge Earthquake (top left), Expected Ground Motion (top right), and the Ratio (bottom) Showing Spatial Correlation of Residuals

The impact of these spatial patterns and the interaction with the distribution of risks or assets in a portfolio can generate very different loss estimates. Indeed the next earthquake that occurs, even if it occurs on the Northridge fault, is not going to look like the map in Figure 51c. Using actual ground motion recordings as well as the spatial correlation model, the AIR model can generate ground motion footprints of any historical events that are consistent with recorded peak ground motion parameters. By generating these accurate and consistent simulated maps

dozens or even hundreds of times, the model produces a realistic distribution of losses and one that is consistent with observed losses.

Figure 52 shows an example of this concept, again applied to the 1994 Northridge earthquake. The figure shows four of 50 simulated ground motion maps of the Northridge earthquake that are consistent with recorded ground motions and allow for spatial correlation. The chart on the right shows the resulting loss distribution from all 50 simulations. The observed (reported) losses for Northridge fall very close to the middle of the distribution.

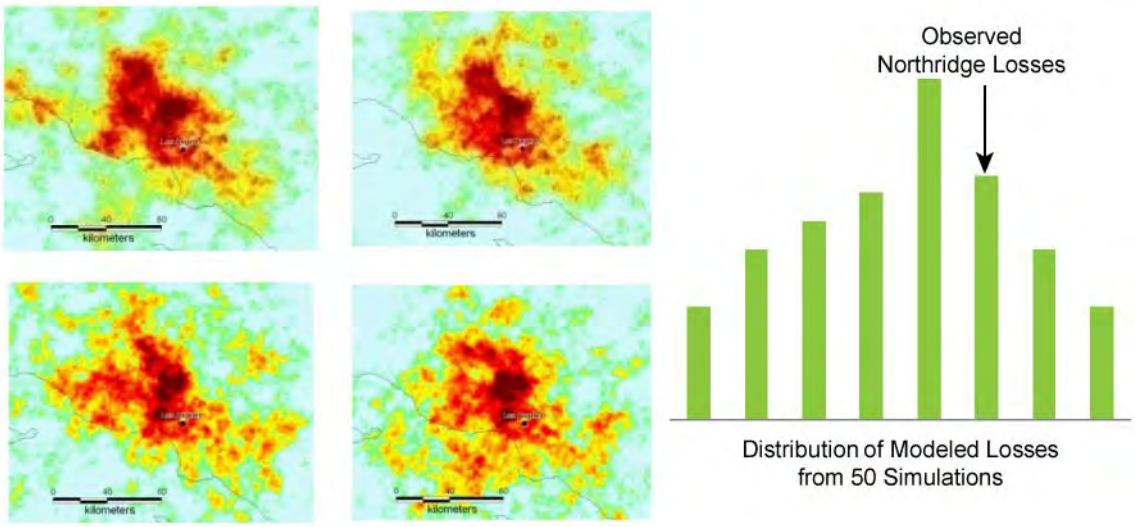

Figure 52. Multiple Ground Motion Maps with Spatial Correlation and the Corresponding Distribution of Modeled Losses for the 1994 Northridge Earthquake

Effects of Spatial Correlation on Portfolio Losses

As mentioned earlier, site-to-site correlation increases as the distance between the sites decreases, producing pockets of unexpectedly high or low ground motion. This of course means that the correlated residuals have a greater effect on clustered exposures, which has important implications for portfolios of properties. For example, the pockets of high or low ground motion may be very large and encompass an entire metropolitan area. When a high ground-motion pocket occurs in a densely populated area, the losses will be much larger than expected everywhere in that area. The converse is true when a lower-than-expected ground motion pocket occurs in a densely populated area.

While large portfolios that are distributed over a large area will, in general, be less affected by spatial correlation than smaller, more concentrated portfolios, in both cases failure to account for ground motion correlation will underestimate the probability of both very high and very low losses, the former being the more serious matter.

Figure 53 shows the impact on the loss exceedance curve. When ground motion uncertainty is considered with spatial correlation, the annual exceedance probability tends to drop more steeply for frequently exceeded losses, thereby lowering the overall losses in this part of the curve. However, the annual exceedance probability then levels and extends farther to include the larger and less frequent losses. Because the exceedance probability curves generated using spatial correlation are based on many more simulations and hence more information, they are more robust—particularly in the tails of the distribution.

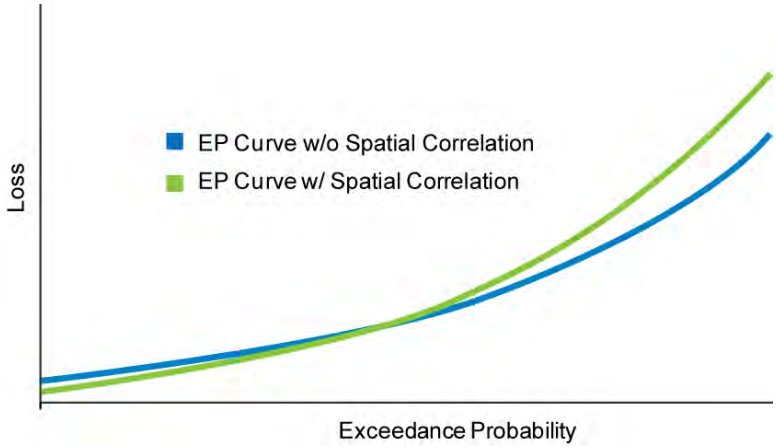

Figure 53. Loss Exceedance Curves with (Green) and without (Blue) Spatial Correlation

4.6 Validating Local Intensity Calculations

This section provides a variety of exhibits illustrating the comprehensive process undertaken by AIR researchers to validate the local intensity module of the AIR Earthquake Model for the United States.

Validating the NGA Equations

As discussed in Section 4.2, the next generation attenuation (NGA) equations implemented by the USGS in the 2008 seismic hazard maps were developed based in the largest, most robust database of ground motion recordings available—a database more than three times larger than had previously been available. In turn, the NGA equations are more reliable and scientifically defensible than any previously produced.

Because the NGA equations themselves have been thoroughly validated by their developers, AIR's implementation of them in the model validates AIR's approach to ground motion modeling.

Figure 54 and Figure 55 show median ground motion and one standard deviation as generated by the NGA equations for the 1989 Loma Prieta and 1994 Northridge earthquakes, respectively.

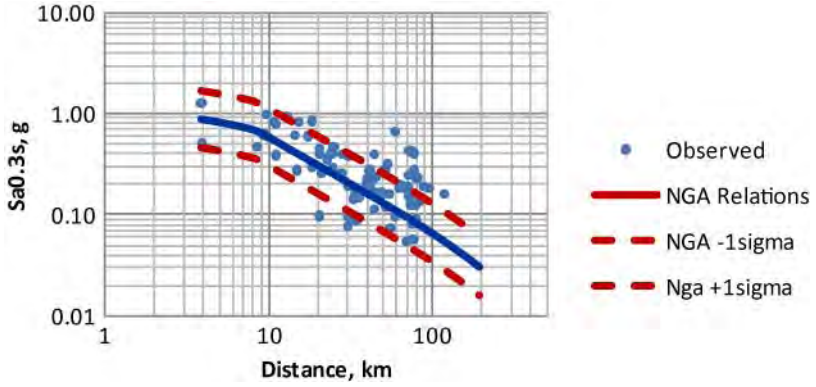

Figure 54. Comparison between Observed and NGA Predicted Mean Ground Motion with Uncertainty for the 1989 Loma Prieta Earthquake

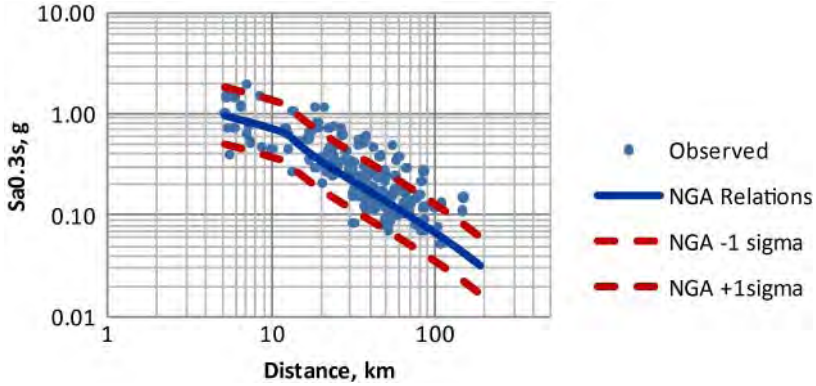

Figure 55. Comparison between Observed and NGA Predicted Mean Ground Motion with Uncertainty for the 1994 Northridge Earthquake

What we see in the Northridge comparison is the higher-than-expected ground motion for the Northridge event due to spatial correlation (localized "hot spots" in areas of high exposure) as discussed above in Section 4.5. The NGA attenuations show here reflect the median of the ground motion of many earthquakes.

Comparing AIR and USGS Ground Motion Hazard

To validate the modeled earthquake hazard, the details from earthquakes at locations across the entire country were compared to data recorded by the USGS. This validation is based on both the distribution of events and the ground motion for each event.

For each of the cities, whose locations are shown in Figure 56, AIR computed the hazard using the 475-year return period ground motion hazard in terms of the peak ground acceleration (PGA), the 0.3 second spectral acceleration (for high-frequency, low-rise, rigid structures), and the 1.0 second spectral acceleration (for flexible structures).

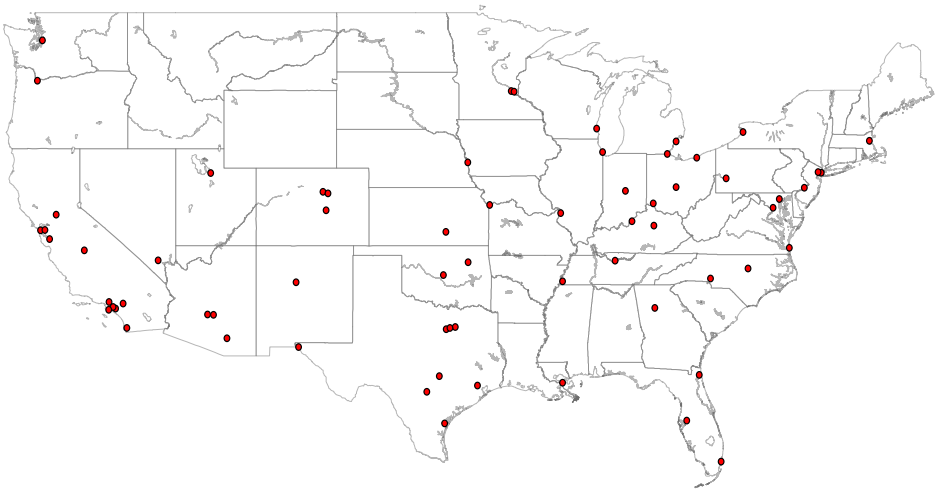

Figure 56. U.S. Locations Used for Ground Motion Validation

As can be seen in Figure 57, Figure 58 and Figure 59, the clustering of data points near the 45-degree line indicates consistency between the AIR and USGS models. There are subtle differences, but the deviations are within an acceptable range, given the complexity of the hazard calculations.

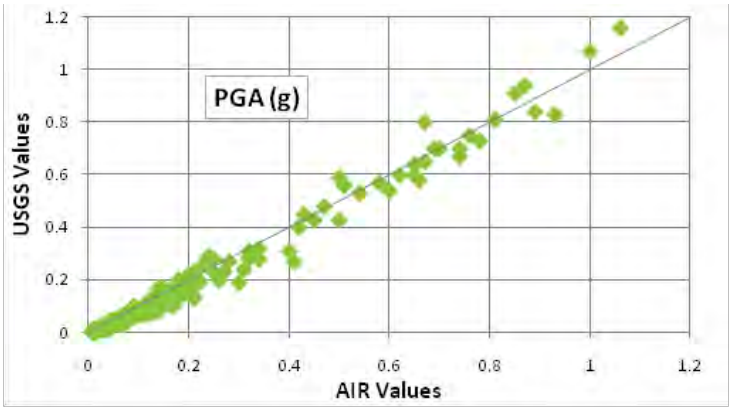

Figure 57. USGS vs. AIR 475-Year Return Period PGA Values

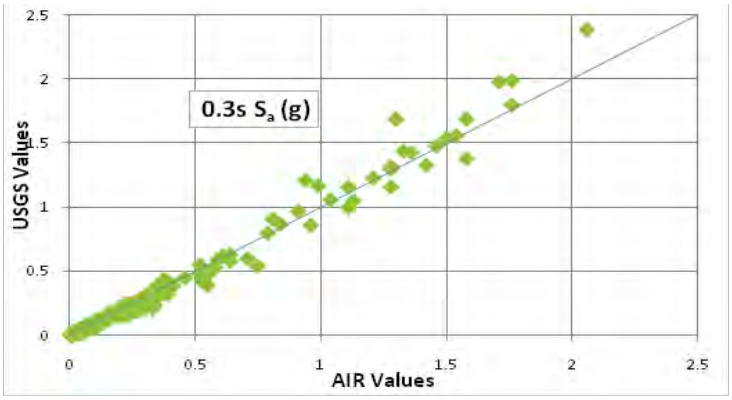

Figure 58. USGS vs. AIR 475-Year Return Period 0.3 s S_a Values

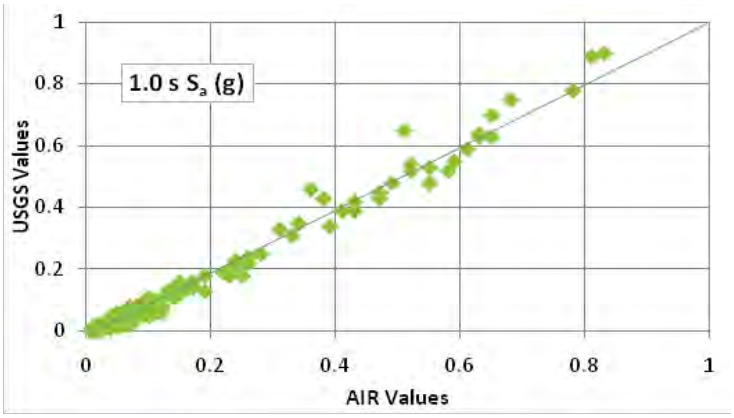

Figure 59. USGS vs. AIR 475-Year Return Period 1.0 s S_a Values

Validating the Liquefaction Module

Because it is difficult to separate the damage caused by shaking from damage caused by liquefaction in claims data, the best method for validating the liquefaction model is by comparing it to historical occurrences of liquefaction due to earthquakes.

The following figures show the liquefaction severity for simulated historical events at ZIP Code resolution, along with observed liquefaction sites from the actual historical earthquakes. In the figures, liquefaction severity refers to the amount of settlement and shifting of the soil that takes place, which depends on both the liquefied state of the soil and the amount of shaking amplification that takes place due to the soil conditions.

For the Loma Prieta earthquake of 1989, observations of liquefaction occurred around San Francisco; however the earthquake rupture was farther south (outside the area shown in Figure 60) and liquefaction farther south may not have been recorded as accurately, due to the wetlands in that area. The simulations of

possible liquefaction severity coincide with observed sites in urban areas, but also show more damage south of these sites. This is due to both the water depth table data and simulated shaking from the earthquake itself.

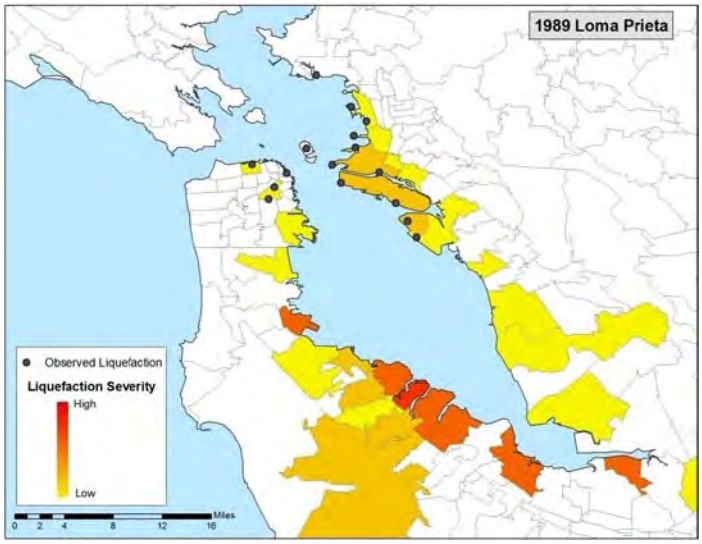

Figure 60. Simulated Liquefaction Severity and Observed Liquefaction Sites, 1989 Loma Prieta Earthquake

The observed liquefaction sites from the San Francisco earthquake of 1906 are consistent with simulated locations (Figure 61). The simulation shows the heaviest severity in almost the same areas as the simulation for Loma Prieta.

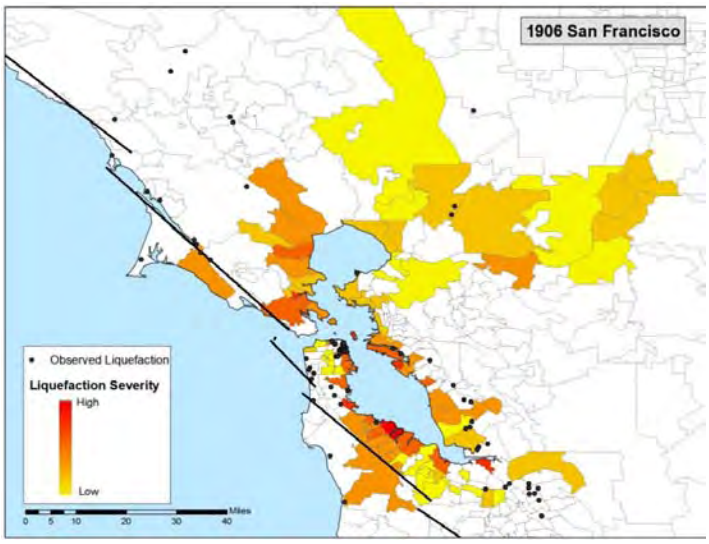

Figure 61. Simulated Liquefaction Severity and Observed Liquefaction Sites, 1906 San Francisco Earthquake

The observed liquefaction sites from the Northridge earthquake of 1994 show a very good consistency with simulated locations, as shown in Figure 62.

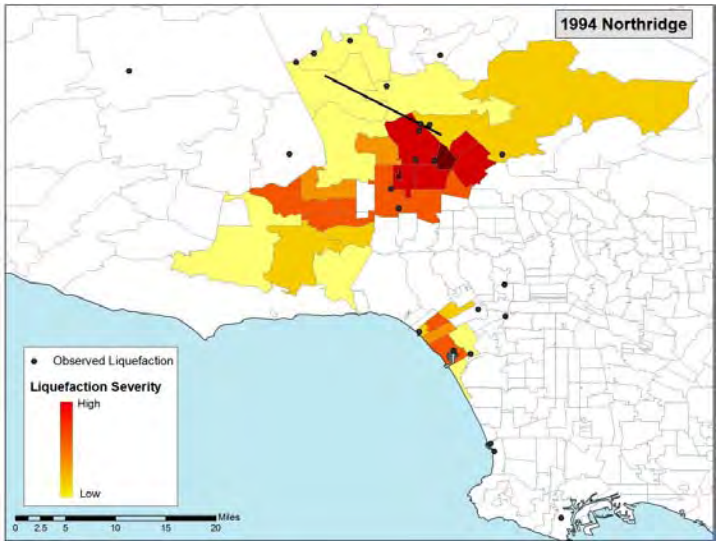

Figure 62. Simulated Liquefaction Severity and Observed Liquefaction Sites, 1994 Northridge Earthquake

The observed liquefaction sites from the Nisqually earthquake of 2001 show a very good consistency with simulated severity (Figure 63). As in the Loma Prieta earthquake, the areas immediately next to the rupture are less prone to liquefaction damage than sites farther away that have the soil and groundwater conditions that can lead to liquefaction during an earthquake.

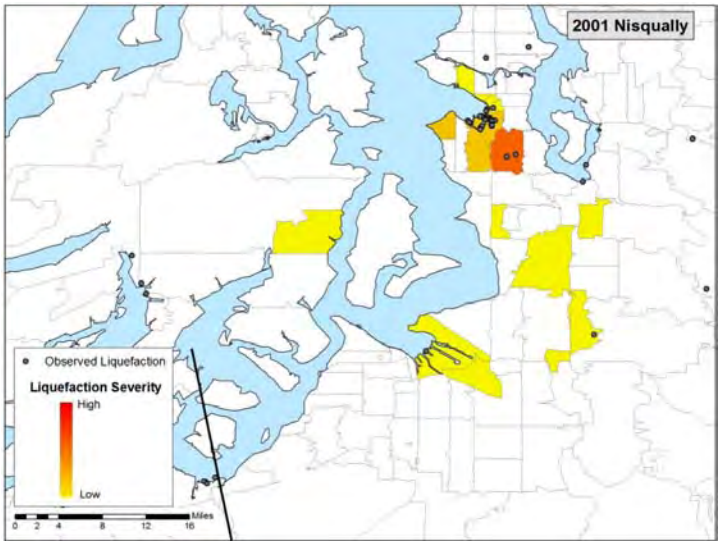

Figure 63. Simulated Liquefaction Severity and Observed Liquefaction Sites, 2001 Nisqually Earthquake

5 Damage Estimation

The vulnerability module of the AIR Earthquake Model for the United States estimates losses caused by ground shaking to residential, commercial and industrial assets, and to automobiles. In addition, the model takes into account the possibility of losses caused by soil liquefaction as a result of ground shaking, and by fire that may ignite as a result of earthquake damage (ruptured electrical and gas lines, chemical spills, damage to tanks and oil refineries, etc.).

Damage functions are used to compute the losses to assets of different construction classes. A damage function is a statistical relationship between the intensity of the ground motion and the fraction of the replacement cost of the asset that is needed to repair the damage. This fraction is known as the damage ratio (DR). Damage functions differ for assets belonging to different construction classes and are formulated based on characteristics of the asset (e.g., construction materials, lateral force structural resisting system, building height, and vintage) that affect the asset's vulnerability to ground shaking.

The ground motion intensity parameters used in the model to predict building performance vary by construction type and height, as shown in Table 9. Using different measures of intensity allows the model to exploit the higher correlation between different ground motion intensities and responses of various building classes.

Table 9. Independent Variables for Different Construction Classes

Construction Class	Height	Independent Variable
Wood Frame	Low-Rise	S_a(0.3s)
Masonry Veneer	Low-Rise	S_a(0.3s)
Unreinforced Masonry – Bearing Wall and Frame	Low-Rise/Mid-Rise	S_a(0.3s)
Reinforced Masonry Shear Wall–With and Without MRF	Low-Rise/Mid-rise	S_a(0.3s)
	High Rise	S_a(1s)
Reinforced Concrete Shear Wall–With and without MRF; Reinforced Concrete MRF–Ductile and Non-Ductile; Tilt-Up and Pre-Cast Concrete	Low Rise	S_a(0.3s)
	Mid-Rise	S_a(1s)
	High Rise	S_a(3s)
Light Metal, Braced Steel Frame, Steel MRF–Perimeter and Distributed	Low-Rise/Mid-Rise	S_a(1s)
	High Rise	S_a(3s)
Long-Span	N/A	S_a(3s)
Mobile Homes, Industrial Facilities (400+ class) and other Construction Classes (200+)	N/A	PGA

Note that not all the height classes in the table are applicable to all construction classes. For instance, mid-rise and high-rise heights are not applicable to tilt-up and light metal buildings.

5.1 Building Classification

This section describes some of the most prominent of these classes, and how each is affected by ground shaking due to earthquakes.

Wood Frame Construction

In the continental United States, the residential building stock is dominated by wood frame construction. About 98% of all types of homes in the earthquake-prone west, from low-cost subsidized dwellings to mansions, are wood frame structures. In addition to residential assets, a significant percentage of commercial structures are wood frame as well. The AIR Earthquake Model for the United States supports two types of wood structures: wood frame, and wood frame with masonry veneer.

Several historical events brought about changes in wood frame construction practices including World War II, the post-war economic and construction boom, the constantly evolving standard of living, and the adoption of modern construction methods such as mass production. However the most significant events that have affected the current building codes for wood frame construction are the earthquakes that occurred along the West Coast over the last 100 years. During this time, each earthquake brought about new lessons, which have since been incorporated in building codes in an effort to improve the seismic performance of these structures.

A typical modern wood frame home in the United States has one to three floors, and sometimes includes a basement. The foundations are often made of a concrete slab-on-grad or, in the case of some older wood frame houses, of spread concrete footings. The exterior walls are finished with stucco, wood siding or shingles, vinyl, or aluminum cladding. Interior walls in older homes are usually finished with plaster; in newer ones they are finished with gypsum boards. The pitched roofs on homes of all ages are usually covered by shingles or tiles, and newer homes sometimes have composition shingles. Flat roofs are usually covered by tar and gravel.[10]

[10] For a detailed examination of wood frame housing construction, see *Review of Structural Materials and Methods for Home Building in the United States: 1900 to 2000,* U.S. Department of Housing and Urban Development (Washington, DC) prepared by National Association of Home Builders (NAHB) Research Center (Upper Marlboro, MD, 2001)

Masonry Construction

Another common type of construction used for residential and commercial dwellings in the United States is masonry. For modeling purposes, AIR divides masonry into two categories: unreinforced masonry and reinforced masonry.

Unreinforced masonry (URM) buildings include structures that do not have any reinforcement steel within the load-bearing masonry walls. As a result, these structures have limited lateral load-resistance capacity and are very vulnerable to the lateral loads generated by earthquakes. This poor performance of URM structures has been observed in all past earthquakes. In 1986, the California Seismic Safety Commission enacted the "URM Law" in order to reduce the vulnerability of these structures. This law requires the local governments in the state's highest seismic hazard regions (defined as Zone 4 in the now obsolete Uniform Building Code) to retrofit URM buildings following specific guidelines. In the eastern part of the country, new construction of unreinforced masonry is still permitted and URM structures are more common.

Reinforced masonry (RM) contains load-bearing walls of brick or concrete block masonry reinforced by steel bars. The reinforced brick, or reinforced hollow concrete block shear walls, which extend from the foundation to the roof, provide lateral load-resistance to the structure. Although the performance of modern reinforced masonry structures is likely to be similar to the modern engineered construction of reinforced concrete structures, older RM structures can have enough deficiencies to perform as badly during earthquakes as URM structures. The deficiencies that affect their performance depend on the construction practices that were in place in a particular region at a particular time. For example, the quality of the grout depends on its age and determines the strength of the bond between reinforcement steel and masonry. High-quality grout is instrumental in providing good lateral resistance during earthquakes.

Steel and Concrete Construction

Steel and reinforced concrete is used for a large number of commercial and industrial buildings, and for residential apartment buildings. These structures consist of steel or reinforced concrete elements (e.g., beams, columns, and shear walls), which make up the primary lateral load-resisting system. These elements as well as the partition walls, façade, floors, etc., of these structures are generally designed and constructed according to similar guidelines, so their performance during earthquakes is usually more uniform than that of the non-engineered wood-frame construction. However, the configuration and the construction methods used for the primary lateral load-resisting systems of these structures vary considerably between different building classes. As a result, typical

buildings belonging to these classes may show significantly different behavior during ground shaking. For example, reinforced concrete buildings with shear walls usually respond better to ground shaking than reinforced concrete frame buildings.

5.2 Impact of Regional Construction on Building Vulnerability

The AIR Earthquake Model for the United States takes into account regional variations in building vulnerability, which are due to the different design requirements and construction practices. Therefore, AIR developed distinct damage functions for the three areas of the country with distinctly different hazard levels: California, Washington and Oregon, and all other states.

The model takes into consideration the building codes adopted in each area over time. For the purpose of deriving damage functions for different construction types, in California, a "high code" is used due to more rigorous seismic design requirements, in Washington and Oregon a "moderate code" is used, and in the rest of the country, a "low code" is used. Structures built before 1940 are considered to be "pre-code."

The awareness for earthquake-resistant design and construction is higher in California, and seismic guidelines for building codes were adopted earlier in earthquake-prone counties. Therefore, buildings in California generally perform better than comparable buildings in other regions when subjected to the same level of ground shaking. Historically, there has also been some awareness of earthquake-resistant design in Oregon and Washington, and many structures there have been designed with earthquakes in mind. However, in the remainder of the country, buildings have been primarily designed only for gravity loads and, in some cases, wind loads. In all these states, for many categories of buildings, the design of the lateral load resisting system is controlled by design wind loads rather than earthquake loads.

Lateral load resisting systems for wind loads provide resistance from seismic loads as well. Therefore, when assessing the lateral strength of a building for damage function development purposes, the AIR model takes into consideration design wind loads throughout the entire continental U.S. This plays an important role for the development of damage functions in the eastern US, especially along the coast, where although the buildings are not designed for earthquakes, the wind load design helps these structures to resist the lateral loads from earthquakes.

5.3 Impact of Year Built on Building Vulnerability

A building's age plays a significant role in its vulnerability, especially for concrete structures. The reinforced concrete (RC) structures that were built in California before 1975 are generally very brittle and are therefore unable to accommodate large deformations that may be generated by intense ground shaking. Hence, these structures have a higher risk of collapse than those of similar construction built more recently. Other nonductile structures include RC frames that are designed to withstand gravity loads only, which are quite common in the central and eastern parts of the United States. For steel structures, age is not as important, although older steel structures are generally more vulnerable than newer ones. For example, many steel moment-resisting frame buildings built in southern California before 1994, which engineers considered to be almost indestructible, are unexpectedly brittle and incurred fractures in the steel column-beam connections during the M6.7 Northridge earthquake. Steel moment-resisting frame buildings designed and built after 1994 are expected to behave in a more ductile manner and show improved seismic performance.

A building's age typically identifies the building code that guided its design, and the construction techniques that were used when it was built. Thus older buildings are generally more vulnerable to shake damage than newer ones, since newer codes tend to have stricter design guidelines and are more rigorously enforced.

In the AIR Earthquake Model for the United States, the age bands for engineered construction, such as steel and reinforced concrete buildings, reflect the evolution of the seismic code provisions and are supported by the findings of post-earthquake damage reconnaissance reports. The age bands for non-engineered (or less engineered) construction classes, such as wood frame, were derived with more emphasis on the damage and loss data caused by historical earthquakes rather than by the evolution of code regulations.

It is interesting to note that for non-engineered (or less engineered) structures newer does not necessarily imply better seismic performance. For example, during the 1994 Northridge earthquake, wood frame buildings dating from the 1940s and 1950s performed, on average, better than those built in the 1960s. This is mainly because earlier houses were generally smaller in size, with smaller rooms and smaller and fewer openings in the façade, and had simpler plans and vertical layouts. The buildings in the 1960s were architecturally more daring with more open layouts, larger rooms, and large wrap-around windows, which are characteristics that compromised their seismic performance.

Figure 64 shows the average damage ratio for five different age bands (S_a(0.3s) = 0.75-1.25g), based on a statistical study of an extensive set of data from a claims database. The damage ratios are for wood frame structures in California that were damaged during the 1994 Northridge earthquake.

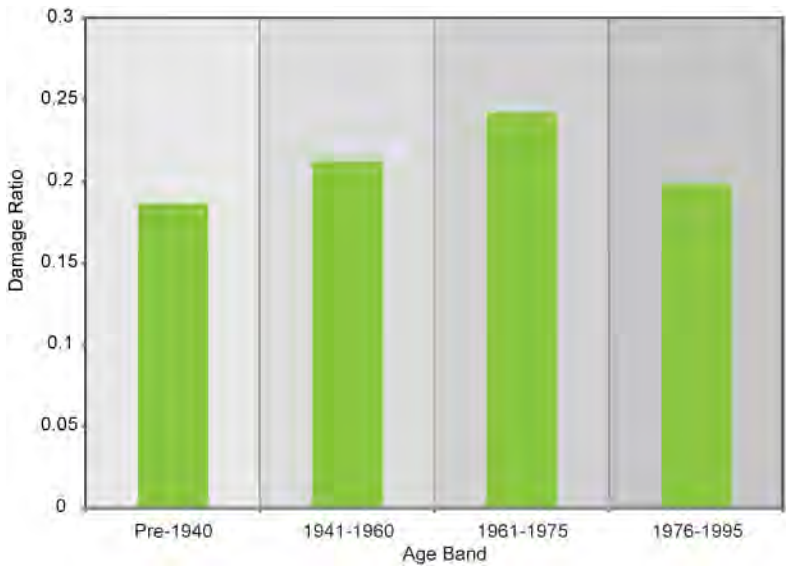

Figure 64. Damage Ratios of Wood Frame Structures of Different Ages after the 1994 Northridge Earthquake

The AIR model uses age bands that consolidate the results of all the building code review effort and statistical studies of damage and loss data from AIR engineers. Note that the age bands are not identical for the same construction classes in different regions of the United States, since codes and construction practices were not uniformly adopted at the same time across the country.

5.4 Building Damage Functions

The damage functions implemented in the AIR model correlate an appropriate ground-motion intensity measure with the building damage ratio (the ratio of the building's repair cost to its replacement value).

If an infinite amount of damage and loss data, including records of ground motion at each building location, were available for buildings of all construction classes and age bands, then the derivation of damage functions would only entail a statistical exercise involving regression techniques. However, such large databases are not available, for several reasons, the primary one being that damaging earthquakes do not occur frequently enough to provide extensive data. The result is that data is generally scarce and the data that do exist is often poorly recorded. Therefore, the most accurate damage functions for all construction

classes, all age bands, and all regions, can only be derived using a combination of engineering and statistical tools.

Hence, the AIR damage functions are based on engineering analyses, damage data collected after historical earthquakes, claims data at both property and aggregated levels, loss estimates for past earthquakes, and a careful evaluation of the prescription in the building codes. The balance in the adoption of these tools varies with different construction classes.

All engineering analyses performed for the purpose of evaluating the response of a building to different levels of ground shaking follow the conceptual flow-chart depicted in Figure 65.

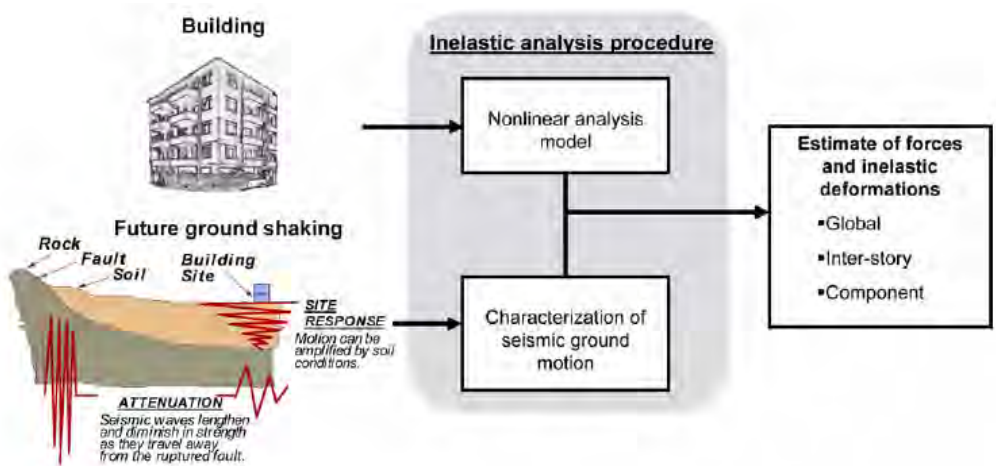

Figure 65: Conceptual Flow of Analyses Adopted for Building Damage Functions (adapted from FEMA 440)

The engineering analyses require the use of a computer representation of a building, and of the characterization of ground motions that such a building may be subjected to in the future. The following sections discuss in some detail the nonlinear analyses that can be performed to estimate the response of the building (i.e., mostly induced deformation such as roof and story drifts but also forces in structural members) when subjected to different ground motion intensities.

5.5 The Capacity Spectrum Method and the Use of Nonlinear Static Analysis

To estimate a building's response to different levels of ground shaking, a computerized model of the building is subjected to a lateral load pattern that represents the force generated by the ground motion (see Figure 66). The total load is then increased in successive steps to create a relationship between the intensity of the applied load (measured in terms of base shear) and the

deformation of the building (measured in terms of roof drift). The analysis terminates when the building (virtually) collapses. This static nonlinear procedure is often called pushover analysis and the force/deformation curve obtained is called a pushover curve. The shape of the load vector is an approximate representation of the accelerations associated with the fundamental mode of the structure's vibration.

When one is interested in predicting the response of a building to a specific ground motion in an expedited manner, then an available analysis method is the Capacity Spectrum Method (CSM), in which the quantities in the full building pushover curve are transformed into response measurements of an equivalent single-degree-of-freedom oscillator, such as the pendulum shown in Figure 66. The oscillator has the same natural frequency and degraded stiffness, after yielding, as that of the modeled building. More precisely, the applied load is translated into spectral acceleration, and the building deformation is translated into spectral displacement.[11] The pushover curve represented by these two parameters (which are related to the equivalent oscillator) is called the capacity curve. A building's capacity curve reflects various seismic characteristics of the building, such as its stiffness, its material brittleness or ductility, and its strength. This curve correlates the lateral deformation that a building is subjected to (in terms of spectral displacement) to a specific level of dynamic demand (expressed in terms of spectral acceleration).

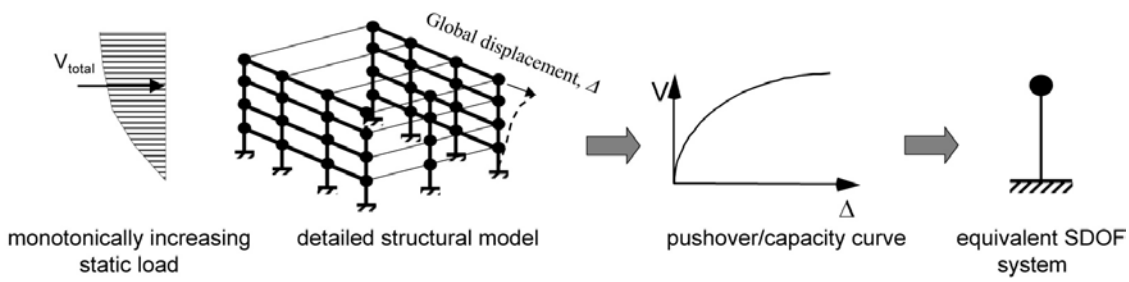

Figure 66: Schematic Depiction of Static Pushover Analysis used in the Capacity Spectrum Method (excerpted from FEMA 440)

As will be discussed later, any anticipated ground motion that may affect a building can be modeled in a more comprehensive form as a *time history* of ground acceleration. However, several simplified representations are also available to engineers, one of which is the response spectrum. In the response spectrum representation, which is convenient to use in the framework for the Capacity Spectrum Method, the demand on a building imposed by ground

[11] Spectral acceleration and spectral displacement are two response measures of oscillators with given vibration period and damping.

motion is represented by the maximum acceleration and displacement of a series of oscillators. The response of this collection of pendulums can be plotted as a curve of acceleration/displacement pairs known as the demand curve.

In Figure 67, a series of simple oscillators are subjected to ground shaking. The peak responses of the oscillators are plotted on the graph to the right, showing the spectral acceleration against the spectral displacement. The radial lines on the graph represent the periods of the oscillators.

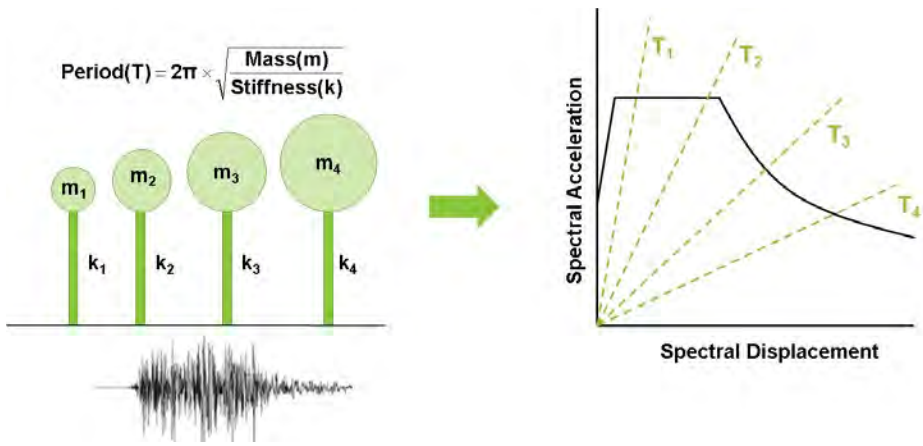

Figure 67. Maximum Acceleration and Displacement of a Series of Oscillators

The demand curve and the capacity curve are represented by the same parameters and can be plotted in the same figure. The intersection of the demand curve and the building capacity curve plotted on the spectral acceleration vs. spectral displacement plane corresponds, within a constant, to the maximum roof displacement of the building relative to the ground in response to that ground motion.

Figure 68 shows the intersection of the demand and capacity curves, which represents the peak response of the structure.

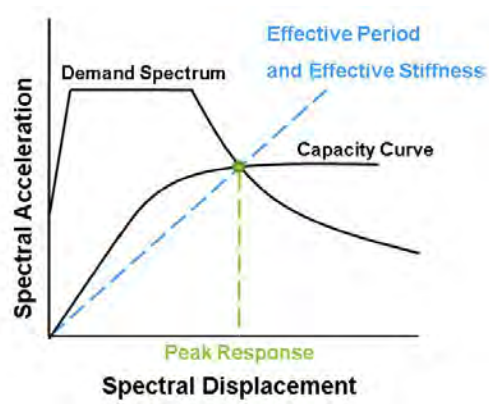

Figure 68. The Peak Response of a Structure Determined by its Capacity Curve

A capacity curve representing a single building of a certain construction class will have a unique intersection with different response spectra for different ground motion intensities. Similarly, different capacity curves representing different buildings of the same class will have unique intersections with the same response spectrum from a given ground motion intensity, as illustrated in the left panel of Figure 69. These attributes provide the ability to distinguish between the responses of various building classes to different ground motion intensities.

During ground shaking, the amount of deformation incurred by the different stories of a building can be derived, given certain assumptions, from the deformation at the roof level. The story deformations can be related to the damage suffered by all types of components, both structural (e.g., columns and beams) and non-structural (e.g., cladding, partitions, ceiling tiles, etc.) at each story and, therefore, to the repair strategies that are expected due to the predicted damage. The repair strategies for each damaged component can be priced and expressed in terms of a fraction of the replacement cost of the entire building.

Therefore, each intersection between a ground motion demand curve and a building capacity curve generates one point of the damage function for that building; the entire damage function is subsequently generated from multiple intersections. The right panel of Figure 69 shows conceptual damage functions generated for three buildings: A, B, and C, which belong to the same construction class. This is the essence of the Advanced Component Method (ACM), which AIR introduced in 2000. A similar approach has also been adopted in the current version of the model for developing damage functions for a few construction classes for which damage data, or claims data, or detailed nonlinear time-history analysis results are not available.

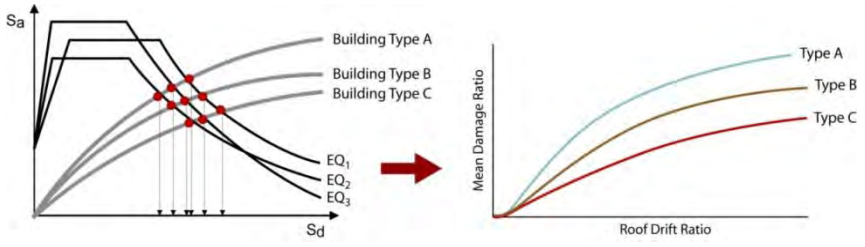

Figure 69. Maximum Displacement and Building Damage Depends on Ground Motion and Building Characteristics

5.6 Nonlinear Dynamic Analysis

The capacity spectrum method, which uses pushover analysis for assessing responses of buildings to ground shaking, is a perfectly viable analysis technique for addressing the inelastic response of buildings that respond predominantly in the fundamental mode of vibration. However, because of its inherent assumptions, CSM analysis may lose accuracy in predicting the seismic response of long-period buildings, whose higher modes of vibration need to be considered, and of other buildings with complex post-elastic behavior. In particular, pushover analysis has been shown to overestimate the displacement of brittle structures, especially stiff ones (e.g., old, low- and mid-rise concrete buildings) and of stiff, ductile structures (e.g., wood frames), and to underestimate the displacement of flexible, ductile structures (e.g., high-rise steel buildings).

With the release of the current model, AIR engineers have taken yet another step in the advancement of objective, engineering-based earthquake vulnerability assessment with the introduction of nonlinear dynamic analysis (NDA) to replace static pushover analysis. Computationally very expensive and practicable only as a result of major advances in computing power, NDA is today the current state-of-the-art methodology for predicting building response to earthquake ground motion.

The framework within which NDA is incorporated is the same as in ACM**.** The primary difference is in how the relationship between ground motion intensity and building response is established.

As with CSM (and ACM), the first step in NDA analysis is to create a computer representation of a building that captures the nonlinear post-elastic behavior of a building's structural elements that undergo damage (see Figure 70). A large number of historical ground motion records of varying intensities are loaded into the software to perform time-history (dynamic) analysis. Essentially, the virtual building is shaken (rather than pushed) using the recorded ground motions in the same way that it would be shaken by an actual earthquake.

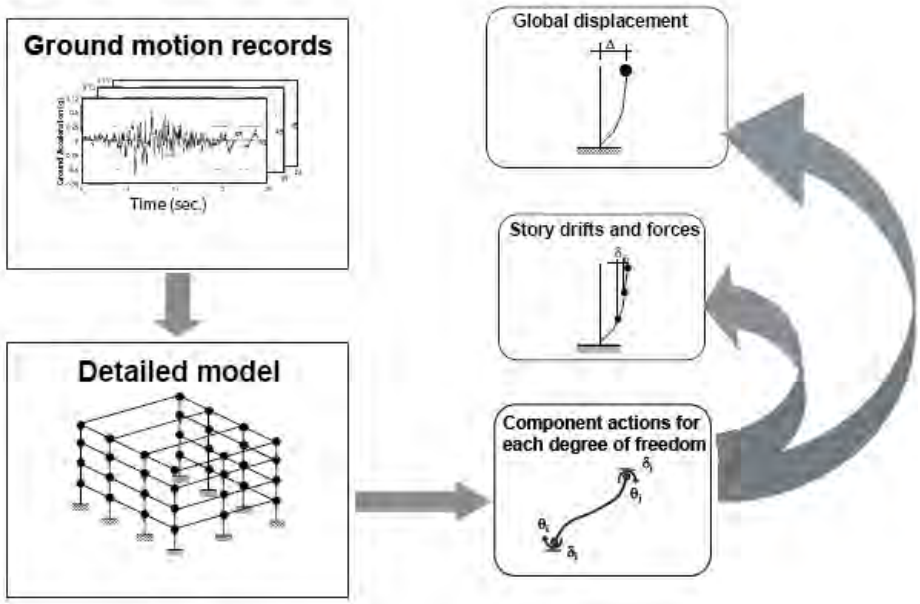

Figure 70. Flow Chart Depicting the Use of NDA to Determine Building Response (Excerpted from FEMA 440)

The use of time-history analysis allows an explicit consideration of the effects of the duration of the earthquake shaking on the cumulative damage of building components. In each analysis, the forces and deformations occurring in all structural members of the model are computed and used to evaluate the global response measures such as maximum peak inter-story drifts and forces, roof displacement, and peak story accelerations.

An example of the estimates of maximum peak inter-story drift and peak floor acceleration obtained via NDA by applying ground motions from 100 earthquakes to a 10-story steel moment-resisting frame building is shown in Figure 71 below. The peak inter-story drift is the highest lateral displacement between two consecutive floors, normalized by the inter-story height. The *maximum* peak inter-story drift is the maximum drift among all stories that is observed over the entire duration of the earthquake. This quantity is well correlated with the damage of structural elements (e.g., beams and columns) and of deformation-sensitive non-structural elements (e.g., wall partitions). The peak floor acceleration (PFA) is the highest acceleration of a particular floor in response to ground shaking. Similarly, the *maximum* peak floor acceleration is the highest PFA found along the entire height of the building. This quantity is well correlated with damage to acceleration-sensitive nonstructural components (e.g., suspended ceilings), and to contents.

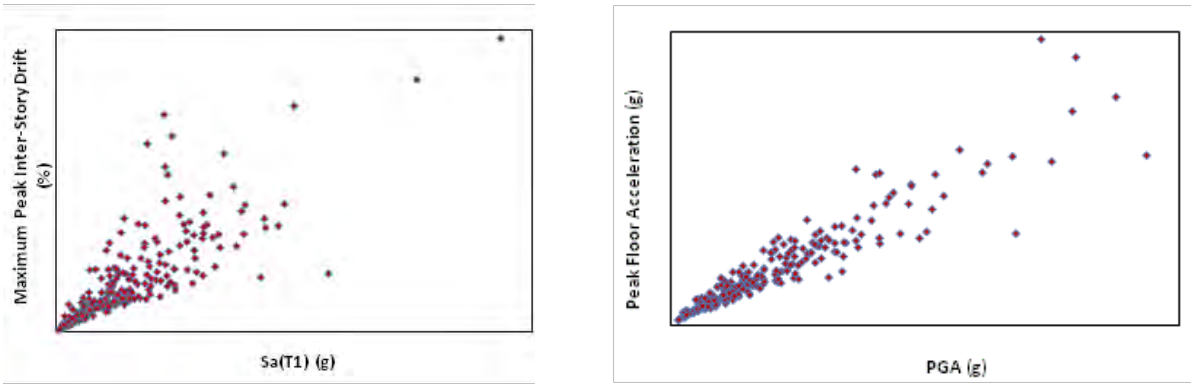

Figure 71. Maximum Peak Inter-Story Drift Ratios (MIDR) and Maximum Peak Floor Accelerations (MPFA)

Regression analysis can then be performed on the results in Figure 71 to establish the best relationships between the ground motion intensity parameters (e.g., spectral acceleration at the fundamental period of the building or Sa(T), and its peak ground acceleration or PGA) and the building's global response measurements (e.g., maximum peak inter-story drift and peak floor acceleration). Note that a special statistical treatment was applied to account for ground motions that cause the complete collapse of the building (this response is not shown in the figure below). The use of ground motions from multiple earthquakes allows the model to obtain not only an estimate of the mean response given a certain level of ground shaking, but also allows it to account for the variability in the buildings' nonlinear response generated by different records of the same intensity.

Figure 72 shows the expected maximum peak interstory drift and interstory drift at different stories found by regression analysis for the same 10-story steel moment-resisting frame whose responses to non-collapsing ground motions were shown in Figure 71. The figure shows the relationship between the global response parameters and the intensity of the ground motion when the collapse cases are (correctly) considered (solid lines) or disregarded (dotted lines). Collapse cases must be considered since the building will not withstand indefinitely large deformation without failing.

NDA directly provides, without any limiting assumptions, the force imposed on a building by ground motion. Deformation levels (or story acceleration levels, when necessary) are then used to determine component damage and the associated repair strategy, and the monetary loss for the entire building is estimated by combining component repair costs.

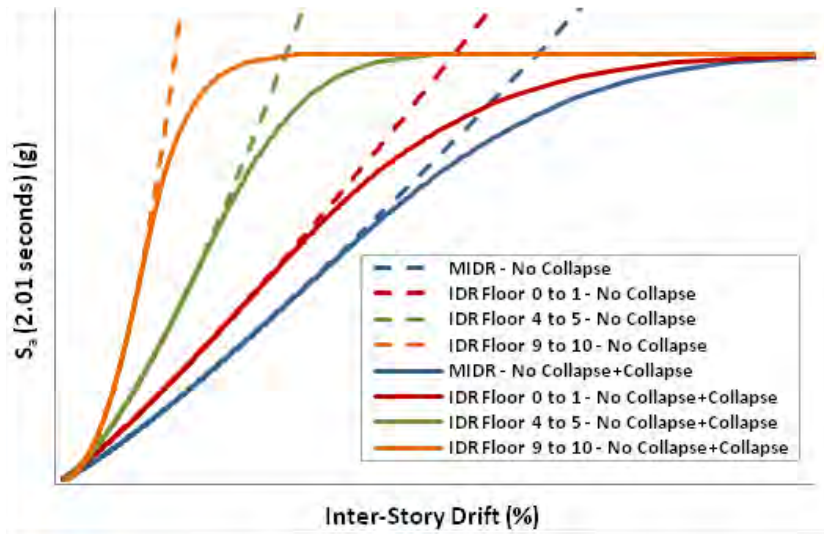

Figure 72. Relationship between Spectral Accelerations at the Fundamental Period of a Building and the Induced MIDR and IDR.

Note that with NDA, building deformation at each story is computed from a fully detailed model of the building. Because building response is calculated along the height of the building, NDA allows higher modes of vibration to be captured as well as different failure modes, as shown in Figure 73.

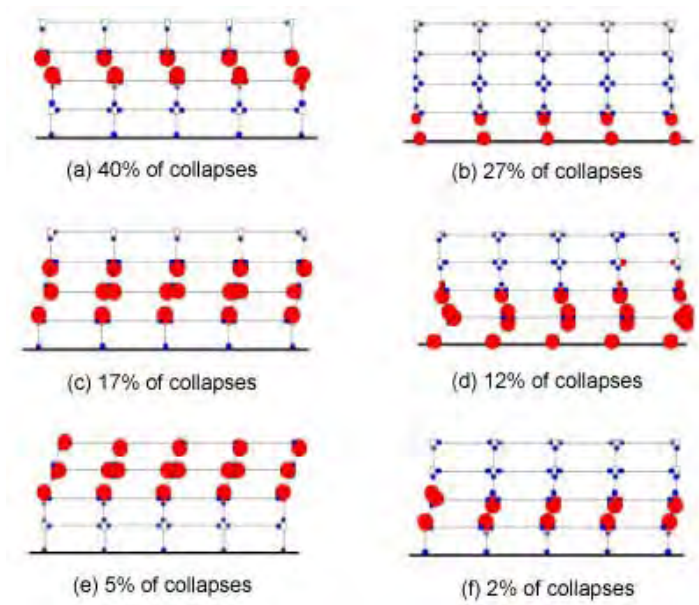

Figure 73. Six Failure Modes Captured by NDA for a Four-Story Concrete Moment-Resisting Frame Building (courtesy of Dr. Curt B. Haselton, California State University)

5.7 Development of Damage Functions for Different Construction Classes

As mentioned earlier, damage functions for different building construction classes are developed using a combination of tools that include engineering analyses, evaluation of building codes prescriptions, and damage and loss data.

Engineering analyses are more critical and, therefore, heavily used when empirical data is scarce. NDA was heavily used for the following types of buildings:

- Low-rise, mid-rise, and high-rise brittle and ductile reinforced concrete (RC) frame buildings in California
- Low-rise, mid-rise, and high-rise modern moment-resisting steel frame buildings throughout the continental United States

NDA was also considered, but to a lesser degree, for developing damage functions for wood frames in California, as will be discussed later.

For each of these construction classes, the nonlinear dynamic analyses were performed by both AIR engineers and other researchers, for multiple buildings within each class, to acquire an understanding of building-to-building response to similar ground shaking. The details of such engineering analyses were discussed in the previous section using an illustrative example of a 10-story steel moment-resisting frame building. NDA analyses performed for other buildings may differ in some details but they are conceptually equivalent to those described above.

For single-family wood frame (WF) residences in California, damage functions are based on engineering analyses, on claims data from the 1994 Northridge earthquake, and on damage and loss data from a number of historical events, including the 1989 Loma Prieta earthquake, the 2003 San Simeon earthquake, and the 2008 Chino Hills earthquake. About 98% of the residences in California are of wood frame construction.

The claims data for the Northridge earthquake include 450,000 policies filed with the California Department of Insurance (DOI) and another 27,000 policies from private insurers. The distribution of claims data from the private insurers is shown in Figure 74.

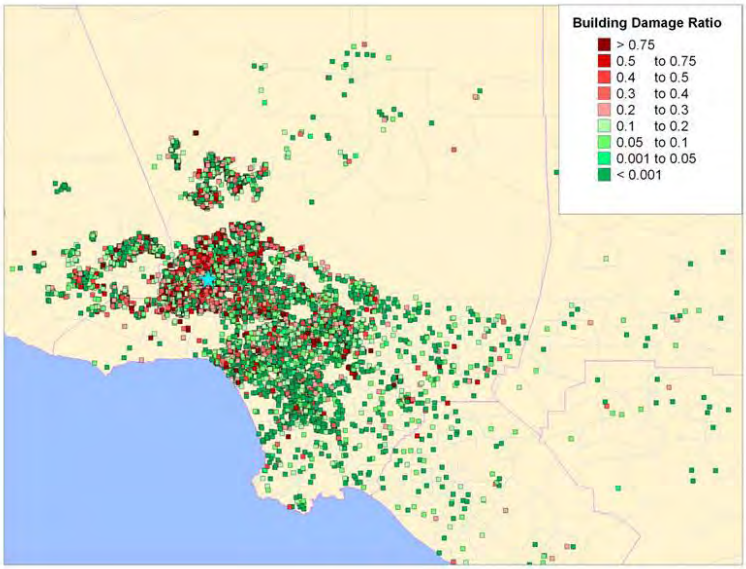

Figure 74. Claims Data from the 1994 Northridge Earthquake (Private Insurers)

When such claims data are available, one can plot the damage ratio vs. the intensity of the ground motion parameter of choice at each claim location using data from the ground motion maps published by the USGS for the causative event (in this case, the 1994 Northridge earthquake).

A scatter plot of the damage ratio versus the intensity parameter (in this example spectral acceleration at a period of 0.3s, which is relevant for wood frame houses) is shown in Figure 75 for wood frame houses constructed between 1976 and 1994.

The overall trend in the data is obscured by the large variability in the dataset. However, the trend can be easily uncovered by simply plotting the mean damage ratio of the data points grouped in spectral acceleration bins, as shown in Figure 76. The blue dots in the figure indicate the average damage ratios calculated from the claims data shown in the pink dots in Figure 75, for a set of spectral accelerations bins. The red squares in Figure 76, which are extracted from the larger dataset from the DOI, are in excellent agreement with those of the smaller dataset.

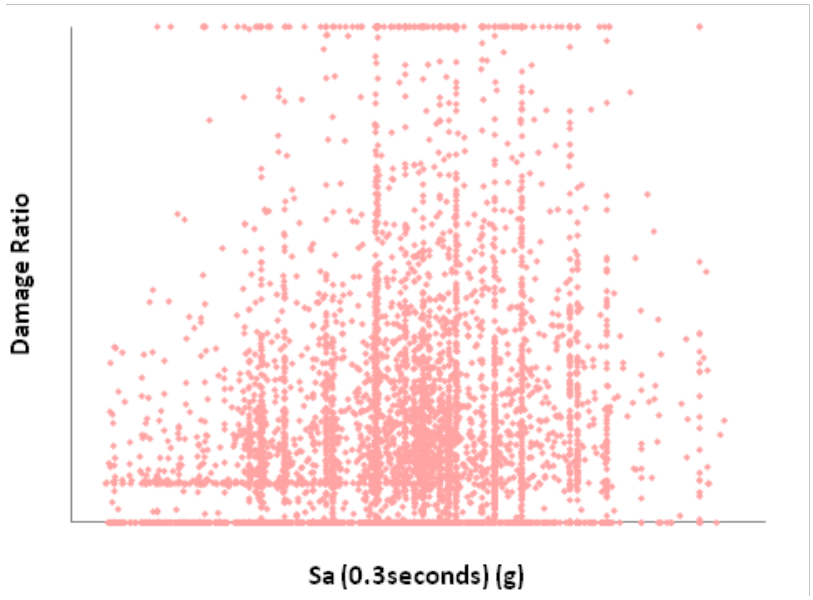

Figure 75. Damage Data from the 1994 Northridge Earthquake for Wood Frame Houses Built after 1976

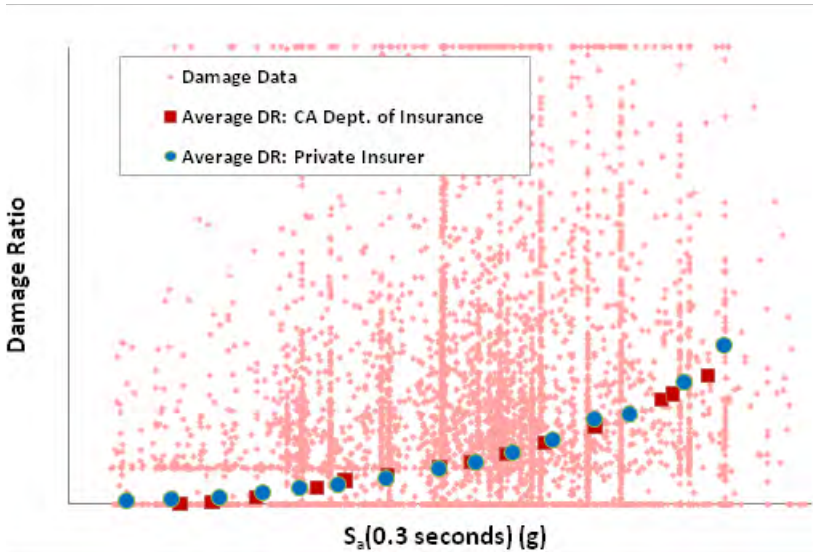

Figure 76. Average Damage Ratios for a Set of Spectral Accelerations

Note, however, that the claims data shown in the previous two figures do not convey any information about losses below deductibles that are suffered by many properties. In statistical jargon, claims data can be categorized as *censored* data. The issue of censored data is carefully accounted for in the empirical derivation of the damage functions to avoid a positive bias in the damage ratio estimates. The description of the censored data analysis is omitted here for brevity.

The empirical information, such as that shown in the previous figures, can then be considered along with results from engineering analyses. Figure 77 shows analysis results for wood frame houses of similar vintage. In the figure, each green dot represents the result of non-linear dynamic analysis on a ground motion record. The green dots near the top of the chart represent analyses that caused the structure to collapse. The damping ratio (ζ) is 5% of critical damping.

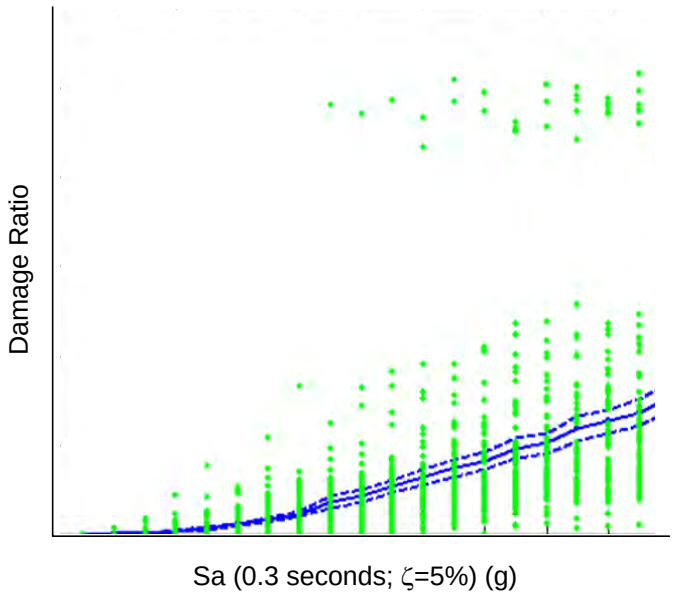

Figure 77. Damage Ratios vs. 0.3 s Spectral Acceleration for Wood Frame Houses Built around 1980

Despite the availability of empirical data, engineering analyses are still vital since the quality of the empirical data is not accurate enough to differentiate houses with different characteristics (e.g., foundation type or number of stories). The effects on damage ratios caused by these differences can easily be modeled using engineering analyses. In synthesis, the combination of empirical claims data and engineering analyses is the best tool to generate credible and realistic damage functions.

Extensive databases of claims data, such as those shown for wood frame structures, are unfortunately not available for other construction classes. There are, however, detailed databases of historical damage data, rather than claims data, for several construction classes other than wood frame. In place of the loss from a claim, the damage data provides detailed descriptions of the damage caused to an asset at a given location. Of course, the damage data can be used to estimate the repair cost and, after normalization by the replacement cost of the building, the damage ratio. Datasets of damage data are available for a variety of construction types, including:

- Concrete tilt-up buildings
- Unreinforced masonry buildings
- Steel moment-resisting frame buildings
- Concrete moment-resisting frame buildings

For illustrative purposes, the following section provides some details on the damage data available for tilt-up and unreinforced masonry buildings. The damage data from the 1994 Northridge earthquake, available for moment-resisting steel frame and reinforced concrete (RC) buildings, is more limited and therefore it was used only to validate the results of the engineering analyses.

Figure 78 shows the location of about 100 tilt-up buildings that were damaged during the Northridge earthquake, along with a brief synopsis of the types of damage that were incurred. Figure 79 shows the corresponding post-occupancy tag that inspectors assigned to each building. The tags also give an indication of the downtime of such buildings.

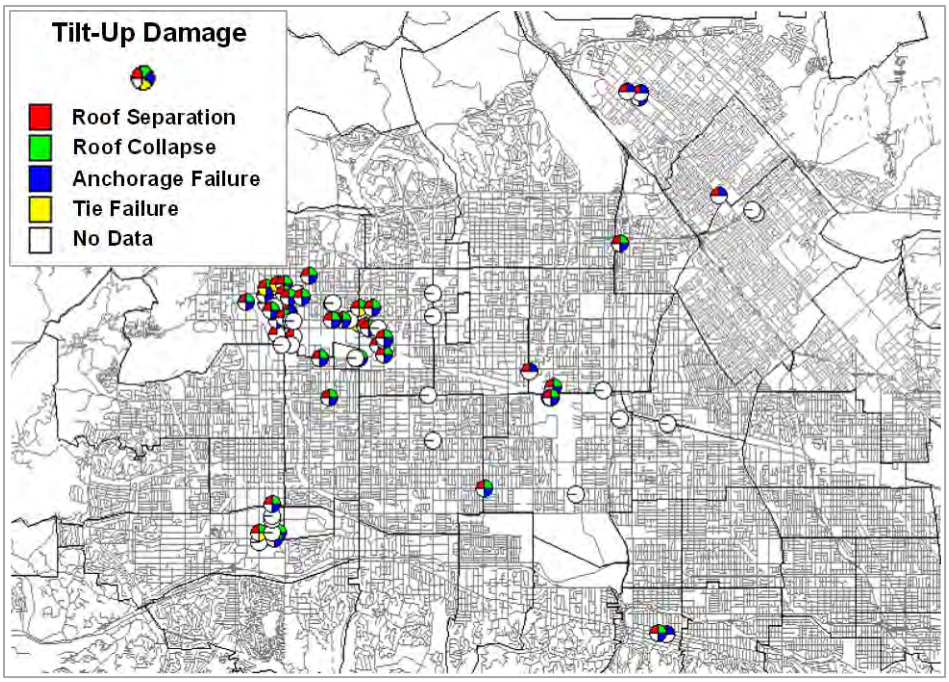

Figure 78. Damage to Approximately 100 Concrete Tilt-Up Structures after the 1994 Northridge Earthquake

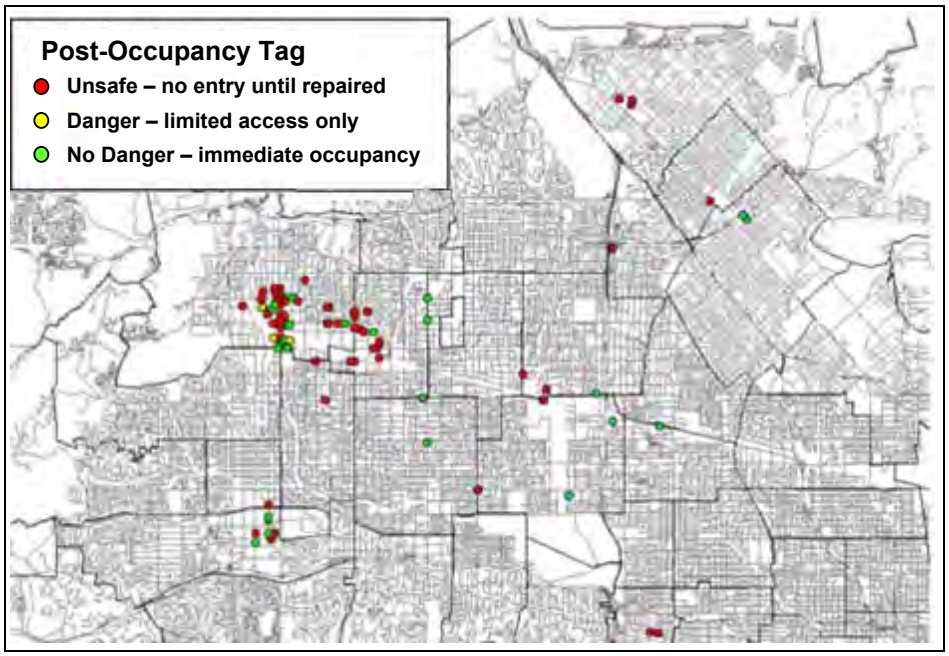

Figure 79. Post-Occupancy Tags Corresponding to the Damaged Tilt-Up Structures after the 1994 Northridge Earthquake

For unreinforced masonry (URM) buildings, damage data from several historical earthquakes is available. Most of the data used for developing the AIR damage functions were collected by the Office of Emergency Services (OES) in California, after the 1989 Loma Prieta and the 1994 Northridge earthquakes. The data covers 850 buildings damaged by the Loma Prieta earthquake, shown in Figure 80, and 3500 buildings damaged by the Northridge earthquake, shown in Figure 81.

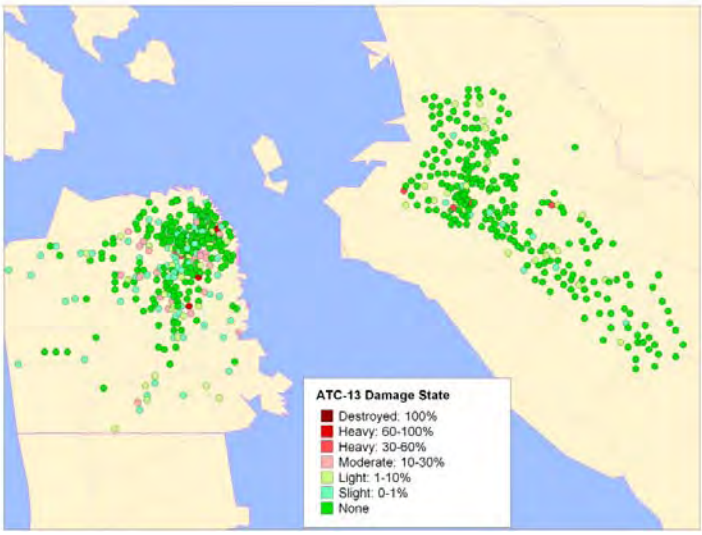

Figure 80. Damage Distribution for URM Buildings, 1989 Loma Prieta Earthquake

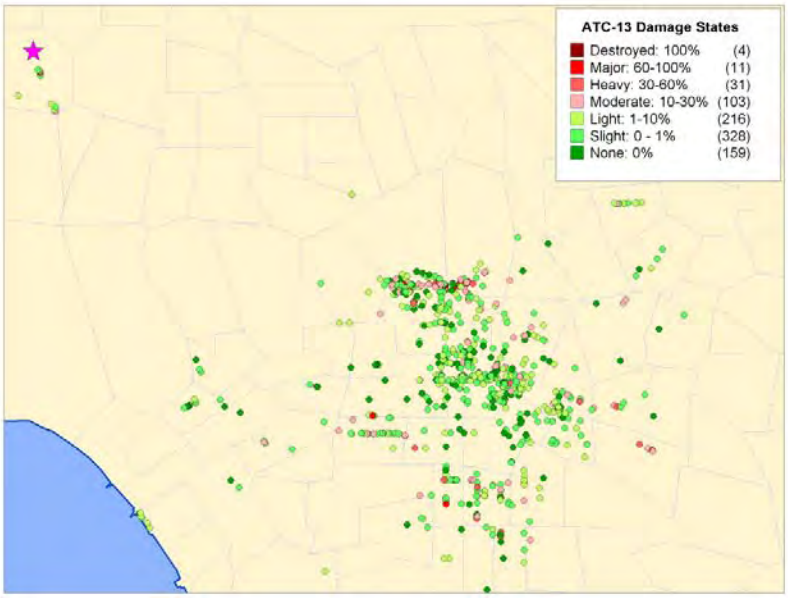

Figure 81. Damage Distribution for URM Buildings, 1994 Northridge Earthquake

Figure 82 shows the scatter plot of the damage ratio inferred for these damaged URM buildings versus the spectral acceleration that was likely observed at the buildings' site during those earthquakes.

The figure also shows the average of the damage ratio for different spectral acceleration bins. For comparison purposes, blue squares indicate the average of the damage ratio from a very large set of URM damage data collected by the Italian Department of Civil Protection covering earthquakes that have occurred in Italy since 1975. Interestingly, the similarity of the trends between the data from the U.S. and Italy is striking—despite inter-country differences in URM building practices.

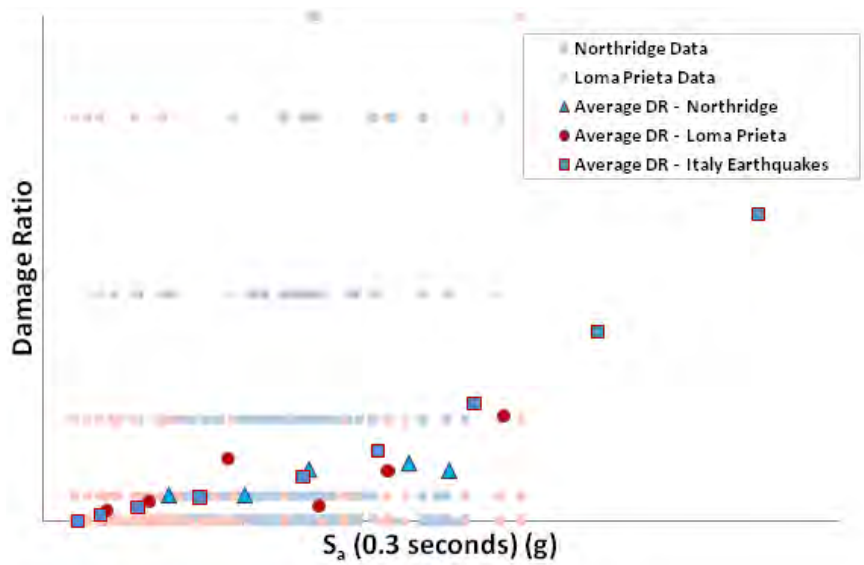

Figure 82. Damage Ratios for URM Buildings for Earthquakes in California and Italy

Figure 83 shows the final damage functions for California for selected construction types.

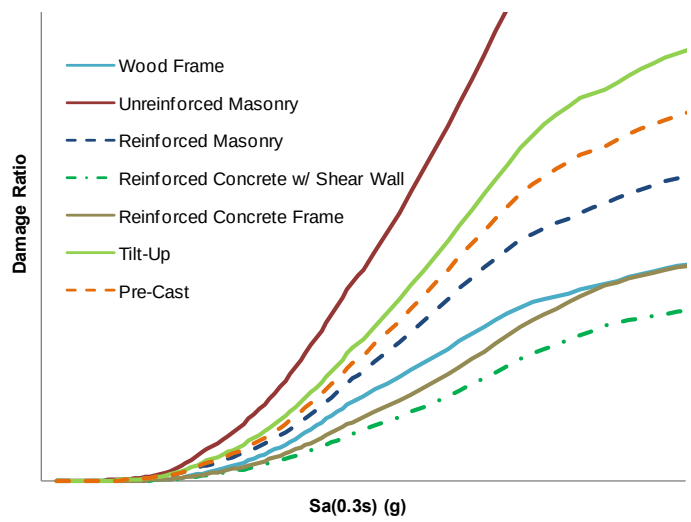

Figure 83. Damage Functions for Various Construction Types in California

The preceding discussions have described the development of damage functions for construction classes in California. The damage functions for buildings in other regions of the U.S. were developed by modifying the damage functions for corresponding buildings in California, accounting for the different design loads and construction practices. Adequate consideration has also been given to specific studies on for the damageability of buildings in the central and eastern United States performed by the Mid-America Earthquake (MAE) Center (e.g., Ellingwood

et al., 2007 and 2008) and to relevant information in HAZUS.[12] The resulting damage functions for low-rise RC frame buildings in the three seismicity regions considered are displayed in Figure 84.

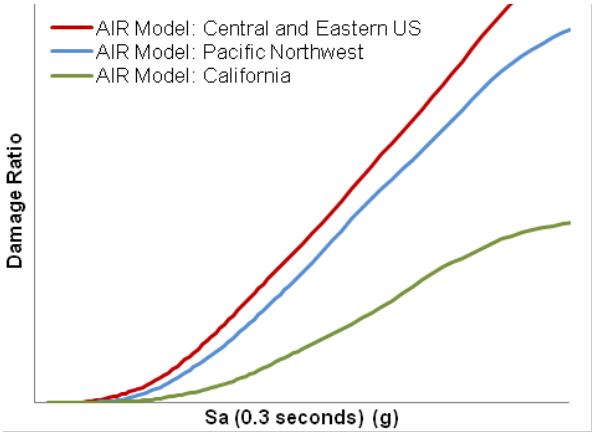

Figure 84. Damage Functions for Low-Rise RC Frame Buildings

The Distribution of Damage: Uncertainty in Damage Estimation

The model's damage functions provide estimates of the mean, or expected, damage ratio corresponding to median ground motion at each affected site. However, as is commonly seen in the course of damage surveys in the aftermath of earthquakes, similar structures at the same location experience different levels of damage. This variation in building damage can arise due to the inherent randomness in building response or to differences in building characteristics, construction materials or workmanship. AIR has developed a distribution around the mean damage ratio to capture this uncertainty in damage, as illustrated in the sample damage function shown in Figure 85.

Observations have shown that, after an earthquake, similar buildings within close range of one another sustain a wide range of damage. Many will be severely damaged or completely destroyed while others in the same vicinity sustain only very light damage or none at all. These damage patterns are commonly represented by a beta distribution, which accounts for this variation in damage.

However, after an extensive study of claims data, AIR engineers have found that a combination of two beta distributions (referred to here as a bi-beta distribution) provides a much better fit to the observed damage patterns in past earthquakes. Therefore, the AIR model has adopted the bi-beta distribution, which shows a much higher level of accuracy when used for insured loss estimations.

[12] A GIS-based natural-hazard loss-estimation software package developed by the U.S. Federal Emergency Management Agency (FEMA).

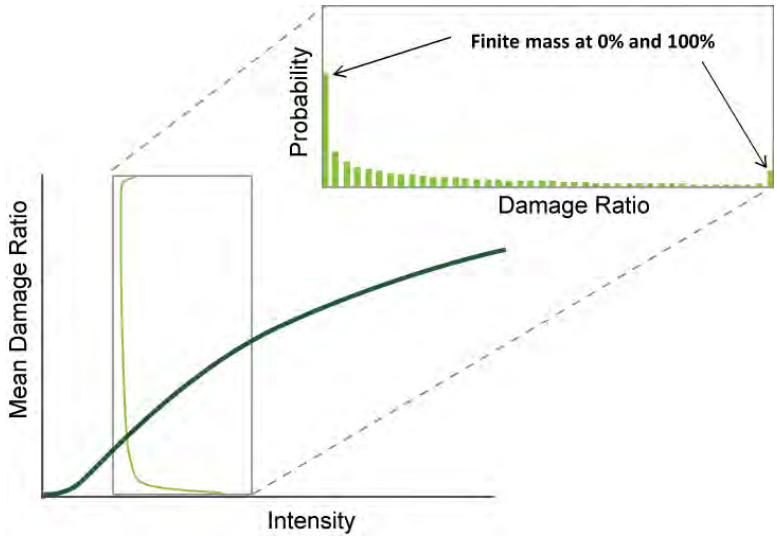

Figure 85. Sample Damage Function and Distribution with Non-zero Probabilities of 0% and 100% Loss

5.8 Damage Functions that Include Ground Motion Uncertainty

The development of mean damage functions discussed in the previous sections are based on fixed levels of ground motion intensities. However, there is a significant amount of variability in the estimation of ground motion intensity at any site for any given earthquake. A damage function that has modified the mean values by taking into account the uncertainty of the ground motion is referred to here as an "integrated" damage function.

Mean damage functions are most appropriate when there is little uncertainty in the estimation of ground motion intensity. For example, they can be used to accurately assess losses suffered during an historical earthquake by buildings that are located close to recording stations, since the uncertainty at those sites is in this case fairly limited. In all other cases, a more realistic loss assessment is achieved when ground motion uncertainty is considered. Integrated damage functions are used in the AIR model to estimate the mean damage for events in the stochastic catalog, as well as for older historical events that have little or no instrumentally recorded data.

Figure 86 shows the mean and integrated damage functions for wood frame structures in California and for the typical variability of the ground motion intensity at a given value of S_a (0.3 s).

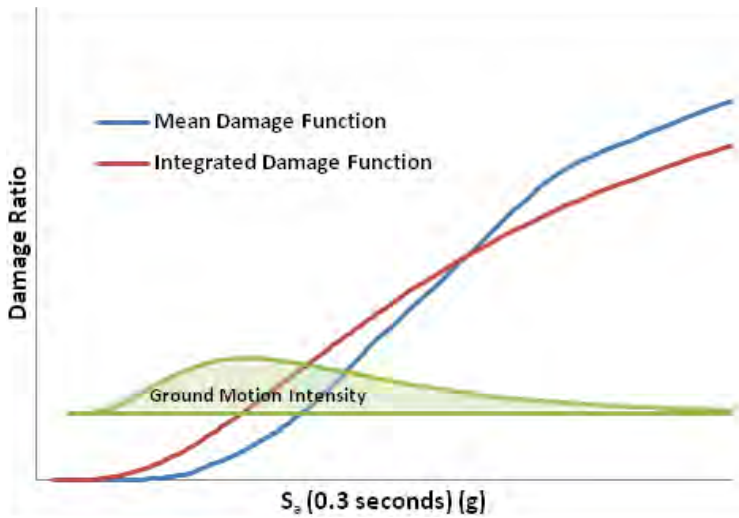

Figure 86. Mean and Integrated Damage Functions for Wood Frame Structures in California

Derivation of the Integrated Damage Functions from the Mean Damage Functions

The mean damage function (the solid blue line in Figure 86) gives the mean damage ratio DR(i) at each level of intensity, *Sa(i)*. The value *Sa(i)* is, however, the mean value of a *distribution* of possible ground-motion intensities (as shown by the green line) that can be generated at a site by an event of given magnitude. Each level of ground motion in that distribution, if it were to occur, would generate a damage ratio that is generally different from DR(i).

The value of the integrated damage function at Sa(i) is simply the weighted average of all the damage ratios generated by all possible ground motion levels in the green distribution. The weights are equal to the likelihood of the occurrence of each ground motion level as calculated from the green distribution. By taking the variability of ground motion into account, the integrated damage function is less steep than the original damage function, as can be seen in the figure.

Using ShakeMap for Damage Function Calibration

The AIR method for simulating ground motion discussed throughout Section 4 is especially useful when modeling historical earthquakes for which there are few or no reliable recordings. Also, the AIR method provides a realistic distribution of losses by using the integrated damage functions that account for spatial correlation of ground motion residuals, as discussed above.

However, in some cases USGS ShakeMap is particularly useful for calibrating the models damage functions. These are shaking and intensity maps based on a variety of data from historical earthquakes including ground motion recordings,

geological conditions, and earthquake location and magnitude. It produces the best set of ground motions within a fine grid cell, so the damage functions calibrated to these maps for historical events take into consideration a range of ground motion levels at sites throughout the region, depending on the distance from the earthquake and different geological conditions at each site.

Calibrating damage functions to information-rich ShakeMaps produces realistic losses for a wide range of portfolios. The accuracy of the ShakeMaps can be illustrated by comparing them to actual recorded ground motion intensities for two well-known and well-recorded historical earthquakes: the 1994 Northridge and the 1989 Loma Prieta events. Comparisons are shown using both PGA and spectral acceleration values.

Figure 87 compares modeled and observed ground motion intensities for the 1994 Northridge earthquake; measurements are in terms of peak ground acceleration (PGA).

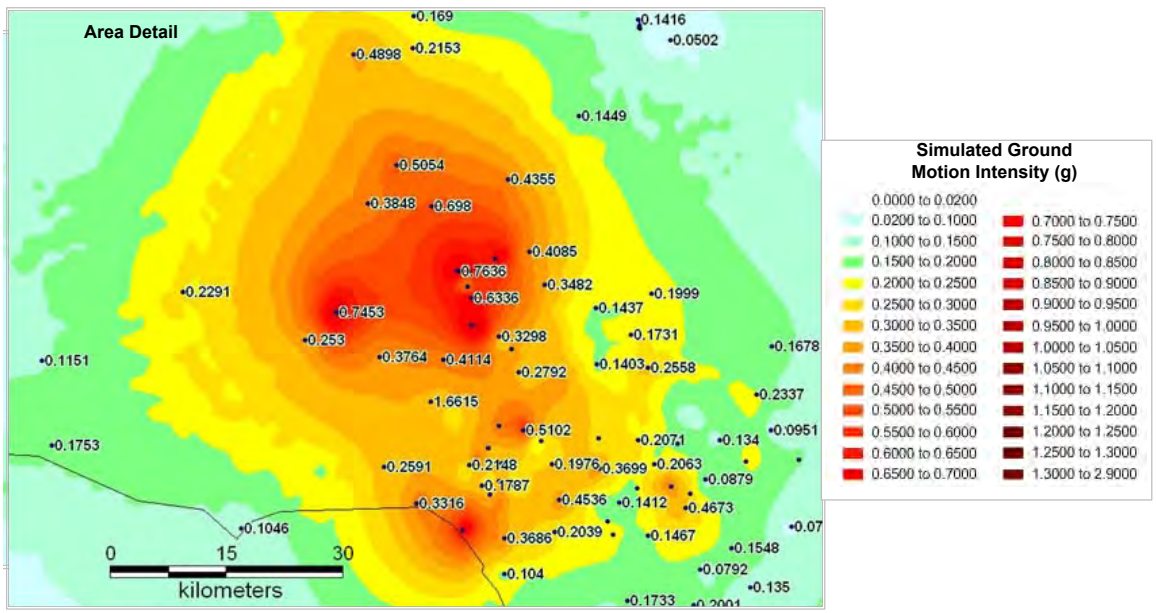

Figure 87. Simulated ShakeMap (colors) vs. Observed (numbers) PGA, 1994 Northridge Earthquake

Figure 88 and Figure 89 compare the ShakeMap ground motion against observed spectral accelerations at periods of 0.3 second and 1.0 second, respectively. At periods between 0.2 and 0.3 second, the intensity is generally higher and typically provides the maximum amount of shake damage. Therefore the intensities for 0.3 second are higher than those for 1.0 second or the PGA.

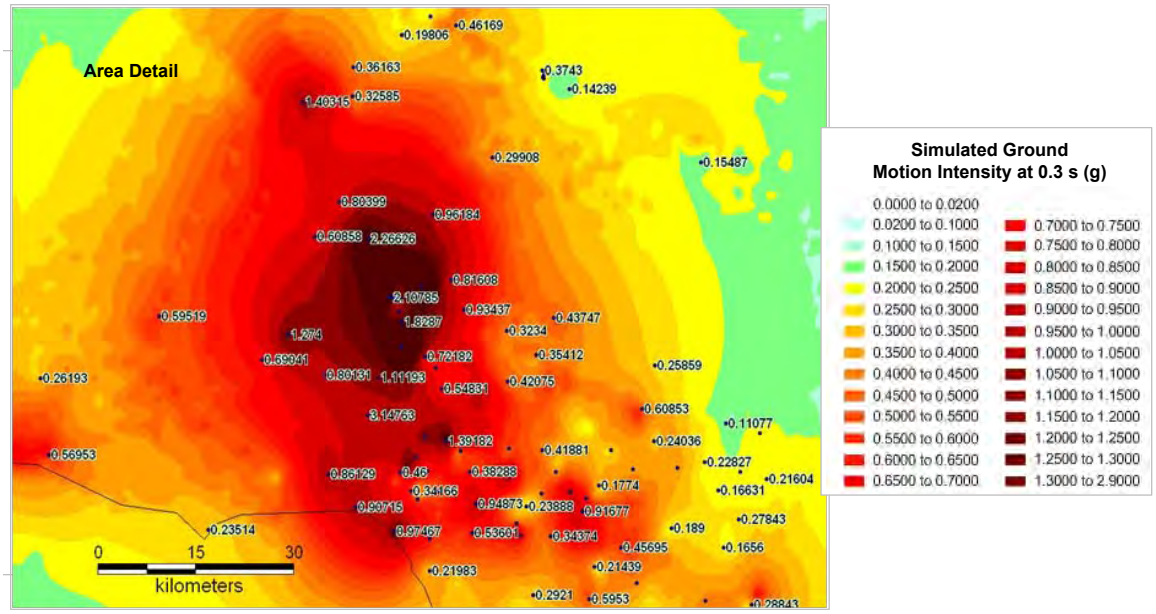

Figure 88. Modeled vs. Observed Sa at 0.3 second (g), 1994 Northridge Earthquake

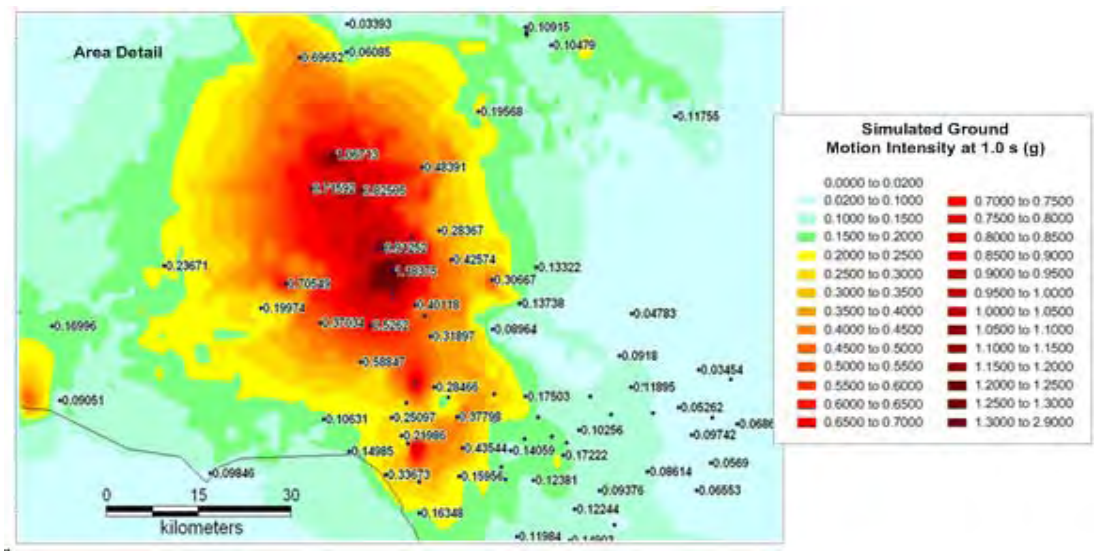

Figure 89. Modeled vs. Observed Sa at 1.0 second (g), 1994 Northridge Earthquake

Figure 90 compares modeled and observed ground motion for the 1989 earthquake at Loma Prieta; measurements are in terms of peak ground acceleration (PGA).

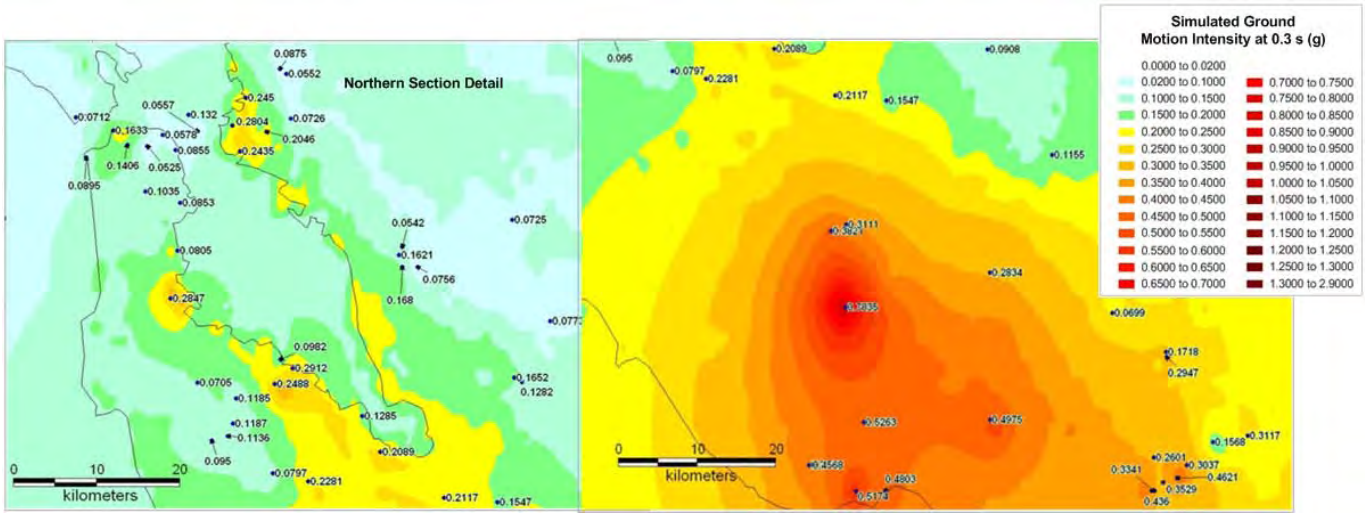

Figure 90. Modeled vs. Observed PGA, 1989 Loma Prieta Earthquake

Figure 91 and Figure 92 compare the simulated ground motion against observed spectral accelerations at periods of 0.3 second and 1.0 second, respectively. Again, at periods between 0.2 and 0.3 second, the intensity is generally higher and typically provides the maximum amount of shake damage. Therefore the intensities for 0.3 second are higher than those for 1.0 second or the PGA.

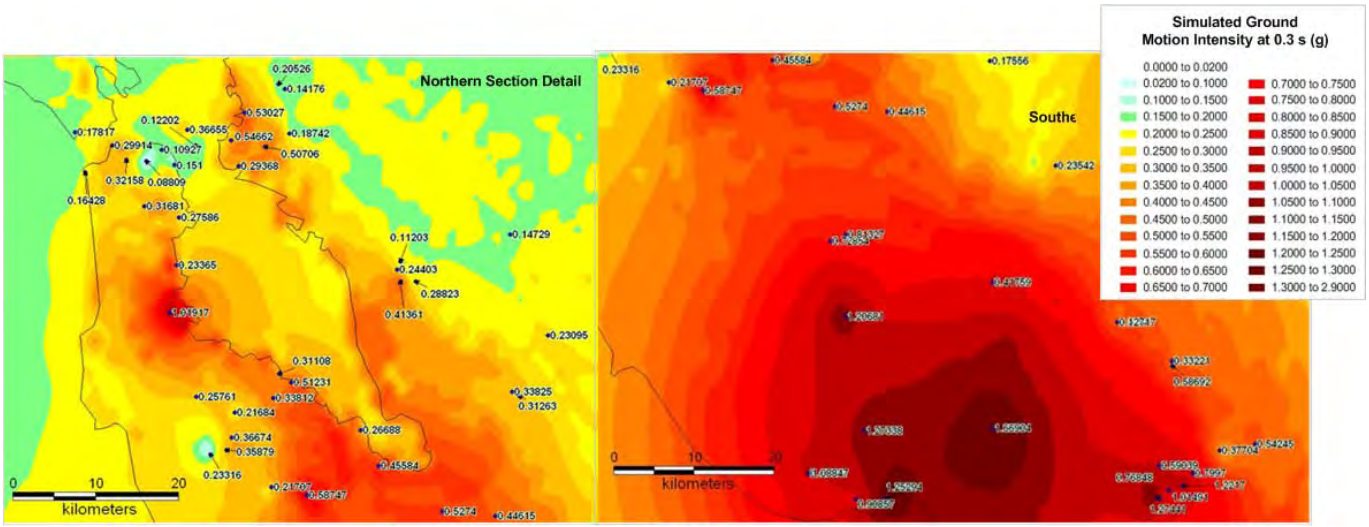

Figure 91. Modeled vs. Observed Sa at 0.3 second (g), 1989 Loma Prieta Earthquake

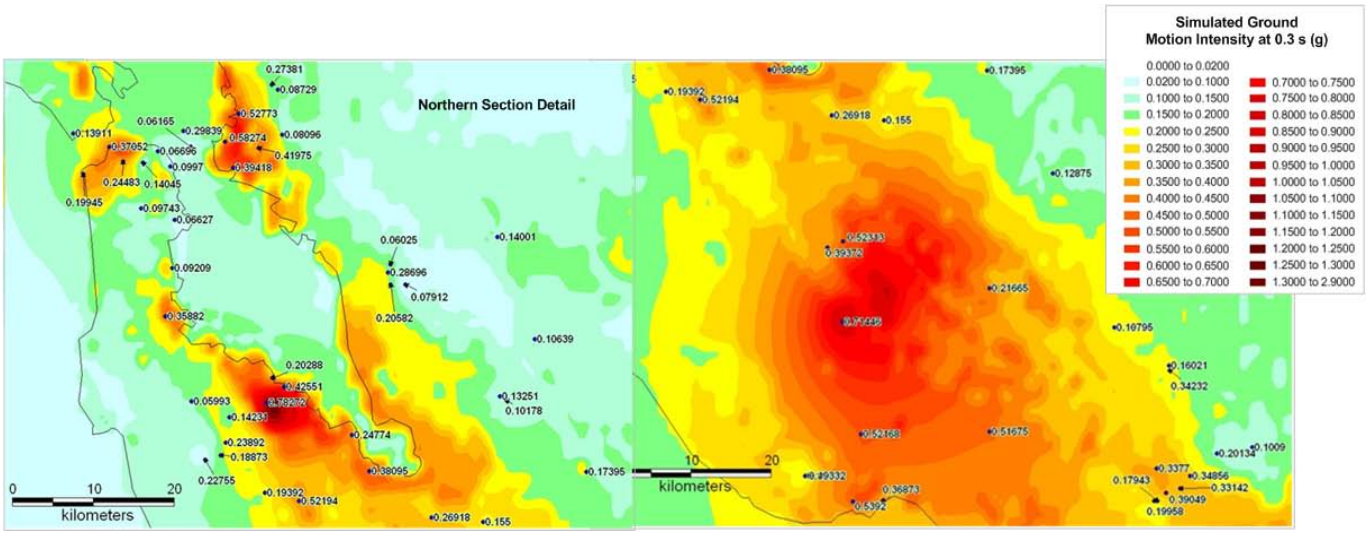

Figure 92. Modeled vs. Observed Sa at 1.0 second (g), 1989 Loma Prieta Earthquake

5.9 Contents Damage

In the AIR Earthquake Model for the United States, contents damage is a function of spectral acceleration (see Section 4) and also of the occupancy class. (Each occupancy class is associated with a set of typical contents and their vulnerability to shake damage.) Contents damage is generally higher in commercial occupancies than residential ones, and higher in industrial facilities than in commercial facilities.

At low levels of shaking, the primary determinant of contents damage is floor acceleration, which imposes inertial lateral forces. At higher levels of shaking, contents damage depends on both inertial forces and building damage. For example, contents may be damaged due to the collapse of both structural and nonstructural components, including ceilings, beams, and columns. Content damage generally increases at higher levels of shaking. Unreinforced masonry structures have the highest content damage of the construction classes.

5.10 Additional Living Expenses

Damage functions are also included for time element, or additional living expenses, for residential structures. The AIR ALE damage functions take into account the time that people may need to stay in a hotel or elsewhere while their home is repaired. It also takes into consideration any necessary time taken off work due to the inability to get to their place of employment, or necessary time spent with contractors.

ALE loss is a function of the mean building damage, which in turn is used to estimate the number of days required to repair or rebuild the structure, and an estimate of per diem ALE costs. The damage functions were calibrated to and validated by actual claims data, primarily from the Northridge earthquake.

5.11 Business Interruption

Downtime, or the number of days before a business can return to full operation, is the primary parameter for estimating business interruption (BI) losses. The AIR BI estimation method, as illustrated schematically in Figure 93, utilizes an event tree approach, incorporating the latest research and findings from an extensive analysis of claims data. For each damage state, a probability is assigned to two possible outcomes: continued operations or cessation of operations at the location. If operations cannot continue at the location, a probability is assigned to whether the company will relocate. These probabilities vary by occupancy. For example, while relocation is feasible for an office, it is not for a hotel. Thus the two will take different paths to recovery, and hence will have different downtimes in the event of business interruption.

Downtime is calculated for each stage of the damage assessment and recovery process. The first stage is the time before repairs can get underway (pre-repair). Damage must be assessed, repair costs negotiated with contractors, and the building permit obtained. The next stage is the repair time. Some businesses choose to relocate rather than wait for repairs, but relocation takes time as well. Once repairs are completed, revenues may not resume immediately at the pre-disaster level; it may take some time to regain market share, or to rebuild a labor force that may have been dislocated.

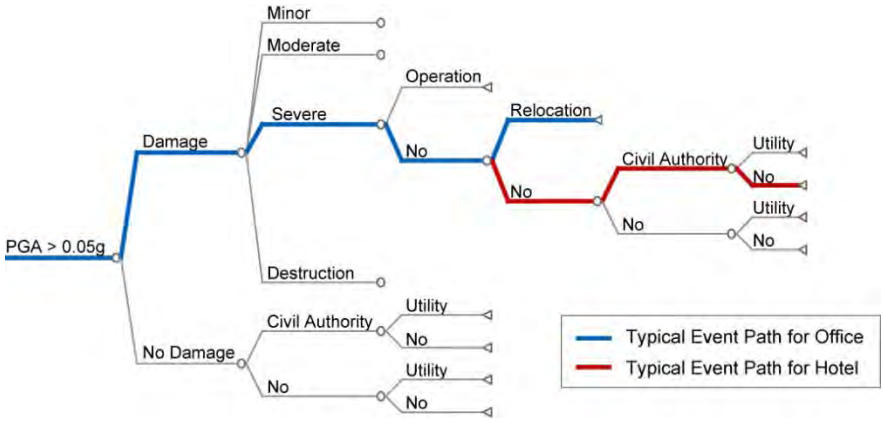

Figure 93. Hypothetical Event Tree of BI Estimation for an Office and a Hotel

In the AIR model, the estimated number of days needed to restore the business to full operation depends on a number of key factors, including the level of damage sustained, the size of the building (as approximated by building height) and its architectural complexity (as approximated by occupancy class).

For a given damage ratio, a 2,500 square meter hotel will take significantly longer to repair than a 450 square meter professional office. Since floor area is usually not directly available, it is estimated using building height. For a given floor area, buildings with significant architectural complexity will also take more time to repair. Warehouses can be quite large, but repairs are likely to take place quickly because of their architectural simplicity. Interior finishes must also be taken into account. Hotels are not only typically larger than offices, but can take more time to repair due to the higher quality of interior finishing.

Some types of businesses, such as hospitals, are more resilient than others and may be able to restart operations before repairs are complete, or they may have had disaster management plans in place that allow them to relocate quickly. For other businesses, such as hotels, location is everything and relocation is not an option. Since many parameters (such as building size, complexity, and business resiliency) critical to determining business interruption are generally not available for input into the model, occupancy class is used as a proxy to measure these parameters.

Occupancy is also used to estimate the probability that there may be business interruption at a dependent building within the damage footprint—such as the supplier of a necessary manufacturing input—that will exacerbate BI losses at the principal building. Estimation of the impact of the dependent building(s) damage on the principal building requires the knowledge of the location and the degree of interdependence between dependent and principal buildings. Since this level of detailed information is generally not available, logical assumptions are made to estimate the impact of the dependent building(s) on the principal building's downtime. The methodology for estimating BI losses relies in part on loss experience data and in part on expert judgment in the face of limited available exposure information.

5.12 Automobile Damage

Automobile damage during an earthquake is caused by both ground shaking and debris falling from damaged buildings. In the AIR model, automobile damage functions, which represent the vulnerability of four-wheeled automotive vehicles for passenger transport, were developed based on ATC-13 guidelines in which auto damage is a function of peak ground acceleration, or PGA.

5.13 Liquefaction Damage

Areas that are at risk of liquefaction include locations where the soil is saturated with groundwater and becomes liquefied due to violent ground motion. Heavy property damage can result if the soil supports building foundations, or contains buried pipes and lines. Significant damage due to liquefaction was observed in the Marina District of San Francisco during the Loma Prieta earthquake in 1989.

The model assesses liquefaction damage for the seven regions that have sufficient groundwater depth data along with a history of liquefaction during earthquakes. These areas are the greater San Francisco and Los Angeles areas; Portland, Oregon; Seattle, Washington; Salt Lake City, Utah; and the New Madrid and Charleston seismic zones.

In the AIR model, building damage resulting from liquefaction is modeled as a function of peak ground acceleration.

For more information on the causes and effects of liquefaction, liquefaction occurrences during historical earthquakes, and on AIR's assessment of liquefaction damage, see Section 4.

Finally, note that in the AIR Earthquake Model for the United States losses caused by ground shaking and losses caused by liquefaction are combined and are not separable in the software.

5.14 Fire Following Damage

A separate dynamic simulation is used to estimate losses from fires following earthquakes. The components of this damage-estimation module are illustrated in Figure 94.

In the AIR Earthquake Model for the United States, multiple fire simulations can be run for each earthquake event. This allows for variations in probabilistically selected simulation parameters for a single earthquake event. For each historical earthquake, several dozen simulations are run, and the mean fire damage ratio and loss are calculated for each ZIP Code and fire class. This procedure provides an estimate of the expected fire-following losses were an historical event to recur. In contrast, for each simulated event in the 10,000-year stochastic catalog, ten fire simulations are run in order to produce a wider range of possible fire following losses while still providing expected values based on a number of potential scenarios for each event.

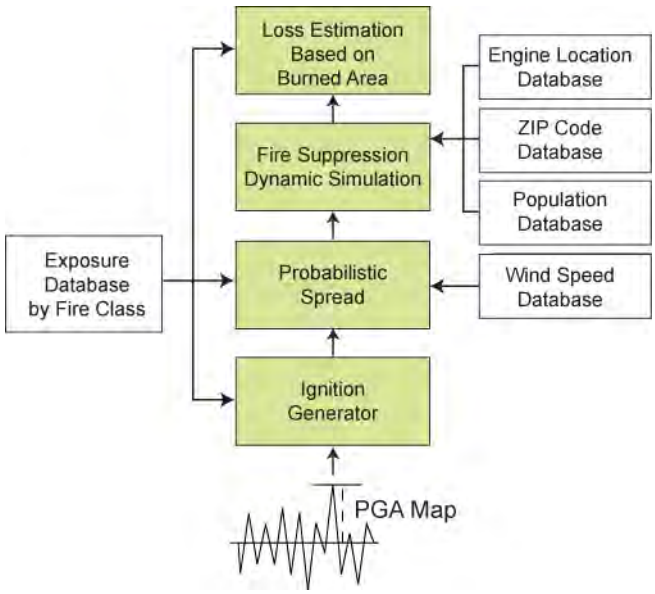

Figure 94. Primary Model Components in Fire Damage Estimation

Databases

A number of databases are used in the fire-following damage estimation module. These include databases of exposure, fire engines, population, and wind speeds. The data collectively affect fire ignition, spread, suppression, and loss estimation.

Exposure: Certain aspects of the industry exposure data are relevant to the fire–following peril. In particular, exposures for residential and commercial lines of business are divided into combustible and noncombustible categories. All types of wood construction are considered combustible, while other construction types are considered noncombustible. Each exposure record is assigned to one of five fire classes: residential combustible, residential noncombustible, commercial combustible, commercial noncombustible, and mobile home. The exposure density in a given area is used to categorize the type of urban environment, which determines the building size and spacing parameters used in the model for the exposures in that area.

Fire Engines*:* An extensive fire engine database is incorporated in the model. It includes detailed data for 350 of the largest cities and towns in the contiguous United States (Figure 95) obtained from local fire departments. For areas not in the database, the model uses a regression technique to estimate the number of fire engines in each area based on the population.

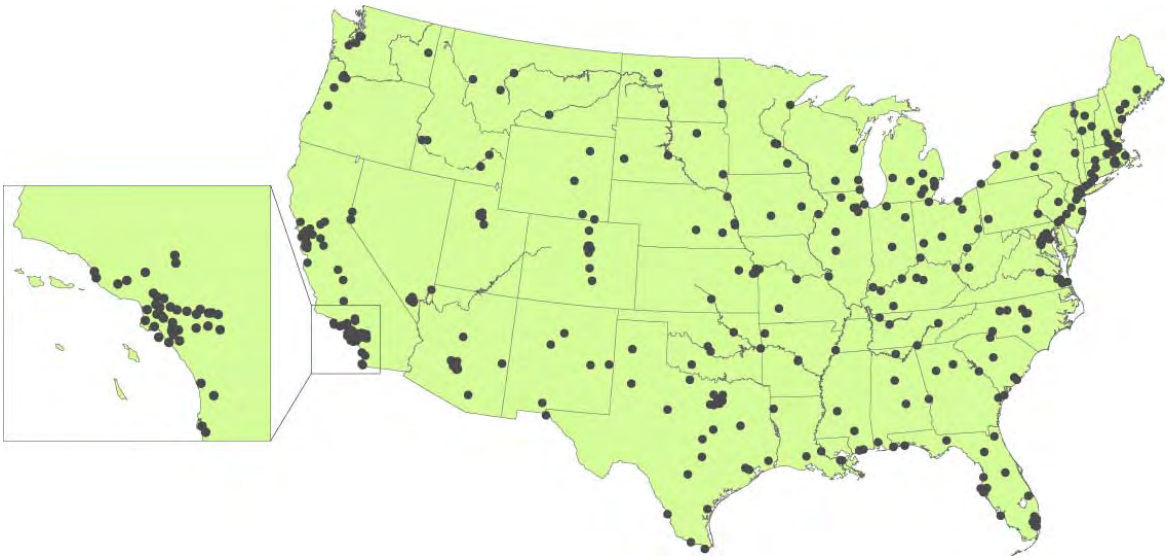

Figure 95. Source Locations for Fire Engine Data – Continental U.S. and Zoom-in of Los Angeles Area

Population: Population data for each ZIP Code are used to determine the number of fire engines that are assigned to areas for which actual fire-engine data were not available. These are typically smaller cities and towns. The source of the population data is the U.S. Census Bureau.

Wind Speeds: The model uses a wind speed algorithm to determine the wind speed during a fire outbreak, using data collected from Weather Underground. The wind speed is selected from a distribution that corresponds to the weighted average of historical wind speed distributions from weather stations surrounding the area affected by the earthquake.

Fire Ignition

The AIR Earthquake Model for the United States features a stochastic fire-ignition algorithm that is based on historical data. During an earthquake, fires may ignite when devices powered by gas or electricity overturn, break, or are struck by another object, generating open flames or chemical reactions, electrical wiring short circuits, or gas lines rupture.

Generally there is a positive correlation between fire-ignition rate and earthquake intensity. Higher levels of ground motion tend to produce higher ignition rates. Thus, the ignition rate, in ignitions per million square feet of building floor area, is a function of peak ground acceleration (PGA). Figure 96 shows ignition rates for several historical earthquakes.

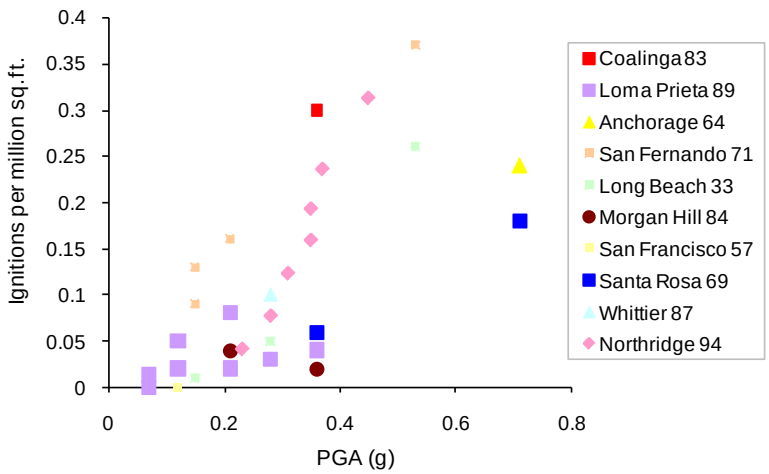

Figure 96. Fire Ignition Data for Selected Historical Earthquakes

Adjustments are made to account for the observation that different fire classes exhibit noticeably different ignition rates. For example, there is a lower probability of fire ignition in a million square feet of commercial high-rise property than there is in a million square feet of single-family residential property for a given level of ground motion. Commercial high-rise buildings typically adhere to more stringent building codes.

For a particular PGA value, the model includes a distribution in ignition rates around the mean, as illustrated in Figure 97. For a given fire class and PGA combination, the model stochastically selects an ignition rate from such a distribution to more realistically capture the variability in ignition rates.

After fire ignitions are generated, they are stochastically placed within their ZIP Code.

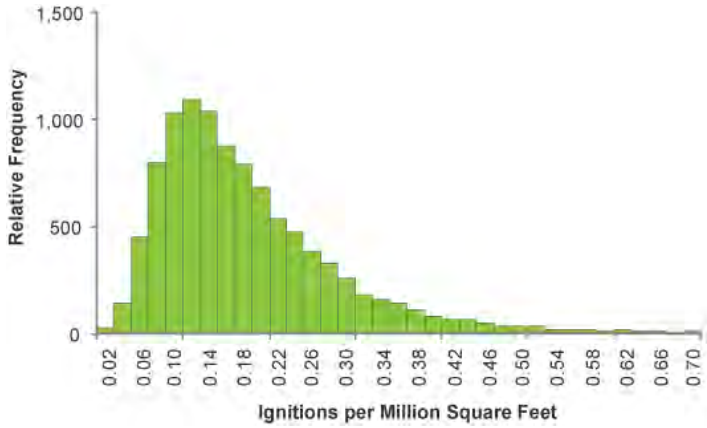

Figure 97. Sample Ignition Rate Distribution at PGA of 0.4 g

Fire Spread and Suppression

The model incorporates distributions in fire-discovery and fire-report times, and fire-engine speeds to determine how much time elapses between each ignition and the beginning of active suppression of the resulting fire.

Fire spread to adjacent buildings is estimated using the Hamada (1975) fire-spread model. Updated Hamada building parameters are based on six different types of urban environments, including very dense urban, dense urban, moderately dense urban, suburban, intermediate suburban-rural, and rural. For each of these urban environments, Hamada building parameters are defined for four different types of buildings: residential single-family houses, mobile homes, commercial, and apartments/condos.

The fire-spread rate in the Hamada model is a function of wind speed. The spread rate is highest in the downwind direction, lowest in the upwind direction, and intermediate in the crosswind direction.

For each fire simulation, a wind speed is drawn from a probability distribution appropriate for the affected area. The probability distribution used corresponds to the weighted average mean historical wind speed for surrounding weather stations. The weighting factor for each weather station is $1/r^2$, where r is the distance from the station to the ignition centroid. The ignition centroid is the mean longitude and latitude of all the simulated ignitions for the fire simulation.

For historical events, the wind-speed distribution is a Rayleigh distribution, which is a Weibull distribution with the shape parameter k equal to two. For stochastic events, the wind-speed distribution is a hybrid Weibull distribution which uses a Rayleigh distribution for the lowest 70% of the wind-speed samples and a Weibull distribution with k equal to one for the highest 30%. While a k value of two is common (Pavia and O'Brien 1986), using this value alone would not fit the tail adequately. Therefore, the tail of the distribution is modeled as a Weibull distribution with a k value of one.

Fire suppression is modeled for each event using estimates of fire-engine speed, fire-engine capacity, and water availability as a function of the PGA in the area affected by the earthquake. Intense earthquakes are more likely to render roads impassable, break water mains, or result in other situations that affect suppression capability.

Fire spread and fire suppression are modeled as a dynamic process, as both components of the model work together to determine how the fire simulation proceeds and how each individual fire grows and is eventually suppressed. As a fire continues to grow, it requires more fire engines. The additional fire engines

are assigned to the fire if they are available. The time it takes to suppress the fire is a function of its size and the number of engines at the site. As fires are suppressed, engines are rerouted to other fires.

The AIR Earthquake Model for the United States takes into account the existence of firebreaks, which are gaps between buildings that are wider than the typical building separation within a city block. Examples are streets and wider boulevards. Fires may be stopped by a firebreak, or they may—with some probability—jump across to the next group of buildings. The crossing probability is a function of the firebreak width and wind speed. Each fire generated in the model has some probability of stopping at each firebreak it encounters, even if there is no active fire suppression.

Fire Damage Estimation

Fire damage is computed for each fire by multiplying the amount of building floor area burned by an estimate of the construction cost per square foot. That cost is then multiplied by a scaling factor to include damage to contents and time element (business interruption) losses. Maximum burn ratios are assigned to each fire class, and total losses for each fire in a ZIP Code are capped by the total exposure.

5.15 Workers' Compensation Losses due to Earthquakes

The AIR Earthquake Model for the United States offers an auxiliary damage estimation component that generates losses due to injuries and deaths that occur under workers' compensation insurance policies. When ground shaking during an earthquake damages a workplace, employees who are in or near the building at the time can sustain a wide variety of injuries, with severity ranging from minor to fatal. Depending on the time of day the earthquake occurs, the number of people at work at the time, and other factors, a significant percentage of the total insured losses can be due to workers' compensation.

The AIR model offers a complex analysis that incorporates the most likely types of injuries that are incurred in buildings of different construction types, with different levels of damage, along with a large number of other factors that affect workers' compensation losses. These include the number of injuries and deaths as a function of the injury rates, the nature of the damage sustained by the buildings where the workers are located, and the number of workers who are at risk at the time of the earthquake. The model does not account for any loss of income due to these injuries.

Types of Building Damage that Cause Injury

The primary cause of injury during earthquakes is due to debris falling inside damaged buildings and, in the most severe cases, the collapse of occupied buildings. Therefore, the nature and severity of injuries from earthquakes are modeled as a function of building damage. For each construction type and occupancy class, the AIR model divides the full distribution of building damage into four distinct damage states: minor, moderate, extensive, and complete.

Note that "complete" damage means that a building is not recoverable; it does not necessarily mean that a building has collapsed. However, the state of collapse of a building has significant consequences in a workers' compensation loss estimation, since building collapse typically increases the number of fatalities and severe injuries. In the AIR model, the probability of collapse is used to create two categories within the complete damage state: "complete damage without collapse" and "complete damage with collapse."

Building construction, and its effect on a building's ability to withstand ground shaking, has been shown to affect injury and fatality rates significantly. For example, the 1995 Great Hanshin earthquake in Kobe, Japan, which occurred at 5:46 a.m., caused more than 5,000 deaths. In contrast, the 1994 Northridge earthquake, which occurred at 4:30 a.m., resulted in fewer than 60 deaths. The earthquakes were of similar magnitude and both occurred during early morning hours when most people were not yet at work. The difference in fatality counts can be largely explained by differences in building construction. As construction practices vary widely by location, it is inadvisable to use international damage and casualty experience when estimating workers' compensation losses in the United States.

However, within the continental United States, the structural requirements for buildings and the degree to which they are enforced vary greatly with location. In earthquake-prone areas, structural requirements are generally more stringent than in areas where there has been little historical earthquake activity. The AIR model takes these requirements into consideration, since they have a significant effect on a building's ability to withstand ground shaking.

Probability of Collapse

The probability of collapse for any given building is determined primarily by its construction class. Masonry buildings, for example, are more likely to collapse than concrete buildings. Steel buildings may experience significant deformation under severe ground shaking, but collapse is less likely.

The collapse probabilities used in the AIR model are adopted from the HAZUS MR4 Technical Manual (FEMA 2009), with adjustments made based on engineering judgment and damage reports from building collapses due to earthquakes in the United States. Table 10 shows examples of the collapse probability used in the AIR model.

Table 10: Collapse Probabilities Used in the AIR Earthquake Model for the United States

Construction Type	Probability of Collapse (%) Given Complete Damage State
Wood Frame, Low-Rise	2
Masonry, Low-Rise	12
Masonry, Mid-Rise	9
Reinforced Concrete, Low-Rise	10
Reinforced Concrete, Mid-Rise	8
Reinforced Concrete, High-Rise	4
Steel, Low-Rise	8
Steel, Mid-Rise	5
Steel, High-Rise	3

Injuries Due to Earthquakes

Historical evidence shows that most of the injuries resulting from small to moderate earthquakes are lacerations, sprains, and contusions caused by non-structural building components falling on people. Life-threatening or fatal injuries are typically caused by the structural damage that occurs with larger magnitude events.

Table 11 shows the percentage of nonfatal injury types for five historical earthquakes of moderate magnitude in California. The data used to construct this table comes from various sources, including studies by Aroni and Durkin (1985). Because these statistics come from multiple studies, the “Other” category contains injuries such as fractures, pain/soreness, respiratory or inhalation injuries, eye injuries, and unspecified injuries, which may not be represented the same way in each study.

Table 11: Distribution of Nonfatal Injuries for Five California Earthquakes

Earthquake		Lacerations	Sprains	Contusions	Cardiovascular	Neurological/ Psychological	Other
Santa Barbara (1978)	**M5.7**	33%	19%	23%	2%	2%	21%
Imperial County (1979)	**M6.4**	25%	14%	18%	0%	13%	30%
Coalinga (1983)	**M6.7**	32%	14%	23%	1%	5%	25%
Loma Prieta (1989)	**M6.9**	7%	39%	22%	N/A	0%	32%
Northridge (1994)	**M6.7**	31%	13%	6%	11%	4%	35%

The AIR model also estimates the probabilities, or rates, of injury severity for each of the damage states of each construction class. There are four injury severity levels used in the AIR model, as shown in Table 12.

Table 12. Injury Severity Levels Used for Workers' Compensation (FEMA 2009)

Severity Level	Description
Minor	Basic medical aid that can be administered by paraprofessionals is sufficient. Examples are sprains, severe cuts requiring stitches, minor burns (first or second degree on a small part of the body), and bumps on the head without loss of consciousness.
Moderate	A greater degree of medical care is necessary. The use of medical technology such as x-rays or surgery is needed, but the injury is not life-threatening. Examples include second or third degree burns over large parts of the body, bumps on the head that cause loss of consciousness, fractured bones, dehydration, or exposure.
Life-Threatening	Injuries pose an immediate life-threatening condition if they are not treated expeditiously. Examples include: uncontrolled bleeding, internal injuries such as punctured organs, spinal injuries, and crush syndrome.
Fatal	Person is instantaneously killed or mortally injured.

Calculating the Number of Casualties

To estimate the number of casualties that correspond to different combinations of damage states and injury severity levels, the AIR model uses an event-tree framework, such as the one shown in Figure 98. By following the event tree, the

number of casualties for each of the four injury severity levels is estimated separately for each building damage state. The casualty numbers are then combined according to their associated probabilities to produce the total injury estimation for a building.

This calculation is completed for the damage states for each construction type. Casualty rates depend to a large degree on construction type. For example, the casualty rate for a wooden house differs significantly from that of a high-rise concrete building.

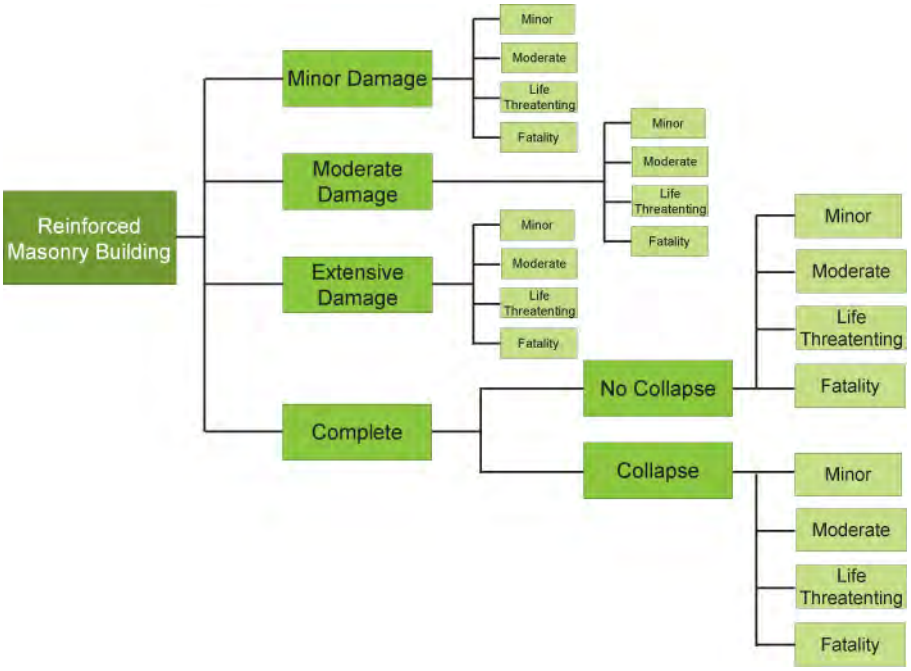

Figure 98: Injury Severity Level by Building Damage State for a Reinforced Masonry Building

Calculating the number of casualties due to an earthquake is a complex process because each building damage state must be correlated with the likelihood of injury and the severity level. Injury rates are separately derived for each injury level and are conditional on the building's damage state. They are derived using casualty data from historical earthquakes in the United States (FEMA 2009 and Peek-Asa et al. 2000).

Estimating Workers' Compensation Losses

For each injury severity category an estimate of the number of workers that are injured is calculated using a probabilistic process that accounts for inherent uncertainties. First, the injury rate distribution is applied to the number of employees present in the building. The cost of the injuries, which also varies by

their severity, is then applied and summed probabilistically to achieve an estimate of total workers' compensation losses for that building (Figure 99).

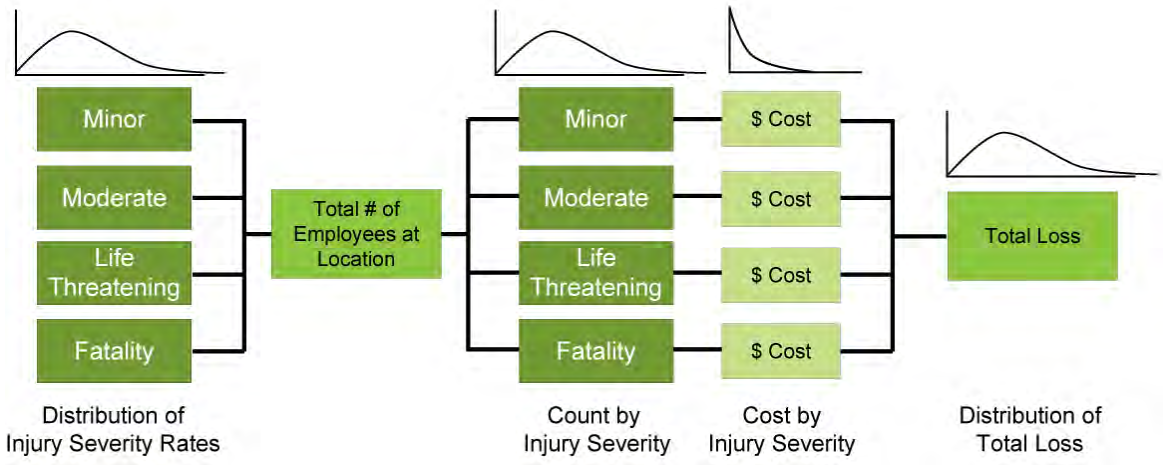

Figure 99: Calculation of Workers' Compensation Loss for an Individual Building

The total number of workers at each location is derived using a comprehensive business demographics database of U.S. businesses and employee counts from a premier market research company. In the AIR model, the estimate of the percentage of workers who are injured depends on the day of the week and the time of day that the earthquake took place.

The model utilizes a six-day work week (since many businesses operate on Saturday or Sunday). Daytime is defined as the hours from 9 a.m. to 5 p.m., while night is defined as 7 p.m. to 7 a.m. Separating these time periods are two commuting periods: one from 7 a.m. to 9 a.m. and another from 5 p.m. to 7 p.m. Therefore, for the days Monday-Saturday, the model assumes an 8-hour working period, 4 hours of commute time, and a 12-hour night. (Sunday falls into the same category as night.) This means that there is less than a 30% probability that an earthquake, which can occur at any time of day or night with equal probability, will occur during the hours when the majority of employees are at work.

The model's default assumptions about workplace occupancy are derived from FEMA (2009). The default industrial occupancy rates are as follows: 80% of employees are assumed to be at work during the daytime hours, 10% are at work during night hours, and 50% are at work during commuting hours. Commercial occupancy rates are 98% for daytime hours, 2% for night hours, and 50% for commuting hours.

The difference in the number of workers during each of the three time periods has a direct consequence on the estimated number of casualties. Table 13 shows the results from a scenario study of the 1994 Northridge earthquake. Two scenarios of

the Northridge earthquake are assumed, one at night and the other during the day, with day and night hours as defined in this section. The table includes ranges for the estimated number of workers who are injured at each of the four injury levels. For each range, the lower bound indicates the number of casualties incurred during an event at night while the upper bound indicates the number of casualties incurred during an event during the day.

Table 13: Model Estimates of the Number of Casualties for Two Scenarios of the 1994 Northridge Earthquake

Injury Severity Level	Number of Workers
Minor	346 – 14,624
Moderate	219 – 9,356
Life-Threatening	35 – 1,519
Fatal	17 – 717
Total Casualties	**617 – 26,216**

Developing Default Injury Costs and Benefit Levels

Estimates of workers' compensation losses are calculated based on the number of employees who have sustained injuries at each severity level and on the cost of the injury, which depends on its severity as well as the location of the workplace. In cases where claims costs are not provided by the client, the model uses objective average costs, specific for each state, as reported to the National Council on Compensation Insurance (NCCI).

The model's default assumptions about average workers' compensation claim costs are derived from observational data obtained from the NCCI Annual Statistical Bulletin. Losses are developed on an ultimate settlement basis by the NCCI, and AIR adjusts the historical observational data to include current cost and benefit levels. This is done by state and NCCI injury type, and is separate from medical and indemnity claims. Any changes in benefits, or in legislation that affects coverage, are accounted for using information from each state. Losses are also normalized to the current time period using the changes in claim costs as shown in the NCCI reports.

The mental stress that usually accompanies catastrophic events is also taken into consideration. An adjustment is made to the average cost of nonfatal injuries to incorporate an increased level of mental stress. The amount of the adjustment is based on the "mental stress" historically associated with an injury using observational data from the NCCI.

5.16 Sprinkler Leakage Damage

The AIR Earthquake Model for the United States features a separate module to estimate losses caused by the breakage and subsequent leakage of fire sprinkler pipes[13] due to ground shaking. The module takes into account advances in technology, as well as building code and practice through regional and age modifiers. It also recognizes differences in vulnerability to water damage of individual non-structural building components and different types of contents.

The sprinkler leakage module estimates losses to buildings (non-structural components only) and contents, as well as those stemming from business interruption. The development of the sprinkler leakage damage functions is based on both original and published research, including the work of Comerio and Bertero (2000). In that study, which uses data from the Northridge (1994) and Nisqually (2001) earthquakes, the authors estimate water damage ratios for non-structural building components and contents as a function of building damage state. The damage states, which are consistent with those from SEAOC's Vision 2000, are given as a relative ranking from 0 (complete, or collapse) to 10 (negligible). By mapping these damage states to damage ratios suggested in ATC-13, AIR developed a "base" damage function, which takes the general form illustrated below in Figure 100.

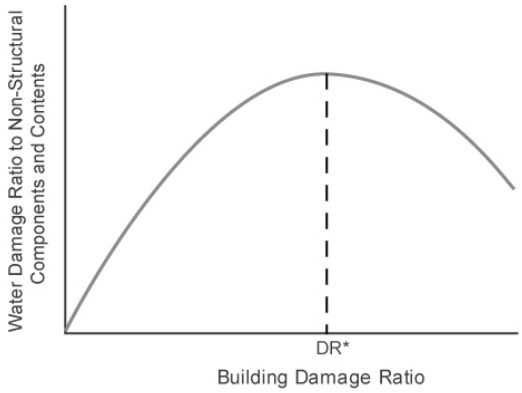

Figure 100: General Form of the AIR Sprinkler Leakage Damage Function

Note that beyond some building damage ratio, DR*, the water damage ratio actually decreases. This threshold damage ratio represents ground shaking sufficiently severe to cause the breakage of the water mains that supply sprinkler systems. Beyond this level of intensity, water pressure and therefore water damage is reduced.

[13] Note that the module includes leakage from all water pipes within a building. However, pipes other than fire sprinkler pipes are much less vulnerable, less prevalent throughout the building and therefore contribute minimally to total losses from water damage.

AIR engineers have developed separate damageability relationships for each of building, contents, and time element for each of more than two dozen occupancy classes. Expert judgment is used to determine the vulnerability of contents, which vary by occupancy, to water damage. A relative ranking of contents vulnerability and thus damage functions by occupancy class is developed, as illustrated schematically in Figure 101.

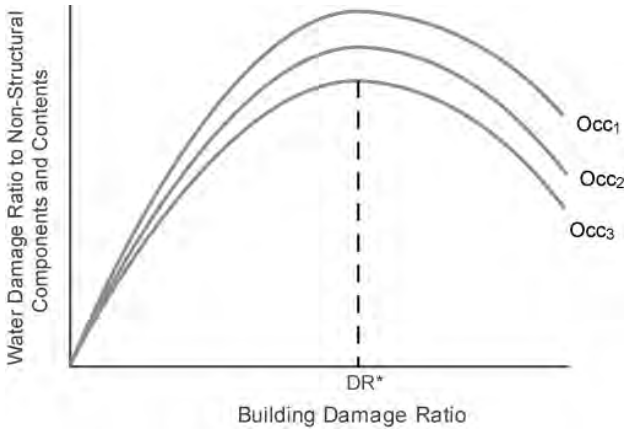

Figure 101: Relative Ranking of Contents Damage Functions by Occupancy Class

In the case of Coverage A, the module assumes that only non-structural components are water-damageable. The value of such non-structural elements as a percentage of total building value for various occupancy classes is provided by the detailed databases that support AIR's property replacement value estimation products. AIR construction engineers estimated the vulnerability to water damage of each component type, including interior walls, ceilings, floor finishes, wiring and fixtures, etc. Similar to the approach used for contents, this information is used to develop a relative ranking of non-structural component damage functions by occupancy class.

Time element damage functions are developed based on the estimates of the number of days needed for repair or replacement of both contents and non-structural building components. Note that these are not additive. In some cases, contents can be replaced while non-structural repairs are underway. In other cases, this may not be true.

Two or more variables (in this case contents and non-structural damage) that have a common source (earthquake ground-shaking), but whose values are not directly correlated, are called "orthogonal" and are appropriately combined by way of the square root of the sum of the squares.

Regional Modifiers

The AIR sprinkler leakage damage module employs regional modifiers. Construction techniques and building practices generally reflect the relative hazard experience of different regions. Because of its historical experience with respect to seismic activity and its stringent seismic code, structures in California are assumed to be the least vulnerable to earthquake shake, while structures in the Central and Eastern United States are the most vulnerable. The Pacific Northwest (Washington and Oregon only) ranks second to California.

Age Modifiers

Age also plays a role in vulnerability, though its effects are complex. The materials used in the non-structural components of newer buildings are generally more vulnerable to water than older materials found in older buildings. Also, newer buildings will, in general, have newer contents, many of which—electronic equipment, in particular—are more vulnerable than older contents.

However, sprinkler systems in newer buildings are less likely to break. Built to more stringent code establishing requirements for longitudinal and lateral bracing, and the amount of clearance around piping, as well as benefiting from technological improvements such as flexible couplings, the sprinkler systems in newer buildings are less vulnerable to earthquake shake. While the effect of overall building vulnerability dominates the vulnerability of either non-structural components or contents, both effects are taken into account in the AIR model.

Secondary Uncertainty

The AIR sprinkler leakage loss module is fully probabilistic and takes into account secondary uncertainty. Damage from sprinkler leakage is modeled as a function of building damage. The model accounts for uncertainty in the level of sprinkler leakage damage given a building damage ratio, as well as uncertainty in the building damage ratio given a level of ground motion. These two distributions are combined by way of simulation to obtain the final damage distribution.

General Impact of Sprinkler Leakage Damage on Earthquake Loss Estimates

The impact of the sprinkler leakage loss module on overall earthquake shake losses is quite small. The probability of sprinkler leakage damage is the product of the probability that pipes will break and the probability that building components and contents are exposed to and actually damaged by water. The first probability is estimated to be quite low.

5.17 Validating the Model's Damage Estimation Module

As discussed in Section 5.7, the model's damage functions report the mean damage ratio for each level of intensity, where the mean damage ratio is the ratio of the repair cost of the building or contents to its replacement value. Thus validating the damage estimation component of the model is inextricably intertwined with validating modeled losses. A discussion of modeled loss validation can be found in Section 7.2. Validating event losses, which accounts for ground motion, vulnerability, and industry inventory data, ensures a model's overall performance.

Nevertheless, a sample of additional validation exhibits relating to the model's damage functions and estimates of fire-following and workers' compensation losses are provided below.

Validating the Model's Damage Functions

Perhaps the most significant advance in the vulnerability module is the shift from static pushover analysis with the more realistic nonlinear dynamic analysis, or NDA. This relatively new theoretical framework for the seismic design of new buildings and the seismic performance evaluation of existing ones has become firmly established in the academic and engineering communities and represents a radical shift from the traditional reliance on prescriptive building codes

When NDA is used on detailed three-dimensional models of buildings, the prediction of the building response is extremely accurate. Figure 102 shows a three-dimensional computer model developed by AIR of a seven-story reinforced concrete moment-resisting frame building in Van Nuys, California, that experienced the Northridge earthquake in 1994.

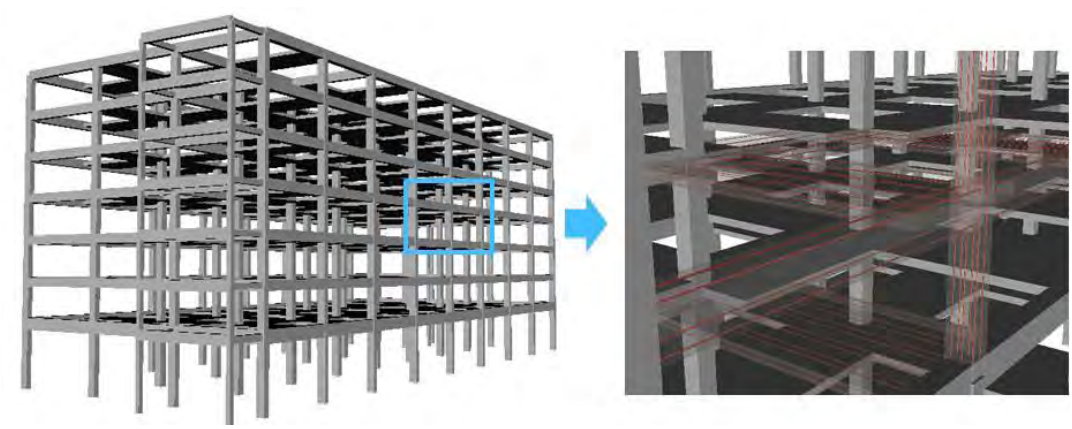

Figure 102. Model of an Existing Reinforced Concrete Frame Building that was Instrumented during the 1994 Northridge Earthquake

The red lines in the image on the right indicate steel reinforcing bars in the columns and slabs of the building. Since this building was instrumented to record its behavior, and its deformation and damage are known, it represents an excellent benchmark for assessing the accuracy of NDA to predict the response of actual buildings to earthquakes.

Figure 103 displays the predicted interstory drift ratio of the building in Figure 102 when subjected to the 1994 Northridge earthquake ground motion recorded at the building site. The figure compares the modeled response of the building (blue line) to its actual response that was recorded during the earthquake (red line). The results show remarkable agreement as testimony to the accuracy that NDA provides when estimating building deformation during ground shaking.

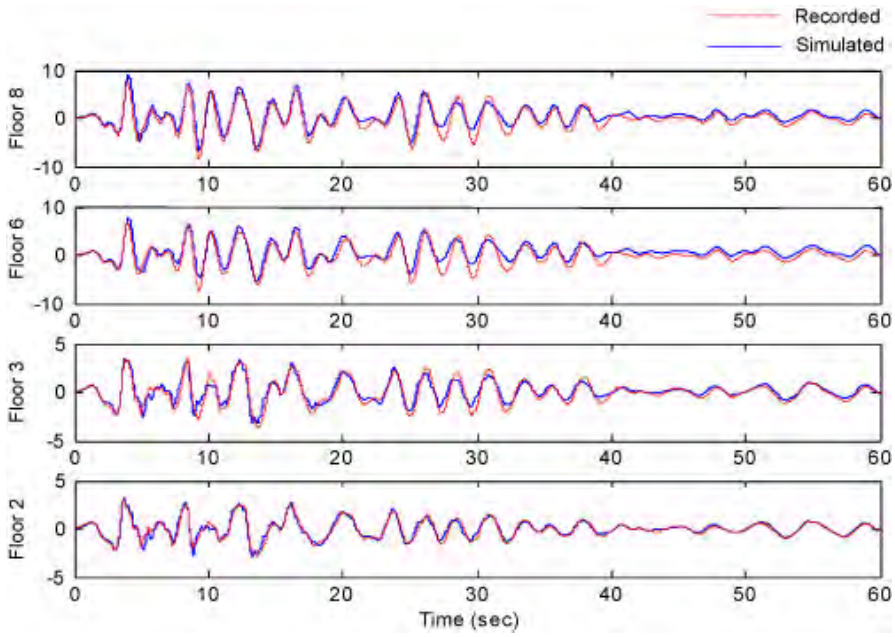

Figure 103. Comparison of Simulated and Recorded Floor Displacement during the 1994 Northridge Earthquake

At the industry level, the damage functions developed using NDA produce realistic damage footprints, as illustrated in Figure 104 and Figure 105.

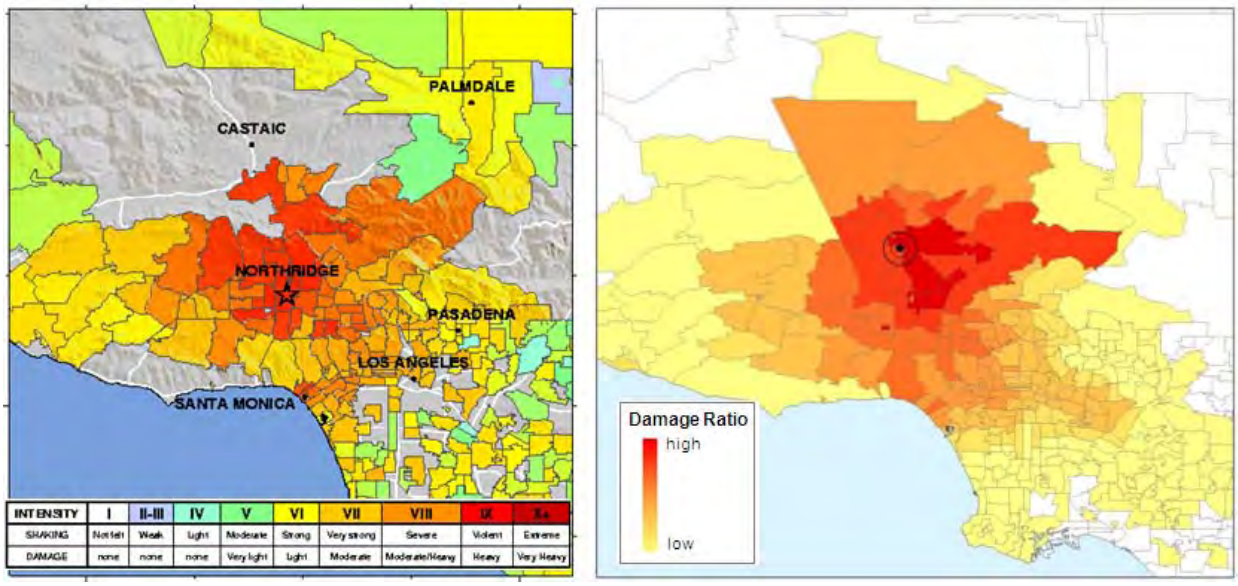

Figure 104. Comparison between USGS MMI Map for the 1994 Northridge Earthquake (left) and AIR Modeled Damage Ratios (right)

Figure 104 provides a comparison between the Modified Mercalli Intensity (MII) map produced by the USGS for the 1944 Northridge earthquake and a map of damage ratios produced by the AIR model for this event. Figure 105 shows a similar comparison but for the 1989 Loma Prieta earthquake. Please note that in these exhibits, damage ratios are being compared to reported intensity. Note, too, that Zip code boundaries have changed since these two events. Nevertheless, both show good agreement.

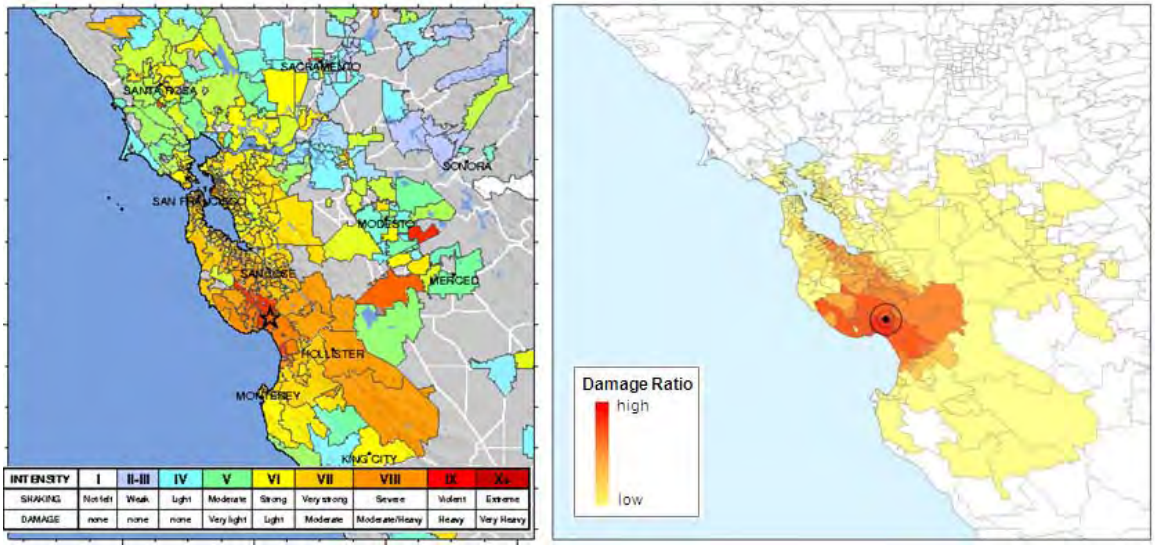

Figure 105. Comparison between USGS MMI Map for the 1989 Loma Prieta Earthquake and AIR Modeled Damage Ratios

As discussed above, contents damage is a function of spectral acceleration and occupancy in the AIR model. Figure 106 shows the comparison of the contents damage function in the model and contents claims data from the 1994 Northridge earthquake.

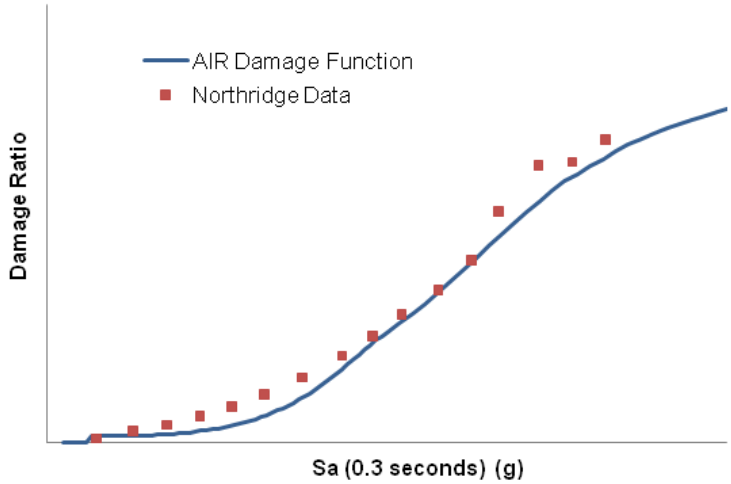

Figure 106. Northridge Claims Data and AIR Damage Function for Residential Contents

As discussed above, Additional Living Expenses, or ALE, loss is a function of the mean building damage. Figure 107 shows a comparison of the AIR damage function and ALE claims from the 1994 Northridge earthquake.

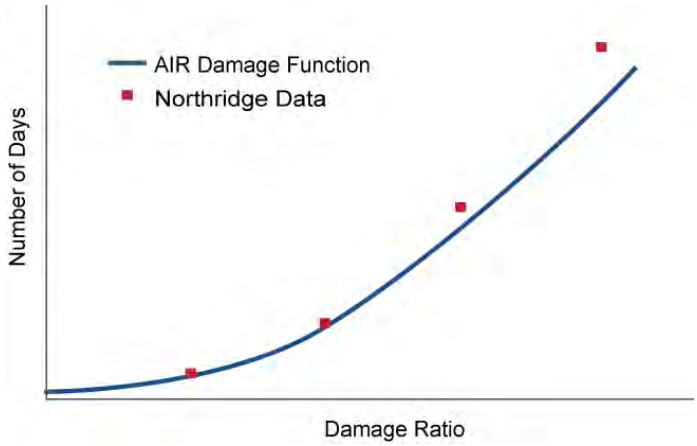

Figure 107. Northridge Claims Data and AIR Damage Function for Residential Additional Living Expenses

Validating the Distribution of Damage

As was discussed in Section 5.7, similar structures at the same location may experience different levels of damage. To capture this uncertainty in damage, the AIR model constructs distributions around the mean damage ratio.

Although beta distributions are commonly used, they do not accurately reflect variation in damage. Following an extensive analysis of claims data, AIR engineers found that a combination of two beta distributions (referred to here as a bi-beta distribution) better represents this uncertainty. Figure 108 and Figure 109 compare the bi-beta modeled and observed damage distributions at mean damage ratios of 0.026136 and 0.17251, respectively. The observed and modeled damage distributions are quite consistent.

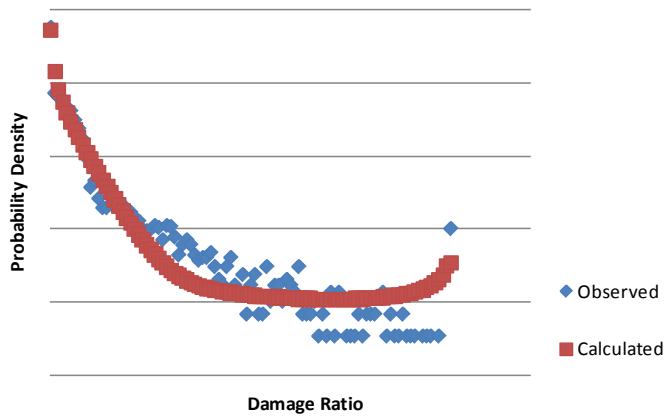

Figure 108. Modeled vs. Observed Probability Distributions, Mean Damage Ratio 0.026136

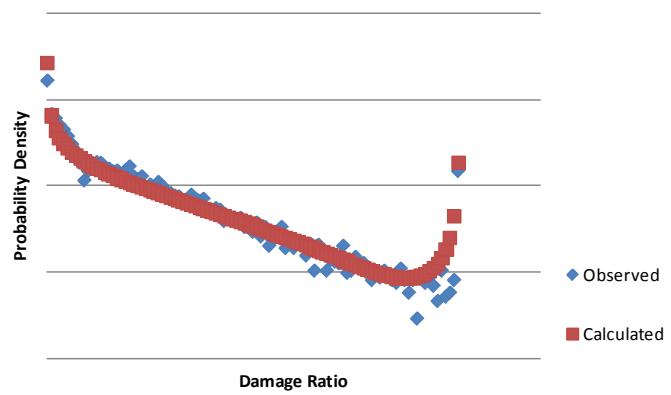

Figure 109. Modeled vs. Observed Probability Distributions, Mean Damage Ratio 0.17251

Validating Fire Following Damage

Figure 110 illustrates the locations of actual fire ignitions associated with the 1994 Northridge earthquake. Figure 111 illustrates the locations of simulated fire ignitions associated with the same event, assuming 2008 exposures. The simulated ignitions are from a single fire simulation. The two figures demonstrate reasonably good agreement regarding the locations of simulated and actual ignitions.

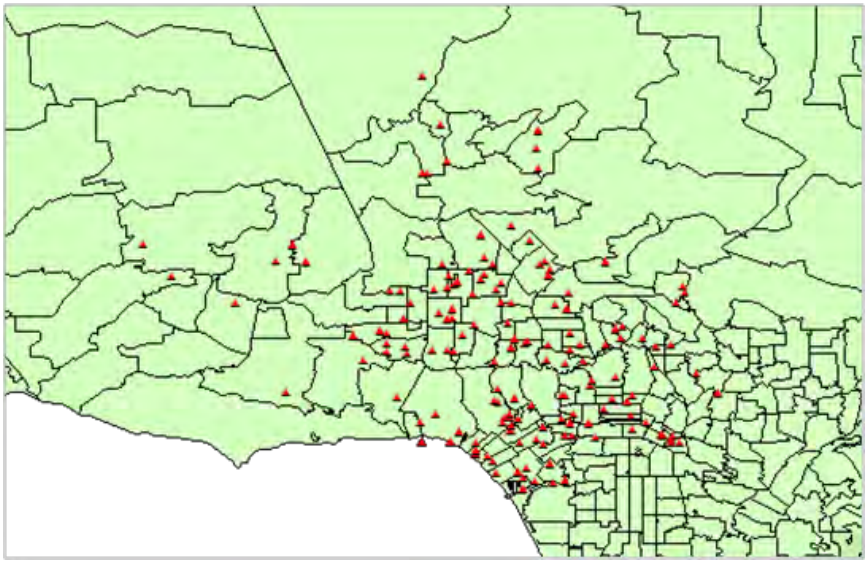

Figure 110. Observed Ignitions for the 1994 Northridge Earthquake

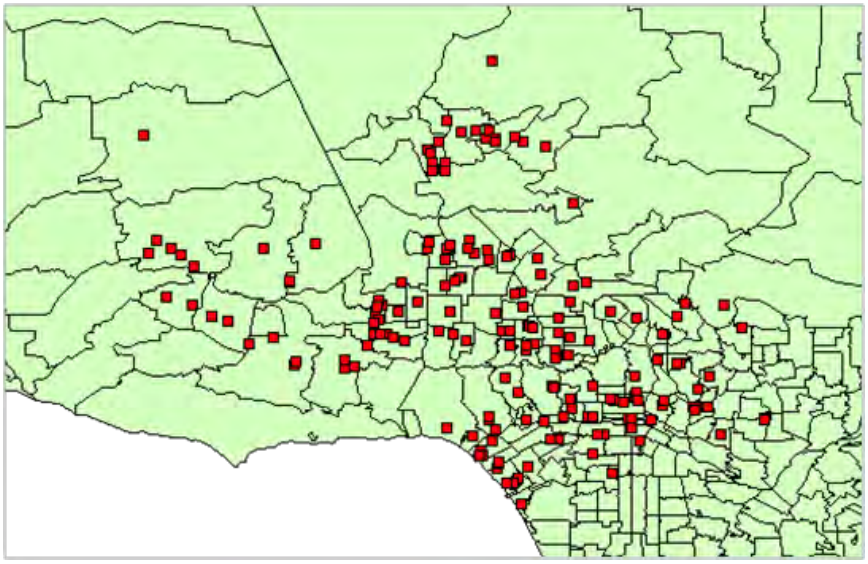

Figure 111. Simulated Ignitions for the 1994 Northridge Earthquake, Assuming 2008 Exposures

Figure 112 illustrates the spatial distribution of exposure density and the modeled peak ground acceleration (PGA) contours associated with a repeat of the 1994 Northridge earthquake. Also shown are the average modeled fire damage ratios for combustible exposures. Figure 113 is similar to except that it shows average modeled fire damage ratios for noncombustible exposures. The modeled fire damage ratios tend to be higher for combustible than for noncombustible exposures, as expected.

The likelihood of fire damage depends on both ground motion and exposure density. For most earthquakes, the locations with the highest levels of ground motion and exposure density do not coincide. Therefore, in most cases, the highest fire damage ratios are likely to occur where either or both the exposure density and ground motion are not at their highest levels.

In the case of the 1994 Northridge earthquake, the model predicts that the highest fire damage ratios occur where there is a relatively high exposure density and slightly less than the highest levels of ground motion. This occurs near the center of Figure 112 , where the concentration of dark-colored squares is highest. A similar pattern is observed in Figure 113.

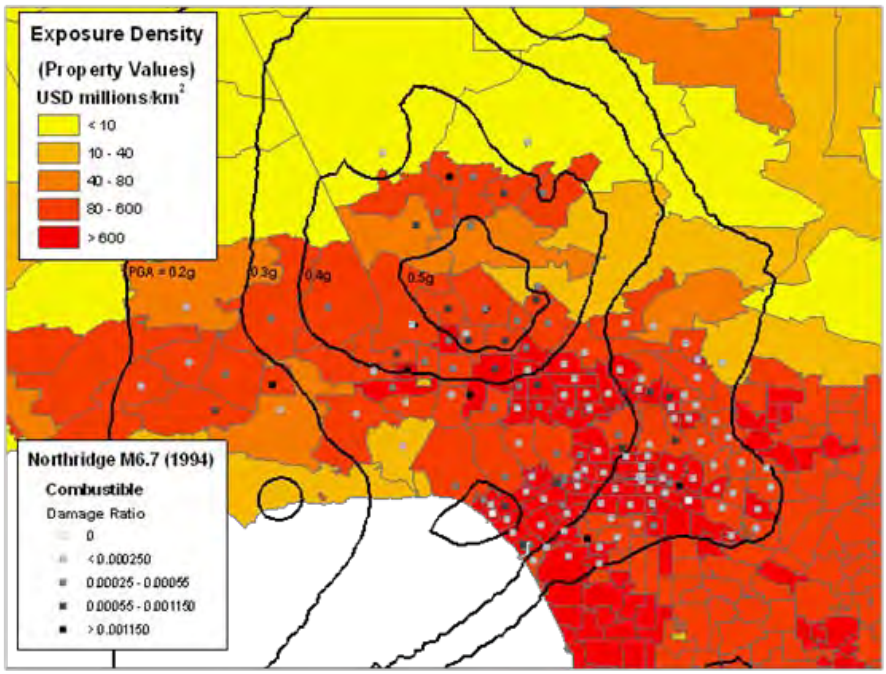

Figure 112. Exposure Density, Simulated PGA Contours, and Mean Damage Ratios for Combustible Exposures, Repeat of the 1994 Northridge Earthquake

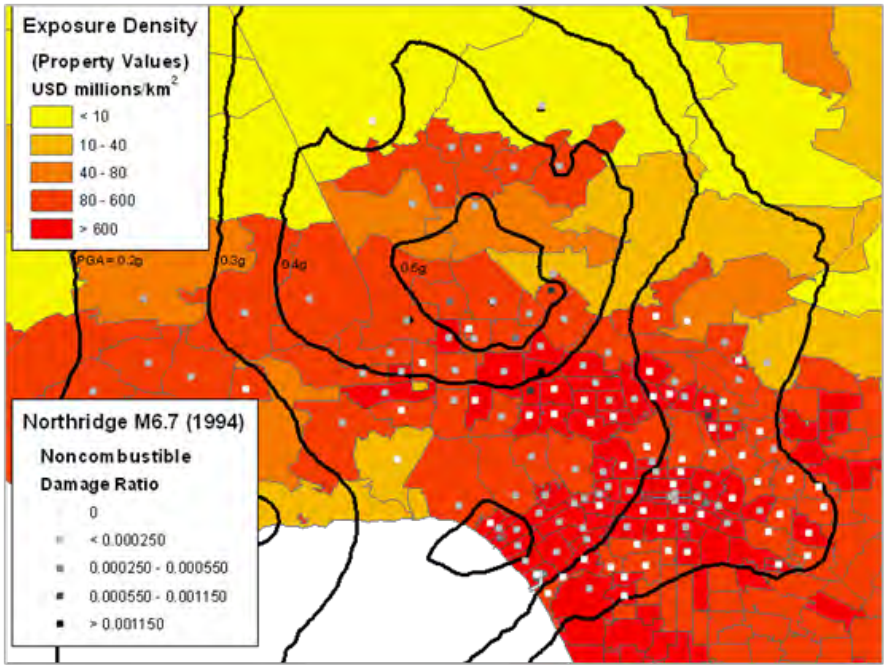

Figure 113. Exposure Density, Simulated PGA Contours, and Mean Damage Ratios for Noncombustible Exposures, Repeat of the 1994 Northridge Earthquake

Figure 114 illustrates the spatial distribution of exposure density and the modeled PGA contours associated with a repeat of the 1906 San Francisco, earthquake. Also displayed are the average modeled fire damage ratios for combustible exposures. Figure 115 is similar to Figure 114 except that it shows the average modeled damage ratios for noncombustible exposures.

In the case of the 1906 San Francisco earthquake, the model predicts that the highest fire damage ratios occur where the exposure density and PGA values are both relatively high, in the lower half of each figure, west, south, and southeast of San Francisco Bay.

The actual earthquake occurred more than 100 years ago and affected a very different exposure distribution. While the AIR Earthquake Model for the United States predicts that in a repeat of the 1906 San Francisco earthquake, with the present exposure distribution, about 15% of the ground-up damage would be due to fire, in the actual event, 80-90% of the damage was due to fire. The difference is explained by a number of reasons. First the building stock in San Francisco in 1906 was not built to withstand earthquakes, so there was more shake damage than would occur today; the higher levels of shake damage resulted in higher ignition rates. Also, a large percentage of the building stock was made of wood and was therefore highly combustible. Finally, much of the fire damage resulted

from the use of dynamite, which was employed in the misguided effort to create firebreaks.

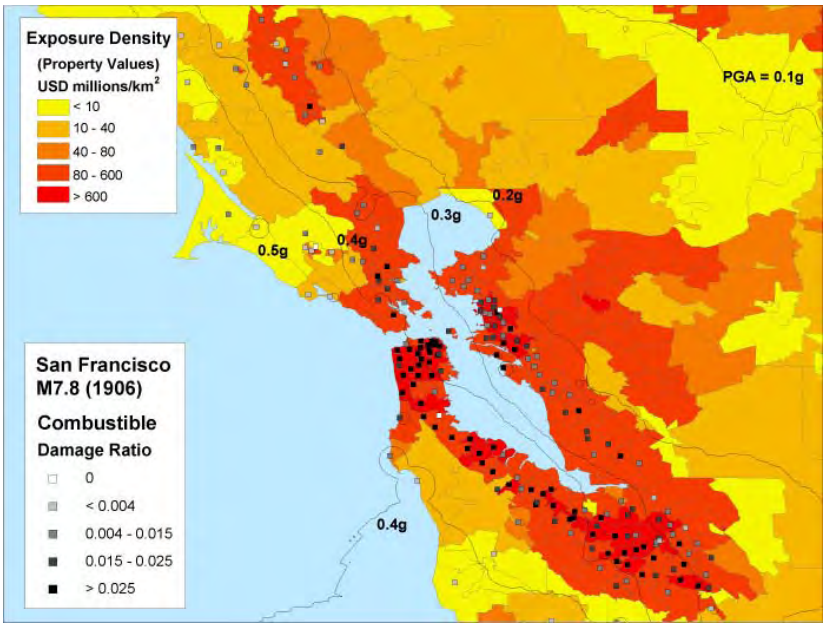

Figure 114. Exposure Density, Simulated PGA Contours, and Damage Ratios for Combustible Exposures, Repeat of the 1906 San Francisco Earthquake

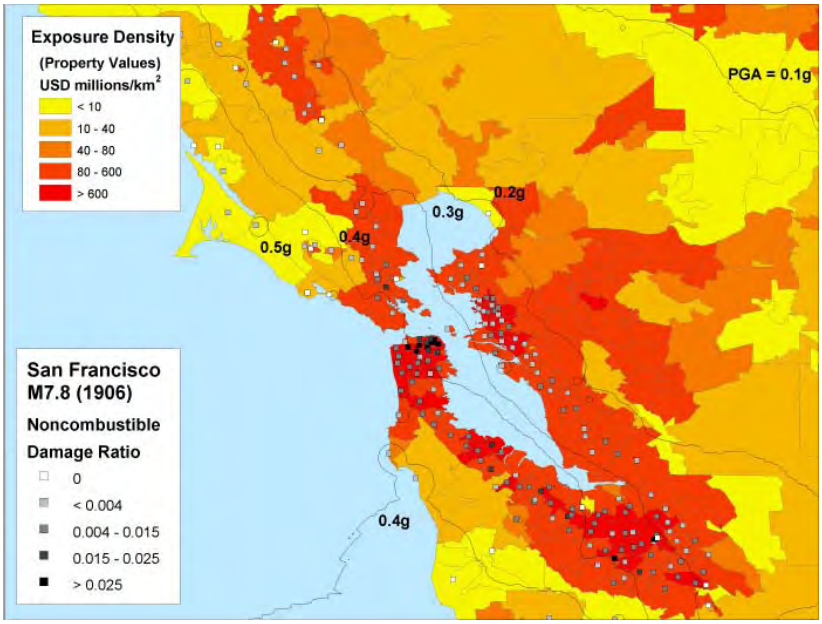

Figure 115. Exposure Density, Simulated PGA Contours, and Damage Ratios for Noncombustible Exposures, Repeat of the 1906 San Francisco Earthquake

Figure 116 illustrates the spatial distribution of exposure density and the modeled PGA contours associated with a repeat of the 1989 Loma Prieta earthquake. Also displayed are the average modeled fire damage ratios for combustible exposures. Figure 117 is similar to Figure 116 except that it shows the average modeled damage ratios for noncombustible exposures.

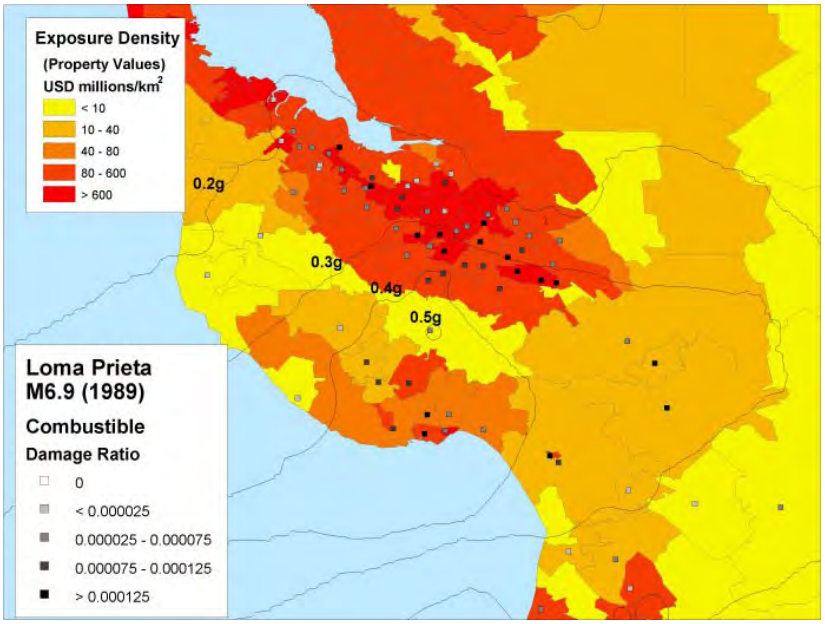

Figure 116. Exposure Density, Simulated PGA Contours, and Damage Ratios for Combustible Exposures, Repeat of the 1989 Loma Prieta Earthquake

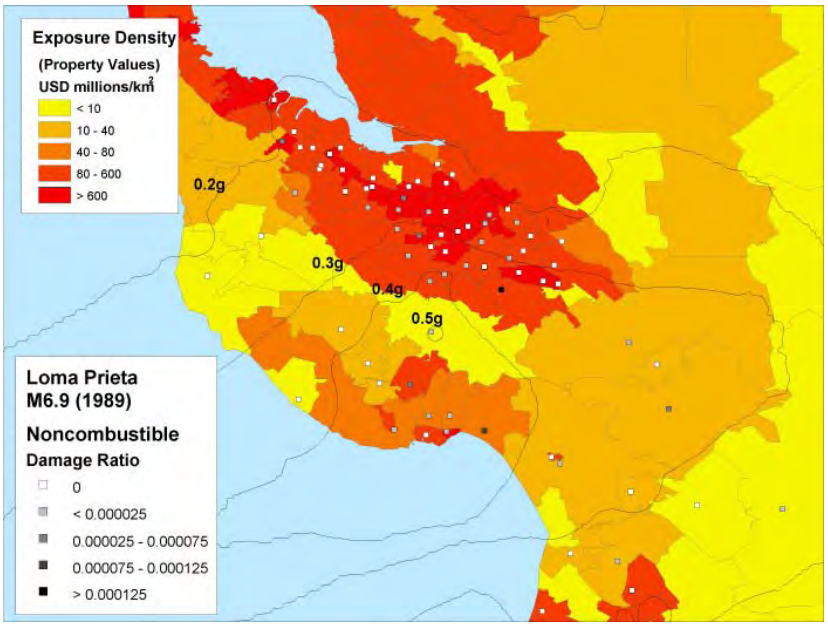

Figure 117. Exposure Density, Simulated PGA Contours, and Damage Ratios for Noncombustible Exposures, Repeat of the 1989 Loma Prieta Earthquake

In the case of the 1989 Loma Prieta earthquake, the model predicts that the highest fire damage ratios occur where the exposure density and PGA values are both relatively high, to the southeast of San Francisco Bay. Reports from the actual earthquake indicate that some of the heaviest fire damage was in Santa Cruz, where two dozen buildings were destroyed by fire caused by the earthquake. As Figure 116 and Figure 117 indicate, the model also predicts heavier damage in those areas. In addition, heavy fire damage was incurred in the Marina District of San Francisco, where 17 fires were reported.

For the 1989 earthquake in Loma Prieta, and the 1994 earthquake in Northridge, actual fire-following losses are compared to the median and mean modeled losses, as shown in Figure 118. The observed loss data is reasonably consistent with both the mean and median modeled losses. For the Northridge earthquake, the mean modeled loss is higher due to the presence of some outliers with large losses among the 50 fire simulations that were run for the event.

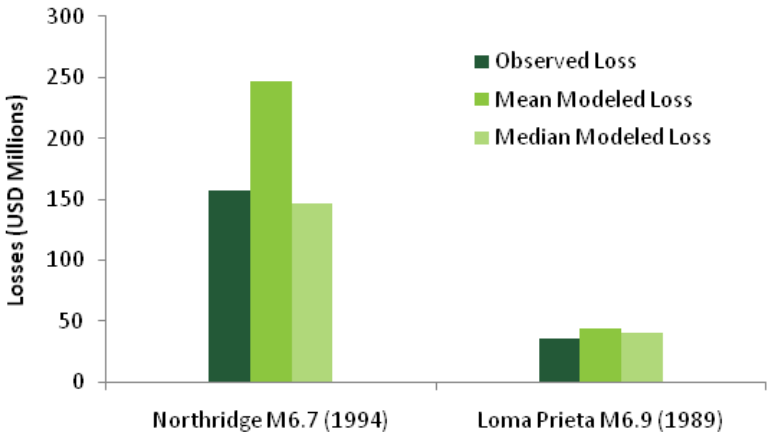

Figure 118. Observed Fire-Following Losses Compared to Mean and Median Modeled Losses for Northridge and Loma Prieta Earthquakes

Validating Modeled Workers' Compensation Losses

The workers' compensation component of the AIR Earthquake Model for the United States relies on published studies of casualty rates as well as data from actual earthquakes. For validation, however, the availability of appropriate data is limited. Some of the challenges are discussed in this section, along with a comparison between modeled and historical injury counts for some recent earthquakes. Note that a meaningful comparison of losses is made more challenging because of the significant changes in benefit levels that have occurred over time. Note that the modeled results reflect industry exposures as of 2008, both in terms of population and exposed properties.

There is only limited information on workers' compensation insurance claims in the United States available to the public. In addition, there is a certain amount of uncertainty regarding the change over time in number of workers and their workplaces. Therefore, a reliable validation uses a comparison between the modeled and historical injury counts based on the total population, rather than on the injury counts of workers.

Table 14 shows the total number of casualties based on observational data after some recent historical earthquakes in California. These observations are compared to the number of casualties that are estimated by the AIR model were these earthquakes to recur today. Given an average population growth of approximately 1.6% annually in California between 1980 and 2008 (U.S. Census Bureau), the number of casualties reported at the time of these events are adjusted based on a formulation (Vranes et al., 2009). These adjusted values provide estimates of the number of casualties that would occur had these events taken place with today's population. With population growth taken into account, the modeled results are within a reasonable range for these earthquakes.

Table 14: Comparison of Observed and Modeled Casualties for Selected Historical Earthquakes in California

Year	Location	Observed Casualties*		Modeled Casualties	
		Nonfatal	Fatal	Nonfatal	Fatal
1987	Whittier	1,913	11	3,015	25
1989	Loma Prieta	5,161	87	8,297	95
1992	Landers	457	1	449	1
1994	Northridge	36,035	76	39,761	81

*Values have been adjusted to account for population growth in California

The uncertainty surrounding the number of injuries and fatalities observed during older earthquake events is considerably greater than for more recent events. This is due to less reliable data for older earthquake, and the fact that the impact of population growth on the number of casualties that would occur if those earthquakes took place today is difficult to predict. Moreover, the improvement in building design as well as increased public awareness of earthquake hazards over the past several decades play an important role in reducing the number of casualties. The combined impact of these factors on the injury counts is not quantifiable, especially in cases where the earthquakes occurred several decades ago.

However, information from all of the past earthquakes can be used to verify the overall model performance. Fatality data from 29 historical earthquakes in the U.S. that occurred between 1886 and 2003 was collected (NOAA, 1972; Cutter et al., 2005; Ramirez et al., 2005; and Vranes et al., 2009) and compared with the model estimates.

Figure 119 shows a scatter plot of observed and modeled fatalities. The horizontal line associated with each event indicates a range of the observed fatalities, suggesting uncertainties in the observed numbers. While the model underestimates the fatalities for some of the events and overestimates for others, the plots are tightly scattered around the 45° line, which indicates that the model estimates in general are reasonable and that the model does not have a bias.

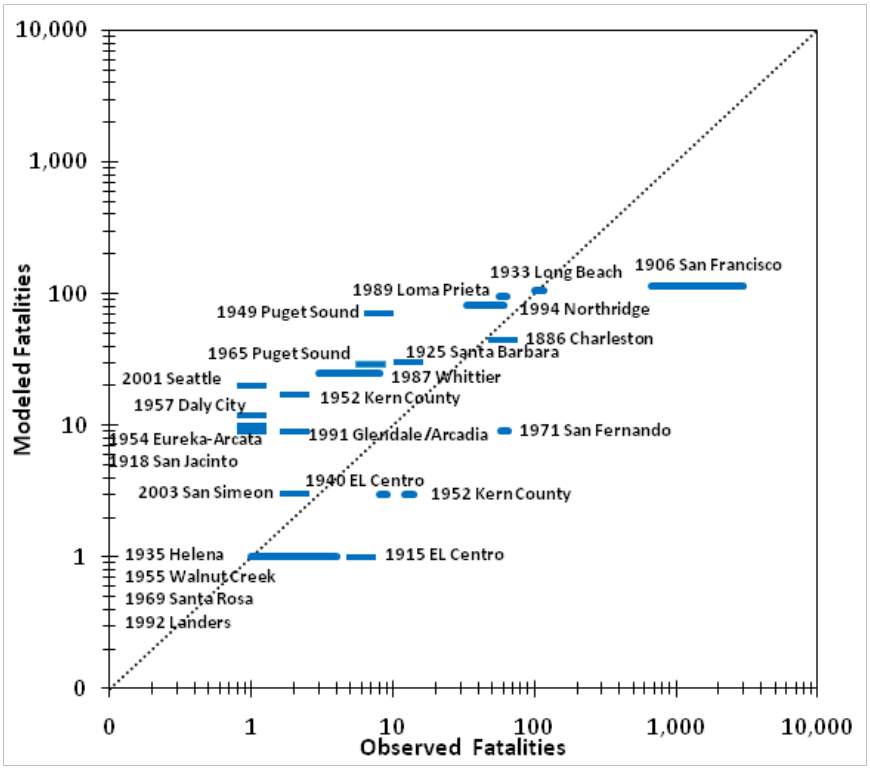

Figure 119: Modeled vs. Observed Fatalities from 29 Historical Earthquakes in the U.S.

The loss estimates produced by the AIR workers' compensation module are well within the range of reasonability when compared to the available historical data. Although there have been no significant casualties from earthquakes since the 1906 event in San Francisco, there is no doubt that earthquakes pose a significant hazard. It is therefore important to use a realistic modeling approach for workers' compensation to determine injuries due to ground shaking from earthquakes.

6 Estimating Damage to Industrial Facilities

The AIR Earthquake Model for the United States assesses property and business interruption (BI) losses for industrial facilities due to earthquake-induced ground shaking, fire following earthquakes and liquefaction. This section focuses on the damage functions used for large industrial facilities. These facilities contain a wide range of components, some of which are shown in Figure 120. The damage functions for large industrial facilities are included with the 400-series of CLASIC/2 occupancy classes.

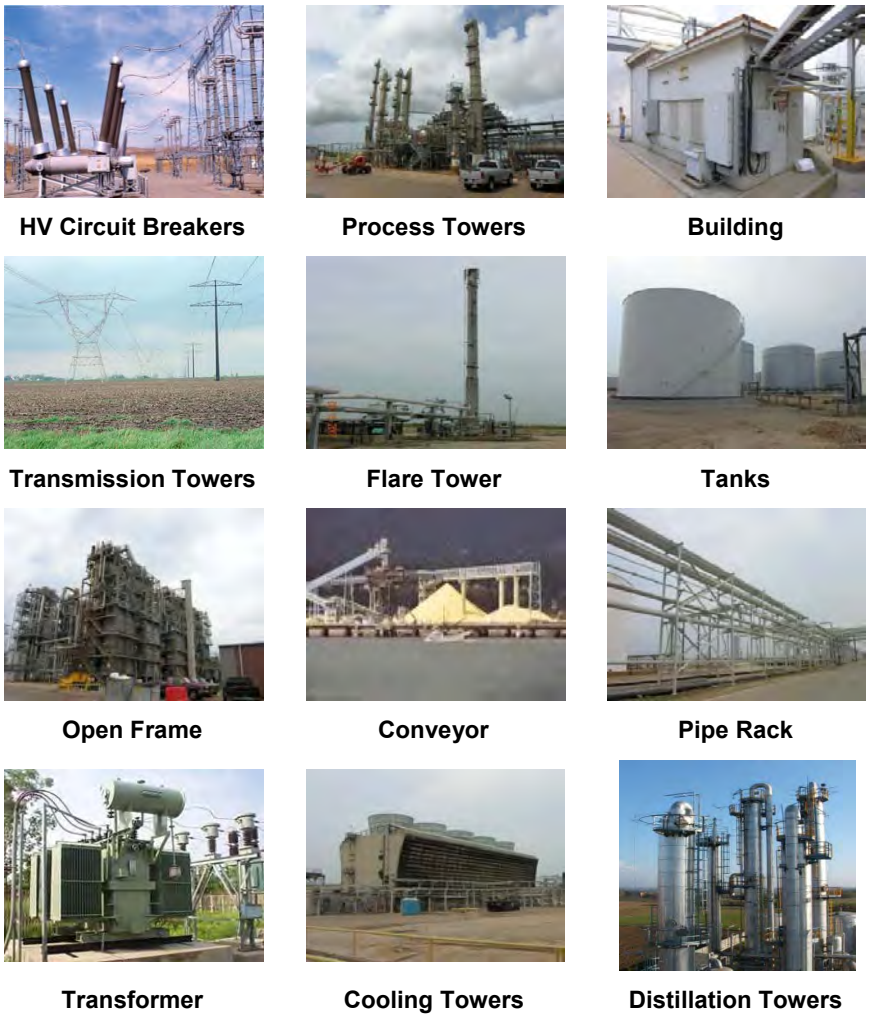

Figure 120. Some Industrial Facility Components

To assess the damage and loss potential to a large facility as a whole, AIR employed a component-based approach, which allows the damage functions to

account for the many primary components intrinsic to this type of facility. These primary components are categorized into classes and subclasses based on their function as well as their vulnerability to ground shaking, and AIR developed separate damage functions for each of more than 400 such components. AIR also obtained the valuation breakdown of a facility according to its components, and combined this information with the component damage functions to derive the damage function for an entire industrial facility.

This approach provides loss estimates that are transparent and consistent across different facilities. Furthermore, the component-based approach is essential for a reliable assessment of business interruption (BI) losses, which depend heavily on the numerous interactions between the various components and lifelines within industrial sites.

Developing Component-Level Damage Functions

To predict the response of an industrial facility exposed to ground shaking, the AIR model uses peak ground acceleration (PGA). Since the components are parts of a larger facility, a unique ground motion parameter has been used to estimate the response of all of the components. Using PGA as a ground motion parameter for assessing vulnerability of industrial components is advantageous for four reasons. First, the majority of components (e.g., machinery and equipment) in industrial plants are anchored and fairly rigid, and therefore PGA correlates well with their performance. Second, as discussed later in this section, the damage functions for an entire industrial facility are obtained using a weighted average of component damage functions. This process can be streamlined without adding uncertainties in the process of aggregation of different components by using the same ground motion parameter for all components. Thirdly, some of the component damage functions developed by different researchers are generally PGA-based and therefore using PGA facilitates the consideration of damage functions already available. Finally, historical damage data for industrial plants is often available along with an estimate of the PGA at the site. Estimates of other ground motion parameters are generally not reported.

Some 400 industrial components are included in the AIR model. The main categories of components are listed in Table 15, but each has many sub-classes. All components chosen for analysis represent actual industrial facilities. They were selected from structural drawings, design specifications and other sources.

Table 15. Industrial Facility Components used in the AIR Earthquake Model for the United States

Industrial Facility Components		
Air Handling Units	Distribution Panels	Open-Frame Structures
Baffles	Electric Power Backup	Paddles
Basins	Electric Transmission Towers	Pipe Racks
Battery Chargers	Elevated Pipes	Pipes and Pipelines
Battery Racks	Engine Generators	Potential Transformers
Boiler/Pressure Vessels	Equipment	Pressurized Reactors
Boilers	Fans	Process Towers
Buildings	Filter Gallery	Pumps
Chillers	Flares	Scrapers
Chlorination Equipment	Generators	Sediment Flocculation Equipment
Circuit Breakers	Highways/Runways/Railroads	Silos
Commercial Backup Power	Large Horizontal Vessels	Stacks/Chimneys
Compressors	Large Motor-Operated Valves	Switch Gears
Control Panels	Large Vertical Vessels with Formed Head	Tanks
Cooling Towers	Lightning Arrestors	Transformers
Coupling Capacitors	Loading Structures (Cranes/Cargo Handling/Conveyor Systems)	Tunnels
Current Transformers	Motor Control Centers	Wells
Dams	Large Motor-Operated Valves	Valves
Disconnect Switches	Motor-Driven Pumps	

The damage functions derived for each component, in general, vary depending on the region where the facility is located. This is because the seismic hazard and, therefore, the design specifications are different in different parts of the United States. Therefore, for each component and subcomponent, AIR developed different damage functions for each of the three seismic regions of the country: California, Washington and Oregon, and all other states.

Figure 121 illustrates damage functions for the most common components found in industrial facilities in California. Similar sets of component functions were obtained for Oregon and Washington, and for all other states.

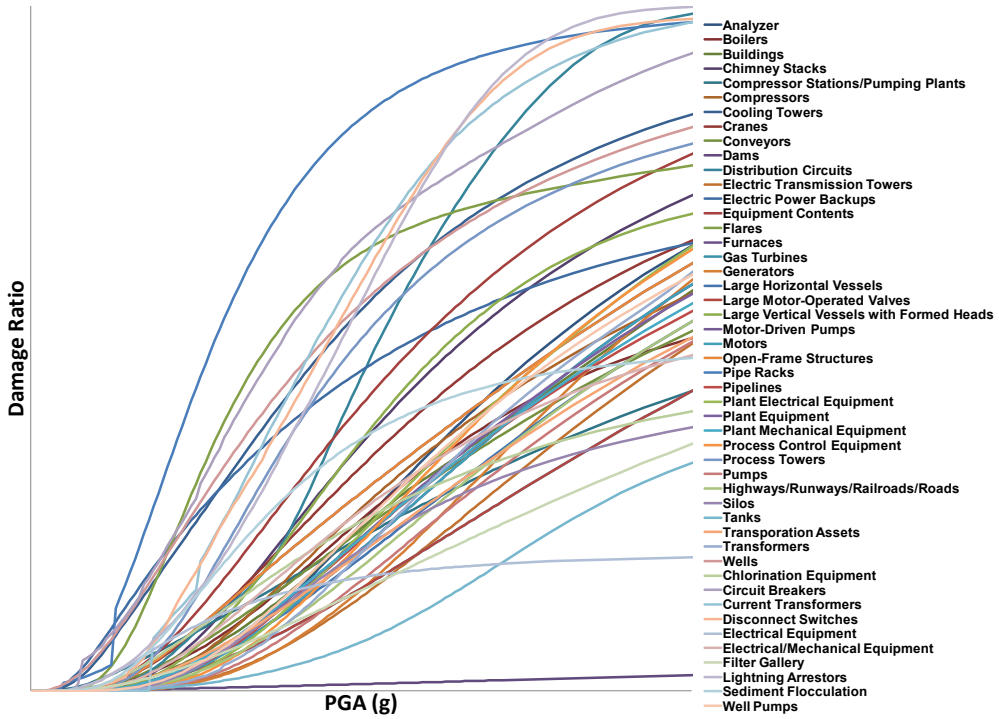

Figure 121. Damage Functions for Industrial Facility Components in California

The following sections describe the different methods that were used to develop the component-level damage functions.

Damage Functions for Buildings

As stated earlier, the damage functions for small industrial facilities were developed with the assumption that the facility comprises primarily buildings and some machinery. The damage functions for small facilities were therefore developed based on the building damage functions for different construction classes. These damage functions are identical to the building damage functions for large industrial facilities. However, since the cost of the components for the large industrial facilities is generally more than 80% of the cost of the facilities, there is significant difference between the damage functions for large and the small facilities. To derive the building damage functions for each type of facility (e.g., heavy fabrication), AIR obtained a weighted average of all the damage functions for different types of low-rise buildings that are present in the industry exposure for that type of facility. The weights assigned to each damage function are simply the fraction of each building type in the mix. This process was completed for each seismic region to obtain a building damage function for each industrial type.

Table 16 shows an example of the weights used to obtain the damage function for buildings within an industrial site in different regions of the United States. The table shows, for each seismic zone, the construction distribution used for low-rise buildings in heavy fabrication and assembly plants.

Table 16. Construction Distribution for Heavy Fabrication and Assembly Plants in each Seismic Zone, for Low-Rise Buildings

Wood		Masonry				Concrete				Steel			
Wood Frame–Modern	Heavy Timber	Unreinforced Masonry–Load-Bearing Wall	Unreinforced Masonry–Load-Bearing Frame	Reinforced Masonry	Reinforced Masonry–Shear Wall with MRF	Reinforced Concrete–Shear wall with MRF	Reinforced Concrete MRF–Ductile	Tilt-up	Poured Concrete	Light Metal	Braced Steel Frame	MRF–Perimeter	MRF – Distributed
California													
34.0%	3.2%	1.3%	0.0%	10.3%	2.1%	10.7%	0.2%	0.5%	3.0%	6.2%	18.4%	5.8%	4.2%
Washington and Oregon													
41.9%	2.2%	1.3%	0.0%	6.5%	1.2%	8.7%	0.7%	1.4%	2.5%	4.3%	16.4%	9.5%	3.5%
All Other States													
27.6%	5.5%	12.2%	0.8%	1.7%	2.4%	1.0%	0.9%	2.9%	2.0%	19.0%	5.7%	7.7%	10.6%

Figure 122 shows the damage functions for the different building construction classes specified in Table 2 that are often found within industrial facilities in California. Since different types of industrial facilities (e.g., chemical plants versus manufacturing plants) have a different mix of building types, the overall damage functions for buildings vary depending on the type of industrial facility. Figure 123 shows the derived building damage functions for various industrial facility types in California.

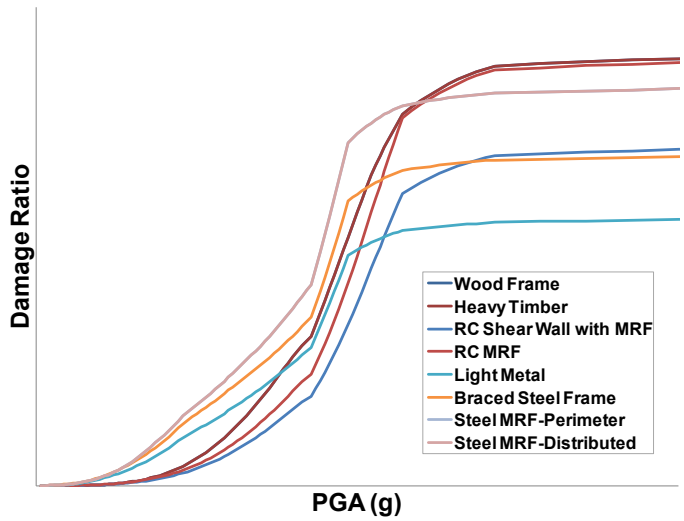

Figure 122. Building Damage Functions in California

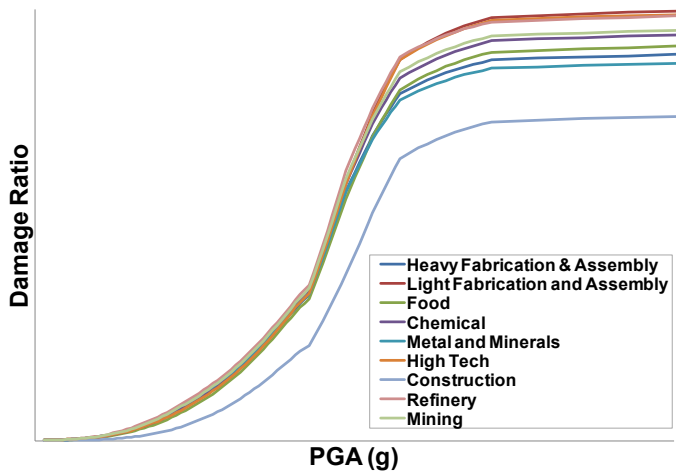

Figure 123. Building Damage Functions for Various Industrial Facilities in California

Damage Functions for Components Derived from Observational Data

For tanks, dams, tunnels, and several other components, damage data are available from historical records and publications. For these components, damage functions have been derived using a combination of observational data from historical earthquakes and engineering studies.

The following figures show damage functions for tanks from published literature. Figure 124 uses the generic tank type (e.g., the average functions of unanchored and anchored, fill-level, etc.). Figure 125 shows on-grade tanks, and tanks with specific anchorage type and fill-level. The final damage function is the average of these damage functions.

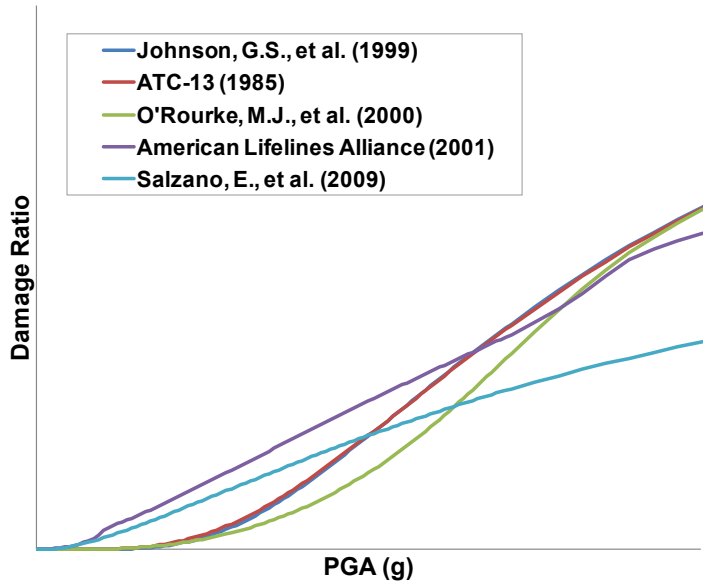

Figure 124. Damage Functions for Tanks Based on Technical Literature and Reviews, Average Damage from Each Source

Figure 125 shows damage functions for tanks with different filling ratios and anchoring conditions, derived from observational data. The moving average of all data, shown with the dotted black line, is seen to cross the middle of these functions. The damage functions in Figure 124 and Figure 125 are combined to obtain the damage functions for tanks with different characteristics.

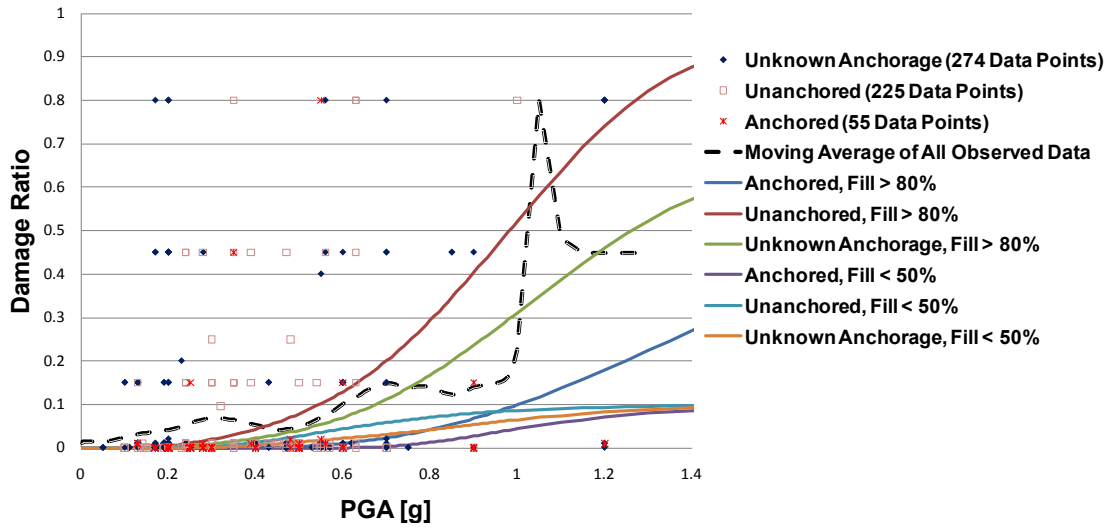

Figure 125. Damage Functions for On-Grade Tanks Based on Observed Damage Data

The data in Figure 125 is observational data collected from 19 historical earthquakes, which are listed in Table 17.

Table 17. Historical Earthquakes Used for Tank Damage Data

Earthquake	Year
Long Beach, CA	1933
Kern County, CA	1952
Alaska	1964
San Fernando, CA	1971
Imperial Valley, CA	1979
Coalinga, CA	1983
Morgan Hill, CA	1984
Loma Prieta, CA	1989
Costa Rica	1992
Landers, CA	1992

Earthquake	Year
Northridge, CA	1994
Kobe, Japan	1995
Chichi (Jiji), Taiwan	1999
Izmit, Turkey	1999
Athens, Greece	1999
Nisqually, WA	2001
Southern Peru	2001
Bam, Iran	2003
San Simeon, CA	2003

Component Damage Functions Derived from Nonlinear Structural Analysis

For many industrial components (e.g., chimneys, cooling towers, flare towers, open-frame structures, pipes, pipe racks, process towers, and silos), there is insufficient damage data or studies in the literature to derive damage functions accurately. In these cases, AIR used engineering analyses—primarily nonlinear static pushover analyses (see Section 5.5 for more detail). Most industrial components are simple structures and vibrate in essentially one mode, which makes static pushover analysis appropriate. All analyses were carried out in accordance with state-of-the-art, performance-based provisions, taking into account the complexity of each component and its characteristic response to shaking.

Structural models were subjected to a progressively increasing lateral force (corresponding to increasing levels of ground motion) to evaluate the trigger of key limit states, ranging from the onset of inelastic response to complete structural collapse. The response of each structure was quantified in terms of a functional relationship between the ground motion intensity (PGA) and the key limit states of the structure (e.g., first yield, buckling, ultimate strength of anchor bolts, instability, etc.). The damage ratio associated with each limit state was derived in accordance with ATC-13 guidelines.

Figure 126 shows pushover analysis results for an open-frame plant structure being displaced in two orthogonal directions. As the figure indicates, under the action of transverse lateral loads, the first limit state is the buckling of a knee

brace (shown by the red dot in the left figure in the top panel), and is associated with a sharp drop in the lateral strength. As the lateral load increases, an additional brace buckles resulting in another drop in the lateral strength.

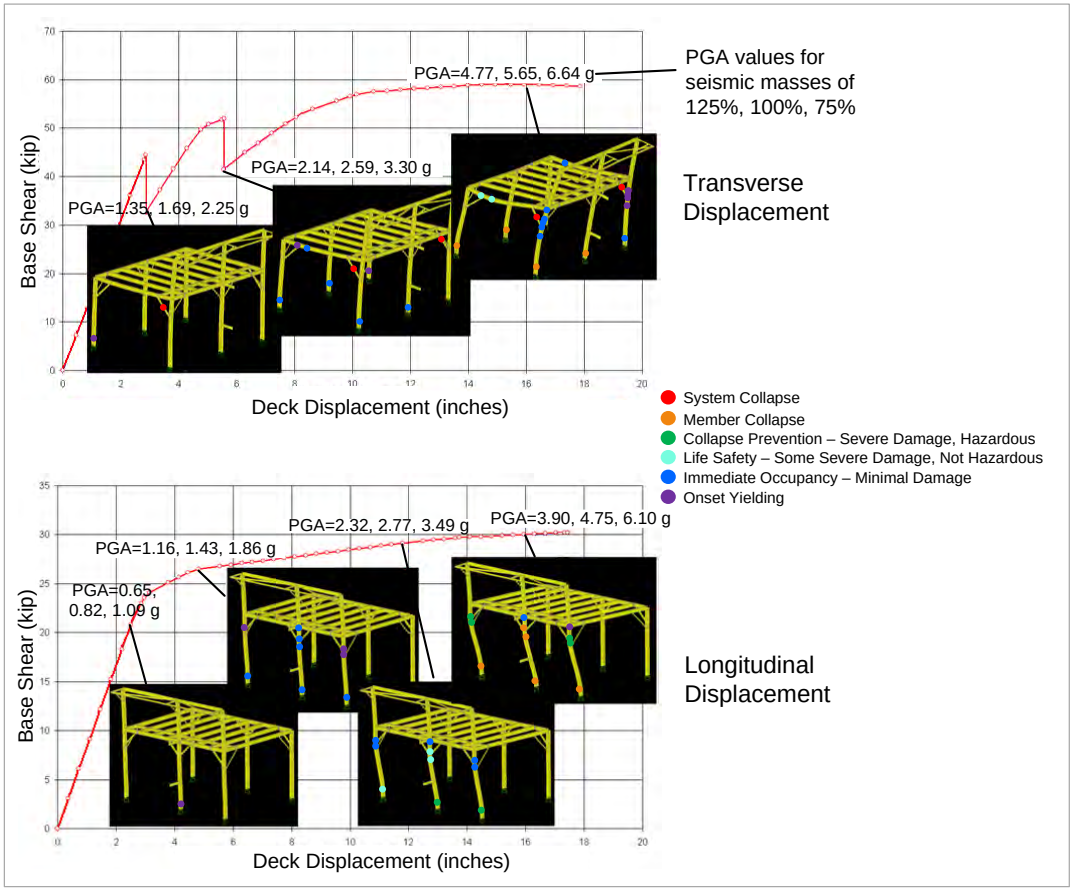

Figure 126. Pushover Analysis Results for an Open-Frame Structure showing PGA Values at Several Limit States

Additional stress in the legs and braces results in more deformation and eventual collapse. With increasing lateral loads in the longitudinal direction, the first plastic hinge forms at the base of a leg, followed by more plastic hinges at the leg bases and braces.

Each engineering analysis takes into account three different loading conditions: light, moderate, and heavy. This is done to take into account the variability in the live load, which affects the performance of structures in earthquakes. The transverse displacement has three limit states while the longitudinal displacement shows four limit states. These correspond to live loads (seismic loads) equal to 75%, 100%, and 125%, respectively, of the dead load of the structure itself. The dead load includes the self-weight of the structure and appurtenances, plus any equipment that it supports. The three PGA values close to each illustration

represent the average ground motion level that brings that structure to the specified level of deformation, for each of the three loading conditions.

With a lighter load, a higher level of PGA is needed to bring the structure to the onset of a specific limit state. For example, at the first longitudinal displacement, a PGA value of 0.65 g is needed to bring this open frame structure with heavy load conditions (i.e., live loads equal to 125% of dead load) to the onset of minor damage. However with moderate loading on the same structure, a higher PGA (0.82 g) is needed, on average, to reach the same level of damage.

The following two figures show damage functions for open-frame structures with different load conditions derived from pushover analysis. Figure 127 shows the damage functions for an open-frame steel plant structure. Figure 128 shows the damage functions for an open-frame steel dock, which has a narrow frame supporting pipes and equipment.

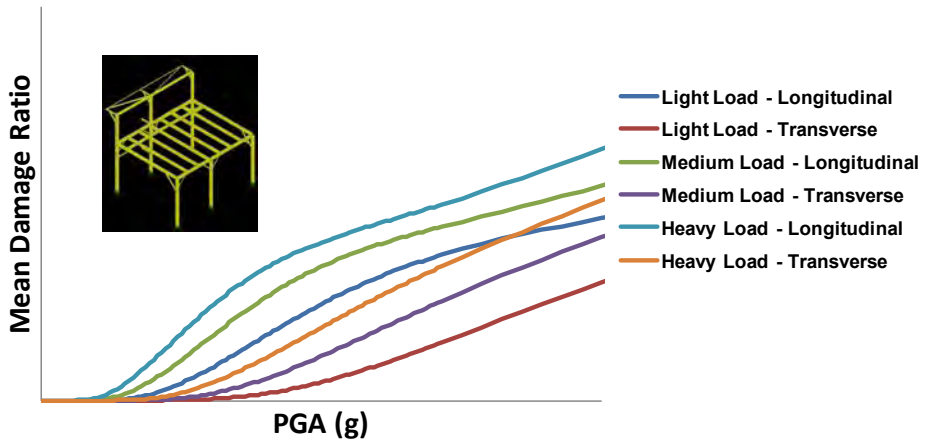

Figure 127. Damage Functions for an Open-Frame Steel Plant Structure

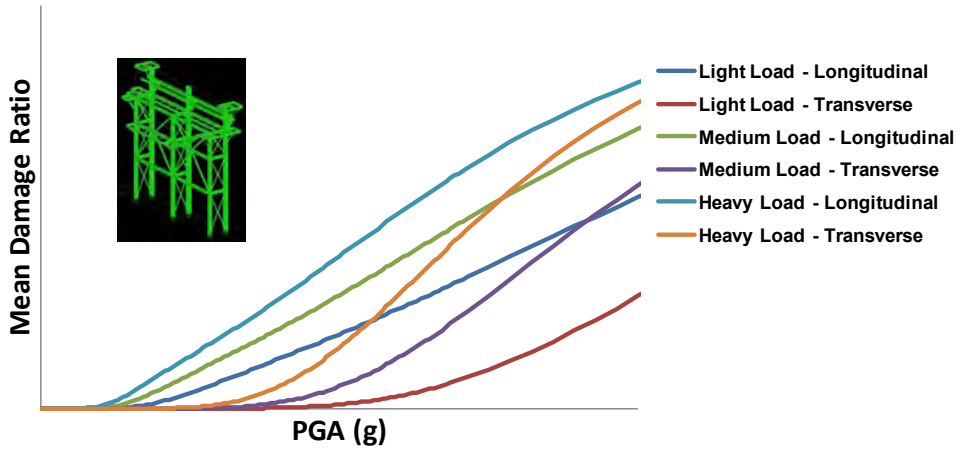

Figure 128. Damage Functions for an Open-Frame Steel Dock Structure

Developing Damage Functions for an Entire Industrial Facility

To develop damage functions at the facility level, AIR adopted an approach similar to that used to develop damage functions for buildings within an industrial facility. For each type of industrial facility, the aggregated damage functions were developed based on the damage functions for the component classes (e.g., tanks) and subcomponent classes (e.g., fully anchored tanks). The damage functions for each component and subcomponent were assigned a weight equal to the ratio between the replacement value of the class to the replacement value of the industrial facility.

The weights for different industrial facilities was derived from three major sources: studies performed by AIR for private industrial corporations (e.g., petrochemical and chemical facilities); ATC-13 1995 (for industrial classes such as heavy and light fabrication and assembly, food and drug, chemicals, metals, high technology, construction, and mining); and HAZUS (hydro- and thermo-power systems, potable and waste water, and gas processing plants). Each source provided, for each seismic region, a distribution of components for each type of facility.

Based on consulting studies, AIR made some reasonable assumptions about the typical characteristics and weight of individual sub-components in an industrial facility to develop the damage functions for different components. For example, AIR assumed different percentages of anchored and unanchored tanks; and tanks with different filling levels and aspect ratios within a facility.

Figure 129 and Figure 130 show damage functions for an oil refinery in California with anchored and unanchored components. The figures show the weighting factors for each component and subcomponent class, which are based on data from oil refineries. For both cases, the facility-level damage function, shown with the thick red line, is a weighted average of the damage functions of individual components.

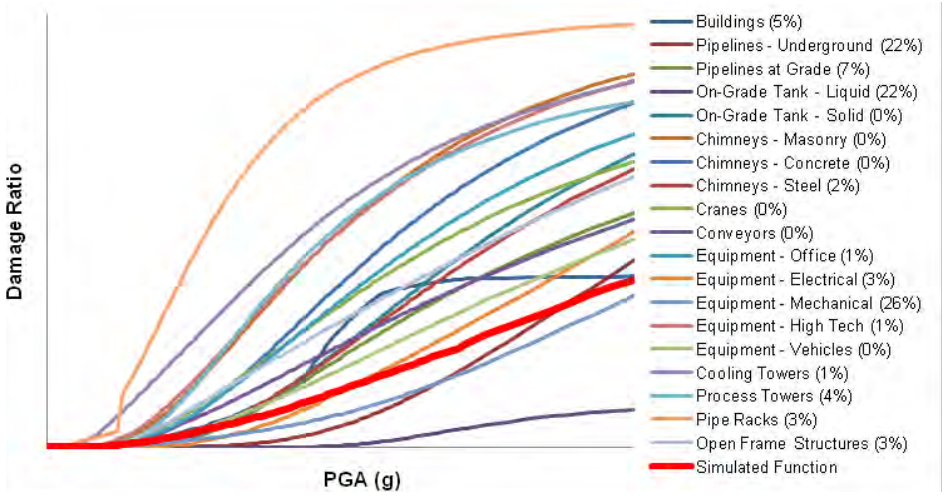

Figure 129. Damage Functions for an "Anchored" Oil Refinery in California

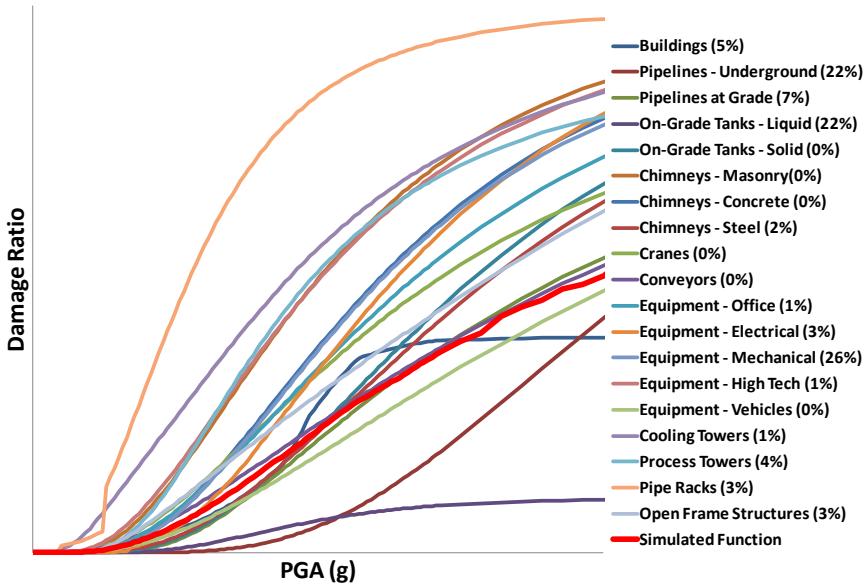

Figure 130. Damage Functions for Unanchored Oil Refinery in California

Customized Composite Damage Functions for a Particular Industrial Facility

As shown above, a plant-level damage function, such as one developed for an oil refinery, uses generalized information for each type of industrial facility (for the 400-level series). For example, the damage functions assume standardized equipment based on that which is commonly found in an industrial plant. Based on this information, estimations are made concerning the replacement values of

those components, and their secondary characteristics (e.g., anchorage type, fill-level of tanks, construction type, etc.).

However the components in each facility vary widely, making each facility unique and sometimes too complex to be accurately captured within a generalized damage function. For example, only a fraction of the components may be anchored, and that fraction varies between facilities. Similarly, the percentage of a particular component can vary widely, creating a wide discrepancy in the replacement value.

To allow for wide variances between industrial facilities, AIR provides flexibility to CLASIC/2 users when applying industrial facility damage functions. Users can customize individual components to change their anchorage, enter their percentage, and make other customizations as needed. Clients can also select any combination of components and sub-components, and enter the relative weights for each. The model will generate customized composite damage functions on the fly using the client's input to match any particular industrial facility.

Developing Damage Functions for Different Regions of the United States and for Unknown Facility Types

To develop damage functions for industrial facilities across the country, AIR engineers studied the differences in the design base shear of components for each of the three major seismic areas: California, Washington and Oregon, and all other states. The values of PGA that induce, on average, the onset of a limit state on the same type of structure (e.g., an open frame structure) in different regions were evaluated by considering the different design base shears.

For unknown facility types, the damage functions for different regions are obtained by performing the same weighted averaging of the damage functions for different industrial facility types in each area. Figure 131 shows the weights used for each type of industrial facility, for each of the three main seismic regions of the United States.

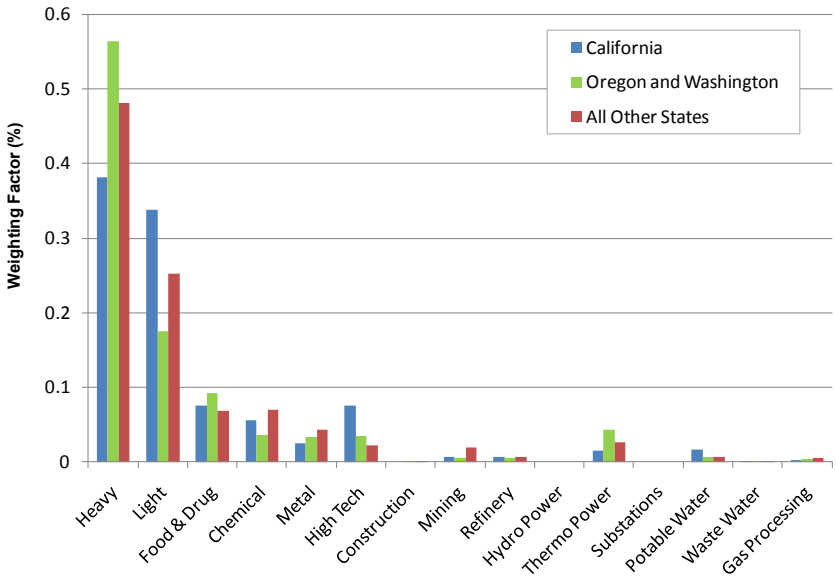

Figure 131. Distribution of Industrial Facility Types for each Seismic Area of the United States

Figure 132, Figure 133, and Figure 134 show the relativity of damage functions for each industrial facility type along with the damage function for an Unknown type of industrial facility, for each of the three seismic areas of the United States. In all three regions, the Unknown facility type (represented by the thick red line) represents a weighted average of the damage functions for the different known industrial facility types.

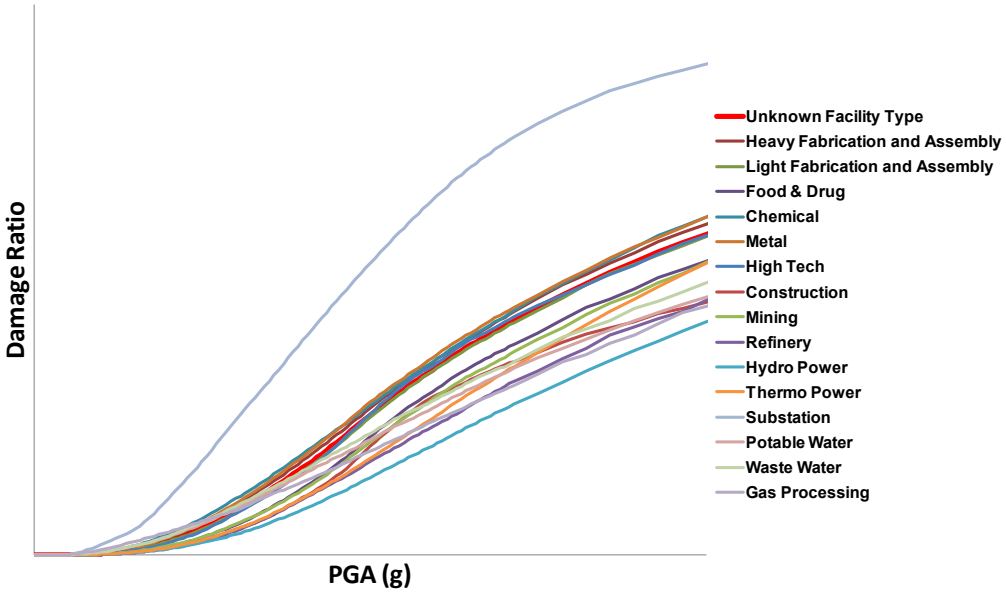

Figure 132. Damage Functions for Industrial Facilities in California

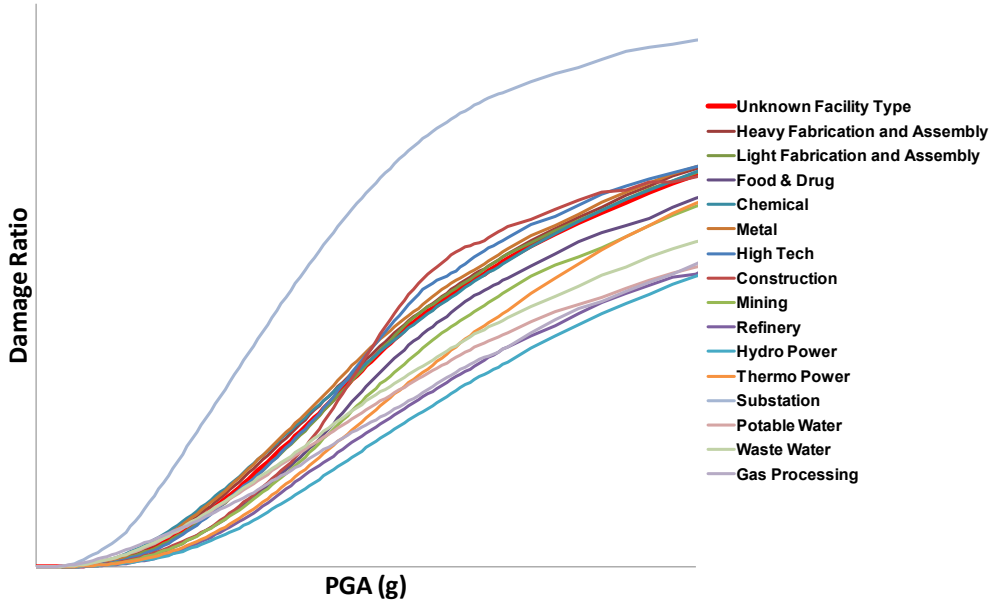

Figure 133. Damage Functions for Industrial Facilities in Oregon and Washington

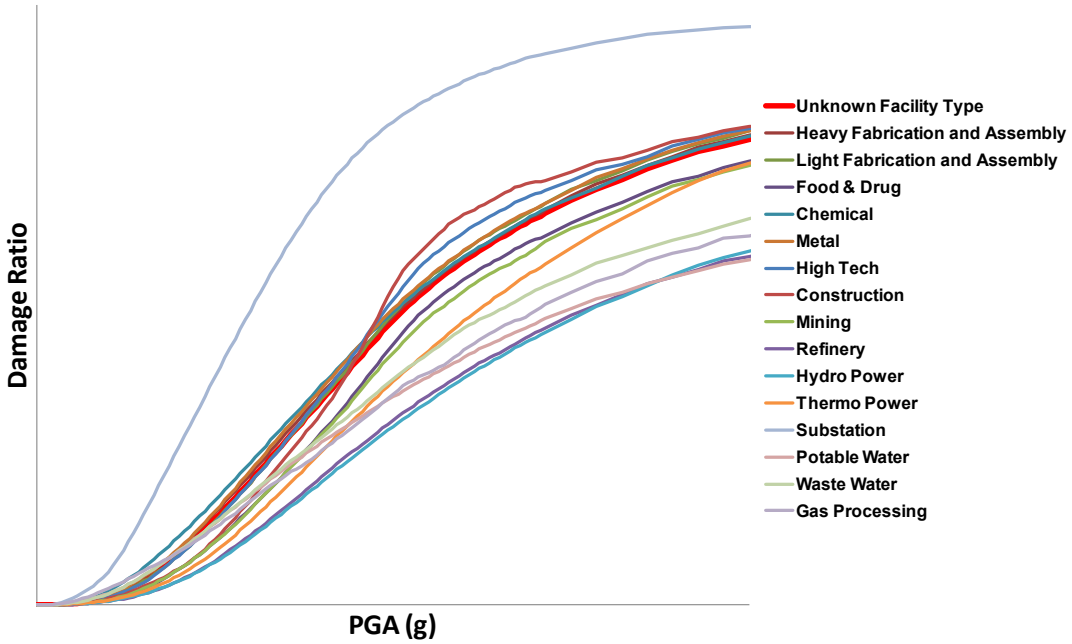

Figure 134. Damage Functions for Industrial Facilities for All States Outside of California, Oregon, and Washington

6.1 Assessment of Business Interruption Losses for Industrial Facilities

Assessing business interruption (BI) loss for industrial facilities is an extremely complex task, particularly in the case of highly integrated facilities with multiple process chains, bottlenecks, and redundancies. The major contribution to BI losses is the loss of revenues incurred when product chains are not functional (either partially or completely). Loss of functionality can occur as a result of physical damage to components and lifelines, such as electricity, water, steam systems, and others.

AIR's approach for the assessment of BI losses for these complex risks is the same as that used for other business lines. Because industrial facilities generally consist of a large number of components, AIR again uses a component-based approach. To assess the possible downtime of an entire industrial facility, AIR starts by determining time element damage functions for each component.

For each component, the time needed for repair or replacement, if necessary, is estimated. As in any other business interruption assessment, the time before repairs can get underway (pre-repair) is determined and added to the time needed for the actual repair. The information on the pre-repair and actual repair time for different components is based both on historical data and on the experience gained by AIR's engineers by consulting with the operators and managers of industrial facilities. In addition, the model takes into account components that are still operable or even undamaged, and therefore have no downtime at all. Once the time element functions are determined for all the components, the model aggregates the functions by determining a weighted average of the component functions—a process similar to that adopted for developing facility level property damage functions.

Figure 135 illustrates downtime functions for industrial facility components of unknown subclass (e.g., type of anchorage, level of liquid fill, type of material, etc.) in California.

.

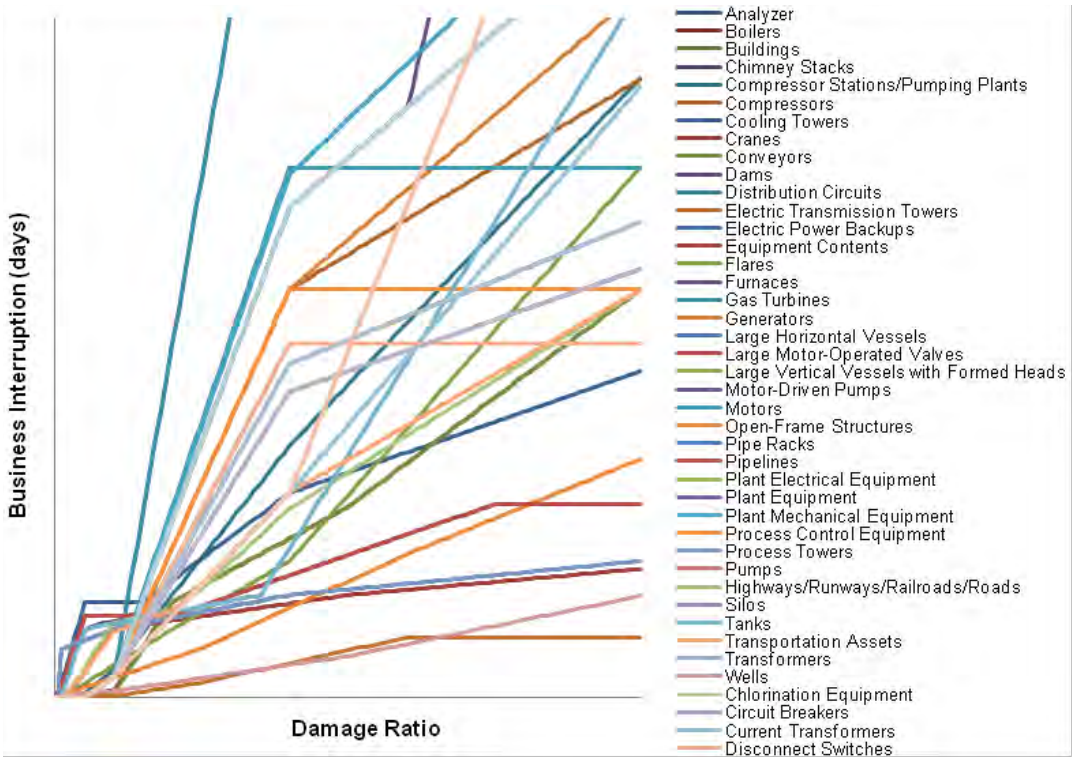

Figure 135. Time Element Functions for Industrial Facility Components

As described above, the business interruption (BI) functions at the facility level are the weighted average downtime functions of the individual component and sub-component class. Figure 136 shows the BI functions for facilities in California. The BI function for the Unknown industrial facility type, represented by the thick red line, is an industry-exposure weighted average of those of all facilities.

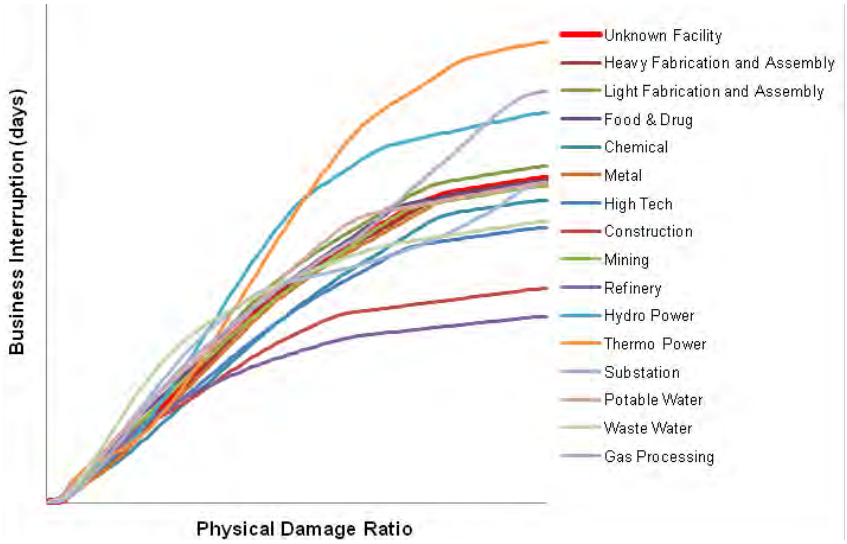

Figure 136. Time Element Functions for Industrial Facilities in California

6.2 Validating Damage Functions for Industrial Facilities

To validate the damage functions (at both the component and facility level), observational damage data to industrial facilities was collected from damage reconnaissance reports after historical earthquakes.

Table 19Table 18 lists 40 historical earthquakes from which damage data was collected for validating the damage functions for industrial facilities.

Table 18. Historical Earthquakes used for Facility and Component Damage Function Validation

Earthquake	Year	Earthquake	Year
Gediz, Turkey	1970	Dinar, Turkey	1995
San Fernando, California	1971	(Hyogo-Ken Nanbu) Kobe, Japan	1995
Imperial Valley, California	1979	Lijiang, Yunnan Province, China	1996
Borah Peak, Idaho	1983	Adana-Cayhan, Turkey	1998
Coalinga, California	1983	El Quindio, Colombia	1999
Morgan Hill, California	1984	Chichi (Jiji), Taiwan	1999
Chile	1985	Kocaeli, Turkey	1999
Michoacan, Mexico	1985	Duzce, Turkey	1999
San Salvador, El Salvador	1986	Nisqually, Washington	2001
Palm Springs, California	1987	Bhuj, India	2001
Whittier Narrows, California	1987	Southern Peru	2001
Tejon Ranch, California	1988	Molise, Italy	2002
Armenia	1988	Denali, Alaska	2002
Loma Prieta, CA	1989	Boumerdes, Algeria	2003
Philippines	1990	San Simeon, CA	2003
Costa Rica	1991	Bam, Iran	2003
Erzincan, Turkey	1992	Tecoman, Mexico	2003
Hokkaido-Nansei-Oki, Japan	1993	Nigata Ken Chuetsu, Japan	2004
Guam	1993	Sumatra, Indonesia	2004
Northridge, CA	1994	Hawaii	2006

Some types of industrial facilities and components, whose damage functions have been validated using damage data from historical earthquakes, are listed in Table 19.

Table 19. Some Facilities and Components Validated with Damage Data from Historical Earthquakes

Facility	Earthquake	Year
Chemical Plants	Borah Peak, ID	1983
	Coalinga, CA	1983
	Morgan Hill, CA	1984
	Chile	1985
	Hokkaido Nansei-Oki, Japan	1993
	Izmit, Turkey	1999
	Athens, Greece	1999
	Bam, Iran	2003
Thermo-Power Plants	San Fernando, CA	1971
	Imperial Valley, CA	1979
	Chile	1985
	Loma Prieta, CA	1989
	Northridge, CA	1994
	Kobe, Japan	1995
	Chichi (Jiji), Taiwan	1999
	Izmit, Turkey	1999
	Athens, Greece	1999
	Southern Peru	2001
	San Simeon, CA	2003
	Sumatra, Indonesia	2005
	Hawaii	2006
Metal Processing Plants	Chile	1985
	Kobe, Japan	1995
	Izmit, Turkey	1999
	San Simeon, CA	2003
Potable Water Systems	Imperial Valley, CA	1979
	Coalinga, CA	1983
	Northridge, CA	1994
	Kobe, Japan	1995
	Central Colombia	1999
	Chichi (Jiji), Taiwan	1999
	Nisqually, WA	2001
	Southern Peru	2001
	Bam, Iran	2003
	San Simeon, CA	2003

Pipes	Imperial Valley, CA	1979
	Coalinga, CA	1983
	Morgan Hill, CA	1984
	Chile	1985
	Loma Prieta	1989
Poles	San Fernando, CA	1971
	Imperial Valley, CA	1979
	Whittier Narrows, CA	1987
	Northridge, CA	1994
	Kobe, Japan	1995
	Chichi (Jiji), Taiwan	1999
Pipe Racks	Loma Prieta, CA	1989

Figure 137, Figure 138 and Figure 139 show facility-level damage functions plotted against observational data from some historical earthquakes.

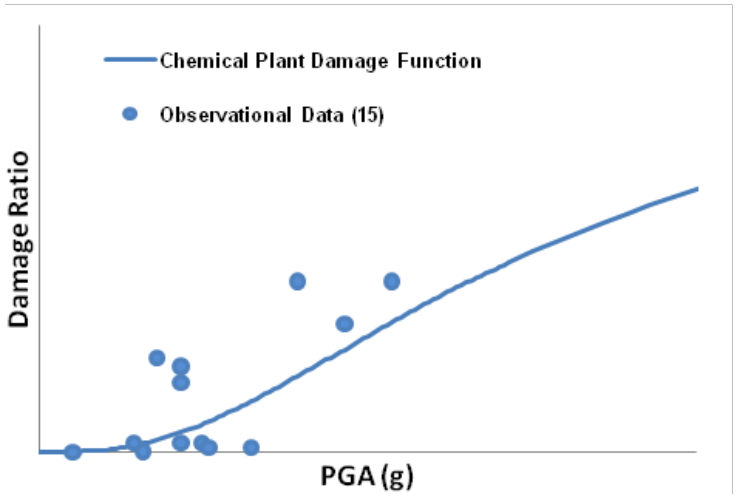

Figure 137. Damage Functions and Observed Damage Data for Chemical Processing Plants in a High Seismicity Area

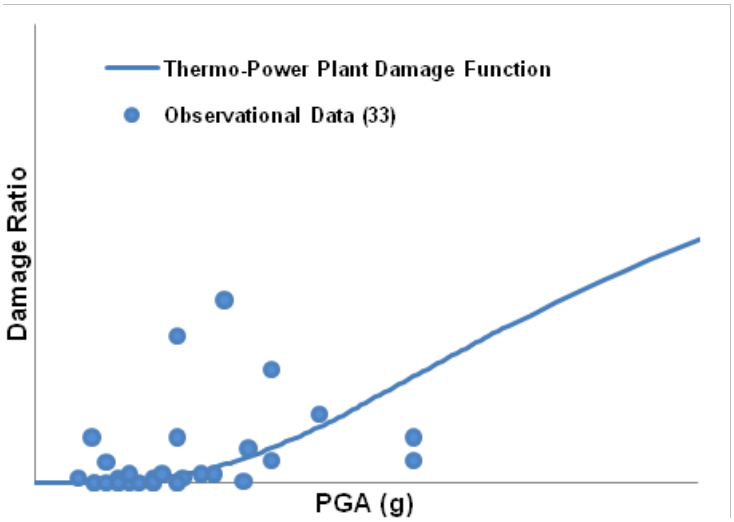

Figure 138. Damage Functions and Observed Damage Data for a Thermo-Power Plant in a High Seismicity Area

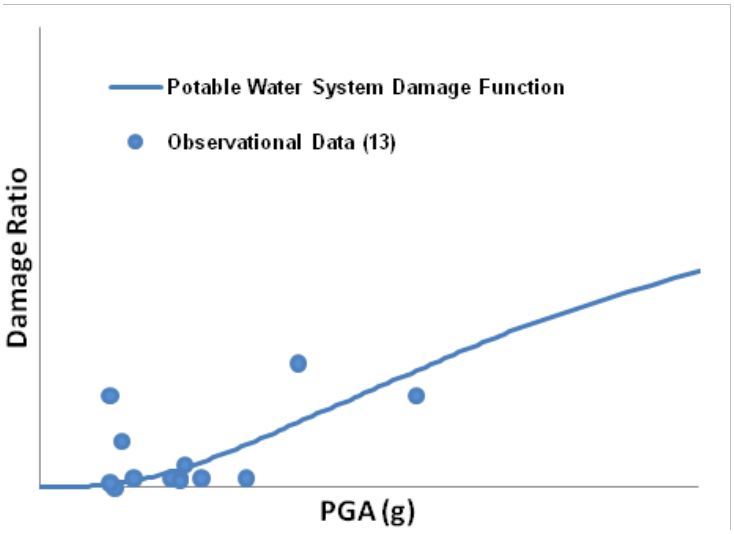

Figure 139. Damage Functions and Observed Damage Data for Potable Water Systems in a High Seismicity Area

7 Insured Loss Calculation

The AIR Earthquake Model for the United States uses a comprehensive cost model to estimate the repair cost of each damaged component in order to translate ground-up damage into monetary losses. Insured losses are calculated by applying policy conditions to the total damage estimates resulting from the damage estimate module. A wide variety of policy conditions are supported in this model, including franchise deductibles, coverage limits, loss triggers and risk-specific reinsurance terms.

7.1 Aggregating Losses Probabilistically

Post-disaster surveys and actual claims data reveal an inherent variability in damage to buildings caused by ground motion. The loss estimates that are generated by the AIR Earthquake Model for the United States capture this variability by accounting for both primary and secondary uncertainty. Primary uncertainty is associated with the randomness in the location and size of future events, which is captured in the stochastic catalog event-generation process. Secondary uncertainty is the uncertainty in the damage of a building resulting from a given earthquake; it includes both the uncertainty in the damage given a level of ground motion at the site and the uncertainty in the actual ground motion experienced at the site. The uncertainty in building damage for a given level of ground motion is due to the variability of the response of buildings of similar construction to a given intensity, and is controlled by the variability in the characteristics, construction materials, workmanship, etc. of buildings of the same construction class. The uncertainty in ground motion generated at a given site by an earthquake of given characteristics, which is included in ground-motion prediction equations with an intra-event variability term, has been considered explicitly in the model.

As was discussed in Section 5, losses are calculated by damage functions that provide, for a given mean ground-motion level, a mean damage ratio (MDR) and a measure of the variability of the damage around the mean which is modeled via a probability distribution. As discussed before, the AIR Earthquake Model for the United States uses integrated damage functions in order to take into account variations in the MDR due to the intra-event variability in ground-motion intensity. The inter-event variability of the ground motion intensity at a site generated by different events with similar parameters (e.g., magnitude) has also been considered. The uncertainty around the mean damage for a given intensity level is modeled as a mixed probability distribution. The damage ratios between

0% and 100% are modeled as a continuous random variable that follows a beta distribution while the important cases of exactly zero damage and complete collapse are modeled with a discrete random variable with finite probability masses at 0% and 100% damage ratios.

The damage functions are used to produce, for each event, a distribution of ground-up loss by location and coverage. Limits, deductibles and reinsurance are applied in the financial module to the ground-up loss distribution to produce gross and net loss estimates. Note that insured losses can accumulate even if the *mean* damage ratio is below the deductible, because some structures are damaged above the mean and the deductible. The distributions are applicable to the analysis of a single exposure and usually have a high degree of uncertainty. The individual distributions are combined to obtain the portfolio distribution, where the uncertainty is lower.

In the financial module, there is clearly a need to aggregate losses probabilistically, at various levels. Specifically, computational techniques are developed for statistically aggregating nonparametric distributions. Even though the ground-up, coverage-level damage distributions typically use parametric distributions, once location and policy terms are applied the distributions cannot be represented parametrically. Further aggregation of such loss distributions are achieved using numerical algorithms.

AIR's software applications include a financial module that allows a wide variety of location, policy, and reinsurance conditions to be applied to a calculation. Location terms may be specified to include limits and deductibles by site or by coverage. Supported policy terms include blanket and excess layers, minimum and maximum deductibles, and sublimits.

Reinsurance terms include facultative certificates and various types of risk-specific and aggregate treaties with occurrence and aggregate limits. Please see product specific documentation available from the client support section of AIR's website (www.air-worldwide.com) as well as details on the industry standard UNICEDE data format (www.unicede.com) for additional information.

7.2 Validating Modeled Losses

The AIR Earthquake Model for the United States has been calibrated for physical damage and monetary losses using USGS ShakeMap, building performance data, post-event damage observation data, and detailed claims data from several insurance companies. Modeled losses have also been validated using the ground-up loss data from events dating as far back as 1900, as reported by several research papers and insurance industry organizations.

Figure 140 compares AIR modeled losses to reported losses for three historical events. It should be noted that for the 1906 San Francisco earthquake, actual loss data is not available. However, even if it were available, it would have little meaning today. The estimated figure (with uncertainty, as depicted by the vertical line) shown in Figure 140 represents published estimates from a variety of researchers.

Note, too, that the estimates and comparisons in Figure 140 are based on ground-up damage on an industrywide portfolio and they have all been normalized to 2008 values. The deductibles and policy conditions for earthquakes have changed over time, as have the take-up rates. Therefore, performing such a comparison on an insured or an industry insurable basis is very challenging.

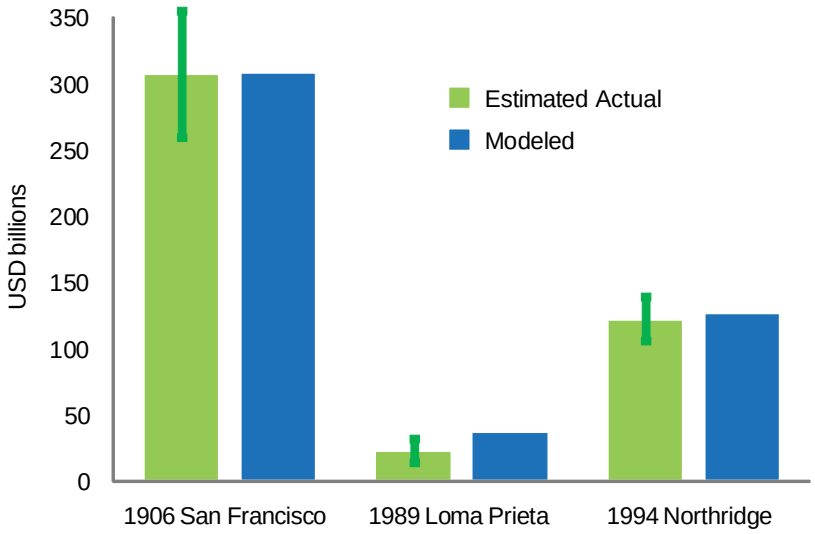

Figure 140. Comparison between Actual and Modeled Losses for Key Historical Events (variation in published reported losses is represented by an error bar)

Figure 141 shows a similar set of exhibits for less severe events. It is important that the model perform well not only for medium-to-high severity events, but also for low-severity events, which have a significant impact on the high-frequency portion of the exceedance probability curve and on average annual losses. Note again that there is considerable uncertainty in the reported losses for the older events.

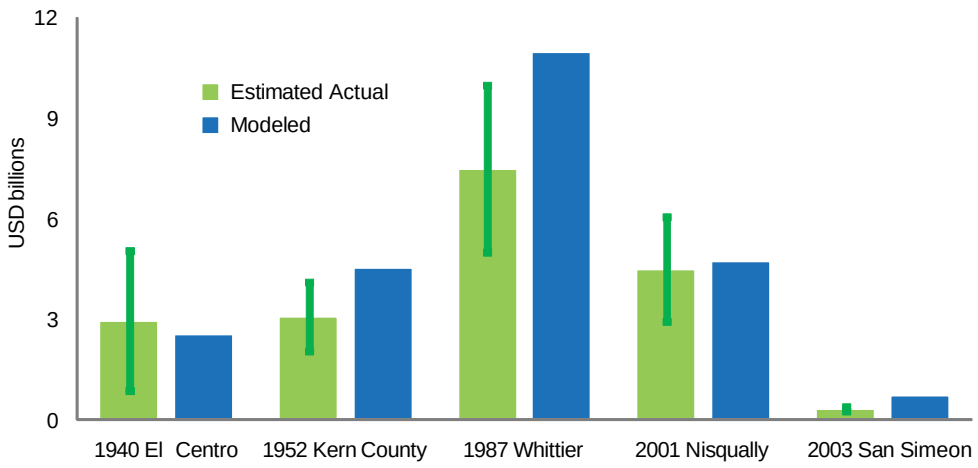

Figure 141. Comparison between Actual and Modeled Losses for Less Severe Historical Events (variation in published reported losses is represented by an error bar)

Validating the Distribution of Losses by Coverage

For the Northridge earthquake, we can show the relative distribution of losses between Building, Contents, and Business Interruption. Figure 142 compares the modeled loss distribution to reported loss data from the Institute for Building and Home Safety (1998). As can be seen in the figure, the two distributions compare favorably.

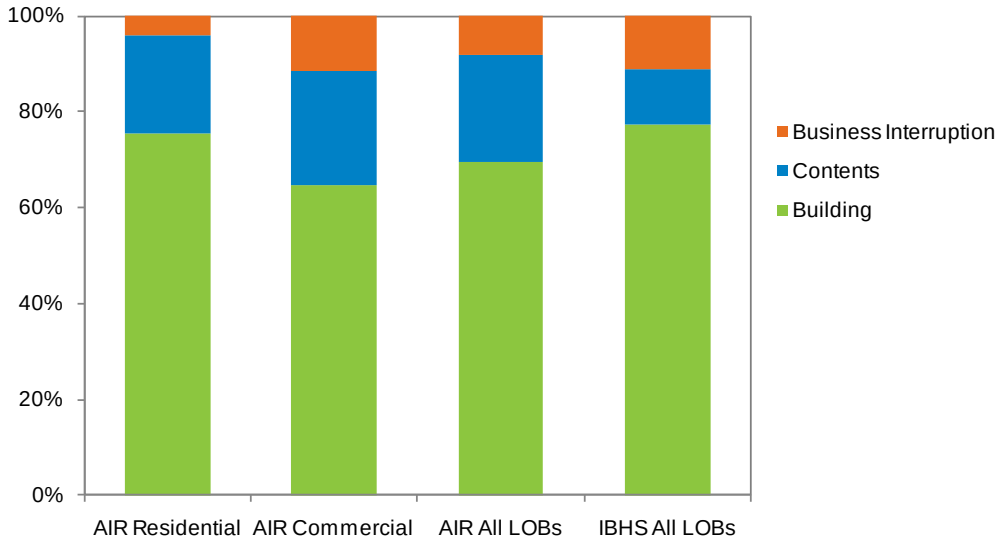

Figure 142. Relative Distribution of Modeled vs. Reported Insurable Losses, 1994 Northridge Earthquake

8 Selected References

Abrahamson, N. A., and W. J. Silva 2008, "Summary of the Abrahamson & Silva NGA Ground Motion Relations," *Earthquake Spectra,* 24, 67–97.

Al-Faris, K., and B. Tan 1996, "Northridge Earthquake Insurance Loss Report," State of California Department of Insurance, August 1, 1996.

American Lifelines Alliance 2001, "Seismic Fragility Formulations for Water Systems, Part 1: Guideline," a report written under contract by the American Lifelines Alliance, a partnership between the Federal Emergency Management Agency and the American Society of Civil Engineers. Available at: http://www.americanlifelinesalliance.org/pdf/Part_1_Guideline.pdf

Applied Technology Council 1985, "Earthquake Damage Evaluation Data for California," Report 13, funded by Federal Emergency Management Agency.

Armbruster, J., and L. Seeber 1992, "Earthquake Catalog for the Eastern U. S.," National Center for Earthquake Engineering Research (NCEER- 91) Lamont-Doherty Geological Observatory of Columbia University, Palisades, New York.

Aroni, S., and M. Durkin 1985, "Injuries and Occupant Behavior in Earthquakes," Proceedings of the Joint U.S.-Romanian Seminar on Earthquakes and Energy, Bucharest, Romania, September 2–9, 1985.

ATC-13 "Earthquake Damage Evaluation Data for California," 1985.

Atkinson, G. M., and D. M. Boore 2006, "Earthquake Ground Motion Prediction Equations for Eastern North America," *Bulletin of the Seismological Society of America,* 96, 2181–2205.

Atkinson, G. M., and D. M. Boore 2003, "Empirical Ground Motion Relations for Subduction-Zone Earthquakes and their Application to Cascadia and Other Regions," *Bulletin of Seismological Society of America,* 93, 1703–1729.

AXCO Insurance Information Services, Global Statistics. Available at: http://www.axcoinfo.com/statsmain.html

Bauer, R. A., W. Su, R. C. Counts, M. D. Karaffa 2007. "Shear Wave Velocity, Geology and Geotechnical Data of Earth Materials in the Central U.S. Urban Hazard Mapping Areas," Final Technical Report, USGS External Research Grant (Award No. 06-HQ-GR-0192)

Bazzurro, P., J. Park, P. Tothong, and N. Jayaram 2008, "Effects of Spatial Correlation of Ground Motion Parameters for Multi-Site Seismic Risk

Assessment," Collaborative Research with J. Baker of Stanford University and AIR Worldwide Report December, 2008. Available at: http://earthquake.usgs.gov/research/external/reports/07HQGR0032.pdf.

Beeson, M. H. et al. 1991. "Geologic Map of the Portland Quadrangle, Multnomah and Washington Counties," Oregon Geological Survey.

Boore, D. M., and G. M. Atkinson 2008, "Ground-Motion Prediction Equations for the Average Horizontal Component of PGA, PGV, and 5%-damped PSA at Spectral Periods between 0.01 s and 10.0 s," *Earthquake Spectra,* 24, 99–138.

Borcherdt, R. D., 1994, "Estimates of Site-Dependent Response Spectra for Design (Methodology and Justification),"*Earthquake Spectra,* 10, 617–653.

Bryant, B. 1990. "Geological Map of the Salt Lake City 30′ x 60′ Quadrangle, North-Central Utah, and Unita County, Wyoming, scale 1:100,000," Utah Geological Survey.

California Department of Insurance, Earthquake Insurance Coverage Study. Available at: http://www.insurance.ca.gov/0400-news/0200-studies-reports/0300-earthquake-study/index.cfm

California Geological Survey, Geological Maps 1950–1990, Available at: http://www.conservation.ca.gov/cgs/rghm/rgm/250k_index/Pages/250k_index.aspx

Campbell, K. W., and Y. Bozorgnia 2003, "Updated Near-Source Ground-Motion (Attenuation) Relations for the Horizontal and Vertical Components of Peak Ground Acceleration and Acceleration Response Spectra," *Bulletin of the Seismological Society of America,* 93, 314–331.

Campbell, K. W. , 2003, "Prediction of Strong Ground Motion using the Hybrid Empirical Method and its use in the Development of Ground-Motion (Attenuation) Relations in Eastern North America," *Bulletin of the Seismological Society of America,* 93, 1012–1033.

Campbell K. W., and Y. Bozorgnia 2008, "NGA Ground Motion Model for the Geometric Mean Horizontal Component of PGA, PGV, PGD and 5% Damped Linear Elastic Response Spectra for Periods Ranging from 0.01 to 10s," *Earthquake Spectra,* 24, 139–171.

The Catastrophe Bulletin, a monthly release by Insurance Services Office, Property Claims Services.

Celik, O. C., and B. R. Ellingwood 2008. "Modeling Beam-Column Joints in Fragility Assessment of Gravity Load Designed Reinforced Concrete Frames," *Journal of Earthquake Engineering,* 12.

Central United States Earthquake Consortium (CUSEC) State Geologists, Geological Maps 2007. Available at: http://www.isgs.illinois.edu/research/earthquake-hazards/cusec/emaps.shtml

Chen, W. F., and C. Scawthorn 2003, *Earthquake Engineering Handbook.* Boca Raton, Florida: CRC Press LLC.

Chiou, B. S. J., and R. R. Youngs 2008, "Chiou-Youngs NGA Ground Motion Relations for the Geometric Mean Horizontal Component of Peak and Spectral Ground Motion Parameters," *Earthquake Spectra,* 24, 173–215.

Choi, Y., J. P. Stewart and R. W. Graves 2005, "Empirical Model for Basin Effects that Accounts for Basin Depth and Source Location," *Bulletin of the Seismological Society of America,* 95, 1412–1427.

Comerio, M. and V. Bertero, "Economic Benefits of a Disaster-Resistant University"; Earthquake Loss Estimation for University of California Berkeley; April 12, 2000.

Connecticut Geological and Natural History Survey 2000, Geological Map 1998. Available at: http://www.ct.gov/dep/cwp/view.asp?a=2698&q=323114

Cutter, S. L., and C. Emrich 2005, "Are Natural Hazards and Disaster Losses in the U.S. Increasing?," *Transactions of the American Geophysical Union,* 86, 381–396.

Day, S. M., J. Bielak, D. Dreger., R. Graves, S. Larsen, K. Olsen., A. Pitarka, and L. Ramirez-Guzman 2006, "Numerical Simulation of Basin Effects on Long-Period Ground Motion," Paper 1857, Proceedings of the Eighth National Conference on Earthquake Engineering, San Francsico, California, April 18–22, 2006.

Eguchi, R. T., J. D. Goltz, C. E. Taylor, S. E. Chang, P. J. Flores, L. A. Johnson, H. A. Seligson, and N. C. Blais 1998, "Direct Economic Losses in the Northridge Earthquake: A Three-Year Post-Event Perspective," *Earthquake Spectra,* 14, 245–264.

Ellingwood , B. R., O. C. Celik, and K. Kinali 2007. "Fragility assessment of building structural systems in Mid-America," *Earthquake Engineering and Structural Dynamics,* 36, 1935–1952.

Emergency Events Database (EMDAT). Available at: http://www.emdat.be/Database/DisasterList/list.php

Engdahl, E. R., and W. A. Rinehart 1991, "Seismicity Map of North America," in Slemmons, D. B., E. R. Engdahl, M. D. Zoback, and D. B. Blackwell 1991, *The Decade of North American Geology.* Boulder, Colorado: Geological Society of America, 1991.

Engdahl, E. R., and A. Villaseñor, "Global Seismicity: 1900–1999," in W. H. K. Lee, H. Kanamori, P. C. Jennings, and C. Kisslinger 2002, *International Handbook of Earthquake and Engineering Seismology*, St. Louis, Missouri: Academic Press.

Federal Emergency Management Association 1991, *HAZUS Technical Manual.* Atlanta, Georgia: Federal Emergency Management Association.

Felzer, K., and T. Cao, "Appendix H: WGCEP Historical California Earthquake Catalog," in Stein, R. (Working Group on California Earthquake Probabilities) 2007, *Earthquake Rate Model 2.2.* Menlo Park, California: United States Geological Survey. Available at: http://pubs.usgs.gov/of/2007/1437/h/of2007-1437h.pdf

Frankel, A., C. Mueller, T. Barnhard, D. Perkins, E. Leyendecker, N. Dickman, S. Hanson, and M. Hopper 1996, "National Seismic Hazard Maps, June 1996," United States Geological Survey Open-File Report 1996-532.

Fumal, T. E., 1978, "Correlations Between Seismic Wave Velocities and Physical Properties of Near-Surface Geologic Materials in the Southern San Francisco Bay Region, California," United States Geological Survey, Open-File Report 78-167.

Gardner, J. K., and L. Knopoff 1974, "Is the Sequence of Earthquakes in Southern California, with Aftershocks Removed, Poissonian?," *Bulletin of the Seismological Society of America,* 64, 1363–1367.

Geological Survey of South Carolina, Geological Maps 2003. Available at: http://www.dnr.sc.gov/geology/publications.htm#ggms

Gregor, N. J., W. J. Silva, I. G. Wong and R. R. Youngs 2002, "Ground-Motion Attenuation Relationships for Cascadia Subduction Zone Megathrust Earthquakes Based on a Stochastic Finite-Fault Model," *Bulletin of the Seismological Society of America,* 92, 1923–1932.

Idriss, I. M. and R. W. Boulanger 2008. *Soil Liquefaction During Earthquakes*. Monograph MNO-12, Earthquake Engineering Research Institute, Oakland, California, 261 pp.

Illinois State Geological Survey, Geological Maps 1995, Revision 2004. Available at: http://www.isgs.illinois.edu/maps-data-pub/maps.shtml

Institute for Building and Home Safety 1998,"The Insured Cost of Natural Disasters: A Report on the IBHS Paid Loss Database," Institute for Building and Home Safety, October 1998.

Insurance Information Institute, Earthquake Insurance Facts File. Available at: http://www.iii.org/media/facts/statsbyissue/earthquakes/

Insurance Services Office (ISO), Propety Claim Services. Available at: http://www.iso.com/Products/Property-Claim-Services/Property-Claim-Services-PCS-info-on-losses-from-catastrophes.html

International Conference of Building Officials 1997, *Uniform Building Code*. Whittier, California: International Conference of Building Officials.

Ishihara, K. and M. Yoshimine 1992, "Evaluation of Settlements in Sand Deposits Following Liquefaction During Earthquakes, "*Soils and Foundations*, JSSMFE, 32, 173–188.

Jacob, K., N. Edelblum, and J. Arnold 2000. "NEHRP Site Classes for Census Tracks in Manhattan, New York City," NYCEM Technical Report , Lamont Doherty Earth Observatory of Columbia University

Johnson, G. S., R. E. Sheppard, M. D. Quilici, S. J. Eder, and C. Scawthorn 1999, "Seismic Reliability Assessment of Critical Facilities: A Handbook, Supporting Documentation and Model Code Provisions," Technical Report, MCEER-99-0008, Multi-disciplinary Center for Earthquake Engineering Research, SUNY-Buffalo, Buffalo, New York.

Kanno, T., A. Narita, N. Morikawa, H. Fujiwara, and Y. Fukushima 2006, "A New Attenuation Relation for Strong Ground Motion in Japan based on Recorded Data," *Bulletin of the Seismological Society of America*, 96, 879–897.

Kostrov, V. V., 1974, "Seismic Moment and Energy of Earthquakes and Seismic Flow of Rocks," *Physics of the Solid Earth*, 1, 23–44.

Martin, G. M., 1994, Proceedings of the NCEER/SEAOC/BSSC Workshop on Site Response during Earthquakes and Seismic Code Revisions, University of Southern California, Los Angeles, California, November 1992.

Massachusetts Geographic Information Systems (MassGIS), Geological Maps 1999. Available at: http://www.mass.gov/mgis/sg.htm

Morton, D. M. 1999, "Preliminary Digital Geologic Map of the Santa Ana 30' x 60' Quadrangle, Southern California," United States Geological Survey Open-File Report 99-172, version 2.1

Munich Re Group (Münchener Rück) 2000, "Major Natural Catastrophes in Insurance History," MunichRe Group (Münchener Rück) 2000.

National Association of Home Builders Research Center 2001, "Review of Structural Materials and Methods for Home Building in the United States: 1900 to 200," a report for the U.S. Department of Housing and Urban Development, January 25, 2001.

National Earthquake Information Center. Available at: http://earthquake.usgs.gov/regional/neic/

National Geophysical Data Center (NGDC) of NOAA Satellite and Information Service. Available at: http://www.ngdc.noaa.gov/hazard/int_srch.shtml

National Oceanic and Atmospheric Administration (NOAA) 1972, "A Study of Earthquake Losses in the San Francisco Bay Area–Data and Analysis," a report prepared for the Office of Emergency Preparedness: U.S. Department of Commerce.

New Jersey Geological Survey, Geological Maps 1999 – 2008 http://www.state.nj.us/dep/njgs/

New York State Museum Technology Center, Geological Maps 1999. Available at: http://www.nysm.nysed.gov/gis/

The Northern California Earthquake Data Center. Available at: http://www.ncedc.org/

O'Rourke, M. J., and S. Pak 2000, "Seismic Fragility Curves for On-Grade Steel Tanks," *Earthquake Spectra,* 16, 801–815.

Oregon Department of Geology and Mineral Industries, Geological Maps 2004–2009. Available at: http://www.oregongeology.org/sub/publications/GMS/gms-map.htm

The Pacific Northwest Seismic Network. Available at: http://www.pnsn.org/SEIS/EQ_Special/WEBDIR_01022818543p/.

Pancha, A., J. G. Anderson, and C. Kreemer 2006, "Comparison of Seismic and Geodetic Scalar Moment Rates across the Basin and Range Province," *Bulletin of the Seismological Society of America,* 96, 11–32.

Park, J., P. Bazzurro, and J. W. Baker 2007, "Modeling Spatial Correlation of Ground Motion Intensity Measures for Regional Seismic Hazard and Portfolio Loss Estimation" Proceedings of the 10th International Conference on Application of Statistic and Probability in Civil Engineering , Tokyo, Japan, July 31–August 4, 2007.

Park, S., and S. Elrick 1998, "Predictions of Shear-Wave Velocities in Southern California using Surface Geology," *Bulletin of the Seismological Society of America,* 88, 677–685.

Park, S., and S. Elrick 1998, "Predictions of Shear-Wave Velocities in Southern California using Surface Geology," *Bulletin of the Seismological Society of America,* 88, 677–685.

Pavia, E. G., and J. O'Brien 1986, "Weibull Statistics of Wind Speed over the Ocean," *Journal of Climate and Applied Meteorology*, 25, 324.

Peek-Asa, C., M. R. Ramirez, K. Shoaf, H. Seligson, and J.F. Kraus 2000, "GIS Mapping of Earthquake-Related Deaths and Hospital Admissions from the 1994 Northridge, California, Earthquake," *Annals of Epidemiology,* 10, 5–13.

Personal Insurance Federation of California 2005, "A Factual Guide To: The California Earthquake Authority for California Legislators," *2005 Insurance Reference Manual*, The Personal Insurance Federation of California, Sacramento, California.

Petak, W. J., and S. Elahi 2000, "The Northridge Earthquake, USA and its Economic and Social Impact," Proceedings of The Euro Conference on Global Change and Catastrophe Risk Management, Earthquake Risks in Europe, International Institute for Applied Systems Analysis, Laxenberg, Austria, July 6–9, 2000.

Petersen, M. D., A. D. Frankel, S. C. Harmsen, C. S. Mueller, K. M. Haller, R. L. Wheeler, R. L. Wesson, Y. Zeng, O. S. Boyd, D. M. Perkins, N. Luco, E. H. Field, C. J. Wills and K. S. Rukstales 2008, *Documentation for the 2008 Update of the United States National Seismic Hazard Maps*, United States Geological Survey Open-File Report 2008-1128.

Ramirez, M., and C. Peek-Asa 2005, "Epidemiology of Traumatic Injuries from Earthquakes," *Epidemiology Review,* 27, 47–55.

Resource Management Services 2004, "The State of Montana Multi-Hazard Mitigation Plan and Statewide Hazard Assessment" report prepared for the stat e of Montana Department of Military Affairs, Disaster and Emergency Services, October 2004. Available at: http://dma.mt.gov/des/Library/PDM/PDM-Final%20Draft/Table%20of%20Contents.pdf

Richison, T., 1998, "Cat-9: Current Issues in Earthquake Insurance," Market and Financial Update, California Earthquake Authority, March 1998. Available at: http://www.casact.org/library/ratsem98/cat9h2.pdf

Sadigh, K., C. Y. Chang, J. Egan, F. Makdisi and R. Youngs 1997, "Attenuation Relationships for Shallow Crustal Earthquakes Based on California Strong Motion Data," *Seismological Research Letters,* 68, 180–189.

Salzano E., A. G. Agreda, A. Di Carluccio, and G. Fabbrocino 2009, "Risk Assessment and Early Warning Systems for Industrial Facilities in Seismic Zones," *Reliability Engineering & System Safety*, 94, 1577–1584

Sanford, A. R., K. Lin, I. Tsai and L. Jaksha 1995, "Preliminary Listing and Discussion of New Mexico Earthquakes 1962–1994 with Duration Magnitudes of 3.0 and Greater," Geophysics Open-File Report 79, New Mexico Institute of Mining and Technology.

Sanford, A. R., T. Mayeau, J. Schlue, R. Aster and L. Jaksha 2004, "Earthquake Catalogs for New Mexico and Bordering Areas II—1999–2004," *New Mexico Geology*, 28, 99–109.

Scawthorn, C., and W. Chen 2003, *Earthquake Engineering Handbook*, Boca Raton, Florida: CRC Press

SEAOC (1995). "Vision 2000–A Framework for Performance Based Earthquake Engineering." Vol. 1, January, 1995.

Shoaf, K. I., L.H. Nguyen, H. R. Sareen and L. B. Bourque 1998, "Injuries as a Result of California Earthquakes in the Past Decades," *Disasters*, 22, 218–235.

Silva, W. J., and K. Lee 1987, "WES RASCAL Code for Synthesizing Earthquake Ground Motions, State-of-the Art for Assessing Earthquake Hazards in the United States," Report 24, United States Army Engineers Waterways Experiment Station, Paper S–73–1.

Silva, W., N. Gregor and R. Darragh 2002, "Development of Hard Rock Attenuation Relations for Central and Eastern North America," Internal Report from Pacific Engineering, November 2002. Available at: http://www.pacificengineering.org/CEUS/Development%20of%20Regional%20Hard_ABC.pdf

Sipkin, S. A., W. J. Person, and B. W. Presgrave 2000, Preliminary Determination of Epicenters (PDE) catalog at the USGS National Earthquake Information Center (NEIC), (Golden, Colorado).

Somerville, P., N. Collins, N. Abrahamson, R. Graves, and C. Saikia 2001, "Ground Motion Attenuation Relations for the Central and Eastern United States—Final report, June 30, 2001," Report Submitted to the United States Geological Survey for Award 99HQGR0098.

The Southern California Earthquake Data Center. Available at: http://www.data.scec.org/index.html

Stover, C. W., G. Reagor and S. T. Algermissen 1984, "United States Earthquake Data File," United States Geological Survey Open-File Report 1984-225.

Stover, C. W., and J. L. Coffman 1993, "A Catalog of Principal Earthquakes in the United States, 1568 – 1989" (USHIS Catalog) United States Geological Survey.

Stover, C. W., and J. L. Coffman 1993, "Seismicity of the United States, 1568–1989 (revised)," United States Geological Survey Professional Paper 1527.

Swiss Re 1996, "Natural Catastrophes and Major Losses in 1995," Sigma Insurance Research, number 2, 1996 Swiss Re, Zurich.

Swiss Re 2002, "Natural Catastrophes and Man-Made Disasters in 2001," Sigma Insurance Research, number 1, 2002 Swiss Re, Zurich.

Tavakoli, B., and S. Pezeshk 2005, "Empirical-Stochastic Ground-Motion Prediction for Eastern North America," *Bulletin of the Seismological Society of America,* 95, 2283–2296.

Tinti, S., and F. Mulargia 1985, "Effects of Magnitude Uncertainties on Estimating the Parameters in the Gutenberg-Richter Magnitude-Frequency Law," *Bulletin of the Seismological Society of America* 75, 1681–1697.

Toro, G. R. 2002, "Modification of the Toro et al. (1997) Attenuation Equations for Large Magnitudes and Short Distances," report by Risk Engineering, Inc. Available at: http://www.riskeng.com/PDF/atten_toro_extended.pdf

Toro, G. R., N. A. Abrahamson, and J. F. Schneider 1997, "A Model of Strong Ground Motions from Earthquakes in Central and Eastern North America—Best Estimates and Uncertainties," *Seismological Research Letters,* 68, 41–57.

The United States Census Bureau, "State and County Quick Facts–California QuickLinks." Available at: http://quickfacts.census.gov/qfd/states/06000lk.html

The United States Geological Survey. Available at: http://www.usgs.gov/hazards/earthquakes/

The United States Geological Survey, 1:500,000 Geologic Maps in 47 states, digitized from 1997–2007. Available at: http://pubs.usgs.gov/of/2005/1324/index_map.htm

Vermont Geological Survey, Geological Maps 2008. Available at: http://www.anr.state.vt.us/dec/geo/statemap.htm

Vranes, K., and R. Pielke 2008, "Normalized Earthquake Damage and Fatalities in the United States: 1900–2005," *Natural Hazards Review,* 10 , 84–101.

Wald, D. J., and T. I. Allen 2007, "Topographic Slope as a Proxy for Seismic Site Conditions and Amplification," *Bulletin of the Seismological Society of America*, 97, 1379–1395.

Wald, D. J., B. C. Worden, V. Quitoriano, and K. l. Pankow 2006, *ShakeMap Manual: Technical Manual, User's Guide, and Software Guide*. The United States Geological Survey. Available at: http://pubs.usgs.gov/tm/2005/12A01/pdf/508TM12-A1.pdf

Walling, M., W. Silva and N. Abrahamson 2008, "Nonlinear Site Amplification Factors for Constraining the NGA Models," *Earthquake Spectra*, 24, 243–255.

Washington Division of Geology and Earth Resources, Geological Maps 2005. Available at: http://www.dnr.wa.gov/Search/Results.aspx?k=geological%20map%202005

Washington State Department of Natural Resources, Geological Maps 1993. Available at: http://www.dnr.wa.gov/Search/Results.aspx?k=open-file%20report%2093

Wentworth, C. M. 1997" General Distribution Of Geologic Materials In The San Francisco Bay Region, California: A Digital Map Database," United States Geological Survey Open-File Report 97-744

Williams, R. A., J. K. Odum, W. J. Stephenson and R. B. Herrmann 2007, "Shallow P- and S-wave Velocities and Site Resonances in the St. Louis Region Missouri-Illinois," *Earthquake Spectra*, 23, 711–726.

Williams, R. A., S. Wood, W. J. Stephenson, J. K. Odum, M. E. Meremonte and R. Street 2003, "Surface Seismic-Refraction/Reflection Measurement Determinations of Potential Site Resonances and the Areal Uniformity of NEHRP Site Class D in Memphis, Tennessee," *Earthquake Spectra*, 19, 159–189.

Wills, C. J., M. Petersen, W. A. Bryant, M. Reichle, G. J. Saucedo, S. Tan, G. Taylor, and J. Treiman 2000, "A Site-Conditions Map for California Based on Geology and Shear-Wave Velocity," *Bulletin of the Seismological Society of America*, 90, S187–S208.

Wills, V. J., and W. Silva 1998, "Shear Wave Velocity Characteristics of Geologic Units in California," *Earthquake Spectra*, 14, 533–556.

Wills, C. J., M. Peterson, W. A. Bryant, M. Reichle, G. J. Saucedo, S. Tan, G. Taylor, and J. Treiman 2000, "A Site Conditions Map for California based on Geology and Shear Wave Velocity," *Bulleting of the Seismological Society of America*, 90, S187–S208.

Wong, I., J. Bouabid, W. Graf, C. Huyck, A. Porush, W. Silva, T. Siegel, G. Bureau, R. Eguchi, and J. Knight 2005, "Potential Losses in a Repeat of the 1886 Charleston, South Carolina, Earthquake," *Earthquake Spectra*, 21, 1157–1184.

The World Factbook, the Central Intelligence Agency online reference manual. Available at: https://www.cia.gov/library/publications/the-world-factbook/

Working Group on California Earthquake Probabilities. Available at: http://www.scec.org/research/projects/WGCEP/

Yerkes, R. F. and S. E. Graham 1997, "Preliminary Geologic Map of the Los Angeles 7.5' Quadrangle, Southern California: A Digital Database" United States Geological Survey Open-File Report 97-432

Youd, T. L. and I. M. Idriss 2001. "Liquefaction Resistance of Soils: Summary Report from the 1996 NCEER and 1998 NCEER/NSF Workshops on Evaluation of Liquefaction Resistance of Soils, " *Journal of Geotechnical and Geoenvironmental Engineering*, pp 297–313

Youngs, R. R., S. J. Chiou, W. J. Silva, and J. R. Humphrey 1997, "Strong Ground Motion Attenuation Relationships for Subduction Zone Earthquakes," *Seismological Research Letters*, 68, 58–73.

Zhao J. X., J. Zhang, A. Asano, Y. Ohno, T. Oouchi, T. Takahashi, H. Ogawa, K. Irikura, H. Thio, P. Somerville, and Y Fukushima 2006, "Attenuation Relations of Strong Ground Motion in Japan Using Site Classification Based on Predominant Period," *Bulletin of the Seismological Society of America*, 96, 898–913.

9 About AIR Worldwide

AIR Worldwide (AIR) is the scientific leader and most respected provider of risk modeling software and consulting services. AIR founded the catastrophe modeling industry in 1987 and today models the risk from natural catastrophes and terrorism in more than 50 countries. More than 400 insurance, reinsurance, financial, corporate and government clients rely on AIR software and services for catastrophe risk management, insurance-linked securities, site-specific seismic engineering analysis, and property replacement cost valuation. AIR is a member of the ISO family of companies and is headquartered in Boston with additional offices throughout North America, Europe and Asia. For more information, please visit www. air-worldwide.com.

Superseded Schedule Items

Please note that all items on the following pages are items, which have been replaced by a newer version. The newest version is located with the appropriate schedule on previous pages. These items are in date order with most recent first.

Creation Date:	Schedule	Schedule Item Name	Replacement Creation Date	Attached Document(s)
11/07/2011	Supporting Document	P&C Actuarial Justification	11/15/2011	Explanatory Exhibits.pdf (Superceded)
11/28/2011	Supporting Document	HPCS-Homeowners Premium Comparison Survey	11/30/2011	USAA HPCS-Revised 11-28-11.XLS (Superceded) CIC HPCS-Revised 11-28-11.XLS (Superceded) GIC HPCS-Revised 11-28-11.XLS (Superceded) Garrison HPCS-Revised 11-28-11.XLS (Superceded)
11/15/2011	Supporting Document	HPCS-Homeowners Premium Comparison Survey	11/28/2011	12a. USAA HPCS-Revised 11-21-11.XLS (Superceded) 12b. CIC HPCS-Revised 11-21-11.XLS (Superceded) 12c. GIC HPCS-Revised 11-21-11.XLS (Superceded) 12d. GARR HPCS-Revised 11-21-11.XLS (Superceded)
11/07/2011	Supporting Document	HPCS-Homeowners Premium Comparison Survey	11/15/2011	7. AR HPCS.XLS (Superceded)

USAA Group
Arkansas
Fire and Allied Lines Filing Memorandum

USAA Group (USAA, USAA-CIC, USAA-GIC, and Garrison) wishes to revise our Fire and Allied Lines program with an overall effect of 13.1%. The effects by form apply as follows:

USAA Fire	5.0%
USAA Allied Lines	20.0%
USAA Misc	0.0%
USAA Combined	13.0%

USAA-CIC Fire	5.0%
USAA-CIC Allied Lines	19.9%
USAA-CIC Misc	0.0%
USAA-CIC Combined	13.4%

USAA-GIC Fire	5.0%
USAA-GIC Allied Lines	19.9%
USAA-GIC Misc	0.0%
USAA-GIC Combined	13.4%

Garrison Fire	5.0%
Garrison Allied Lines	19.9%
Garrison Misc	0.0%
Garrison Combined	13.4%

USAA Group Combined	13.1%

The proposed changes include revising the Fire and Allied Lines Base Rates. The attached exhibits support these revisions.

An effective date of February 8, 2012 for these revisions will apply to all policies. Details of these revisions are attached.

USAA Group
Arkansas
Fire and Allied Lines Filing Memorandum

Attachments in support of this filing:

Explanatory Memo-Fire

Exhibit I-Fire	Indicated Rate Change
Exhibit II-Fire	Premium Trend
Exhibit III-Fire	Large Loss Adjustment
Exhibit IV-Fire	Loss Development
Exhibit V-Fire	Loss Trend
Exhibit VI-Fire	Loss Adjustment Expense (LAE)
Exhibit VII-Fire	Expected Net Fire Following Earthquake Loss and LAE Ratio
Exhibit VIII-Fire	Expenses
Exhibit IX-Fire	Underwriting Profit Provision

Explanatory Memorandum-Allied Lines

Exhibit I-Allied Lines	Indicated Rate Change
Exhibit II-Allied Lines	Premium Trend
Exhibit III-Allied Lines	Large Loss Adjustment
Exhibit IV-Allied Lines	Loss Development
Exhibit V-Allied Lines	Loss Trend
Exhibit VI-Allied Lines	Loss Adjustment Expense (LAE)
Exhibit VII-Allied Lines	Expected Net Hurricane Catastrophe Loss and LAE Ratio
Exhibit VIII-Allied Lines	Expected Net Severe Thunderstorm Loss and LAE Ratio
Exhibit IX-Allied Lines	Expected Net Winter Storm Loss and LAE Ratio

USAA Group
Arkansas
Fire and Allied Lines Filing Memorandum

Exhibit X-Allied Lines	Expenses
Exhibit XI-Allied Lines	Underwriting Profit Provision

USAA Group
Arkansas
Explanatory Memorandum
Fire

The attached exhibits are in support of the Fire Rate revision in Arkansas with a proposed effective date of 02/08/2012. Exhibits I-Fire through IX-Fire develop the rate level indication.

Exhibit I-Fire - illustrates USAA Group's Arkansas experience for the latest five accident years ending March 31, 2011 as of June 30, 2011. The indicated rate level change is developed in this exhibit. The proposed change is also provided. A large loss procedure was applied to the losses, which is detailed in Exhibit III-Fire.

Exhibit II-Fire - provides the calculation of the premium trend factors to reflect increasing amounts of insurance, as well as all other distributional changes. The selected factors are based on USAA Group Arkansas data. The current amount factors are based on actual trend to current in average earned premium at present rates (EPPR). The trended amount factor was selected based on the change in annual average EPPR. The data was fitted to an exponential curve.

Exhibit III-Fire - shows the 10-year smoothing technique USAA uses to reflect the excess loss potential in Arkansas. The Large Loss Adjustment establishes an excess loss cut-off as a percentage of the average amount of insurance written for each year. The procedure then removes the portion of developed loss in excess of the cut-off, ratios the excess losses to the developed non-excess (normal) losses, and selects a weighted average of this ratio as the excess loss factor.

Exhibit IV-Fire - displays the calculation of USAA Group loss development factors for Arkansas. Loss data used for these calculations excludes catastrophes.

Exhibit V-Fire - shows the loss trend underlying the rate level indication. Various exponential fits including 20-, 16-, 12-, 8-, and 4-points are shown. The selected current cost factor (CCF) and trended cost factor (TCF) are based on the results of these exponential fits. (Due to the volatility and lack of credibility in Arkansas, the selected Arkansas loss trend was credibility weighted with USAA countrywide loss trend data excluding CA, FL & TX.) The Arkansas credibility-weighted current cost factor and trended cost factor are displayed on Page 2.

Exhibit VI-Fire - develops the loss adjustment expense (LAE) factor used in calculating the indication in Exhibit I-Fire. The factor is based upon USAA countrywide data for calendar-accident years 2007, 2008, and 2009.

Exhibit VII-Fire - displays the expected fire following earthquake catastrophe loss and LAE ratio calculation based on a fire following earthquake simulation model developed by AIR Worldwide (AIR), Inc., of Boston, Massachusetts. AIR's Catastrophe Loss Analysis Service models fire following earthquake based on geological, engineering, and property damage data. The models estimate damage by five digit ZIP code based on

various earthquake causative characteristics, including ignition, population, and fire suppression ability. The model generates a large sample of simulated events which are then superimposed on USAA's geographical distribution of exposures by county and ZIP code within the state. USAA uses the statewide estimated average annual loss provided by AIR in calculating the overall indication.

Exhibit VIII-Fire - shows the development of the variable permissible loss and LAE ratio for Arkansas on Page 1. Provisions for other expense categories are based on countrywide data from the Insurance Expense Exhibit while taxes, licenses, and fees are based upon actual Arkansas experience for USAA Group. The calculation of the selected annual expense trend is shown on Page 2. The trend is derived by taking a weighted average of the Employment Cost Index and the Consumer Price Index. The expense trend is used to trend fixed expenses, which are used to develop the indication shown in Exhibit I-Fire.

Exhibit IX-Fire - details USAA Group's method for selecting its underwriting profit and contingency provision, which is included in the permissible loss ratio. A separate explanatory memorandum is included with the exhibit.

USAA Group
Arkansas
Indicated Rate Change
Fire Forms
As of 06/30/2011

Calendar/ Accident Year Ending (1)	Earned Premium at Present Rates (2)	Premium Trend Factor [A] (3)	Prospective Earned Premium at Present Rates (4) = (2) * (3)	Smoothed Developed Incurred Losses Excluding Catastrophes [B] (5)	Loss Trend Factor [C] (6)	LAE Factor [D] (7)	Prospective Incurred Losses and LAE Excluding Catastrophes (8) = (5) * (6) * (7)	Prospective Loss and LAE Ratio Excluding Catastrophes (9) = (8) / (4)	Weight (10)
03/31/2007	$583,866	1.211	$707,062	$151,658	0.791	1.120	$134,357	0.190	0.100
03/31/2008	644,873	1.167	752,567	1,023,672	0.823	1.120	943,580	1.254	0.150
03/31/2009	696,052	1.175	817,861	413,990	0.857	1.120	397,364	0.486	0.200
03/31/2010	813,131	1.104	897,697	1,017,170	0.893	1.120	1,017,333	1.133	0.250
03/31/2011	925,208	1.072	991,823	890,541	0.931	1.120	928,585	0.936	0.300

Five Year Weighted Loss and LAE Ratio Excluding Catastrophes =		0.868
Fire Following Earthquake Catastrophe Loss and LAE Ratio [E] =		0.007
Trended Fixed Expense Ratio [F] =		0.117
Variable Permissible Loss and LAE Ratio [G] =		0.825
Indicated Rate Level Change =	(.868+ 0.007 + 0.117) / 0.825 - 1	20.2%
Proposed Rate Level Change =		5.0%

[A] Developed in Exhibit II-Fire
[B] Developed in Exhibit III-Fire
[C] Developed in Exhibit V-Fire , Page 2 of 2
[D] Developed in Exhibit VI-Fire
[E] Developed in Exhibit VII-Fire
[F] Developed in Exhibit VIII-Fire, Page 2 of 2
[G] Developed in Exhibit VIII-Fire, Page 1 of 2

USAA Group
Arkansas
Premium Trend
Fire Forms

Year Ending Quarter (1)	Total Earned Premium at Present Rates (2)	Earned Exposures (3)	Average Earned Premium at Present Rates (4)	Annual Change (5)	Current Amount Factors 295.50 / (4)
2006/2	562,095.27	2,161.00	260.11		1.136
2006/3	569,140.10	2,188.00	260.12		1.136
2006/4	574,664.22	2,213.00	259.68		1.138
2007/1	583,866.26	2,233.00	261.47		1.130
2007/2	596,346.40	2,265.00	263.29	1.2%	1.122
2007/3	613,543.29	2,314.00	265.14	1.9%	1.115
2007/4	630,740.88	2,358.00	267.49	3.0%	1.105
2008/1	644,872.61	2,376.00	271.41	3.8%	1.089
2008/2	658,333.13	2,401.00	274.19	4.1%	1.078
2008/3	670,917.80	2,445.00	274.40	3.5%	1.077
2008/4	690,319.10	2,515.00	274.48	2.6%	1.077
2009/1	696,051.59	2,581.00	269.68	-0.6%	1.096
2009/2	718,912.29	2,654.00	270.88	-1.2%	1.091
2009/3	742,430.83	2,729.00	272.05	-0.9%	1.086
2009/4	774,900.39	2,798.00	276.95	0.9%	1.067
2010/1	813,131.22	2,834.00	286.92	6.4%	1.030
2010/2	834,404.32	2,894.00	288.32	6.4%	1.025
2010/3	862,465.85	2,961.00	291.28	7.1%	1.014
2010/4	885,576.58	3,051.00	290.26	4.8%	1.018
2011/1	925,207.57	3,131.00	295.50	3.0%	1.000

Trended Amount Factor:

Least Squares Results

Exponential Fits	20 pt	16 pt	12 pt	8 pt	4 pt
Annualized Change:	2.6%	2.8%	3.2%	5.3%	2.9%
R-squared Value:	0.891	0.836	0.757	0.912	0.764
Selected Annual Trend Factor:	1.030				

Premium Trend Factor

Accident Year Ending	Current Amount Factors (1)	Trended Amount Selection (2)	Trended Amount Period [A] (3)	Trended Amount Factors (4) = (2) ^ (3)	Premium Trend Factors (5) = (1) * (4)
03/31/2007	1.130	1.030	2.360	1.072	1.211
03/31/2008	1.089	1.030	2.360	1.072	1.167
03/31/2009	1.096	1.030	2.360	1.072	1.175
03/31/2010	1.030	1.030	2.360	1.072	1.104
03/31/2011	1.000	1.030	2.360	1.072	1.072

[A] From the average earned date in the most recent accident year, 09/30/2010, to the average earned date in the effective period, 02/08/2013

USAA Group
Arkansas
Large Loss Adjustment
Fire Forms
As of 06/30/2011

Calendar/ Accident Year Ending (1)	Average Amount of Insurance (2)	Cutoff 25% of (2) (3)	Incurred Losses Excluding Catastrophes (4)	Loss Development Factors (5)[A]	Developed Losses Excluding Catastrophes (6)	Number of Excess Losses (7)	Large Losses (8)	Excess Losses (9) = (8) - (7) * (3)	Normal Losses (10) = (6) - (9)	Excess Ratio (11) = (9) / (10)	Smoothed Developed Incurred Losses Ex Cats (12)[C]
03/31/2002	$102,390	$25,598	$148,568	1.0000	$148,568	3	$132,551	$55,757	$92,811	0.601	$190,912
03/31/2003	104,958	$26,240	43,975	1.0000	$43,975	0	$0	0	43,975	0.000	$90,457
03/31/2004	118,403	$29,601	228,828	1.0000	$228,828	3	$192,297	103,494	125,334	0.826	$257,812
03/31/2005	133,866	$33,467	39,848	1.0000	$39,848	0	$0	0	39,848	0.000	$81,967
03/31/2006	143,875	$35,969	287,165	1.0000	$287,165	3	$270,394	162,487	124,678	1.303	$256,463
03/31/2007	151,060	$37,765	171,876	1.0000	$171,876	1	$135,913	98,148	73,728	1.331	$151,658
03/31/2008	160,900	$40,225	1,015,172	1.0000	$1,015,172	8	$839,319	517,519	497,653	1.040	$1,023,672
03/31/2009	165,380	$41,345	634,221	1.0000	$634,221	4	$598,342	432,962	201,259	2.151	$413,990
03/31/2010	174,666	$43,667	1,066,657	1.0000	$1,066,657	9	$965,168	572,165	494,492	1.157	$1,017,170
03/31/2011	182,031	$45,508	734,702	1.0051	$738,449	7	$624,073	305,517	432,932	0.706	$890,541
								$2,248,049	$2,126,710		

Weighted Average Excess Ratio [B] = 1.057

Weighted Average Excess Factor = 2.057

[A] Developed in Exhibit IV-Fire

[B] Weighted Average Excess Ratio = Sum of Column (9) / Sum of Column (10)

[C] (12) = (10) * Weighted Average Excess Factor

USAA Group
Arkansas
Loss Development
Incurred Losses Excluding Catastrophes
Fire Forms

Accident Year Ending	15 months	27 months	39 months	51 months	63 months
03/31/2002					148,568
03/31/2003				43,975	43,975
03/31/2004			228,828	228,828	228,828
03/31/2005		39,848	39,848	39,848	39,848
03/31/2006	287,165	287,165	287,165	287,165	287,165
03/31/2007	197,936	171,876	171,876	171,876	171,876
03/31/2008	1,021,991	1,037,758	1,015,172	1,015,172	
03/31/2009	634,221	634,221	634,221		
03/31/2010	1,010,651	1,066,657			
03/31/2011	734,702				

Age-to-Age Factors

Accident Year Ending	15 to 27 Months	27 to 39 Months	39 to 51 Months	51 to 63 Months
03/31/2002				
03/31/2003				1.0000
03/31/2004			1.0000	1.0000
03/31/2005		1.0000	1.0000	1.0000
03/31/2006	1.0000	1.0000	1.0000	1.0000
03/31/2007	0.8683	1.0000	1.0000	1.0000
03/31/2008	1.0154	0.9782	1.0000	
03/31/2009	1.0000	1.0000		
03/31/2010	1.0554			
Latest 3-year Average	1.0236	0.9927	1.0000	1.0000
Latest 4-year Average	0.9848	0.9946	1.0000	1.0000
Latest 5-year Average	0.9878	0.9956	1.0000	1.0000
Latest 3-out-of-5-year Average	1.0051	1.0000	1.0000	1.0000
Selected Age-to-Age Factors	1.0051	1.0000	1.0000	1.0000

Cumulative Factors [A]

	15 to Ultimate	27 to Ultimate	39 to Ultimate	51 to 63 Months
Selected Cumulative Factors	1.0051	1.0000	1.0000	1.0000

[A] Cumulative factors are adjusted to ultimate with a factor of 1.0000

USAA Group
Arkansas
USAA Group CW Excl CA, FL, & TX
Fire Forms

	Calendar Year Paid Frequency				Calendar Year Paid Severity				Calendar Year Paid Pure Premium			
Year Ending Quarter	Series 1 [A]	Annual Change	Series 2 [B]	Annual Change	Series 1 [A]	Annual Change	Series 2 [B]	Annual Change	Series 1 [A]	Annual Change	Series 2 [B]	Annual Change
2006/3	0.0027		0.0035		76,714		30,361		210.37		106.86	
2006/4	0.0014		0.0037		123,270		30,583		167.11		111.75	
2007/1	0.0009		0.0038		87,326		28,797		78.21		110.43	
2007/2	0.0040		0.0037		28,013		30,351		111.31		113.60	
2007/3	0.0065	136.4%	0.0038	7.0%	33,874	-55.8%	32,630	7.5%	219.58	4.4%	122.92	15.0%
2007/4	0.0085	525.7%	0.0039	5.9%	37,662	-69.4%	30,740	0.5%	319.44	91.2%	118.99	6.5%
2008/1	0.0114	1168.8%	0.0040	3.1%	35,876	-58.9%	33,091	14.9%	407.69	421.3%	130.87	18.5%
2008/2	0.0125	214.5%	0.0041	9.4%	29,612	5.7%	31,818	4.8%	369.99	232.4%	130.25	14.7%
2008/3	0.0127	95.6%	0.0042	11.4%	33,876	0.0%	29,950	-8.2%	429.51	95.6%	125.72	2.3%
2008/4	0.0119	40.6%	0.0041	5.8%	27,626	-26.6%	30,043	-2.3%	329.53	3.2%	123.06	3.4%
2009/1	0.0101	-11.4%	0.0040	0.4%	26,258	-26.8%	30,092	-9.1%	264.51	-35.1%	119.47	-8.7%
2009/2	0.0060	-51.8%	0.0040	-1.9%	34,402	16.2%	27,891	-12.3%	207.40	-43.9%	112.05	-14.0%
2009/3	0.0066	-48.0%	0.0039	-6.3%	21,452	-36.7%	28,983	-3.2%	141.49	-67.1%	113.93	-9.4%
2009/4	0.0068	-43.1%	0.0037	-8.7%	31,181	12.9%	29,958	-0.3%	211.74	-35.7%	112.00	-9.0%
2010/1	0.0081	-19.4%	0.0040	-0.5%	38,138	45.2%	27,443	-8.8%	309.52	17.0%	108.40	-9.3%
2010/2	0.0100	66.2%	0.0039	-3.5%	34,409	0.0%	26,076	-6.5%	344.80	66.2%	101.12	-9.8%
2010/3	0.0088	33.1%	0.0042	7.1%	38,241	78.3%	24,143	-16.7%	335.79	137.3%	101.69	-10.7%
2010/4	0.0088	30.3%	0.0045	20.1%	31,696	1.7%	21,744	-27.4%	280.50	32.5%	97.60	-12.9%
2011/1	0.0073	-9.5%	0.0045	13.5%	31,819	-16.6%	22,951	-16.4%	233.74	-24.5%	102.87	-5.1%
2011/2	0.0081	-19.5%	0.0047	20.3%	41,380	20.3%	22,818	-12.5%	333.81	-3.2%	106.47	5.3%
Exponential Fits	R-squared Value	Annualized Change	R-squared Value	Annualized Change	R-squared Value	Annualized Change	R-squared Value	Annualized Change	R-squared Value	Annualized Change	R-squared Value	Annualized Change
20-point fit	0.190	30.7%	0.595	3.8%	0.286	-13.5%	0.652	-6.5%	0.117	13.1%	0.256	-2.9%
16-point fit	0.099	-5.3%	0.415	3.5%	0.031	2.1%	0.868	-9.9%	0.032	-3.3%	0.779	-6.7%
12-point fit	0.207	-9.2%	0.351	4.4%	0.256	10.2%	0.835	-11.6%	0.005	0.0%	0.799	-7.7%
8-point fit	0.127	9.6%	0.845	13.0%	0.365	22.4%	0.856	-16.5%	0.300	34.2%	0.444	-5.6%
4-point fit	0.445	-16.2%	0.873	13.0%	0.065	10.1%	0.133	-4.5%	0.019	-7.7%	0.480	7.9%

[A] Series 1 is based on USAA Group Arkansas data

[B] Series 2 is based on USAA Group CW Excl CA, FL, & TX data

USAA Group
Arkansas
USAA Group CW Excl CA, FL, & TX
Fire Forms

	Series 1 Frequency[A]	Series 2 Frequency[B]	Cred-Weighted Frequency[C]	Series 1 Severity[A]	Series 2 Severity[B]	Cred-Weighted Severity[C]	Cred-Weighted Pure Premium
Current Cost Selection	1.000	1.040	1.038	1.030	0.920	0.925	0.96
Trended Cost Selection	1.000	1.070	1.067	1.100	0.900	0.910	0.971

Loss Trend Factor

Accident Year Ending	Current Cost Selection (1)	Current Cost Period[D] (2)	Current Cost Factor (3) = (1) ^ (2)	Trended Cost Selection (4)	Trended Cost Period[E] (5)	Trended Cost Factor (6) = (4) ^ (5)	Loss Trend Factor (7) = (3) * (6)
03/31/2007	0.960	4.250	0.841	0.971	2.110	0.940	0.791
03/31/2008	0.960	3.250	0.876	0.971	2.110	0.940	0.823
03/31/2009	0.960	2.250	0.912	0.971	2.110	0.940	0.857
03/31/2010	0.960	1.250	0.950	0.971	2.110	0.940	0.893
03/31/2011	0.960	0.250	0.990	0.971	2.110	0.940	0.931

[A] Series 1 is based on USAA Group Arkansas data

[B] Series 2 is based on USAA Group CW Excl CA, FL, & TX data

[C] USAA Group Arkansas is 4.9% credible based on 26 claims; used the Square Root method with a full credibility standard of 10,623 claims.

[D] From the average date of loss in the respective accident year to 12/31/2010

[E] From 12/31/2010 to the average date of loss in the effective period, 02/08/2013

USAA Group
Countrywide
Loss Adjustment Expense (LAE) Factor
All Forms Combined
As of 6/30/2010

Non-Catastrophe Loss Adjustment Expense Factor

Calendar/Accident Year Ending	Incurred Losses	Loss Adjustment Expense	LAE Ratio
12/31/2007	90,452,699	10,382,432	0.115
12/31/2008	91,517,758	11,240,055	0.123
12/31/2009	108,159,666	13,712,416	0.127
Average LAE Ratio			0.122
Selected Non-Catastrophe LAE Factor			1.120

USAA Group

Arkansas

Expected Net Fire Following Earthquake Loss and LAE Ratio

Fire Forms

(1) Expected Annual Net Fire Following Earthquake Cat Loss	$6,598
(2) Prospective Earned Premium at Present Rates	$991,823
(3) Fire Following Earthquake Catastrophe Loss and LAE Ratio (1) / (2)	0.007
Selected Fire Following Earthquake Catastrophe Loss and LAE Ratio	0.007

[A] Based on Applied Insurance Research, Inc. (AIR) methodology and assumptions; net losses are based on exposure levels as of 05/31/2010 and trended for loss severity

USAA Group
Arkansas
Fixed and Variable Expense Provisions
Fire Forms

	2009	2010	2-Year Straight Average	Selected
(1) Average General Expenses Per Earned Exposure [A]	$4.18	$3.54		
(2) Selected Annual Expense Trend [B]	2.0%	2.0%		
(3) Trend Period [C]	3.61	2.61		
(4) Projected Average General Expenses Per Earned Exposure (1) * [1.02] ^ (3)	$4.49	$3.73	$4.11	$4.11
(5) Average Other Acquisition Expense Per Written Exposure [A]	$28.03	$32.06		
(6) Selected Annual Expense Trend [B]	2.0%	2.0%		
(7) Trend Period [D]	3.11	2.11		
(8) Projected Average Other Acquisition Expense Per Written Exposure (5) * [1.02] ^ (7)	$29.81	$33.43	$31.62	$31.62
(9) Average Licenses and Fees Expense Per Written Exposure [E]	$1.43	$0.72		
(10) Selected Annual Expense Trend [B]	2.0%	2.0%		
(11) Trend Period [D]	3.11	2.11		
(12) Projected Average Licenses and Fees Expense Per Written Exposure (9) * [1.02] ^ (11)	$1.52	$0.75	$1.14	$1.14
(13) Total Fixed Expense (4) + (8) + (12)				$36.87
(14) Average Projected Premium at Present Rates [F]				$316.27
(15) Projected Fixed Expense Provision (13) / (14)				0.117
(16) Commission and Brokerage	0.0%	0.0%	0.0%	0.0%
(17) Taxes [G]	2.4%	2.5%	2.5%	2.5%
(18) Profit and Contingencies Provision [H]				15.0%
(19) Total Variable Expenses (16) + (17) + (18)				17.5%
(20) Variable Permissible Loss and LAE Ratio 1 - (19)				82.5%

[A] USAA Group Countrywide data
[B] Developed in Exhibit VIII-Fire, Page 2 of 2
[C] From the midpoint of the respective year to the average earned date in effective period, 02/08/2013
[D] From the midpoint of the respective year to the average written date in effective period, 08/08/2012
[E] Arkansas USAA Group data
[F] Arkansas USAA Group data for Fire Forms only
[G] Arkansas USAA Group data as a percent of direct written premium
[H] Developed in Exhibit IX-Fire

USAA Group
Countrywide
Calculation of Annual Expense Trend

(1)	Employment Cost Index - Financial activities, excluding incentive paid occupations (annual change over latest 2 years ending 03/31/2011) U.S. Department of Labor	2.1%
(2)	% of Total Acquisition and General Expenses used for Salaries and Employee Relations & Welfare - USAA Group Insurance Expense Exhibit, 2010	54.4%
(3)	Consumer Price Index, All Items - (annual change over latest 2 year ending 03/31/2011)	2.5%
(4)	Annual Expense Trend - { (1) * (2) } + { (3) * [1 - (2)] }	2.3%
Selected Annual Expense Trend		2.0%

USAA GROUP
ARKANSAS FIRE
UNDERWRITING PROFIT PROVISION
EXPLANATORY MEMORANDUM

This exhibit is submitted in support of the underwriting profit and contingency provision included in the permissible loss ratio.

UNDERWRITING PROFIT PROVISION

The target underwriting profit and contingency provision needed to achieve our desired overall profit level is developed on Page 2. The selected target rate of return is 10.0% on GAAP (generally accepted accounting principles) equity.

The target underwriting return on an after-tax basis is derived by subtracting the after-tax investment rate of return on GAAP surplus from the target rate of return. This target underwriting rate of return is then adjusted to a before-tax basis, using the current corporate tax rate of 35.0%, and then divided by the premium-to-surplus ratio to yield the target underwriting profit and contingency provision.

TARGET RATE OF RETURN

Results from the Capital Asset Pricing Model (CAPM), commonly used in evaluating investments, suggest a required rate of return around 8.0%. Historically, the CAPM has consistently supported a 10.0% rate of return. However, the unusually poor market performance in recent years has impacted the results. We still believe 10.0% is a reasonable rate of return and is consistent with our historical selection.

The data points used in the CAPM method are published historical values from Value Line, Inc.'s *Investment Survey* (as of 7/30/10) and from Ibbotson Associates' 2010 Stocks, Bonds, Bills & Inflation (SBBI) Yearbook. The companies composing the "P&C Insurance Industry", as identified by Value Line, Inc., were selected to determine the appropriate rate of return for a P&C company.

INVESTMENT RATE OF RETURN

The investment rate of return is determined by dividing the estimated investment earnings by the Countrywide Fire allocation of USAA Group surplus. The estimated investment earnings are calculated by applying a selected after-tax rate of return to the total funds subject to investment.

The selected after-tax rate of return is a weighted average after-tax return, using the projected proportion of the portfolio held in each component as weight. The composition of the portfolio is projected for 2011 and 2012 and an after-tax return for each year is calculated.

USAA GROUP
ARKANSAS FIRE
UNDERWRITING PROFIT PROVISION

A.	Target Rate of Return (% of GAAP Surplus)		
	1.	Capital Asset Pricing Model	8.0%
	2.	Selected Target Rate of Return	10.0%
B.	Target Underwriting Rate of Return (% of GAAP Surplus)		
	1.	Investment Rate of Return After Tax	1.9%
	2.	Target Underwriting Return After Tax (A2) - (B1)	8.1%
	3.	Target Underwriting Return Before Tax (B2) / (1.00 - 0.35)	12.5%
C.	Target Underwriting Profit Provision (% of Direct Earned Premium)		
	1.	Direct Written Premium / GAAP Surplus Ratio	0.661
	2.	Indicated Underwriting Profit Provision (B3) / (C1)	18.9%
	3.	Selected Underwriting Profit Provision	15.0%

USAA Group
Arkansas
Explanatory Memorandum
Allied Lines

The attached exhibits are in support of the Allied Lines Rate revision in Arkansas with a proposed effective date of 02/08/2012. Exhibits I-Allied Lines through XI-Allied Lines develop the rate level indication.

Exhibit I-Allied Lines - illustrates USAA Group Arkansas experience for the latest five accident years ending March 31, 2011 as of June 30, 2011. The indicated rate level change is developed in this exhibit. The proposed change is also provided. A large loss procedure was applied to the losses, which is detailed in Exhibit III-Allied Lines.

Exhibit II-Allied Lines - provides the calculation of the premium trend factors to reflect increasing amounts of insurance, as well as all other distributional changes. The selected factors are based on USAA Group Arkansas data. The current amount factors are based on actual trend to current in average earned premium at present rates (EPPR). The trended amount factor was selected based on the change in annual average EPPR. The data was fitted to an exponential curve.

Exhibit III-Allied Lines - shows the 10-year smoothing technique USAA uses to reflect the excess loss potential in Arkansas. The Large Loss Adjustment establishes an excess loss cut-off as a percentage of the average amount of insurance written for each year. The procedure then removes the portion of developed loss in excess of the cut-off, ratios the excess losses to the developed non-excess (normal) losses, and selects a weighted average of this ratio as the excess loss factor.

Exhibit IV-Allied Lines - displays the calculation of USAA Group loss development factors for Arkansas. Loss data used for these calculations excludes catastrophes.

Exhibit V-Allied Lines - shows the loss trend underlying the rate level indication. Various exponential fits including 20-, 16-, 12-, 8-, and 4-points are shown. The selected current cost factor (CCF) and trended cost factor (TCF) are based on the results of these exponential fits. (Due to the volatility and lack of credibility in Arkansas, the selected Arkansas loss trend was credibility weighted with USAA countrywide loss trend data excluding CA, FL & TX.) The Arkansas credibility-weighted current cost factor and trended cost factor are displayed on Page 2.

Exhibit VI-Allied Lines - develops the loss adjustment expense (LAE) factor used in calculating the indication in Exhibit I-Allied Lines. The factor is based upon USAA countrywide data for calendar-accident years 2007, 2008, and 2009.

Exhibit VII-Allied Lines - displays the expected hurricane catastrophe loss and LAE ratio calculation based on a hurricane simulation model developed by AIR Worldwide (AIR), Inc., of Boston, Massachusetts. AIR's Catastrophe Loss Analysis Service models hurricanes based on meteorological, engineering, and property damage data. The models estimate wind speeds by five-digit zip code based on various hurricane characteristics,

including landfall location, size, intensity, storm track, direction, and wind speed. The model generates a large sample of simulated hurricanes, with the resultant hurricane characteristics superimposed on USAA's geographical distribution of exposures by county and zip code within the state. USAA uses the statewide estimated average annual hurricane loss provided by AIR in calculating the overall indication.

Exhibit VIII-Allied Lines - displays the expected severe thunderstorm catastrophe loss and LAE ratio calculation based on a severe thunderstorm simulation model developed by Applied Insurance Research (AIR), Inc., of Boston, Massachusetts. AIR's Severe Thunderstorm Model is based on meteorological, engineering, and property damage data. This service estimates thunderstorm damage by five digit ZIP code based on various thunderstorm characteristics, including size, intensity, and storm track. The model generates a large sample of simulated severe thunderstorm events superimposed on USAA's geographical distribution of exposures by county and ZIP code within the state. USAA uses the statewide estimated average annual severe thunderstorm loss provided by AIR in calculating the overall indication.

Exhibit IX-Allied Lines - displays the expected winter storm catastrophe loss and LAE ratio calculation based on a winter storm simulation model developed by Applied Insurance Research (AIR), Inc., of Boston, Massachusetts. AIR's Winter Storm Model is based on meteorological, engineering, and property damage data. This service estimates winter storm damage by five digit ZIP code based on various winter storm characteristics, including size, intensity, and storm track. The model generates a large sample of simulated winter storm events superimposed on USAA's geographical distribution of exposures by county and ZIP code within the state. USAA uses the statewide estimated average annual winter loss provided by AIR in calculating the overall indication

Exhibit X-Allied Lines - shows the development of the variable permissible loss and LAE ratio for Arkansas on Page 1. Provisions for other expense categories are based on countrywide data from the Insurance Expense Exhibit while taxes, licenses, and fees are based upon actual Arkansas experience for USAA Group. The calculation of the selected annual expense trend is shown on Page 2. The trend is derived by taking a weighted average of the Employment Cost Index and the Consumer Price Index. The expense trend is used to trend fixed expenses, which are used to develop the indication shown in Exhibit I-Allied Lines.

Exhibit XI-Allied Lines - details USAA Group's method for selecting its underwriting profit and contingency provision, which is included in the permissible loss ratio. A separate explanatory memorandum is included with the exhibit.

USAA Group
Arkansas
Indicated Rate Change
Allied Lines Forms
As of 06/30/2011

Calendar/ Accident Year Ending (1)	Earned Premium at Present Rates (2)	Premium Trend Factor [A] (3)	Prospective Earned Premium at Present Rates (4) = (2) * (3)	Smoothed Developed Incurred Losses Excluding Catastrophes [B] (5)	Loss Trend Factor [C] (6)	LAE Factor [D] (7)	Prospective Incurred Losses and LAE Excluding Catastrophes (8) = (5) * (6) * (7)	Prospective Loss and LAE Ratio Excluding Catastrophes (9) = (8) / (4)	Weight (10)
03/31/2007	$942,880	1.226	$1,155,971	$242,472	1.822	1.120	$494,798	0.428	0.100
03/31/2008	1,045,262	1.177	1,230,273	383,980	1.646	1.120	707,875	0.575	0.150
03/31/2009	1,130,424	1.182	1,336,161	274,655	1.487	1.120	457,421	0.342	0.200
03/31/2010	1,357,239	1.081	1,467,175	1,334,291	1.343	1.120	2,006,987	1.368	0.250
03/31/2011	1,512,263	1.072	1,621,146	442,862	1.214	1.120	602,151	0.371	0.300

Five Year Weighted Loss and LAE Ratio Excluding Catastrophes =	0.651
Hurricane Catastrophe Loss and LAE Ratio [E] =	0.008
Severe Thunderstorm Catastrophe Loss and LAE Ratio [F] =	0.317
Winter Storm Catastrophe Loss and LAE Ratio [G] =	0.035
Trended Fixed Expense Ratio [H] =	0.094
Variable Permissible Loss and LAE Ratio [I] =	0.826
Indicated Rate Level Change = (0.651 + 0.008 + 0.317 + 0.035 + 0.094) / 0.826- 1	33.8%
Proposed Rate Level Change =	20.0%

[A] Developed in Exhibit II-Allied Lines
[B] Developed in Exhibit III-Allied Lines
[C] Developed in Exhibit V-Allied Lines, Page 2 of 2
[D] Developed in Exhibit VI-Allied Lines
[E] Developed in Exhibit VII- Allied Lines
[F] Developed in Exhibit VIII-Allied Lines
[G] Developed in Exhibit IX- Allied Lines
[H] Developed in Exhibit X-Allied Lines, Page 2 of 2
[I] Developed in Exhibit X-Allied Lines, Page 1 of 2

USAA Group
Arkansas
Premium Trend
Allied Lines Forms

Year Ending Quarter (1)	Total Earned Premium at Present Rates (2)	Earned Exposures (3)	Average Earned Premium at Present Rates (4)	Annual Change (5)	Current Amount Factors 483.00 / (4)
2006/2	918,088.87	2,161.00	424.84		1.137
2006/3	924,398.47	2,188.00	422.49		1.143
2006/4	928,712.38	2,213.00	419.66		1.151
2007/1	942,879.55	2,233.00	422.25		1.144
2007/2	965,036.32	2,265.00	426.06	0.3%	1.134
2007/3	994,341.55	2,314.00	429.71	1.7%	1.124
2007/4	1,022,897.13	2,358.00	433.80	3.4%	1.113
2008/1	1,045,261.74	2,376.00	439.92	4.2%	1.098
2008/2	1,067,660.04	2,401.00	444.67	4.4%	1.086
2008/3	1,088,504.75	2,445.00	445.20	3.6%	1.085
2008/4	1,120,924.37	2,515.00	445.70	2.7%	1.084
2009/1	1,130,423.95	2,581.00	437.98	-0.4%	1.103
2009/2	1,173,623.17	2,654.00	442.21	-0.6%	1.092
2009/3	1,220,048.42	2,729.00	447.07	0.4%	1.080
2009/4	1,285,143.69	2,797.00	459.47	3.1%	1.051
2010/1	1,357,238.65	2,833.00	479.08	9.4%	1.008
2010/2	1,395,917.49	2,894.00	482.35	9.1%	1.001
2010/3	1,435,218.19	2,961.00	484.71	8.4%	0.996
2010/4	1,458,909.76	3,051.00	478.17	4.1%	1.010
2011/1	1,512,263.15	3,131.00	483.00	0.8%	1.000

Trended Amount Factor:

Least Squares Results

Exponential Fits	20 pt	16 pt	12 pt	8 pt	4 pt
Annualized Change:	3.2%	3.6%	4.1%	5.5%	-0.4%
R-squared Value:	0.884	0.860	0.789	0.768	0.046
Selected Annual Trend Factor:	1.030				

Premium Trend Factor

Accident Year Ending	Current Amount Factors (1)	Trended Amount Selection (2)	Trended Amount Period [A] (3)	Trended Amount Factors (4) = (2) ^ (3)	Premium Trend Factors (5) = (1) * (4)
03/31/2007	1.144	1.030	2.360	1.072	1.226
03/31/2008	1.098	1.030	2.360	1.072	1.177
03/31/2009	1.103	1.030	2.360	1.072	1.182
03/31/2010	1.008	1.030	2.360	1.072	1.081
03/31/2011	1.000	1.030	2.360	1.072	1.072

[A] From the average earned date in the most recent accident year, 09/30/2010, to the average earned date in the effective period, 02/08/2013

USAA Group
Arkansas
Large Loss Adjustment
Allied Lines Forms
As of 06/30/2011

Calendar/ Accident Year Ending (1)	Average Amount of Insurance (2)	Cutoff 25% of (2) (3)	Incurred Losses Excluding Catastrophes (4)	Loss Development Factors (5)[A]	Developed Losses Excluding Catastrophes (6)	Number of Excess Losses (7)	Large Losses (8)	Excess Losses (9) = (8) - (7) * (3)	Normal Losses (10) = (6) - (9)	Excess Ratio (11) = (9) / (10)	Smoothed Developed Incurred Losses Ex Cats (12)[C]
03/31/2002	$102,390	$25,598	$128,353	1.0000	$128,353	0	$0	$0	$128,353	0.000	$135,541
03/31/2003	104,958	$26,240	226,839	1.0000	$226,839	2	$67,252	14,772	212,067	0.070	$223,943
03/31/2004	118,403	$29,601	187,142	1.0000	$187,142	2	$66,168	6,966	180,176	0.039	$190,266
03/31/2005	133,866	$33,467	147,798	1.0000	$147,798	0	$0	0	147,798	0.000	$156,075
03/31/2006	143,875	$35,969	279,124	1.0000	$279,124	1	$65,405	29,436	249,688	0.118	$263,671
03/31/2007	151,052	$37,763	234,063	1.0000	$234,063	1	$42,212	4,449	229,614	0.019	$242,472
03/31/2008	160,689	$40,172	363,617	1.0000	$363,617	0	$0	0	363,617	0.000	$383,980
03/31/2009	165,333	$41,333	389,857	1.0000	$389,857	1	$171,100	129,767	260,090	0.499	$274,655
03/31/2010	174,667	$43,667	1,271,264	1.0000	$1,271,264	2	$95,065	7,731	1,263,533	0.006	$1,334,291
03/31/2011	182,031	$45,508	414,527	1.0117	$419,377	0	$0	0	419,377	0.000	$442,862
								$193,121	$3,454,313		

Weighted Average Excess Ratio [B] = 0.056

Weighted Average Excess Factor = 1.056

[A] Developed in Exhibit IV-Allied Lines

[B] Weighted Average Excess Ratio = Sum of Column (9) / Sum of Column (10)

[C] (12) = (10) * Weighted Average Excess Factor

USAA Group
Arkansas
Loss Development
Incurred Losses Excluding Catastrophes
Allied Lines Forms

Accident Year Ending	15 months	27 months	39 months	51 months	63 months
03/31/2002					128,353
03/31/2003				227,157	226,839
03/31/2004			187,142	187,142	187,142
03/31/2005		147,798	147,798	147,798	147,798
03/31/2006	276,704	279,124	279,124	279,124	279,124
03/31/2007	238,472	234,063	234,063	234,063	234,063
03/31/2008	362,194	364,117	363,617	363,617	
03/31/2009	381,783	389,857	389,857		
03/31/2010	1,210,733	1,271,264			
03/31/2011	414,527				

Age-to-Age Factors

Accident Year Ending	15 to 27 Months	27 to 39 Months	39 to 51 Months	51 to 63 Months
03/31/2002				
03/31/2003				0.9986
03/31/2004			1.0000	1.0000
03/31/2005		1.0000	1.0000	1.0000
03/31/2006	1.0087	1.0000	1.0000	1.0000
03/31/2007	0.9815	1.0000	1.0000	1.0000
03/31/2008	1.0053	0.9986	1.0000	
03/31/2009	1.0211	1.0000		
03/31/2010	1.0500			
Latest 3-year Average	1.0255	0.9995	1.0000	1.0000
Latest 4-year Average	1.0145	0.9997	1.0000	1.0000
Latest 5-year Average	1.0133	0.9997	1.0000	0.9997
Latest 3-out-of-5-year Average	1.0117	1.0000	1.0000	1.0000
Selected Age-to-Age Factors	1.0117	1.0000	1.0000	1.0000

Cumulative Factors [A]

	15 to Ultimate	27 to Ultimate	39 to Ultimate	51 to 63 Months
Selected Cumulative Factors	1.0117	1.0000	1.0000	1.0000

[A] Cumulative factors are adjusted to ultimate with a factor of 1.0000

USAA Group
Arkansas
USAA Group CW Excl CA, FL, & TX
Allied Lines Forms

	Calendar Year Paid Frequency				Calendar Year Paid Severity				Calendar Year Paid Pure Premium			
Year Ending Quarter	Series 1 [A]	Annual Change	Series 2 [B]	Annual Change	Series 1 [A]	Annual Change	Series 2 [B]	Annual Change	Series 1 [A]	Annual Change	Series 2 [B]	Annual Change
2006/3	0.0379		0.0169		4,296		5,715		162.95		96.50	
2006/4	0.0384		0.0173		3,602		5,745		138.33		99.44	
2007/1	0.0327		0.0184		4,129		6,241		134.99		114.60	
2007/2	0.0305		0.0192		3,866		6,472		117.77		124.57	
2007/3	0.0238	-37.3%	0.0203	20.2%	3,641	-15.2%	6,517	14.0%	86.53	-46.9%	132.24	37.0%
2007/4	0.0212	-44.8%	0.0204	18.1%	4,272	18.6%	6,720	17.0%	90.58	-34.5%	137.38	38.2%
2008/1	0.0244	-25.3%	0.0208	13.1%	4,413	6.9%	6,949	11.4%	107.73	-20.2%	144.36	26.0%
2008/2	0.0312	2.5%	0.0211	9.7%	4,957	28.2%	6,750	4.3%	154.85	31.5%	142.49	14.4%
2008/3	0.0368	54.9%	0.0205	1.3%	4,995	37.2%	6,990	7.2%	183.87	112.5%	143.63	8.6%
2008/4	0.0370	74.4%	0.0203	-0.7%	4,720	10.5%	6,923	3.0%	174.53	92.7%	140.58	2.3%
2009/1	0.0353	44.4%	0.0217	4.7%	4,576	3.7%	6,977	0.4%	161.35	49.8%	151.73	5.1%
2009/2	0.0305	-2.3%	0.0224	6.0%	4,067	-17.9%	7,074	4.8%	124.14	-19.8%	158.30	11.1%
2009/3	0.0370	0.5%	0.0232	12.8%	7,622	52.6%	6,923	-1.0%	282.07	53.4%	160.45	11.7%
2009/4	0.0436	18.0%	0.0234	15.2%	7,724	63.6%	6,918	-0.1%	336.91	93.0%	161.89	15.2%
2010/1	0.0515	46.2%	0.0238	9.4%	7,375	61.1%	6,967	-0.1%	380.05	135.5%	165.68	9.2%
2010/2	0.0591	93.6%	0.0236	5.4%	7,009	72.3%	6,982	-1.3%	414.18	233.6%	164.69	4.0%
2010/3	0.0550	48.7%	0.0241	3.9%	4,664	-38.8%	7,062	2.0%	256.77	-9.0%	169.98	5.9%
2010/4	0.0482	10.5%	0.0247	5.6%	4,386	-43.2%	6,889	-0.4%	211.32	-37.3%	170.19	5.1%
2011/1	0.0383	-25.6%	0.0255	7.4%	4,422	-40.0%	6,877	-1.3%	169.48	-55.4%	175.65	6.0%
2011/2	0.0341	-42.2%	0.0261	10.5%	5,024	-28.3%	6,973	-0.1%	171.51	-58.6%	181.69	10.3%
Exponential Fits	R-squared Value	Annualized Change	R-squared Value	Annualized Change	R-squared Value	Annualized Change	R-squared Value	Annualized Change	R-squared Value	Annualized Change	R-squared Value	Annualized Change
20-point fit	0.321	10.7%	0.957	8.4%	0.224	8.6%	0.576	3.3%	0.318	20.2%	0.925	11.9%
16-point fit	0.493	20.4%	0.931	7.2%	0.096	7.0%	0.297	0.9%	0.286	28.8%	0.958	8.2%
12-point fit	0.138	9.1%	0.949	8.8%	0.001	-0.6%	0.046	-0.2%	0.029	8.4%	0.937	8.5%
8-point fit	0.038	-6.8%	0.901	6.9%	0.771	-30.6%	0.000	0.0%	0.509	-35.3%	0.922	6.8%
4-point fit	0.979	-48.6%	0.992	11.5%	0.240	9.7%	0.176	-1.6%	0.873	-43.6%	0.896	9.7%

[A] Series 1 is based on USAA Group Arkansas data

[B] Series 2 is based on USAA Group CW Excl CA, FL, & TX data

USAA Group
Arkansas
USAA Group CW Excl CA, FL, & TX
Allied Lines Forms

	Series 1 Frequency[A]	Series 2 Frequency[B]	Cred-Weighted Frequency[C]	Series 1 Severity[A]	Series 2 Severity[B]	Cred-Weighted Severity[C]	Cred-Weighted Pure Premium
Current Cost Selection	1.130	1.080	1.085	1.020	1.020	1.020	1.107
Trended Cost Selection	1.000	1.090	1.081	1.020	1.000	1.002	1.083

Loss Trend Factor

Accident Year Ending	Current Cost Selection (1)	Current Cost Period[D] (2)	Current Cost Factor (3) = (1) ^ (2)	Trended Cost Selection (4)	Trended Cost Period[E] (5)	Trended Cost Factor (6) = (4) ^ (5)	Loss Trend Factor (7) = (3) * (6)
03/31/2007	1.107	4.250	1.540	1.083	2.110	1.183	1.822
03/31/2008	1.107	3.250	1.391	1.083	2.110	1.183	1.646
03/31/2009	1.107	2.250	1.257	1.083	2.110	1.183	1.487
03/31/2010	1.107	1.250	1.135	1.083	2.110	1.183	1.343
03/31/2011	1.107	0.250	1.026	1.083	2.110	1.183	1.214

[A] Series 1 is based on USAA Group Arkansas data

[B] Series 2 is based on USAA Group CW Excl CA, FL, & TX data

[C] USAA Group Arkansas is 10.2% credible based on 110 claims; used the Square Root method with a full credibility standard of 10,623 claims.

[D] From the average date of loss in the respective accident year to 12/31/2010

[E] From 12/31/2010 to the average date of loss in the effective period, 02/08/2013

USAA Group
Countrywide
Loss Adjustment Expense (LAE) Factor
All Forms Combined
As of 6/30/2010

Non-Catastrophe Loss Adjustment Expense Factor

Calendar/Accident Year Ending	Incurred Losses	Loss Adjustment Expense	LAE Ratio
12/31/2007	90,452,699	10,382,432	0.115
12/31/2008	91,517,758	11,240,055	0.123
12/31/2009	108,159,666	13,712,416	0.127
Average LAE Ratio			0.122
Selected Non-Catastrophe LAE Factor			1.120

USAA Group
Arkansas
Expected Net Hurricane Catastrophe
Loss and LAE Ratio
Allied Lines Forms

(1) Expected Annual Net Hurricane Catastrophe Loss and LAE [A]	$12,273
(2) Prospective Earned Premium at Present Rates	$1,621,146
(3) Hurricane Catastrophe Loss and LAE Ratio (1) / (2)	0.008
Selected Hurricane Catastrophe Loss and LAE Ratio	0.008

[A] Based on Applied Insurance Research, Inc. (AIR) methodology and assumptions; net losses are based on exposure levels as of 05/31/2010 and trended for loss severity

USAA Group

Arkansas

Expected Net Severe Thunderstorm Loss and LAE Ratio

Allied Lines Forms

(1) Expected Annual Net Severe Thunderstorm Cat Loss	$513,137
(2) Prospective Earned Premium at Present Rates	$1,621,146
(3) Severe Thunderstorm Catastrophe Loss and LAE Ratio (1) / (2)	0.317
Selected Severe Thunderstorm Catastrophe Loss and LAE Ratio	0.317

[A] Based on Applied Insurance Research, Inc. (AIR) methodology and assumptions; net losses are based on exposure levels as of 05/31/2010 and trended for loss severity

USAA Group

Arkansas

Expected Net Winter Storm Loss and LAE Ratio

Allied Lines Forms

(1) Expected Annual Net Winter Storm Cat Loss	$56,599
(2) Prospective Earned Premium at Present Rates	$1,621,146
(3) Winter Storm Catastrophe Loss and LAE Ratio (1) / (2)	0.035
Selected Winter Storm Catastrophe Loss and LAE Ratio	0.035

[A] Based on Applied Insurance Research, Inc. (AIR) methodology and assumptions; net losses are based on exposure levels as of 05/31/2010 and trended for loss severity

USAA Group
Arkansas
Fixed and Variable Expense Provisions
Allied Lines Forms

	2009	2010	2-Year Straight Average	Selected
(1) Average General Expenses Per Earned Exposure [A]	$5.36	$4.70		
(2) Selected Annual Expense Trend [B]	2.0%	2.0%		
(3) Trend Period [C]	3.61	2.61		
(4) Projected Average General Expenses Per Earned Exposure (1) * [1.02] ^ (3)	$5.76	$4.95	$5.36	$5.36
(5) Average Other Acquisition Expense Per Written Exposure [A]	$36.09	$42.16		
(6) Selected Annual Expense Trend [B]	2.0%	2.0%		
(7) Trend Period [D]	3.11	2.11		
(8) Projected Average Other Acquisition Expense Per Written Exposure (5) * [1.02] ^ (7)	$38.38	$43.96	$41.17	$41.17
(9) Average Licenses and Fees Expense Per Written Exposure [E]	$2.38	$1.15		
(10) Selected Annual Expense Trend [B]	2.0%	2.0%		
(11) Trend Period [D]	3.11	2.11		
(12) Projected Average Licenses and Fees Expense Per Written Exposure (9) * [1.02] ^ (11)	$2.53	$1.20	$1.87	$1.87
(13) Total Fixed Expense (4) + (8) + (12)				$48.40
(14) Average Projected Premium at Present Rates [F]				$516.95
(15) Projected Fixed Expense Provision (13) / (14)				0.094
(16) Commission and Brokerage	0.0%	0.0%	0.0%	0.0%
(17) Taxes [G]	2.4%	2.4%	2.4%	2.4%
(18) Profit and Contingencies Provision [H]				15.0%
(19) Total Variable Expenses (16) + (17) + (18)				17.4%
(20) Variable Permissible Loss and LAE Ratio 1 - (19)				82.6%

[A] USAA Group Countrywide data
[B] Developed in Exhibit X-Allied Lines, Page 2 of 2
[C] From the midpoint of the respective year to the average earned date in effective period, 02/08/2013
[D] From the midpoint of the respective year to the average written date in effective period, 08/08/2012
[E] Arkansas USAA Group data
[F] Arkansas USAA Group data for Allied Lines Forms only
[G] Arkansas USAA Group data as a percent of direct written premium
[H] Developed in Exhibit XI-Allied Lines

USAA Group
Countrywide
Calculation of Annual Expense Trend

(1)	Employment Cost Index - Financial activities, excluding incentive paid occupations (annual change over latest 2 years ending 03/31/2011) U.S. Department of Labor	2.1%
(2)	% of Total Acquisition and General Expenses used for Salaries and Employee Relations & Welfare - USAA Group Insurance Expense Exhibit, 2010	54.4%
(3)	Consumer Price Index, All Items - (annual change over latest 2 year ending 03/31/2011)	2.5%
(4)	Annual Expense Trend - { (1) * (2) } + { (3) * [1 - (2)] }	2.3%
Selected Annual Expense Trend		2.0%

USAA GROUP
ARKANSAS EXTENDED COVERAGE
UNDERWRITING PROFIT PROVISION
EXPLANATORY MEMORANDUM

This exhibit is submitted in support of the underwriting profit and contingency provision included in the permissible loss ratio.

UNDERWRITING PROFIT PROVISION

The target underwriting profit and contingency provision needed to achieve our desired overall profit level is developed on Page 2. The selected target rate of return is 10.0% on GAAP (generally accepted accounting principles) equity.

The target underwriting return on an after-tax basis is derived by subtracting the after-tax investment rate of return on GAAP surplus from the target rate of return. This target underwriting rate of return is then adjusted to a before-tax basis, using the current corporate tax rate of 35.0%, and then divided by the premium-to-surplus ratio to yield the target underwriting profit and contingency provision.

TARGET RATE OF RETURN

Results from the Capital Asset Pricing Model (CAPM), commonly used in evaluating investments, suggest a required rate of return around 8.0%. Historically, the CAPM has consistently supported a 10.0% rate of return. However, the unusually poor market performance in recent years has impacted the results. We still believe 10.0% is a reasonable rate of return and is consistent with our historical selection.

The data points used in the CAPM method are published historical values from Value Line, Inc.'s *Investment Survey* (as of 7/30/10) and from Ibbotson Associates' 2010 Stocks, Bonds, Bills & Inflation (SBBI) Yearbook. The companies composing the "P&C Insurance Industry", as identified by Value Line, Inc., were selected to determine the appropriate rate of return for a P&C company.

INVESTMENT RATE OF RETURN

The investment rate of return is determined by dividing the estimated investment earnings by the Texas Extended Coverage allocation of USAA Group surplus. The estimated investment earnings are calculated by applying a selected after-tax rate of return to the total funds subject to investment.

The selected after-tax rate of return is a weighted average after-tax return, using the projected proportion of the portfolio held in each component as weight. The composition of the portfolio is projected for 2011 and 2012 and an after-tax return for each year is calculated.

USAA GROUP
ARKANSAS EXTENDED COVERAGE
UNDERWRITING PROFIT PROVISION

A.	Target Rate of Return (% of GAAP Surplus)		
	1.	Capital Asset Pricing Model	8.0%
	2.	Selected Target Rate of Return	10.0%
B.	Target Underwriting Rate of Return (% of GAAP Surplus)		
	1.	Investment Rate of Return After Tax	1.8%
	2.	Target Underwriting Return After Tax (A2) - (B1)	8.2%
	3.	Target Underwriting Return Before Tax (B2) / (1.00 - 0.35)	12.6%
C.	Target Underwriting Profit Provision (% of Direct Earned Premium)		
	1.	Direct Written Premium / GAAP Surplus Ratio	0.661
	2.	Indicated Underwriting Profit Provision (B3) / (C1)	19.1%
	3.	Selected Underwriting Profit Provision	15.0%

SERFF Tracking Number:	*USAA-127801012*	*State:*	*Arkansas*
First Filing Company:	*Garrison Property and Casualty Insurance Company, ...*	*State Tracking Number:*	
Company Tracking Number:	*AR1114530*		
TOI:	*01.0 Property*	*Sub-TOI:*	*01.0002 Personal Property (Fire and Allied Lines)*
Product Name:	*Dwelling Fire Program*		
Project Name/Number:	*Rate Revision/AR1114530*		

Attachment "USAA HPCS-Revised 11-28-11.XLS" is not a PDF document and cannot be reproduced here.

SERFF Tracking Number:	*USAA-127801012*	*State:*	*Arkansas*
First Filing Company:	*Garrison Property and Casualty Insurance Company, ...*	*State Tracking Number:*	
Company Tracking Number:	*AR1114530*		
TOI:	*01.0 Property*	*Sub-TOI:*	*01.0002 Personal Property (Fire and Allied Lines)*
Product Name:	*Dwelling Fire Program*		
Project Name/Number:	*Rate Revision/AR1114530*		

Attachment "CIC HPCS-Revised 11-28-11.XLS" is not a PDF document and cannot be reproduced here.

SERFF Tracking Number:	*USAA-127801012*	*State:*	*Arkansas*
First Filing Company:	*Garrison Property and Casualty Insurance Company, ...*	*State Tracking Number:*	
Company Tracking Number:	*AR1114530*		
TOI:	*01.0 Property*	*Sub-TOI:*	*01.0002 Personal Property (Fire and Allied Lines)*
Product Name:	*Dwelling Fire Program*		
Project Name/Number:	*Rate Revision/AR1114530*		

Attachment "GIC HPCS-Revised 11-28-11.XLS" is not a PDF document and cannot be reproduced here.

SERFF Tracking Number:	*USAA-127801012*	*State:*	*Arkansas*
First Filing Company:	*Garrison Property and Casualty Insurance Company, ...*	*State Tracking Number:*	
Company Tracking Number:	*AR1114530*		
TOI:	*01.0 Property*	*Sub-TOI:*	*01.0002 Personal Property (Fire and Allied Lines)*
Product Name:	*Dwelling Fire Program*		
Project Name/Number:	*Rate Revision/AR1114530*		

Attachment "Garrison HPCS-Revised 11-28-11.XLS" is not a PDF document and cannot be reproduced here.